АВТОМАТИКА
И
ТЕЛЕМЕХАНИКА

Vol. 22, No. 2, February, 1961

Translation Published September, 1961

SOVIET INSTRUMENTATION AND
CONTROL TRANSLATION SERIES

Automation and Remote Control

(The Soviet Journal *Avtomatika i Telemekhanika* in English Translation)

■ This translation of a Soviet journal on automatic control is published as a service to American science and industry. It is sponsored by the Instrument Society of America under a grant in aid from the National Science Foundation, continuing a program initiated by the Massachusetts Institute of Technology.

SOVIET INSTRUMENTATION AND CONTROL TRANSLATION SERIES

■ This translation of the Soviet Journal *Avtomatika i Telemekhanika* is published and distributed at nominal subscription rates under a grant in aid to the Instrument Society of America from the National Science Foundation. This translated journal, and others in the Series (see back cover), will enable American scientists and engineers to be informed of work in the fields of instrumentation, measurement techniques, and automatic control reported in the Soviet Union.

The original Russian articles are translated by competent technical personnel. The translations are on a cover-to-cover basis and the Instrument Society of America and its translators propose to translate faithfully all of the scientific material in *Avtomatika i Telemekhanika*, permitting readers to appraise for themselves the scope, status, and importance of the Soviet work. All views expressed in the translated material are intended to be those of the original authors and not those of the translators nor the Instrument Society of America.

Publication of *Avtomatika i Telemekhanika* in English translation started under the present auspices in April, 1958, with Russian Vol. 18, No. 1 of January, 1957. The program has been continued with the translation and printing of the 1958-1961 issues.

Transliteration of the names of Russian authors follows the system known as the British Standard. This system has recently achieved wide adoption in the United Kingdom, and is currently being adopted by a large number of scientific journals in the United States.

Readers are invited to submit to the Instrument Society of America comments on the quality of the translations and the content of the articles. Pertinent correspondence will be published in the Society's monthly publication, the ISA JOURNAL. Space will also be made available in the ISA JOURNAL for such replies as may be received from Russian authors to comments or questions by the readers.

1961 Volume 22 Subscription Prices:

Per year (12 issues), starting with Vol. 22, No. 1

General:	*United States and Canada*	$35.00
	Elsewhere	38.00
Libraries of nonprofit academic institutions:		
	United States and Canada	$17.50
	Elsewhere	20.50
Single issues to everyone, each		$ 6.00

1957 Volume 18, 1958 Volume 19, 1959 Volume 20, and 1960 Volume 21 issues also available. Prices upon request.

See back cover for combined subscription to entire Series.

Subscriptions and requests for information on back issues should be addressed to the:

Instrument Society of America
530 William Penn Place, Pittsburgh 19, Penna.

Translated and printed by Consultants Bureau Enterprises, Inc.

Automation and Remote Control

A translation of Avtomatika i Telemekhanika, a publication of the Academy of Sciences of the USSR

Vol. 22, No. 2 Russian Original Dated February, 1961 September, 1961

CONTENTS

	PAGE	RUSS. PAGE
The Theory of Dual Control. IV. A. A. Fel'dbaum	109	129
A Two-Channel Servo System with Antisymmetric Feed-Back in the Case of Random Disturbances. A. A. Krasovskii	122	144
Optimum Servo Drive with Two Control Parameters. A. E. Bor-Ramenskii and Sung Chien	134	157
The Estimation of Self-Oscillation Parameters in Nonlinear Automatic Control Systems. V. R. Andrievskii	146	171
Transitional Processes in a System of Extremal Control with a Dynamic Sensitive Unit. A. P. Yurkevich	151	176
Limiting Dynamic Characteristics of Power Servo System Components. II. G. A. Nadzhafova	159	185
Elements and Units of a Digital Computer One-Cycle Parallel Arithmetic Device which Uses Ferrite Transistor Cells. M. I. Petrukhin	172	199
Electronic Decoding and Coding Function Generators. V. B. Smolov	180	209
Determination of the Required Measuring Frequency for Discrete Control. É. L. Itskovich	186	216
Self-Saturating Magnetic Amplifier with a Voltage Doubling Circuit. R. A. Lipman and A. I. Moskalev	193	224
A High Efficiency DC Reverse Magnetic Amplifier. O. A. Kossov and E. A. Manychkina	199	231
Second Harmonic Magnetic Modulator with a Quadrature Phase Shift Supply Circuit. M. A. Rakov and L. A. Sinitskii	205	238
The Use of Magnetic Amplifiers for Impedance Measurements by Means of Magnetically Coupled Circuits. O. G. Malkina	209	243
Some Circuits for Half-Wave (High-Speed) Magnetic Amplifiers for Servomotors. V. G. Leskov, A. I. Chizhov, and I. I. Chicherin	215	250
On the Pulse Feed of Measuring Bridge Circuits with Semiconductor Resistors in Two-Position Temperature Control Devices. V. F. Bakhmut-skii, I. I. Vinshtein, and S. E. Sas	222	259
New Developments Concerning High-Frequency Remote Control Channels. Ya. L. Bykhovskii, R. A. Izrailev, G. Y. Mikutskii, V. S. Skital'tsev, and V. B. Sokolov	225	263
Transformation of Some Nonelectrical Quantities into Electrical Signals in Application to Contactless Remote Control Devices. M. V. Kazhdarov	233	271

CONTENTS (continued)

	PAGE	RUSS. PAGE
REVIEWS AND BIBLIOGRAPHY		
Review of B. Ya. Kogan's Book "Electronic Simulating Devices and Their Application in Investigating Automatic Control Systems" (Fizmatgiz, 1959). M. N. Babushkin, S. Ya. Berezin, and A. A. Birshtein	235	274
List for 1959 of Domestic Papers on the Theory of Relay Circuits and Final Automatic Devices. V. D. Kazakov and O. P. Kuznetsov	236	275
List for 1959 of Foreign Literature on Magnetic Components Used in Automation, Remote Control, and Computer Techniques	239	277
EVENTS		
Seminar on Technical Contributions to Mathematical Logic (1959 – 1960). V. P. Goncharov	251	292

THE THEORY OF DUAL CONTROL. IV

A. A. Fel'dbaum (Moscow)

Translated from Avtomatika i Telemekhanika, Vol. 22, No. 2, pp. 129-142, February, 1961
Original article submitted June 6, 1960

A generalized algorithm is derived for the optimal strategy of a dual-control system for an object with several inputs and outputs, and a memory. An example is given of the application of the algorithm. In conclusion, we consider the directions that further development of the theory of dual control should take.

Derivation of a Generalized Algorithm for the Optimum Strategy of Dual Control

In the second paper of this series (see [1]), an algorithm was derived for the optimal strategy of a dual control, where it was assumed that the object of control did not have a memory, and had one output and one input. We consider below a generalization of this theory to an object with a memory and with several inputs and outputs.

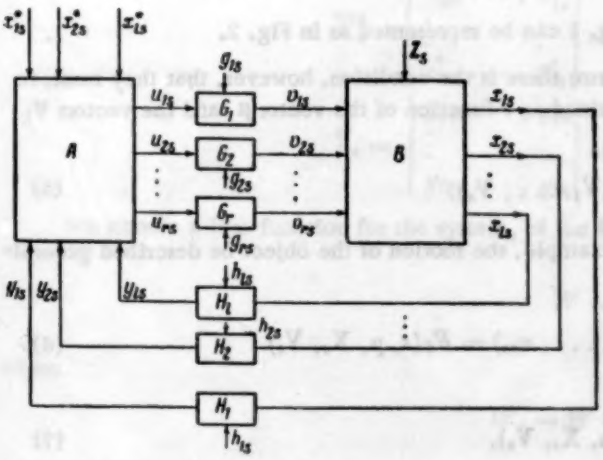

Fig. 1.

The block diagram of the system we are considering is shown in Fig. 1. All quantities will be assumed to be functions of a discrete time $t = s$ ($s = 0, 1, \ldots, n$). The controlling parameters $u_{1s}, u_{2s}, \ldots, u_{rs}$ from the output of the control section A, arrive at the controlled object B through transmission channels $G_1, G_2, \ldots, G_r$, in which the useful signal is mixed with the interference components $g_{1s}, g_{2s}, \ldots, g_{rs}$, respectively. At the object B, the controlling quantities $v_{1s}, v_{2s}, \ldots, v_{rs}$ arrive from the transmission channels. Moreover, the object is subjected to the interference $\mathbf{Z}_s$, which is generally a vector, i.e., it is the combination of interferences applied, perhaps, at various parts of the object B:

$$\mathbf{Z}_s = \mathbf{Z}_s(s, \mu), \tag{1}$$

where μ is the parameter vector

$$\mu = (\mu_1, \mu_2, \ldots, \mu_m). \tag{2}$$

The outputs $x_{1s}, x_{2s}, \ldots, x_{ls}$ from the object B pass through channels $H_1, H_2, \ldots, H_l$ to the input of the control section A. In the channels $H_1, H_2, \ldots, H_l$ the interference $h_{1s}, h_{2s}, \ldots, h_{ls}$ acts, and so the outputs $y_{1s}, y_{2s}, \ldots, y_{ls}$ from the channels generally differ from the inputs $x_{1s}, x_{2s}, \ldots, x_{ls}$ to these channels. In the control section A, the quantities $y_{1s}, y_{2s}, \ldots, y_{ls}$ can generally be compared with certain given quantities $x^*_{1s}, x^*_{2s}, \ldots, x^*_{ls}$. In certain cases (for example, in obtaining the minimum of some quantity $\underline{x}$), such a comparison can be omitted.

In particular cases, for certain inputs, there will be only one scalar quantity x_s at the object output; such a

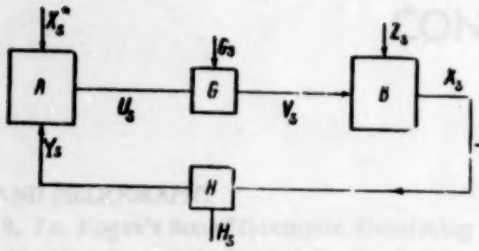

Fig. 2.

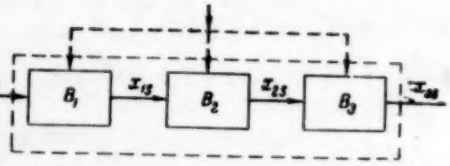

Fig. 3.

case is found in systems of automatic optimization. In other types of systems, the controlling action u_s is transmitted to the object through only one channel, while several quantities x_{is} ($i = 1, \ldots, l$) are measured at the output.

We introduce vectors made up of the values of our parameters all taken for the same time $t = s$:

$$\begin{aligned} \overset{\cdot}{\mathbf{X}}_s &= (\overset{\cdot}{x}_{1s}, \overset{\cdot}{x}_{2s}, \ldots, \overset{\cdot}{x}_{ls}), & \mathbf{X}_s &= (x_{1s}, x_{2s}, \ldots, x_{ls}), \\ \mathbf{Y}_s &= (y_{1s}, y_{2s}, \ldots, y_{ls}), & \mathbf{U}_s &= (u_{1s}, u_{2s}, \ldots, u_{rs}), \\ \mathbf{V}_s &= (v_{1s}, v_{2s}, \ldots, v_{rs}), & \mathbf{G}_s &= (g_{1s}, \ldots, g_{rs}), \\ \mathbf{H}_s &= (h_{1s}, \ldots, h_{ls}). \end{aligned} \tag{3}$$

These space vectors must differ from the time vectors, which are denoted by lower-case letters:

$$\begin{aligned} \overset{\cdot}{\mathbf{x}}_{is} &= (\overset{\cdot}{x}_{i0}, \overset{\cdot}{x}_{i1}, \ldots, \overset{\cdot}{x}_{is}), & \mathbf{x}_{is} &= (x_{i0}, x_{i1}, \ldots, x_{is}); \\ \mathbf{y}_{is} &= (y_{i0}, y_{i1}, \ldots, y_{is}) & (i &= 1, 2, \ldots, l); \\ \mathbf{u}_{js} &= (u_{j0}, u_{j1}, \ldots, u_{js}); & \mathbf{v}_{js} &= (v_{j0}, v_{j1}, \ldots, v_{js}) \qquad (j = 1, 2, \ldots, r). \end{aligned} \tag{4}$$

If this vector notation is used, then the system in Fig. 1 can be represented as in Fig. 2.

The equations for the object B can have arbitrary form; there is the condition, however, that they must, in principle, be solvable, and so the vector $\mathbf{X}_s$ can be determined as a function of the vector $\boldsymbol{\mu}$ and the vectors $\mathbf{V}_k$ ($k = 0, 1, \ldots, s$)

$$\mathbf{X}_s = \mathbf{X}_s(\mu, \mathbf{V}_0, \mathbf{V}_1, \ldots, \mathbf{V}_s). \tag{5}$$

We will consider various particular cases. Let, for example, the motion of the object be described generally by the nonlinear, finite difference equations

$$x_{i,s+1} = F_i(s, Z_s, x_{1s}, \ldots, x_{ls}, v_{1s}, \ldots, v_{rs}) = F_i(s, \mu, \mathbf{X}_s, \mathbf{V}_s) \tag{6}$$

or

$$\mathbf{X}_{s+1} = \mathbf{F}(s, \mu, \mathbf{X}_s, \mathbf{V}_s), \tag{7}$$

where $\mathbf{F}$ is the vector with components $F_1, \ldots, F_l$. When the initial values $\mathbf{X}_0$ and $\mathbf{V}_0$ of the vectors $\mathbf{X}$ and $\mathbf{V}$ are specified, then from this formula we obtain the vector

$$\mathbf{X}_1 = \mathbf{F}(0, \mu, \mathbf{X}_0, \mathbf{V}_0) = \mathbf{F}_1(\mu, \mathbf{V}_0). \tag{8}$$

If we know $\mathbf{X}_1$, we can find the vector

$$\mathbf{X}_2 = \mathbf{F}(1, \mu, \mathbf{X}_1, \mathbf{V}_1) = \mathbf{F}_2(\mu, \mathbf{V}_0, \mathbf{V}_1)$$

etc. To sum up, we obtain a formula of the type (5) for the vector $\mathbf{X}_s$.

As another example, we can use the block diagram shown in Fig. 3 for the object B. The parts B_1 and B_3 of the object are linear, with transfer functions

$$x_{1s} = \sum_{k=0}^{s} a_{1k}(s, \mu)\, v_{s-k}; \qquad x_{2s} = \sum_{k=0}^{s} a_{2k}(s, \mu)\, x_{2, s-k}. \tag{9}$$

The section B_2 is noninertial nonlinear, with the equation

$$x_{2s} = F(s, \mu, x_{1s}). \tag{10}$$

The dependence of x_{2s} on x_{1s} is continuous and single-valued (but its inverse is not necessarily single-valued).

From Eqs. (9) and (10), it is obvious that we can express x_{1s}, x_{2s}, and x_{3s} as functions of μ and $\nu_s = (v_0, v_1, \ldots, v_s)$, i.e., we can obtain a relation of the type (5).

We will first of all assume that such a relation has been obtained by some method or other.

We introduce the space-time matrices

$$\overline{U}_s = \begin{vmatrix} u_{10}, u_{11}, \ldots, u_{1s} \\ u_{20}, u_{21}, \ldots, u_{2s} \\ \vdots \\ u_{r0}, u_{r1}, \ldots, u_{rs} \end{vmatrix} = \begin{vmatrix} \mathbf{u}_{1s} \\ \mathbf{u}_{2s} \\ \vdots \\ \mathbf{u}_{rs} \end{vmatrix} = |\mathbf{U}_0, \mathbf{U}_1, \ldots \mathbf{U}_s|, \tag{11}$$

$$\overline{V}_s = \begin{vmatrix} v_{10}, \ldots, v_{1s} \\ \vdots \\ v_{r0}, \ldots, v_{rs} \end{vmatrix} = \begin{vmatrix} \mathbf{v}_{1s} \\ \mathbf{v}_{2s} \\ \vdots \\ \mathbf{v}_{rs} \end{vmatrix} = |\mathbf{V}_0, \mathbf{V}_1, \ldots, \mathbf{V}_s|, \tag{12}$$

$$\overline{X}_s = \begin{vmatrix} x_{10}, \ldots, x_{1s} \\ \vdots \\ x_{l0}, \ldots, x_{ls} \end{vmatrix} = \begin{vmatrix} \mathbf{x}_{1s} \\ \vdots \\ \mathbf{x}_{ls} \end{vmatrix} = |\mathbf{X}_0, \ldots, \mathbf{X}_s|, \tag{13}$$

$$\overline{X}_s^* = \begin{vmatrix} x_{10}^*, \ldots, x_{1s}^* \\ \vdots \\ x_{l0}^*, \ldots, x_{ls}^* \end{vmatrix} = \begin{vmatrix} \mathbf{x}_{1s}^* \\ \vdots \\ \mathbf{x}_{ls}^* \end{vmatrix} = |\mathbf{X}_0^*, \ldots, \mathbf{X}_s^*|, \tag{14}$$

$$\overline{Y}_s = \begin{vmatrix} y_{10}, \ldots, y_{1s} \\ \vdots \\ y_{l0}, \ldots, y_{ls} \end{vmatrix} = \begin{vmatrix} \mathbf{y}_{1s} \\ \vdots \\ \mathbf{y}_{ls} \end{vmatrix} = |\mathbf{Y}_0, \ldots, \mathbf{Y}_s|. \tag{15}$$

We choose a loss-function for the system, of the form

$$W = \sum_{s=0}^{n} W_s, \tag{16}$$

where

$$W_s = W(s, \mu, \mathbf{X}_s^*, \mathbf{X}_s). \tag{17}$$

An explicit dependence of W_s on μ can exist. For example, if in the system of Fig. 1 there is a unique output x_s given by

$$x_s = \mu_{r+1} + \sum_{i,\, j=1}^{r} a_{ij}(v_{is} - \mu_i)(v_{js} - \mu_j), \tag{18}$$

where $a_{ij} = \text{const}$, v_{js} is the input to the object, and the second term on the right-hand side of Eq. (18) cannot be negative, then the minimum possible value of x_s is μ_{r+1} (for $v_{is} = \mu_i$). The deviation of x_s from the minimum is given by the difference $x_s - \mu_{r+1}$. In the given case, we can therefore take $W_s = x_s - \mu_{r+1}$, and demand the minimization of the mathematical expectation of the corresponding quantity W.

Let the a priori probability density for the vector μ be given, let it be denoted by $P(\mu) = P_0(\mu)$, and let the probability density $P(g_{js})$ $(j = 1, \ldots, r)$ also be given. We will assume that the $P(g_{js})$ are independent of s and, generally speaking, that they are different for different values of j. In the same way, let the probability densities $P(h_{is})$ $(i = 1, \ldots, l)$ be independent of s and different for different values of i.

We will assume that the channels G and H have no memory. Therefore,

$$v_{js} = v_j(g_{js}, u_{js}), \qquad y_{is} = y_i(h_{is}, x_{is}). \tag{19}$$

If we have the above information, we can find the conditional probability densities $P(y_s|x_s)$ and $P(v_s|u_s)$, and also $P(\mathbf{Y}_s|\mathbf{X}_s)$ and $P(\mathbf{V}_s|\mathbf{U}_s)$. We can then find the conditional probability densities

$$P(\mathbf{y}_s|\mathbf{x}_s) = \prod_{i=0}^{s} P(y_s|x_s), \qquad P(\mathbf{v}_s|\mathbf{u}_s) = \prod_{i=0}^{s} P(v_s|u_s), \tag{20}$$

and also the conditional probability densities $P(\overline{\overline{\mathbf{Y}}}_s|\overline{\overline{\mathbf{X}}}_s)$ and $P(\overline{\overline{\mathbf{V}}}_s|\overline{\overline{\mathbf{U}}}_s)$.

The algorithm for the controlling section A of the system is characterized by the probability density Γ_s of its output vector $\mathbf{U}_s$, which, generally speaking, depends on all the previous inputs of the controlling section:

$$P_s(\mathbf{U}_s) = \Gamma_s = \Gamma_s(\mathbf{U}_s|\overline{X}_s^*, \overline{Y}_{s-1}, \overline{U}_{s-1}). \tag{21}$$

We pose the problem of finding a sequence of functions Γ_i $(i = 1, \ldots, n)$, and an initial probability density $\Gamma_0 = P(\mathbf{U}_0)$, such that the risk R is a minimum, where R is the mathematical expectation of the loss-function W.

We can write the expression for R in various forms. We give below an expression for R which has a form which is the most convenient for finding the optimal strategy. This expression is a generalization of a similar formula, given in Section II of the present series of papers. The method of derivation that we use here is somewhat different – it is shorter, but somewhat more formal.

From the equalities (17) and (7), we obtain

$$W_s = W[s, \mu, \mathbf{X}_s^*, \mathbf{X}_s(s, \mu, \overline{V})] = W(s, \mu, \mathbf{X}_s^*, \overline{\overline{V}}). \tag{22}$$

We will limit our derivation of the expression for R to the case of a fixed matrix $\overline{\overline{X}}_s^*$. Let the general conditional probability density $P(\mu, \overline{\overline{U}}_s, \overline{\overline{V}}_s, \overline{\overline{Y}}_{s-1}|\overline{\overline{X}}_s^*)$ for the coupled random vectors and matrices be known.

Here $\overline{\overline{Y}}_{s-1}$ occurs, since, on the basis of (20), $\overline{\overline{U}}_s$ is related to $\overline{\overline{Y}}_{s-1}$. Then the specific risk R_s, corresponding to the instant $t = s$, is

$$R_s = M\{W|\overline{X}_s^*\} = \int_{\Omega(\mu, \overline{U}_s, \overline{V}_s, \overline{Y}_{s-1})} W(s, \mu, \mathbf{X}_s^*, \overline{V}_s) P(\mu, \overline{U}_s, \overline{V}_s, \overline{Y}_{s-1}|\overline{X}_s^*)\, d\Omega(\mu, \overline{U}_s, \overline{V}_s, \overline{Y}_{s-1}) \tag{23}$$

Further, if we use a known theorem concerning the multiplication of probabilities, we obtain

$$P(\mu, \overline{U}_s, \overline{V}_s, \overline{Y}_{s-1}|\overline{X}_s^*) = P(\mu)\, P(\overline{V}_s, \overline{U}_s, \overline{Y}_{s-1}|\mu, \overline{X}_s^*). \tag{24}$$

Here we assume that μ and $\overline{\overline{X}}_s^*$ are independent.

We consider the second factor on the right-hand side of (24):

$$\begin{aligned} P(\overline{V}_s, \overline{U}_s, \overline{Y}_{s-1}|\mu, \overline{X}_s^*) &= P(\overline{U}_s, \overline{Y}_{s-1}|\mu, \overline{X}_s^*)\, P(\overline{V}_s|\overline{U}_s, \overline{Y}_{s-1}, \mu, \overline{X}_s^*) = \\ &= P(\overline{U}_s, \overline{Y}_{s-1}|\mu, \overline{X}_s^*)\, P(\overline{V}_s|\overline{U}_s), \end{aligned} \tag{25}$$

since the probability density of the matrix $\overline{\overline{V}}_s$ is completely determined for one fixed $\overline{\overline{U}}_s$ only, and supplementary information concerning μ and $\overline{\overline{X}}_s^*$ does not change it.

Further,

$$P(\overline{U}_s, \overline{Y}_{s-1} | \mu, \overline{X}_s^*) = P(U_0, Y_0 | \mu, X_0^*) P(U_1, Y_1 | \mu, U_0, Y_0, \overline{X}_1^*) \times$$
$$P(U_2, Y_2 | \mu, \overline{U}_1, \overline{Y}_1, \overline{X}_2^*) \dots P(U_i, Y_i | \mu, \overline{U}_{i-1}, \overline{Y}_{i-1}, \overline{X}_i^*) \dots \quad (26)$$
$$P(U_{s-1}, Y_{s-1} | \mu, \overline{U}_{s-2}, \overline{Y}_{s-2}, \overline{X}_{s-1}^*) P(U_s | \mu, \overline{U}_{s-1}, \overline{Y}_{s-1}, \overline{X}_s^*).$$

We consider a typical factor of this product ($0 < i < s$):

$$P(U_i, Y_i | \mu, \overline{U}_{i-1}, \overline{Y}_{i-1}, \overline{X}_i^*) =$$
$$P(Y_i | \mu, \overline{U}_i, \overline{Y}_{i-1}, \overline{X}_i^*) P(U_i | \mu, \overline{U}_{i-1}, \overline{Y}_{i-1}, \overline{X}_i^*) = \quad (27)$$
$$P(Y_i | i, \mu, \overline{U}_i) \Gamma_i(U_i | \overline{U}_{i-1}, \overline{Y}_{i-1}, \overline{X}_i^*).$$

The probability density Y_i is actually determined for fixed μ and $\overline{U}_i$, and the supplementary fixing of $\overline{\overline{Y}}_{i-1}$ and $\overline{\overline{X}}_i^*$ does not change it.

The second factor is Γ_i – the probability density of U_i (see [21]), which depends only on $\overline{\overline{U}}_{i-1}$, $\overline{\overline{Y}}_{i-1}$, and $\overline{\overline{X}}_i^*$. We note the fact that, in the formula for $P(Y_i)$, it depends on i.

If we substitute (27) in (26), we obtain

$$P(\overline{U}_s, \overline{Y}_{s-1} | \mu, \overline{X}_s^*) = \prod_{i=0}^{s} \Gamma_i \prod_{i=0}^{s-1} P(Y_i | i, \mu, \overline{U}_i). \quad (28)$$

Here we set

$$\Gamma_0 = P_0(U_0, X_0^*). \quad (29)$$

We now substitute (28) in (25), (25) in (24), and (24) in (23), and the expression for R_s becomes

$$R_s = \int_{\Omega(\mu, \overline{V}_s, \overline{U}_s, \overline{Y}_{s-1})} W(s, \mu, X_s^*, \overline{V}_s) P(\mu) P(\overline{V}_s | \overline{U}_s) \prod_{i=0}^{s-1} P(Y_i | i, \mu, U_i) \times \quad (30)$$
$$\prod_{i=0}^{s} \Gamma_i(U_i | \overline{U}_{i-1}, \overline{V}_{i-1}, \overline{X}_i^*) d\Omega(\mu, \overline{V}_s, \overline{U}_s, \overline{Y}_{s-1}).$$

The general risk R is given by

$$R = \sum_{s=0}^{n} R_s. \quad (31)$$

In the particular case when the object B has one input and one output, the space-time matrices in formula (30) become time-vectors, and the space vectors become scalars. The expression (30) now takes the form

$$R_s = \int_{\Omega(\mu, v_s, u_s, y_{s-1})} W(s, \mu, x_s^*, v_s) P(\mu) P(v_s | u_s) \prod_{i=0}^{s-1} P(y_i | i, \mu, u_i) \times \quad (32)$$
$$\prod_{i=0}^{s} \Gamma_i(u_i | u_{i-1}, y_{i-1}, x_i^*) d\Omega(\mu, v_s, u_s, y_{s-1}).$$

Even this expression is more general than formula (40) of the second paper of this series. Actually, W depends here not on the scalar v_s, but on the vector ν_s, and, because of this, it is necessary to take into account the probability density $P(\nu_s | u_s)$. Moreover, $P(y_i)$ depends here not on the value of u_i, but on the vector u_i, i.e., on all the "previous history" of the input to the object B.

In order to determine the optimum strategy, we consider, as in paper II, the specific risk R_n, and assume in the meanwhile that the probability densities Γ_i ($i = 0, 1, \dots, n-1$) are fixed. We set

$$\alpha_k = \alpha_k(\overline{U}_k, \overline{Y}_{k-1}, X_k^*) =$$

$$\int_{\Omega(\mu, \overline{V}_k)} W(k, \mu, X_k^*, \overline{V}_k)\ P(\mu)\ P(\overline{V}_k | \overline{U}_k) \prod_{i=0}^{k-1} P(Y_i | i, \mu, \overline{U}_i)\, d\Omega(\mu, \overline{V}_k). \tag{33}$$

For $k = 0$ we set the quantity $\prod_{i=0}^{k} P(Y_i)$ equal to one. We also set

$$\beta_k = \beta_k(\overline{U}_k, \overline{X}_k^*, \overline{Y}_{k-1}) = \prod_{i=0}^{k} \Gamma_k. \tag{34}$$

Then

$$R_n = \int_{\Omega(\overline{U}_n, \overline{Y}_{n-1})} \alpha_n(U_n, \overline{U}_{n-1}, X_n^*)\, \beta_{n-1} \Gamma_n d\Omega(\overline{U}_n, \overline{Y}_{n-1}) =$$

$$\int_{\Omega(\overline{U}_{n-1}, \overline{Y}_{n-1})} \beta_{n-1} \varkappa_n(\overline{U}_{n-1}, \overline{Y}_{n-1}, \overline{X}_n^*)\, d\Omega(\overline{U}_{n-1}, \overline{Y}_{n-1}), \tag{35}$$

where

$$\varkappa_n(\overline{U}_{n-1}, \overline{Y}_{n-1}, \overline{X}_n^*) =$$

$$\int_{\Omega(U_n)} \alpha_n(U_n, \overline{U}_{n-1}, \overline{Y}_{n-1}, X_n^*)\, \Gamma_n(U_n, \overline{U}_{n-1}, \overline{Y}_{n-1}, \overline{X}_n^*)\, d\Omega(U_n). \tag{36}$$

We now take into consideration the fact that the choice of Γ_n, as for all the probability densities, must satisfy the condition

$$\int_{\Omega(U_n)} \Gamma_n(U_n, \overline{U}_{n-1}, \overline{Y}_{n-1}, \overline{X}_n^*)\, d\Omega(U_n) = 1. \tag{37}$$

It is necessary to select the quantity Γ_n, satisfying condition (37), so that the quantity R_n is a minimum. But this latter quantity will be minimized, if, for any $\overline{U}_{n-1}$ and $\overline{Y}_{n-1}$, the quantity $\varkappa_n$ is minimized, and this will be ensured if we choose

$$\Gamma_n = \delta(U_n - U_n^*). \tag{38}$$

Here δ is the unit impulse function. The quantity U_n^* is determined by the condition

$$\gamma_n^* = \alpha_n(U_n^*, \overline{U}_{n-1}, \overline{Y}_{n-1}, X_n^*) = \min_{U_n \in \Omega(U_n)} \alpha_n(U_n, \overline{U}_{n-1}, \overline{Y}_{n-1}, X_n^*). \tag{39}$$

It is evident that

$$U_n^* = U_n^*(\overline{U}_{n-1}, \overline{Y}_{n-1}, X_n^*). \tag{40}$$

Therefore, the optimal strategy Γ_n is not random, but regular. The choice of the optimal controlling action U_n^* is given by the formulas (39) and (40).

In a similar way, when we consider the sum of the terms $R_{n-1} + R_n$, and then the sum $R_{n-2} + R_{n-1} + R_n$, etc., we can find the optimal strategies Γ_i ($i = n-1, n-2, \ldots$). A similar proof was given in section II of [1]. The result is the following: we introduce the function

$$\gamma_{n-k} = \alpha_{n-k} + \int_{\Omega(Y_{n-k})} \gamma_{n-k+1}^*\, d\Omega(Y_{n-k}), \tag{41}$$

with $\gamma_n = \alpha_n$, and

$$\gamma_{n-k}^* = (\gamma_{n-k})_{U_{n-k} = U_{n-k}^*}, \tag{42}$$

and the value of U^*_{n-k} is obtained from the condition

$$\gamma_{n-k}(U^*_{n-k}, \overline{U}_{n-k-1}, \overline{Y}_{n-k-1}, X^*_{n-k}) = \min_{U_{n-k}\in\Omega(U_{n-k})} \gamma_{n-k}(U_{n-k}, \overline{U}_{n-k-1}, \overline{Y}_{n-k-1}, X^*_{n-k}). \tag{43}$$

Then the optimal strategy Γ^*_{n-k} is given by

$$\Gamma^*_{n-k} = \delta(U_{n-k} - U^*_{n-k}), \tag{44}$$

i.e., it is regular, where U^*_{n-k} is obtained from condition (43), and is a function of $\overline{\overline{U}}_{n-k-1}$, $\overline{\overline{Y}}_{n-k-1}$, and X^*_{n-k}.

If, as in the first part of paper II of this series, the action X^*_{n-k} passes through a noisy channel before entering the control section A, then the optimal strategy becomes more complicated, since it is necessary to include a method for calculating the a posteriori probability density $P_{n-k}(X^*_{n-k})$. The quantity must be calculated by taking into account the preceding values of X^*_{n-k-i} $(i > 0)$, i.e., all the matrices $\overline{\overline{X}}^*_{n-k}$. Therefore, in this case, Γ^*_{n-k} will depend, generally speaking, on all the matrices $\overline{\overline{X}}^*_{n-k}$. In posing such a problem and result, we refer to the case when the aim of the control is not completely explicit, and this aim becomes clearer and clearer during the control process.

An Application of the Generalized Formulas

As an example of the application of the formulas we have derived, we will consider the problem of synthesizing an algorithm for optimizing the control section A for a system of automatic stabilization. The block diagram of the system is shown in Fig. 4. The controlled object B consists of a part B_1 that possesses a memory, and a part B_2 that has no memory. The equations for these parts are:

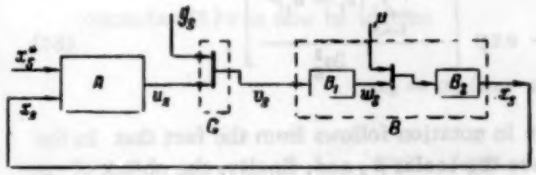

Fig. 4.

$$w_s = \sum_{k=0}^{s} a_k v_{s-k}; \qquad x_s = \mu + w_s. \tag{45}$$

Here a_k are given constants, and μ is a random quantity with a given a priori probability density $P(\mu) = P_0(\mu)$. The general equation for the object B can be written in the form

$$x_s = \mu + \sum_{k=0}^{s} a_k v_{s-k}. \tag{46}$$

The sequence of independent random variables g_s all have the same probability density $q(g_s)$. The functions $P(\mu)$ and $q(g_s)$ are given by the normal-distribution formulas

$$P(\mu) = \frac{1}{\sigma_\mu\sqrt{2\pi}} \exp\left(-\frac{\mu^2}{2\sigma_\mu^2}\right), \quad q(g_s) = \frac{1}{\sigma_g\sqrt{2\pi}} \exp\left(-\frac{g_s^2}{2\sigma_g^2}\right). \tag{47}$$

The quantity u_s is added to the noise g_s in the block G. The output of this block is

$$v_s = g_s + u_s. \tag{48}$$

We will write the specific-loss function in the form

$$W_s = (x_s - x^*_s)^2, \tag{49}$$

and the general loss function will be

$$W = \sum_{s=0}^{n} W_s = \sum_{s=0}^{n} (x_s - x^*_s)^2. \tag{50}$$

In the particular case of systems with one input and one output, from formula (33) we obtain for the function α_k the expression

$$\alpha_k = \alpha_k(u_k,\ y_{k-1},\ x_k^*) =$$

$$\int\limits_{\Omega(\mu,\ v_k)} W(k,\ \mu,\ x_k^*,\ v_k)\, P(\mu)\, P(v_k|u_k) \prod_{i=0}^{k-1} P(y_i|i,\ \mu,\ u_i)\, d\Omega(\mu,\ v_k). \tag{51}$$

In the example considered,

$$\alpha_k = \int\limits_{\Omega(\mu,\ v_k)} (\mu - x_k^* + \sum_{\rho=0}^{k} a_\rho v_{k-\rho})^2 \frac{1}{\sigma_\mu \sqrt{2\pi}} \exp\left(-\frac{\mu^2}{2\sigma_\mu^2}\right) P(v_k|u_k) \times$$

$$\prod_{i=0}^{k-1} P(y_i|i,\ \mu,\ u_i)\, d\Omega(\mu,\ v_k). \tag{52}$$

We will now find expressions for $P(v_k|u_k)$ and $P(y_i|i, \mu, u_i)$.

It follows from (48) that

$$P(v_i|u_i) = q(v_i - u_i) = \frac{1}{\sigma_g \sqrt{2\pi}} \exp\left[-\frac{(v_i - u_i)^2}{2\sigma_g^2}\right]. \tag{53}$$

From the independence of the random variables g_i ($i = 0, 1, \ldots, k$), it follows that

$$P(v_k|u_k| = \prod_{i=0}^{k} P(v_i|u_i) = \frac{1}{\sigma_g^{k+1} (2\pi)^{\frac{k+1}{2}}} \exp\left[-\frac{\sum_{i=0}^{k} (v_i - u_i)^2}{2\sigma_g^2}\right]. \tag{54}$$

We now find that $P(y_i|i, \mu, u_i) = P(x_i|\mu, u_i)$. This change in notation follows from the fact that in the example we are considering $y_i = x_i$, instead of the vector μ we have the scalar μ, and, finally, the object of control is independent of i.

It follows from (46) that

$$x_i - \mu = \sum_{\rho=0}^{i} a_\rho v_{i-\rho} = \sum_{\rho=0}^{i} \nu_\rho, \tag{55}$$

where

$$\nu_\rho = a_\rho v_{i-\rho} = a_\rho (u_{i-\rho} + g_{i-\rho}) = a_\rho u_{i-\rho} + a_\rho g_{i-\rho}. \tag{56}$$

From this it is evident that the quantity ν_ρ is normally distributed, with a mean value $a_\rho u_{i-\rho}$ and a variance $(a_\rho \sigma_g)^2$. Since $u_{i-\rho}$ and μ are taken to be fixed, and the values ν_ρ are independent for fixed $u_{i-\rho}$, it is not difficult to show that x_i is also normally distributed with a mean value

$$(x_i)_{\text{mean}} = \mu + \sum_{\rho=0}^{i} a_\rho u_{i-\rho} \tag{57}$$

and a variance

$$\sigma_i^2 = \sum_{\rho=0}^{i} a_\rho^2 \sigma_g^2 = \sigma_g^2 \sum_{\rho=0}^{i} a_\rho^2. \tag{58}$$

Therefore,

$$P(x_i|\mu,\ u_i) = \frac{1}{\sigma_i \sqrt{2\pi}} \exp\left[-\frac{\left(x_i - \mu - \sum_{\rho=0}^{i} a_\rho u_{i-\rho}\right)^2}{2\sigma_i^2}\right]. \tag{59}$$

The substitution of the expressions (54) and (59) in (52) yields

$$\alpha_k = \alpha_k(\mathbf{u}_k,\ \mathbf{x}_{k-1},\ x_k^*) = \int\limits_{\Omega(\mu,\ \mathbf{v}_k)} \left(\mu - x_k^* + \sum_{\rho=0}^{k} a_\rho v_{k-\rho}\right)^2 \frac{1}{\sigma_\mu \sqrt{2\pi}} \times$$

$$\exp\left(-\frac{\mu^2}{2\sigma_\mu^2}\right) \frac{1}{\sigma_g^{k+1}(2\pi)^{\frac{k+1}{2}}} \exp\left[-\frac{\sum_{i=0}^{k}(v_i - u_i)^2}{2\sigma_g^2}\right] \frac{1}{(2\pi)^{\frac{k}{2}}} \left(\prod_{i=0}^{k-1} \frac{1}{\sigma_i}\right) \times$$

$$\exp\left[-\sum_{i=0}^{k-1} \frac{\left(x_i - \mu - \sum_{\rho=0}^{i} a_\rho u_{i-\rho}\right)^2}{2\sigma_i^2}\right] d\Omega(\mu,\ \mathbf{v}_k). \tag{60}$$

If the object has no memory, and $a_0 = 1$, $a_\rho = 0$ $(\rho > 0)$, then it is not difficult to show that the expression becomes formula (8) of paper III of the present series.

On the basis of (58) we can write

$$\prod_{i=0}^{k-1} \sigma_i = \sigma_g^k \prod_{i=0}^{k-1} \left(\sum_{\rho=0}^{i} a_\rho^2\right)^{\frac{1}{2}} = \sigma_g^k A_{k-1} \tag{61}$$

where A_{k-1} denotes the product.

Formula (61) can now be written

$$\alpha_k = \alpha_k(\mathbf{u}_k,\ \mathbf{x}_{k-1},\ x_k^*) = \frac{1}{\sigma_\mu \sigma_g^{2k+1} A_{k-1} (2\pi)^{k+1}} \times$$

$$\int_{\mu=-\infty}^{\mu=\infty} \int_{v_0=-\infty}^{v_0=\infty} \cdots \int_{v_k=-\infty}^{v_k=\infty} \left(\mu - x_k^* + \sum_{j=0}^{k} a_j v_{k-j}\right)^2 \times$$

$$\exp\left[-\frac{\mu^2}{2\sigma_\mu^2} - \frac{\sum_{j=0}^{k}(v_j - u_j)^2}{2\sigma_g^2} - \sum_{i=0}^{k-1} \frac{\left(x_i - \mu - \sum_{\rho=0}^{i} a_\rho u_{i-\rho}\right)^2}{2\sigma_i^2}\right] d\mu\, dv_0 \ldots dv_k. \tag{62}$$

In this integral, the quantities x_k^*, x_i, and u_i are parameters. We make a change of variables, and introduce the new variables λ_j and the parameters $x_k^{(0)*}$, $x_i^{(0)}$, B_{k-1}, C_{k-1}, and D_{k-1}:

$$\lambda_j = a_{k-j}(v_j - u_j) \quad (j = 0,\ \ldots,\ k), \qquad \lambda_{k+1} = \mu - \frac{B_{k-1}}{2C_{k-1}}, \tag{63}$$

$$x_k^{(0)*} = x_k^* - \sum_{j=0}^{k} a_{k-j} u_j, \qquad x_i^{(0)} = x_i - \sum_{j=0}^{i} a_{i-j} u_j \quad (i = 0,\ \ldots,\ k-1),$$

$$B_{k-1} = \sum_{i=0}^{k-1} \frac{x_i^{(0)}}{\sigma_i^2}, \qquad C_{k-1} = \frac{1}{2}\left(\sum_{i=0}^{k-1} \frac{1}{\sigma_i^2} + \frac{1}{\sigma_\mu^2}\right) > 0,$$

$$D_{k-1} = \sum_{i=0}^{k-1} \frac{(x_i^{(0)})^2}{2\sigma_i^2} > 0, \quad E_k = \frac{B_{k-1}}{2C_{k-1}} - x_k^{(0)*}.$$

Then, after transformation, the formula (62) becomes

$$\alpha_k = \frac{\exp\left(-D_{k-1}+\frac{B_{k-1}^2}{4C_{k-1}}\right)}{\left(\prod_{j=0}^{k} a_{k-j}\right)\sigma_\mu \sigma_g^{2k+1} A_{k-1}(2\pi)^{k+1}} \int_{\lambda_0,\ldots,\lambda_{k+1}=-\infty}^{\lambda_0,\ldots,\lambda_{k+1}=\infty} \cdots \int \left(\sum_{i=0}^{k+1}\lambda_i + E_k\right)^2 \times$$

$$\exp\left(-\frac{1}{2\sigma_g^2}\sum_{i=0}^{k}\lambda_i^2 - C_{k-1}\lambda_{k+1}^2\right) d\lambda_0\, d\lambda_1 \ldots d\lambda_k\, d\lambda_{k+1} =$$

$$\frac{\exp\left(-D_{k-1}+\frac{B_{k-1}^2}{4C_{k-1}}\right)}{\left(\prod_{j=0}^{k} a_{k-j}\right)\sigma_\mu \sigma_g^{2k+1} A_{k-1}(2\pi)^{k+1}} I_k. \tag{64}$$

The integral I_k can be reduced to the following form (see [2], p. 238):

$$I_k = \frac{(2\pi)^{\frac{k+1}{2}}(\sqrt{2}\sigma_g)^{k+1}}{\sqrt{C_{k-1}}} \frac{1}{\theta}\int_{-\infty}^{\infty}(t+E_k)^2 \exp\left[-\left(\frac{t}{\theta}\right)^2\right] dt, \tag{65}$$

where

$$\theta^2 = 2\sigma_g^2(k+1) + \frac{1}{C_{k-1}}. \tag{66}$$

Since we have

$$\int_{-\infty}^{\infty}(t+E_k)^2 \exp\left[-\left(\frac{t}{\theta}\right)^2\right] dt = \theta\sqrt{\pi}\left(\frac{\theta^2}{2}+E_k^2\right), \tag{67}$$

then it follows that

$$I_k = \frac{2^{k+1}\sigma_g^{k+1}(\pi)^{\frac{k}{2}+1}}{\sqrt{C_{k-1}}}\left[\sigma_g^2(k+1)+\frac{1}{2C_{k-1}}+E_k^2\right]. \tag{68}$$

If this expression is substituted in (64), we obtain

$$\alpha_k = \frac{\exp\left(-D_{k-1}+\frac{B_{k-1}^2}{4C_{k-1}}\right)\left[\sigma_g^2(k+1)+\frac{1}{2C_{k-1}}+E_k^2\right]}{\left(\prod_{j=0}^{k} a_{k-j}\right)\sigma_\mu \sigma_g^k A_{k-1}(\pi)^{\frac{k}{2}}\sqrt{C_{k-1}}}. \tag{69}$$

In this formula, only E_k depends on u_k, since

$$E_k = \frac{B_{k-1}}{2C_{k-1}} - x_k^{(0)*} = \frac{1}{2C_{k-1}}\sum_{i=0}^{k-1}\frac{\left(x_i - \sum_{j=0}^{i} a_{i-j}u_j\right)}{\sigma_i^2} - x_k^* + \sum_{j=0}^{k} a_{k-j}u_j. \tag{70}$$

From this and (69) it follows that the minimum of α_n relative to u_n is obtained if u_n^* is such that $E_n = 0$. Therefore,

$$u_n^* = \frac{1}{a_0}\left[x_n^* - \frac{1}{2C_{n-1}}\sum_{i=0}^{n-1}\frac{\left(x_i - \sum_{j=0}^{i} a_{i-j}u_j\right)}{\sigma_i^2} - \sum_{j=0}^{n-1} a_{n-j}u_j\right] = \frac{K_n}{a_0}, \tag{71}$$

where K_n denotes the quantity in the square brackets.

The optimal strategy in the nth cycle has thus been obtained.

In the transition from n to (n − 1), we must integrate $\gamma_n^* = \alpha_n^*$ with respect to x_{n-1}, add the function α_{n-1} to the integral, and then find the value of u_{n-1}^* that minimizes the resulting expression. It is clear from (69) that for $E_n = 0$ the function α_n depends on u_{n-1}, since this quantity enters into the expressions D_{n-1} and B_{n-1}. However, when we use the substitution

$$x_{n-1} - \sum_{j=0}^{n-1} a_{n-1-j} u_j = x_{n-1}^{(0)} \tag{72}$$

and integrate with respect to the new variable $x_{n-1}^{(0)}$ in the range $(-\infty, \infty)$, we see that $\int_{-\infty}^{\infty} \alpha_n^* \, dx_{n-1}$ does not depend on u_{n-1}. Therefore, the minimizing of γ_{n-1} with respect to u_{n-1} reduces to the minimizing of α_{n-1} with respect to u_{n-1}. Similar reasoning shows that, in general, u_k^* can be obtained by minimizing α_k, and this reduces to the condition $E_k = 0$. From this we obtain the optimal strategy in any sth cycle

$$u_s^* = \frac{1}{a_s}\left[x_s^* - \frac{1}{2C_{s-1}} \sum_{i=0}^{s-1} \frac{\left(x_i - \sum_{j=0}^{i} a_{i-j} u_j\right)}{\sigma_i^2} - \sum_{j=0}^{s-1} a_{s-j} u_j\right] = \frac{K_s}{a_s}, \tag{73}$$

where K_s denotes the quantity in the square brackets.

The physical sense of the solution we have obtained becomes clearer when we note that

$$\mu = x_i - w_i = x_i - \sum_{j=0}^{i} a_{i-j} v_j =$$

$$x_i - \sum_{j=0}^{i} a_{i-j}(u_j + g_j) = \left(x_i - \sum_{j=0}^{i} a_{i-j} u_j\right) - \sum_{j=0}^{i} a_{i-j} g_j. \tag{74}$$

The last term in this expression is random, and its variance depends on i. The expression in brackets is the mean value. Thus, the second term in the formula for K_s gives the value of the random quantity μ. The various results of measuring μ enter this value with different weights, since the variance is different for different measurements.

The last term in the formula for K_s represents the mean value of the results of the previous action u_j ($j < s$), which still has an effect because of the presence of the memory in the object at the instant s. It is natural that, in the determination of u_s^*, this residue must be taken into account. Thus, all the terms of the formula (73) have a clear physical meaning.

It can be shown that when $a_\rho < a_0 \varepsilon^\rho$, where $|\varepsilon| < 1$, and for a sufficiently large value of s, the middle term in the formula for K_s reduces to

$$\frac{1}{s} \sum_{i=0}^{s-1} \left(x_i - \sum_{j=0}^{i} a_{i-j} u_j\right),$$

i.e., to the arithmetic mean of the measurements of μ.

In principle, we can extend the results we have obtained to the case of a continuous system. If, in the continuous case, the coupling between w(t) and v(t) is, for example, described by an equation for an inertial link with transfer function $(1 + p\tau_0)^{-1}$, then

$$w(t) = \int_0^t b(\tau) v(t - \tau) \, d\tau, \tag{75}$$

where

$$b(t) = \frac{1}{T_0} \exp\left(-\frac{t}{T_0}\right). \tag{76}$$

In order to make this problem discrete, we set

$$w(t) \approx \sum_{\rho=0}^{s} b(t_\rho)\, v(t - t_\rho)\, \Delta t = \sum_{\rho=0}^{s} a_\rho v(t - t_\rho) = \sum_{\rho=0}^{s} a_\rho v_{1-\rho}, \tag{77}$$

where

$$a_\rho = b(t_\rho)\, \Delta t = \frac{\Delta t}{T_0} \exp\left\{-\frac{\rho \Delta t}{T_0}\right\} \tag{78}$$

$$a_0 = \frac{\Delta t}{T_0}.$$

If we substitute the values of a_ρ in the formula (73) for the optimal strategy, let Δt tend to zero, and set $s\Delta t = t$, we could obtain in the limit the optimal strategy for the continuous case, as in the example in paper III of the series. However, as is also clear from physical considerations, such a limiting operation causes $a_0 \to 0$ and the quantity u_n^* in formula (71) to tend to infinity. The same result is obtained for the other u_s as well. But, for real physical systems, only those solutions for which the value of u_s is bounded have a meaning. We must therefore introduce into the discrete case a further condition, for example, of the type

$$|u_s| \leqslant M. \tag{79}$$

With this condition, however, the optimal strategy changes. For example, instead of (71),we must write

$$u_n^* = \frac{K_n}{a_0} \quad \text{for} \quad \left|\frac{K_n}{a_0}\right| \leqslant M, \qquad u_n^* = \operatorname{sign} \frac{K_n}{a_0} \quad \text{for} \quad \left|\frac{K_n}{a_0}\right| > M. \tag{80}$$

The investigation of this problem shows that now $\int \gamma_n^* \, dx_{n-1}$ depends on u_{n-1}, and this results in a very much more involved calculation.

SUMMARY

The basic content of this series of papers on the theory of dual control is as follows.

A. A new, very general, and practically important problem has been posed. This problem reduces, in its essentials, to that of finding an optimal method of control in an indefinite situation, with incomplete a priori information concerning the object of control (or even concerning the aim of the control), in a closed system with active accumulation of information.

B. A general method of solving this problem and certain of its generalizations was found. This method consists of a succession of alternate minimizations and integrations.

C. Examples were given, from which it followed that only in very simple cases could the solution be completed without the use of computers. In the general case, the control section must contain a very complicated computing device.

The further development in this region was considered, and the following conclusions were reached.

1. Generalizations to cases not yet investigated. Thus, for example, the general solution obtained for a fixed number n of cycles can be extended to include the case when the number of cycles is not fixed beforehand. Examples were given of this in papers III and IV. The extension to the problem of minimizing the time of search is also possible. For example, let $W_s = 0$ for $s < n$, i.e., the weight of the risk is R_n. Then, without fixing n, we can find an optimal strategy $U_s^* = U_s^*(\overline{\overline{U}}_{s-1}, \overline{\overline{Y}}_{s-1}, \overline{\overline{X}}_s^*)$, such that the number of steps n is minimized, as a result of which the risk R_n is less than, or equal to, a certain given quantity. The method of solution of this problem is based on formulas obtained for fixed n, but the general method of solution is more complicated than for fixed n.

It is also of interest to extend the results to the establishment of a regime that has properties equivalent to the consideration of a specific risk of the type

$$R = \lim_{n\to\infty} \frac{1}{n+1} \sum_{s=0}^{n} R_s. \tag{81}$$

Related to this extension is the interesting problem of finding in what cases, with an infinite number of trials, can complete information concerning the object be obtained, i.e., to obtain the limiting a posteriori probability density $P_s(\mu)$ in the form of a δ-function.

Finally, it is interesting to generalize to a continuous system. This does not present any insurmountable difficulties if we do not demand a rigorous approach. Then the method of calculating the set of functions γ_s^* ($s = 0, 1, \ldots, n$) reduces to the solution of a partial differential equation. The idea of taking such a limit exists in the literature (see, for example, [3,4]). One must, however, take into account that, in the case of digital calculating devices, the problem must again be made discrete.

2. The search for practical methods of constructing systems that approximate closely to optimal. This can be related to approximate methods of solving the equations obtained for the strictly optimal strategy by investigating particular types of systems, and establishing their degree of approximation to the optimal solution. This region of development is very important, since, in complex cases, the exact solution is inapplicable in practice because of the complicated computing devices that are necessary.

Finally, other basic problems can be posed, and these will lead to new methods of investigation, and new results.

The present series of papers has therefore described only the first necessary stage of investigations into new, very interesting, and promising regions in the theory and technique of automatic control.

LITERATURE CITED

1. A. A. Fel'dbaum, "The theory of dual control. I, II, and III," Avtomatika i Telemekhanika 21, 9, 11 (1960); 22, 1 (1961).
2. I. M. Ryzhik, Tables of Integrals, Sums, Series, and Products [in Russian] (Gostekhizdat, 1948) 2nd edition.
3. C. W. A. Merriam, III, "Class of optimum control systems," J. Franklin Inst. 267, No. 4 (April, 1959).
4. L. I. Rozonoér, "L. S. Pontryagin's maximum principal in the theory of optimal systems. I, II, and III," Avtomatika i Telemekhanika 20, Nos. 10, 11, and 12 (1959).

A TWO-CHANNEL SERVO SYSTEM WITH ANTISYMMETRIC FEEDBACK IN THE CASE OF RANDOM DISTURBANCES

A. A. Krasovskii (Moscow)

Translated from Avtomatika i Telemekhanika, Vol. 22, No. 2, pp. 143-156, February, 1961
Original article submitted May 24, 1960

The usual methods of analysis for random stationary processes in linear systems are generalized to a system with complex transfer and weight functions.

We investigate the statistical dynamics of two-dimensional systems containing a relay element in the ac channel. Structural circuits are obtained for the mathematical expectations and random components of the coordinates of such relay systems. An estimate is made of the effect of suppressing wideband noise in relay self-oscillating systems.

In [1,2] we considered the dynamics of two-dimensional linear and relay systems with antisymmetric feedback for control systems in the presence of disturbances.

The aim of the present paper is to investigate the statistical dynamics of such systems. We first of all consider linear, stationary systems with complex transfer functions, under the influence of random disturbances. The usual method of investigating stationary, random processes in linear, one-dimensional systems is easily reduced to this case.

Further attention will be concentrated on the statistical dynamics of two-channel servo systems with a relay element in an ac circuit. The basic mode of operation of such systems, relative to the mathematical expectation of the coordinates, is a self-oscillating regime.

In the case of Gauss noise at the input of the relay element, a method is indicated of determining the self-oscillation parameters of the mathematical expectation where this method uses a structural circuit for random components, and the effect of suppressing the noise in the self-oscillating relay system is estimated.

1. Linear Stationary Systems

We consider a linear, stationary, two-channel system with the block diagram shown in Fig. 1. The antisymmetric, crossover feedback is indicated here by dotted lines.

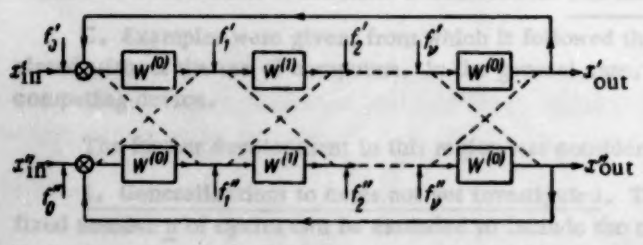

Fig. 1

The complex input to the system consists of a useful component $\bar{x}_{in} = x'_{in} + jx''_{in}$ and interference $\overline{f}_0 = f'_0 + jf''_0$. In addition to the quantities $\bar{x}_{in}$ and $\overline{f}_0$, a further ν disturbance $\overline{f}_i = f'_i + jf''_i$ $(i = 1, \ldots, \nu)$ is applied at various points of the system. All the quantities $\bar{x}_{in}$, $\overline{f}_0$, and $\overline{f}_\nu$ will be assumed to be independent, central, stationary random functions, reducible to white noise. This means that all these random functions, including the useful component of the input, can be represented in the form

$$\bar{x}_{in} = W_{in}\bar{g}_{in} \qquad \bar{f}_i = W_{fi}\bar{g}_i \qquad (i = 0, 1, \ldots, \nu), \tag{1}$$

where W_{in} and W_{f_i} are, in the general case, complex transfer functions of the so-called forming filters [3], and $\bar{g}_{in}$ and $\bar{g}_i$ are independent, centered, random functions with constant spectral densities (white noise). When we use the rules for finding the complex transfer functions linking the two-channel circuits [1], we obtain

$$\overline{\Delta x} = -\frac{1}{1+W}\bar{x}_{in} + \frac{W}{1+W}\bar{f}_0 + \sum_{i=1}^{\nu}\frac{W_i}{1+W}\bar{f}_i, \tag{2}$$

for the block diagram in Fig. 1, where $\overline{\Delta x} = x_{out} - \bar{x}_{in}$, W is the complex transfer function of the system open relative to external negative feedback, W_i is the complex transfer function from the ith input (the quantity f_i) to the output of the system (the quantity $x_{out} = x'_{out} + jx''_{out}$).

When we take into account the transfer functions of the forming filters (1), the expression for the error takes the form

$$\overline{\Delta x} = -\frac{W_{in}}{1+W}\bar{g}_{in} + \frac{WW_{f_0}}{1+W}\bar{g}_0 + \sum_{i=1}^{\nu}\frac{W_iW_{f_i}}{1+W}\bar{g}_i. \tag{3}$$

The impulse transfer (weight) function of the two-channel system for the ith input is the name we give to the reaction of this system to the action of a unit impulse at the ith input. By the action of this impulse, we mean that the δ-function acts on only one (real) channel of the system. However, the case of the simultaneous arrival of an impulse at both channels

$$\bar{f}_i = a\delta(t) + jb\delta(t)$$

can very simply be reduced to the above case, by adding an amplifying circuit with the complex transfer function a + jb. The impulse transfer function of the two-channel system is a complex function of a real variable – the time:

$$\bar{k}(t) = k'(t) + jk''(t).$$

The real part k'(t) gives the reaction at the output of the "real" channel, while the imaginary part k"(t) corresponds to the reaction at the output of the "imaginary" channel.

We call the reaction to a δ-impulse, when the forming filter is taken into account, the generalized impulse transfer (weight) function. Thus, the generalized complex-weight functions of the system we are considering correspond to the transfer functions in the expression (3):

$$\bar{k}(t) \sim -\frac{W_{in}}{1+W}, \qquad k_i(t) \sim \frac{WW_{f_i}}{1+W} \qquad (i, 0, 1, \ldots, \nu). \tag{4}$$

Either directly, or by conversion to a real variable, it is easy to see the justification of the usual representation of the outputs in terms of complex weight functions:

$$\overline{\Delta x}(t) = \int_0^{\infty}\bar{k}(\tau)\bar{g}_{in}(t-\tau)\,d\tau + \sum_{i=0}^{\nu}\int_0^{\infty}\bar{k}_i(\tau)\bar{g}_i(t-\tau)d\tau. \tag{5}$$

If we replace $j = \sqrt{-1}$ by $-j$ in the complex variables, we obtain

$$\overline{\Delta x}^*(t) = \int_0^{\infty}k^*(\tau)\,\bar{g}^*_{in}(t-\tau)\,d\tau + \sum_{i=0}^{\nu}\int_0^{\infty}\bar{k}^*_i(\tau)\bar{g}^*_i(t-\tau)\,d\tau, \tag{6}$$

where the star denotes the complex conjugate.

The mathematical expectation of the product $\bar{x}(t)\bar{x}^*(t')$, as in [4], is called the correlation function of the complex random function $\bar{x}(t)$. The variance of the centered, complex, random function $\bar{x}(t)$ is equal to $M[\bar{x}(t)\bar{x}^*(t)]$. We multiply the expressions (5) and (6), interchange the order of integration, and carry out the operation of calculating the mathematical expectation. Then, if

$$M\,[\overline{g}_{in}(t-\tau)\overline{g}^{*}_{in}(t-\tau')] = S_{in}\delta(\tau-\tau'),$$
$$M\,[\overline{g}_{i}(t-\tau)\overline{g}^{*}_{i}(t-\tau')] = S_{i}\delta(\tau-\tau'),$$
$$M\,[\overline{g}_{i}(t-\tau)\overline{g}^{*}_{q}(t-\tau')] = 0 \qquad (q \neq i),$$
$$M\,[\overline{g}_{in}(t-\tau)\overline{g}^{*}_{i}(t-\tau')] = 0,$$

where S_{in} and S_i are the spectral densities of the white noise, we obtain

$$D = M\,[\overline{\Delta x}(t)\overline{\Delta x}^{*}(t)] = S_{in}\int_0^\infty\int_0^\infty \overline{k}(\tau)\overline{k}^{*}(\tau')\,\delta(t-\tau')\,d\tau\,d\tau' +$$
$$+\sum_{i=0}^{\nu} S_i\int_0^\infty\int_0^\infty \overline{k}_i(\tau)\overline{k}_i^{*}(\tau')\,\delta(\tau-\tau')\,d\tau\,d\tau',$$

or

$$D = S_{in}I_{in} + \sum_{i=0}^{\nu} S_iI_i, \tag{7}$$

where

$$I_{in} = \int_0^\infty |\overline{k}(\tau)|^2\,d\tau, \qquad I_i = \int_0^\infty |\overline{k}_i(\tau)|^2\,d\tau$$

are the integral squares of the generalized complex weight functions.

The expression (7), and all the previous relations, are analogous to the corresponding expressions for one-dimensional (one-channel) systems, and degenerate into the latter for real weight or transfer functions (independent channels, the absence of crossover feedback).

The following geometrical interpretation of the integral-square measure of weight functions is of interest. The complex weight function $\overline{k}(t) = k'(t) + jk''(t)$, in the three-dimensional space of k', k'', and t, corresponds to a space curve (Fig. 2).

The volume of the solid of rotation formed by rotating the space curve corresponding to $\overline{k}(t)$ about the time-axis is

$$\int_0^\infty \pi\,[k'^2(t) + k''^2(t)]dt = \pi\int_0^\infty |\overline{k}(t)|^2\,dt = \pi I_{in}.$$

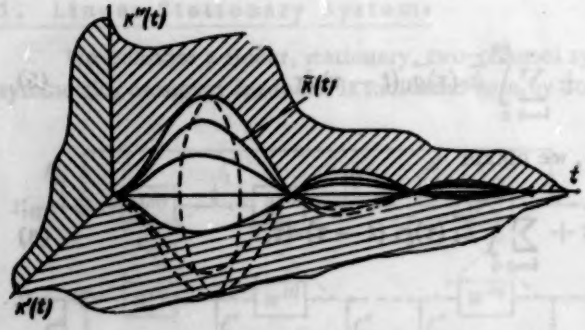

Fig. 2.

Thus, the integral measure of the complex weight function coincides, up to a factor π, with the volume of the solid of rotation swept out by the curve corresponding to this function, when it is rotated about the time axis.

The integral-square measure of a complex weight function is equal to the sum of the square measures of the real functions k' and k'', and for a system with lumped parameters (having rational-fraction transfer functions), this integral-square measure has an analytic expression in terms of these parameters [5,6].

For suitability in calculation for systems of high order, it is more convenient to determine the integral square from the corresponding frequency characteristics.

If we denote the complex transfer function corresponding to the weight function in question [for example, $\overline{k}(t) = k'(t) + jk''(t)$] by

$$\Phi(D) = \Phi'(D) + j\Phi''(D),$$

where D = d/dt, then, from known expressions, the integral measure will be

$$\int_0^\infty |\bar{k}|^2\,dt = \int_0^\infty [k'(t)]^2\,dt + \int_0^\infty [k''(t)]^2\,dt =$$

$$\frac{1}{\pi}\left[\int_0^\infty |\Phi'(j\omega)|^2\,d\omega + \int_0^\infty |\Phi''(j\omega)|^2\,d\omega\right] = \frac{1}{\pi}\int_0^\infty (P'^2 + Q'^2 + P''^2 + Q''^2)\,d\omega,$$

where P and Q are, respectively, the real and imaginary parts of the characteristic

$$\Phi'(j\omega) = P'(\omega) + jQ'(\omega), \qquad \Phi''(j\omega) = P''(\omega) + jQ''(\omega).$$

But

$$P' + jP'' = \frac{\Phi(j\omega) + \Phi(-j\omega)}{2}, \qquad Q' + jQ'' = \frac{\Phi(j\omega) - \Phi(-j\omega)}{2j}.$$

Therefore,

$$\int_0^\infty |\bar{k}|^2\,dt = \frac{1}{2\pi}\int_0^\infty \left(\left|\frac{\Phi(j\omega) + \Phi(-j\omega)}{2}\right|^2 + \left|\frac{\Phi(j\omega) - \Phi(-j\omega)}{2}\right|^2\right)d\omega =$$

$$\frac{1}{2\pi}\int_0^\infty [\,|\Phi(j\omega)|^2 + |\Phi(-j\omega)|^2\,]\,d\omega. \qquad (8)$$

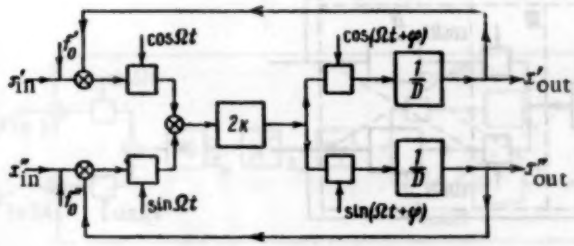

Fig. 3

If the transfer function $\Phi(D)$ is real [$\Phi''(D) = 0$], i.e., the system consists of autonomous channels, then

$$|\Phi(j\omega)|^2 + |\Phi(-j\omega)|^2 = 2|\Phi(j\omega)|^2$$

and the expression (8) takes the usual form

$$\int_0^\infty k^2\,dt = \frac{1}{\pi}\int_0^\infty |\Phi(j\omega)|^2\,d\omega.$$

Example. In Fig. 3, we show the block diagram for a linear, two-channel, servo system with modulation. If the ac channel is assumed to be noninertial for the envelope, and we neglect demodulation harmonics, the influence of which is small for a sufficiently high carrier frequency Ω [2], then the complex transfer function of a system cut off from outside feedback is $W = \frac{ke^{j\varphi}}{D}$. The phase-shift φ can be determined both from the phase-shift of the carrier signal (Fig. 3), and from the phase-shift of the carrier current in the ac channel.

If we represent the useful signal x_{in} as white sound filtered by the inertial circuit with constant time T, and assume that the interference $\overline{f_0}$ is white sound, then we obtain

$$W_{in} = \frac{1}{1+TD}, \qquad W_{f_0} = 1.$$

The expression in (3) is, in the present case,

$$\overline{\Delta x} = -\frac{D}{(1+TD)(D+ke^{j\varphi})}\,\bar{g}_{in} + \frac{ke^{j\varphi}}{D+ke^{j\varphi}}\,\bar{g}_{0}.$$

If we now separate the real and imaginary parts of the transfer function, and apply the formulas for the integral-square measure [6], we obtain

$$I_{in} = \frac{1}{2T\cos\varphi} \frac{kT + \cos\varphi}{1 + 2kT\cos\varphi + k^2T^2}, \qquad I_0 = k\frac{1 + 2\cos^2\varphi}{4\cos\varphi}$$

Thus, the variance of the lack of correlation is equal to

$$D = \frac{S_{in}}{2T\cos\varphi} \frac{kT + \cos\varphi}{1 + 2kT\cos\varphi + k^2T^2} + \frac{S_0 k}{4} \frac{1 + 2\cos^2\varphi}{\cos\varphi}.$$

Only the case when the amplification coefficient is sufficiently large is of practical interest, i.e., when $kT \gg 1$. In fact, for $kT < 1$ or $kT \approx 1$, the variance of the lack of correlation D, even for $S_0 = 0$, is of the order $S_{in}/2T$, which is of the order of the useful signal, i.e., the servo system does not fulfill its basic function.

For $kT \gg 1$, the formula simplifies to

$$D = \frac{S_{in}}{2k^2T^2\cos\varphi} + \frac{S_0 k}{4}\left(\frac{1}{\cos\varphi} + 2\cos\varphi\right).$$

It is easy to see that D has a minimum for $\varphi = 0$, $k = k_{opt} = \frac{1}{T}\sqrt{\frac{2S_{in}}{3S_0}}$ and this minimum is

$$D_{min} = \frac{1}{T}\sqrt{\frac{3}{2}S_0 S_{in}} \qquad (9)$$

For an optimal amplification coefficient, therefore, the greatest servo accuracy is obtained in the given example when there is no crossover feedback between the channels ($\varphi = 0$, see [2]).

It is interesting to note that, for an amplification coefficient greater than optimal ($k = k_{opt}$), the minimum of D occurs with a definite crossover feedback. Thus, for $k \gg k_{opt}$, the minimum occurs for $\varphi = \pi/4$.

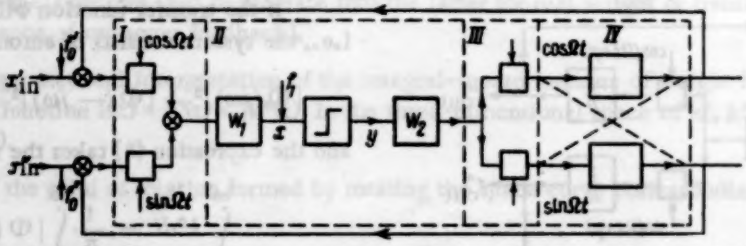

Fig. 4. I) Modulator, II) ac channel, III) demodulator, IV) two-channel part of the circuit.

2. Servo Systems with a Relay Element in the ac Channel and a Two-Channel, Very Low-Frequency Section

The rather general diagram of the system considered in [2] is shown in Fig. 4. Random, independent interference acts both on the input modulator ($\bar{f}_0$) and on the ac channel up to the relay element (f_1).

In order to study the statistical dynamics of such a system, we can apply the approximate method of statistical linearization [4,7,8]. It is obvious, however, that this method cannot be used to clarify certain delicate but important effects of nonlinear filtration. In the case of centered Gauss noise and a relay element with a perfect Z-shaped characteristic, we will make an attempt to obtain a solution to the problem that is accurate in the initial stage, and that will be subsequently simplified.

We will represent the input $\underline{x}$ to the relay element as the sum of the mathematical expectation x_M and a centered random function x_n.

The mathematical expectation of the output from the relay element for a normal distribution of x_n (Gauss noise), as is known [4], is

$$y_M = M(y) = M[\operatorname{sign}(x_M + x_n)] = 2\Phi\left(\frac{x_M}{\sqrt{D_n}}\right), \qquad (10)$$

where $\Phi(z) = \frac{1}{\sqrt{2\pi}} \int_0^z e^{-\frac{z^2}{2}}$ is the probability integral and D_n is the variance of the noise x_n.

A graph of y_M against $\frac{x_M}{\sqrt{D_n}}$ is shown in Fig. 5. In this connection, the block diagram for the mathematical expectation is shown in Fig. 6.

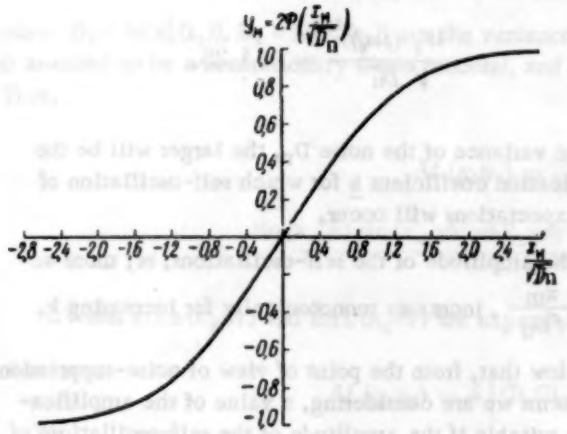

Fig. 5. The relation between the mathematical expectation of the input to the relay element and the mathematical expectation of the output, for a normal distribution.

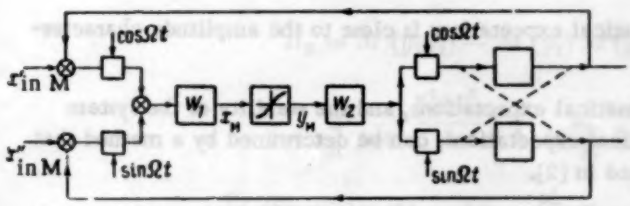

Fig. 6

From the form of the characteristic of the nonlinear element for mathematical expectations it is evident that, according to the mathematical expectancy, the system can be both self-oscillatory and nonself-oscilliatory and practically linear (for small deviations).

We show below that, from the point of view of the possibility of suppressing noise, the self-oscilliatory (for mathematical expectations) regime of operation of the system is most suitable.

The conditions for causing self-oscillation, and the corresponding parameters in the block diagram in Fig. 6 can be determined on the basis of a special form of the harmonic-balance method that has been described in [2]. It is shown in [2] that the harmonic-balance method for two-channel systems with modulation tends to become exact for very large values of the carrier frequency Ω.

For the application of the method, it is necessary to find the amplitude characteristic of the nonlinear element for mathematical expectations, i.e., the ratio of the amplitude of the first harmonic of the quantity y_M to the amplitude of the harmonic output of the quantity $x_M = x_m \sin \omega t$:

$$W_n = \frac{4}{\pi x_m} \int_0^{\pi} \Phi\left(\frac{x_m \sin\varphi}{\sqrt{D_n}}\right) \sin\varphi \, d\varphi$$

$$= \frac{4}{\pi \sqrt{D_n}\, d} \int_0^{\pi} \Phi(d \sin\varphi) \sin\varphi \, d\varphi,$$

where

$$d = \frac{x_m}{\sqrt{D_n}}.$$

A graph of the relation between $W_H\sqrt{D_n}$ and d is shown in Fig. 7. For values of d much larger than one (the amplitude of the self-oscillations will, in this case, be much larger than the mean-square noise-amplitude), we have $W_H \approx \frac{4}{\pi\sqrt{D_n}\, d}$. For $d \ll 1$, we have $d \ll 1 \qquad W_n \approx \sqrt{\frac{2}{\pi}} = 0{,}8.$

The parameters for self-oscillations of the mathematical expectations for $\bar{x}_{in,m} = 0$ (or $\bar{x}_{in,m} = \text{const}$) are, according to [2] and the block diagram shown in Fig. 6, given by the relation

$$W_1(j\omega_0) = -W_n^{-1}, \tag{11}$$

where

$$W_1(j\omega) = \frac{1}{2} W(j\omega) W_1[j(\omega + \Omega)] W_2[j(\omega + \Omega)]$$

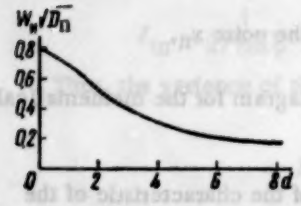

Fig. 7. The amplitude characteristic of the relay element for the mathematical expectations in the presence of Gauss noise.

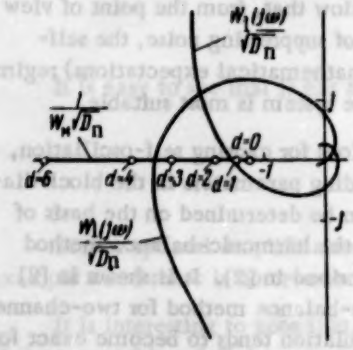

Fig. 8.

is the amplitude-phase characteristic of the linear section, and W(D) is the transfer function of the two-channel section of the circuit. The graph corresponding to this is shown in Fig. 8.

From the relation (11) and Fig. 8, it follows that self-oscillations of the mathematical expectations occur when the amplification coefficient $\underline{k}$ of the linear section exceeds a certain value k_{cr}, given by the relation

$$\frac{W_1(j\omega_0)}{\sqrt{D_n}} = -1{,}25.$$

The higher the variance of the noise D_n, the larger will be the value of the amplification coefficient $\underline{k}$ for which self-oscillation of the mathematical expectations will occur.

For $k > k_{cr}$, the amplitude of the self-oscillations, or, more accurately, the ratio $\frac{x_m}{\sqrt{D_n}}$, increases monotonically for increasing $\underline{k}$.

It is shown below that, from the point of view of noise-suppression in the nonlinear systems we are considering, a value of the amplification coefficient $\underline{k}$ is suitable if the amplitude of the self-oscillations of the mathematical expectations is essentially larger than the mean-square sound amplitude, i.e., $d \gg 1$.

In order to fulfill this condition, we must have

$$\frac{1}{W_n\sqrt{D_n}} \approx \frac{\pi}{4}\frac{x_m}{\sqrt{D_n}},$$

i.e., the amplitude of the characteristic for the mathematical expectations is close to the amplitude characteristic of the original relay element.

The stability of the self-oscillations of the mathematical expectations, and the stability of the system linearized by self-oscillations, relative to the mathematical expectations, can be determined by a method that corresponds exactly to the approximate criteria formulated in [2].

For $d \gg 2$, the transfer function of a system, linearized by self-oscillations with respect to a slowly varying mathematical expectation $\bar{x}_{in,m}$ of the input, will have the form [2]:

$$\bar{x}_{out\ M} = \frac{\frac{2}{\pi x_m}W_1(D)}{1+\frac{2}{\pi x_m}W_1(D)}\bar{x}_{in\ M}. \qquad (12)$$

We now turn to a consideration of the random components of the given system.

Following [3], we write the characteristic of a perfect relay element as

$$y = \operatorname{sign}(x_M + x_n) = \frac{2}{\pi}\int_0^\infty \frac{\sin[(x_M + x_n)u]}{u}du.$$

For brevity, we will denote the coordinates x_n, x_M, and $\underline{y}$ at time $t = t_1$ by the subscript 1, and at time $t = t_2$ by the subscript 2. Then,

$$y_1y_2 = \frac{4}{\pi^2}\int_0^\infty\int_0^\infty \frac{\sin[(x_{M1} + x_{n1})u]\sin[(x_{M2} + x_{n2})v]}{uv}dudv.$$

The mathematical expectation of the signal product in the integrand is

$$M[\sin(x_{M1}+x_{n1})u\sin(x_{M2}+x_{n2})v] =$$

$$= \frac{1}{2}e^{-\frac{D_1u^2+D_2v^2}{2}}[\cos(x_{M1}u-x_{M2}v)\,e^{R_xuv}-\cos(x_{M1}u+x_{M2}v)\,e^{-R_xuv}] =$$

$$= e^{-\frac{D_1u^2+D_2v^2}{2}}[\sin(x_{M1}u)\sin(x_{M2}v)\cosh(R_xuv)+\cos(x_{M1}u)\cos(x_{M2}v)\sinh(R_xuv)],$$

where $D_1 = M[x_n^2(t_1)]$, $D_2 = M[x_n^2(t_2)]$ are the variances of the noise at the times t_1 and t_2 (noise in the general case is assumed to be a nonstationary Gauss process), and $R_x = M[x_n(t_1)\,x_n(t_2)]$ is the correlation function of the noise. Thus,

$$M(y_1y_2) = \frac{4}{\pi^2}\int_0^\infty\int_0^\infty e^{-\frac{D_1u^2+D_2v^2}{2}}\times$$

$$\times\frac{\sin(x_{M1}u)\sin(x_{M2}v)\cosh(R_xuv)+\cos(x_{M1}u)\cos(x_{M2}v)\sinh(R_xuv)}{uv}\,dudv.$$

When $\cosh(R_x uv)$ and $\sinh(R_x uv)$ are expanded in series of powers of $R_x uv$, we obtain

$$M(y_1y_2) = 4\left[\Phi_1\Phi_2+\sum_{\nu=1}^{\infty}\frac{R_x^\nu}{\nu!}\frac{d^\nu\Phi_1}{dx_{M1}^\nu}\frac{d^\nu\Phi_2}{dx_{M2}^\nu}\right],$$

where

$$\Phi_1 = \Phi\left(\frac{x_{M1}}{\sqrt{D_1}}\right),\quad \Phi_2 = \Phi\left(\frac{x_{M2}}{\sqrt{D_2}}\right),\quad \Phi(z) = \frac{1}{\sqrt{2\pi}}\int_0^z e^{-\frac{\xi^2}{2}}\,d\xi.$$

Thus, the correlation function of the relay-element output is

$$R_y = M(y_1y_2)-M(y_1)M(y_2) = 4\sum_{\nu=1}^{\infty}\frac{R_x^\nu}{\nu!}\frac{d^\nu\Phi_1}{dx_{M1}^\nu}\frac{d^\nu\Phi_2}{dx_{M2}^\nu} =$$

$$= \frac{2}{\pi}\rho_x e^{-\frac{\xi_1^2+\xi_2^2}{2}}\left[1+\frac{\rho_x}{2!}\xi_1\xi_2+\frac{\rho_x^2}{3!}(1-\xi_1^2)(1-\xi_2^2)+\right. \tag{13}$$

$$\left.+\frac{\rho_x^3}{4!}(3\xi_1-\xi_1^3)(3\xi_2-\xi_2^3)+\frac{\rho_x^4}{5!}(3-6\xi_1^2+\xi_1^4)(3-6\xi_2^2+\xi_2^4)+\dots\right],$$

where $\rho_x = \dfrac{R_x}{\sqrt{D_1D_2}}$ is the normalized correlation function of the input, and $\xi_1 = \dfrac{x_{M1}}{\sqrt{D_1}}$, $\xi_2 = \dfrac{x_{M2}}{\sqrt{D_2}}$.

It follows from (13) that at the input of the relay element the wideband noise, i.e., the noise with a small correlation time, is transformed into wideband noise at the output of this element, modulated by some function of the mathematical expectations.

Actually, if x_n is white noise,* then $\rho_x = 1$ for $t_1 = t_2$; $\rho_x = 0$ for $t_1 \neq t_2$.

Thus, for $t_1 = t_2$ ($\xi_1 = \xi_2 = \xi = \dfrac{x_M}{\sqrt{D_n}}$),

$$R_y = D_y = \frac{2}{\pi}e^{-\xi^2}\left[1+\frac{1}{2!}\xi^2+\frac{1}{3!}(1-\xi^2)^2+\frac{1}{4!}(3\xi-\xi^3)^2+\dots\right] \tag{14}$$

and $R_y = 0$ for $t_1 \neq t_2$.

*The calculations in connection with white noise are of a formal character. A rigorous proof of the relations we have given can be obtained by applying a limiting process (letting the correlation time tend to zero) for noise having a finite variance.

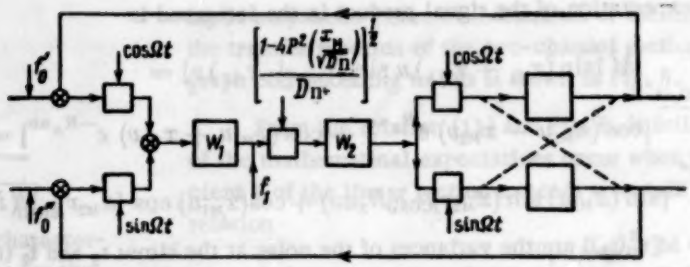

Fig. 9

It can be shown that

$$1-4\Phi^2(\xi)=\frac{2}{\pi}e^{-\xi^2}\left[1+\frac{1}{2!}\xi^2+\frac{1}{3!}(1-\xi^2)^2+\frac{1}{4!}(3\xi-\xi^3)^2+\ldots\right].$$

Thus, the correlation function of the output from the relay element, when the input is effected by white sound, can be written

$$R_y=\rho_x[1-4\Phi^2(\xi)]=R_x\frac{1-4\Phi^2\left(\frac{x_M}{\sqrt{D_n}}\right)}{D_n}. \tag{15}$$

On the other hand, if the white noise passes through a linear element with a variable amplification coefficient k(t), then

$$R_y=R_xk^2(t). \tag{16}$$

A comparison of (15) and (16) shows that the passage of white noise through a relay element is similar to the passage of this noise through a linear element* with, in general, a variable amplification coefficient:

$$k(t)=k(x_M,D_n)=\sqrt{\frac{1-4\Phi^2\left(\frac{x_M}{\sqrt{D_n}}\right)}{D_n}}.$$

Such an element can be considered in the same way as a modulator, i.e., a multiplication link, at one input of which arrives x_n, and at the other the quantity k(t).

We mention that not only for white noise, but also for any Gauss noise, the variance of the output from the relay element will be

$$D_y=D_n\frac{1-4\Phi^2\left(\frac{x_M}{\sqrt{D_n}}\right)}{D_n}=1-4\Phi^2\left(\frac{x_M}{D_n}\right). \tag{17}$$

Thus, from the point of view of the variance, any Gauss noise is transformed in the relay element in the same way as in a multiplying unit with coefficient k(t).

Corresponding to the above description, the equivalent block diagram of the system we are considering for random component coordinates is of the form shown in Fig. 9.

This setup accurately reflects the statistical dynamics of the system with white noise at the input of the relay element, and is approximate for the case of arbitrary Gauss noise (it represents accurately only the transformation of the variance in the nonlinear element).

---

*Since the amplification coefficient k depends on D_n as well as on $x_m(t)$, the element in question can only conventionally be called linear.

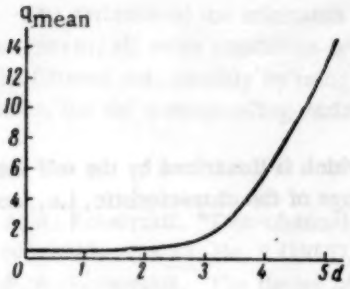

Fig. 10. Dependence of the mean noise-suppression coefficient on the ratio of the amplitude of self-oscillations to the mean-square noise.

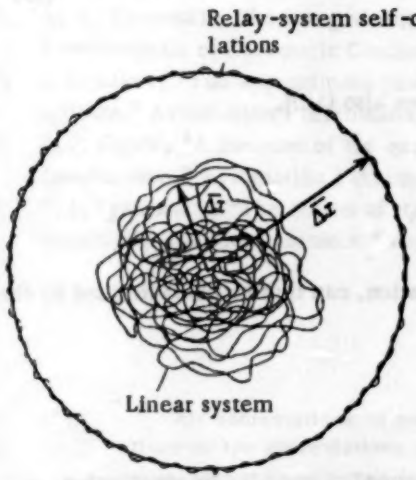

Fig. 11. An illustration of the effect of noise suppression on the self-oscillation in a relay system.

Strictly speaking, Gauss and white noise at the input of the relay element can occur only in the special case when the external noise f_1 and f_0 is of a type not usually occurring in practice. The random component x_n of the signal at the input of the relay element actually includes not only the external noise, but also the random component of the preceding closed circuit, i.e., the component at the input due to the feedback.

Therefore, even if the external noise is white, the quantity x_n contains a component that has been filtered in the inertial part of the system, and is not white noise. Similarly, even if the external noise has a normal distribution, the distribution at the output of the relay element is not normal, and the noncorrelation signal contains a non-Gauss component.

In its passage through the inertial, linear part of the system, however, wideband noise is, on the one hand, weakened and, on the other, "normalized" [9]. This is the weighting basis for the practical application of the idealization considered for the processes.

The block diagram for random components (Fig. 9), generally speaking, must be considered at the same time as the block diagram for mathematical expectations (Fig. 6). In the simultaneous consideration of these block diagrams, it is convenient to use the method of successive approximations. Thus, we start with a rough value of the noise variance at the input of the relay element, this value being obtained from the characteristics of the external noise. We then determine the mathematical expectation, in particular the self-oscillation parameters in the scheme in Fig. 6. When we have obtained x_M, we use an approximate value of D_n to obtain the amplification coefficient

$$D_n^{-\frac{1}{2}}\left[1-4\Phi^2\left(\frac{x_M}{\sqrt{D_n}}\right)\right]^{\frac{1}{2}}$$

in the equivalent scheme for random components (Fig. 9) and, by analyzing the statistical dynamics of this scheme, to determine a more accurate value of D_n. This improved approximation for D_n is used to obtain new values of the self-oscillation parameters for the mathematical expectation; we again turn to the equivalent scheme for the random components, etc.

The convergence of this successive-approximation process is usually rapid enough so that the determination of one or two values of D_n and x_M is sufficient.

It is evident from Fig. 9 that the investigation of the statistical dynamics for the case

$$k=D_n^{-\frac{1}{2}}\left[1-4\Phi^2\left(\frac{x_M}{\sqrt{D_n}}\right)\right]^{\frac{1}{2}}=\text{const}$$

can be carried out by using the usual method described in the first part of this paper.

For the case k = var there is a supplementary modulation, and the processes are nonsteady. A complete investigation demands a special method that is beyond the range of the present work. A rough estimate of the important effect of sound suppression in a self-oscillating relay system can, however, be carried out quite simply by obtaining the signal-to-noise ratio at the input and output of the relay element.

In the self-oscillating system, $x_M = x_m \sin \omega t$, and the noise variance at the relay-element input is

$$D_v = 1 - 4\Phi^2(d \sin \omega t), \qquad (18)$$

where

$$d = \frac{x_m}{\sqrt{D_n}}.$$

On the other hand, the amplification coefficient of the relay circuit (which is linearized by the self-oscillations) for the useful component is equal to the mean value of the rate of change of the characteristic, i.e., according to (10) it is

$$\frac{2}{\pi}\frac{2}{\sqrt{D_n}}\int_0^{\frac{\pi}{2}} \Phi'\left(\frac{x_m \sin\varphi}{\sqrt{D_n}}\right) d\varphi.$$

Thus,

$$y_s = \frac{4}{\pi x_m}\Phi(d)\, x_s, \tag{19}$$

where x_s and y_s are the useful signals at the input and output.

For $d > 2$, $2\Phi(d) \approx 1$, and the amplification coefficient is $2/\pi x_m$ [see also (12)].

It follows from (18) and (19) that

$$\frac{y_s}{\sqrt{D_y}} = \frac{4\Phi(d)}{\pi d\sqrt{1-4\Phi^2(d\sin\omega t)}}\frac{x_s}{\sqrt{D_n}}.$$

Noise suppression in the relay element, in the presence of self-oscillation, can thus be characterized by the coefficient

$$q = \frac{4\Phi(d)}{\pi d\sqrt{1-4\Phi^2(d\sin\omega t)}}.$$

For $d = \frac{x_m}{\sqrt{D_n}} = \text{const}$, q is a periodic function of the time, and it is natural to consider its mean value

$$q_{mean} = \frac{2}{\pi}\int_0^{\frac{\pi}{2}} q\, d\varphi = \frac{8\Phi(d)}{\pi^2 d}\int_0^{\frac{\pi}{2}} \frac{d\varphi}{\sqrt{1-4\Phi^2(d\sin\varphi)}}.$$

The relation between the mean value of the noise-suppression coefficient q_{mean} and the ratio d is shown in Fig. 10. It is evident from this graph that, for $d < 2{,}8$, the mean noise-suppression coefficient is less than one, i.e., when the ratio of the self-oscillation amplitude to the mean-square noise at the relay-element input is small, there is no increase, but a certain decrease, in the signal-to-noise ratio in this element. On the other hand, for $d > 3$, there is a sharp increase in the sound-suppression coefficient and in the signal-to-noise ratio at the relay-element output. For $d \gg 1$, the coefficient has the asymptotic representation

$$q_{mean} \approx 0{,}85\, d^{-\frac{5}{2}} e^{\frac{d^2}{4}},$$

and this shows that q_{mean} increases more rapidly for larger values of d.

Although noise suppression in the relay element occurs only when the amplitude of the self-oscillations is appreciably greater than the mean-square noise, this effect can be practically useful in the systems we are considering. The self-oscillations have, in fact, a strictly determined frequency, and can be filtered out or compensated for in a supplementary device without any noticeable worsening of the dynamic properties of the whole system.

The effect of noise suppression in a self-oscillating relay system is shown in Fig. 11. Particular realizations are shown here of the time-curve for the mismatch Δx for a constant input $\bar{x}_{in} = \text{const}$ in the case of a linear system, and also in the case of a self-oscillating relay system.

The variance of the mismatch in the case of the self-oscillating system is much less than in the case of the linear system, all other conditions being the same. The output component corresponding to the self-oscillations can be filtered out, possibly by using a wavetrap. When the input varies slowly, the center of the time-curve also varies, but the corresponding variance remains the same.

LITERATURE CITED

1. A. A. Krasovskii, "Two-channel automatic-control systems with antisymmetric coupling," Avtomatika i telemekhanika 18, No. 2 (1957).
2. A. A. Krasovskii, "The theory of two-channel servo systems with a relay element and an ac circuit," Avtomatika i telemekhanika 21, No. 9 (1960).
3. G. H. Lining and R. G. Battin, Random Processes in Problems of Automatic Control [Russian translation] (IL, 1958).
4. V. S. Pugachev, The Theory of Random Functions and Its Application in Problems of Automatic Control [in Russian] (Gostekhizdat, 1957).
5. H. James, N. Nicols, and R. Phillips, The Theory of Servo Systems [Russian translation] (IL, 1951).
6. A. A. Krasovskii, The integral-square measure of the effectiveness of control processes," Collection: The Fundamentals of Automatic Control [in Russian] (Mashgiz, 1954).
7. I. Kazakov, "The approximate probability analysis of the precision of operation of essentially nonlinear systems," Avtomatika i telemekhanica 17, No. 5 (1956).
8. E. P. Popov, "A measure of the quality of nonlinear automatic systems in the presence of random interference," Avtomatika i telemekhanika 20, No. 10 (1959).
9. F. I. Pyatintskii, "The action of stationary random processes on a system of automatic control containing an essentially nonlinear element," Avtomatika i telemekhanika 21, No. 4 (1960).

All abbreviations of periodicals in the above bibliography are letter-by-letter transliterations of the abbreviations as given in the original Russian journal. *Some or all of this periodical literature may well be available in English translation.* A complete list of the cover-to-cover English translations appears at the back of this issue.

OPTIMUM SERVO DRIVE WITH TWO CONTROL PARAMETERS

A. E. Bor-Ramenskii and Sung Chien (Moscow)

Translated from Avtomatika i Telemekhanika, Vol. 22, No. 2, pp. 157-170, February, 1961
Original article submitted May 24, 1960

A method of synthesis is described for a servoelectric drive, optimal in speed of action, that is based on the maximum principle developed by L. S. Pontryagin and his associates in [1,2]. A dc motor with two controlled voltages is taken as the actuating element. These parameters are the voltage in the rotor circuit and the exciting voltage. The results obtained from an experimental model are given, where this model was constructed from a dynamoelectric amplifier and a 1-watt dc motor.

In [8], on the basis of the maximum principle in optimal control processes developed by L. S. Pontryagin and his associates, the problem was investigated of the control, optimal in rapidity of action, in an electric servo drive with an electrodynamic amplifier and a dc motor. In the paper referred to, the problem was also solved of the synthesis of optimal control for a simplified system, the motion of which was described by double controls of the first order. In the present paper, we investigate the solution of the problem of synthesis for a system the same as this, except for the fact that the inertia in the EDA is taken into account. In this case, the motion is described by three differential equations of the first order with two controlling parameters: the voltage in the controlling winding of the EDA, and the voltage in the exciting coil of the motor. Using such a theoretical synthesis, we have built an operating model of a real machine with a power of 1 kw. The results of experiment have shown that this system has, during the transitional process, a great advantage over those at present in use. The transitional process in the system developed is close to optimal.

For convenience in what follows, we will use a notation that is not the same as that used in [8].

1. The Equations of Motion

We consider an electrical servo drive with an electrodynamic amplifier (EDA) and a dc motor (Fig. 1). The motion of the closed system can be described by the following set of differential equations:

$$\frac{dA}{dt} = \xi\Omega, \qquad J\frac{d\Omega}{dt} = C(I_e) I_e I_r + M_{ct}, \qquad E_r - C_u(I_e) I_e = I_r R_r$$
$$T_1 \frac{dI_c}{dt} + I_c = k_1 U_1, \qquad T_2 \frac{dI_e}{dt} + I_e = k_2 U_2, \qquad T_3 \frac{dE_r}{dt} + E_r = k_3 I_c \qquad (1) \qquad (1)$$

Here A is the angle of rotation of the object of control, Ω is the rate of rotation of the motor, I_r and I_e are the current in the rotor and excitation winding, respectively, I_c is the current in the control winding of the EDA, E_r is the voltage at the EDA output, U_1 is the voltage at the control coil of the EDA, U_2 is the voltage of the exciting coil of the motor. The variable coefficient $C(I_e)$ characterizes the strength of the magnetic current, and is obtained experimentally.

We made the following assumptions: The static moment is small in comparison with the inertial load, the time constant T_1 is small in comparison with T_3 (for the EDA-12 that we used, $T_1 = 0.1$ sec, $T_3 = 0.7$ sec), the time constant T_2 is also small for the combination of the excitation winding and the tube source ($T_2 = 0.02$ sec). With these assumptions, the system of equations (1) can be simplified and reduced to the following dimensionless form:

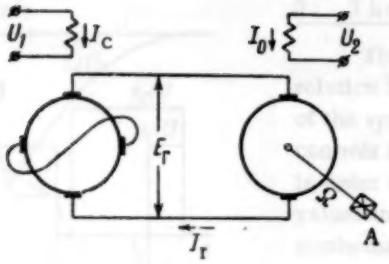

Fig. 1.

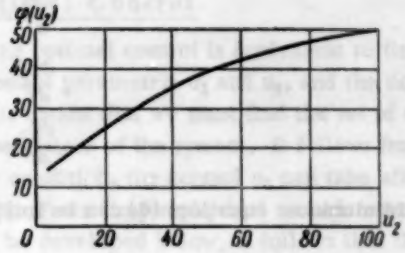

Fig. 2.

$$\frac{d\alpha}{dt} = \lambda\omega,$$

$$\frac{d\omega}{dt} = -\mu C(i_e)\, i_e e_\Gamma + \eta C^2(i_e)\, i_e^2 \omega, \qquad (2)$$

$$\frac{de_\Gamma}{dt} = -\rho e_\Gamma + \rho u_1.$$

Here α, ω, and e_Γ are dimensionless variables corresponding to A, Ω, and E_Γ; λ, μ, η, and ρ are constant coefficients, and

$$i_e = \frac{Ie}{m_{I_e}}, \qquad u_1 = \frac{U_1}{m_{U_1}}.$$

Let the arbitrary stepped signal g_0 arrive at the input. We introduce new coordinates:

$$x_1 = g_0 - \alpha, \qquad x_2 = \frac{dx_1}{dt} = -\lambda\omega, \qquad x_3 = -e_\Gamma, \qquad i_e = u_2. \qquad (3)$$

In these coordinates, the system of equations (2) can be written

$$\frac{dx_1}{dt} = x_2,$$

$$\frac{dx_2}{dt} = \beta\varphi(u_2)\, x_3 - \eta\varphi^2(u_2)\, x_2, \qquad (4)$$

$$\frac{dx_3}{dt} = -\rho x_3 - \rho u_1,$$

where $\varphi(u_2) = C(u_2)u_2$.

The parameters for the EDA and the motor used in the construction of the experimental servo system had the following numerical values:

$$\beta = 4{,}2 \cdot 10^{-3}, \qquad \eta = 1{,}55 \cdot 10^{-3}, \qquad \rho = 5{,}55.$$

The variable coefficient $\varphi(u_2) = C(u_2)u_2$, determined experimentally, is shown in Fig. 2.

2. Optimal Control

For the system of equations (4), we will seek the optimal control $u_1(t)$ and $u_2(t)$ for an arbitrary initial mismatch. For the controls u_1 and u_2, corresponding to the rated data, the following restrictions must be applied:

$$|u_1| \leqslant 120, \qquad 16{,}7 \leqslant u_2 \leqslant 100. \qquad (5)$$

For the system (4) with the limitations (5), we pose the problem of optimal control: Let any initial state of the system, defined by the values $x_1(0)$, $x_2(0)$, $x_3(0)$, be given. We wish to find the controls $u_1(t)$ and $u_2(t)$ satisfying the conditions (5), which will lead the system to an equilibrium position in the shortest possible time. According to the theory of the maximum principle [1], we make up a control system related to (4) for the vector-function ψ with components $\psi_1(t)$, $\psi_2(t)$, and $\psi_3(t)$:

$$\frac{d\psi_1}{dt} = 0,$$

$$\frac{d\psi_2}{dt} = -\psi_1 + \eta\varphi^2(u_2)\,\psi_2, \tag{6}$$

$$\frac{d\psi_3}{dt} = -\beta\varphi(u_2)\,\psi_2 + \rho\psi_3.$$

The simultaneous equations (6) can be integrated directly:

$$\psi_1 = \psi_{10} = \text{const},$$

$$\psi_2(t) = e^{\eta\int_0^t \varphi^2[u_2(\tau)]d\tau}\left(\psi_{20} - \psi_{10}\int_0^t e^{-\eta\int_0^\tau \varphi^2[u_2(\lambda)]d\lambda}\,d\tau\right),$$

$$\psi_3(t) = e^{\rho t}\left(\psi_{30} - \beta\int_0^t \varphi(u_2)\;\psi_2(\tau)\,e^{\rho\tau}d\tau\right) \tag{7}$$

We also form the Hamiltonian

$$H(x, \psi, u) = x_2\psi_1 + \psi_2[\beta\varphi(u_2)\,x_3 - \eta\varphi^2(u_2)\,x_2] + \psi_3[-\rho x_3 - \rho u_1] =$$
$$= G(x_2, x_3, \psi_1, \psi_3) + \psi_2[\beta\varphi(u_2)\,x_3 - \eta\varphi^2(u_2)\,x_2] - \rho\psi_3(t)\,u_1,$$

where

$$G(x_2, x_3, \psi_1, \psi_3) = x_2\psi_1(t) - \rho x_3\psi_3(t).$$

According to the maximum principle, the optimal control at any instant of time, given by $u_1(t)$ and $u_2(t)$, yields the maximum Hamiltonian H for all possible values of u_1 and u_2, i.e.,

$$H(x(t), \psi(t), u(t)) = \max_{\substack{|u_1|\leq 120\\ 16.7\leq u_2\leq 100}} \{G(x, \psi) + \psi_2[\beta\varphi\;(u_2)\,x_3 - \eta x_2\varphi^2(u_2)] - \rho\psi_3(t)\,u_1\}. \tag{8}$$

It follows from the condition (8) that the optimal control described by $u_1(t)$ must have the form

$$u_1(t) = -120\,\text{sign}\,\psi_3(t).$$

We note that the function $\psi_3(t)$, for values of the coefficients ψ_{10}, ψ_{20}, and ψ_{30} not identically equal to zero, differs from zero, and changes sign, in general, not more than twice. Therefore, the optimal control $u_1(t)$, in general, consists of three intervals, in each of which it maintains one of two limiting values, and changes sign in neighboring intervals.

The optimal control $u_2(t)$ is determined from the condition for the maximum of the expression ΔH:

$$\Delta H = \max_{u_2} \psi_2(t)\,[\beta\varphi(u_2)\,x_3 - \eta\varphi^2(u_2)\,x_2].$$

It is obvious that the optimal control u_2 depends here on not only the sign of $\psi_2(t)$, but also on the values of the coordinates x_2 and x_3. We rewrite this condition in the form

$$\Delta H = \max_{u_2} \psi_2(t)\,\eta x_2\left[\left(\varphi(u_2) - \frac{\beta}{2\eta}\frac{x_3}{x_2}\right)^2 - \left(\frac{\beta x_3}{2\eta x_2}\right)^2\right]. \tag{9}$$

The formula (9) shows that the optimal control $u_2(t)$ must be such that the expression in the first set of round brackets has a maximum or minimum value depending on the sign of the product $x_2\psi_2(t)$. In addition, $u_2(t)$ must satisfy the limitations (5).

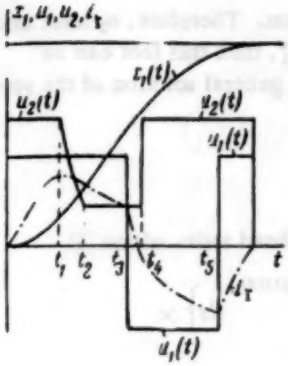

Fig. 3.

3. The Synthesis of Optimal Control

The problem of synthesizing optimal control is equivalent to finding the relation between the optimal-control parameters u_1 and u_2, and the coordinates of the system x_1, x_2, and x_3. This means that we must find the set of optimal controls for all possible initial conditions of the system. It follows from (9) that, in order to satisfy the maximum condition, the control u_2 can take all possible values in the segment [16.7; 100]. From simple physical considerations, and mathematical analysis that will be developed below, it follows that the character of the transitional process can be represented in the form shown in Fig. 3. It is evident that the last part of the optimal trajectory is a braking section, and the value of u_2 (the current in the excitation winding of the motor), must be a maximum. Then the last part of the optimal trajectory can be calculated as follows. We replace t by $-\tau$ in the equations (4), and consider the solution of these equations in inverse form. It can be shown that all the optimal trajectories have initial parts consisting of two curves starting at the origin for $u_1 = +120$ and $u_1 = -120$, respectively. We will denote these curves by L_1^+ and L_1^-. They are given by parametric equations obtained as the solutions of (4), with t replaced by $-\tau$, and with zero initial conditions.

For L_1^+ we have (for $u_1 = 120$ and $u_2 = u_{2\max} = 100$),

$$\begin{aligned} x_1(\tau) &= 2{,}34\,(e^{5{,}55\tau} - 1) - 5{,}7\,(e^{3{,}56\tau} - 1) + 7{,}2\tau, \\ x_2(\tau) &= -13\,(e^{5{,}55\tau} - e^{3{,}65\tau}) - 7{,}2\,(1 - e^{3{,}56\tau}), \\ x_3(\tau) &= 120\,(e^{5{,}55\tau} - 1). \end{aligned} \tag{10}$$

The other curve L_1^- is obtained similarly (for $u_1 = -120$, $u_2 = u_{2\max} = 48$):

$$\begin{aligned} x_1(\tau) &= -120\,(e^{5{,}55\tau} - 1), \\ x_2(\tau) &= 13{,}0\,(e^{5{,}55\tau} - e^{3{,}56\tau}) + 7{,}2\,(1 - e^{3{,}56\tau}). \\ x_3(\tau) &= -120\,(e^{5{,}55\tau} - 1). \end{aligned} \tag{11}$$

The curves L_1^+ and L_2^- are antisymmetric, and they can be obtained one from the other by an antisymmetric mapping.

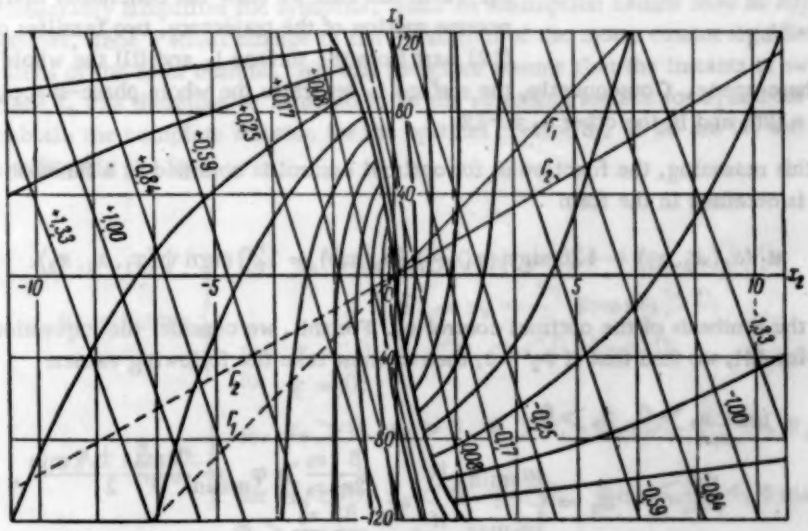

Fig. 4.

The part of the trajectory preceding the last part is also evidently a braking section. Therefore, u_2 must also take a maximum value. Since all optimal trajectories must end on the curves L_1^+ and L_1^-, then this fact can be used as initial conditions for obtaining the second-last sections of the trajectories. The general solution of the system (4) for arbitrary initial conditions, when t is replaced by $-\tau$, is:

$$x_1(\tau) = -\int_0^\tau x_2(s)\,ds + x_{10},$$

$$x_2(\tau) = \left\{ x_{20} - \beta \int_0^\tau \varphi(u_2(s)) \left[x_{30} e^{5,55s} + u_1 (e^{5,55s} - 1) \right] e^{-\eta \int_0^s \varphi^2(u_2(\lambda))\,d\lambda} ds \right\} \times$$

$$\times\, e^{\eta \int_0^\tau \varphi^2(u_2(s))\,ds},$$

$$x_3(\tau) = x_{30} e^{5,55\tau} + u_1 (e^{5,55\tau} - 1). \qquad (12)$$

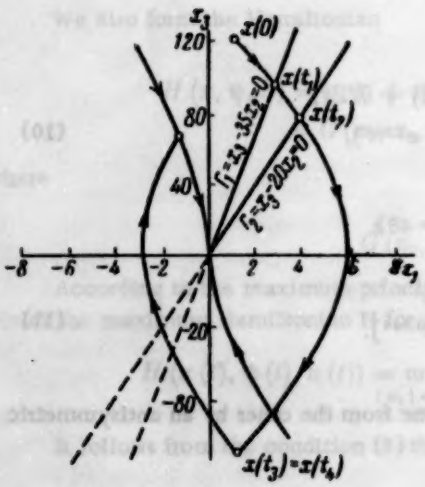

Fig. 5.

If the point (x_{10}, x_{20}, x_{30}) passes along the whole length of L_1^+ and L_1^- with control $u_1 = -120$ and $u_1 = +120$, then we obtain a certain surface L_2, on one-half of which $u_1 = -120$, and on the other half of which $u_1 = +120$. We denote these partial surfaces by L_2^+ and L_2^-. The projection of the surface L_2 on the x_2x_3-plane, obtained from the tabulated results for the solution (12), is shown in Fig. 4, in which the heavy lines show optimal trajectories, and the fine lines are lines of equal value of the surface L_2 as functions of the two variables x_2 and x_3. Analytically, the equation of this surface can be written as

$$\psi(x_1, x_2, x_3) = x_1 - f(x_2, x_3) = 0. \qquad (13)$$

The numerical values of the function $f(x_2, x_3)$ can be reduced to tabular form. It is therefore evident that the second-last and last parts of any optimal trajectory belong to the surface L_2. From this fact we draw the conclusion that, if we consider the reverse motion of the trajectory, two families of integral curves (12) start from the surface L_2 and fill the whole of the remaining three-dimensional phase-space. Consequently, the surface L_2 separates the whole phase-space into two half-spaces, in one of which $u_1 = +120$, and in the other $u_1 = -120$.

As a result of this reasoning, the function u_1 for optimal control is obtained as a function of the coordinates. The optimal control is obtained in the form

$$u_1(x_1, x_2, x_3) = 120 \operatorname{sign}(x_1 - f(x_2, x_3)) = 120 \operatorname{sign} \psi(x_1, x_2, x_3). \qquad (14)$$

We now begin the synthesis of the optimal control u_2. For this, we consider the expression (9). From the maximum condition for ΔH, we find that if $\psi_2 > 0$, then u_2 must take the following values:

for $x_2 > 0,\ x_3 > 0$

$$u_2 = \begin{cases} u_{2\min}, & \text{if} \quad \dfrac{\beta}{2\eta} \dfrac{x_3}{x_2} \geqslant \varphi_{\text{mean}} \dfrac{\varphi_{\max} + \varphi_{\min}}{2}, \\ u_{2\max}, & \text{if} \quad \dfrac{\beta}{2h} \dfrac{x_3}{x_2} < \varphi_{\text{mean}} \end{cases}$$

for $x_2 > 0,\ x_3 < 0$

$$u_2 = u_{2\max}$$

for $x_2 < 0,\ x_3 > 0$

$$u_2 = u_{2\min}$$
$$\text{for} \quad x_2 < 0, \; x_3 < 0$$

$$u_2 = \begin{cases} u_{2\max} & \text{if} \quad \dfrac{\beta}{2\eta}\dfrac{x_3}{x_2} \geqslant \varphi_{\max} \\ \dfrac{\beta}{2\eta}\dfrac{x_3}{x_2}, & \text{if} \quad \varphi_{\min} \leqslant \dfrac{\beta}{2\eta}\dfrac{x_3}{x_2} < \varphi_{\max} \\ u_{2\min} & \text{if} \quad \dfrac{\beta}{2\eta}\dfrac{x_3}{x_2} \leqslant \varphi_{\min} \end{cases}$$

If, on the other hand, $\psi_2 < 0$, then u_2 must be given by:

$$\text{for} \quad x_2 > 0, \; x_3 > 0$$

$$u_2 = \begin{cases} u_{2\max} & \text{if} \quad \dfrac{\beta}{2\eta}\dfrac{x_3}{x_2} \geqslant \varphi_{\text{mean}} \\ \dfrac{\beta}{2\eta}\dfrac{x_3}{x_2}, & \text{if} \quad \varphi_{\min} < \dfrac{\beta}{2\eta}\dfrac{x_3}{x_2} \leqslant \varphi_{\max} \\ u_{2\min} & \text{if} \quad \dfrac{\beta}{2\eta}\dfrac{x_3}{x_2} < \varphi_{\min} \end{cases}$$

$$\text{for} \quad x_2 < 0, \; x_3 > 0$$
$$u_2 = u_{2\min}$$
$$\text{for} \quad x_3 > 0, \; x_3 < 0$$
$$u_2 = u_{2\max}$$
$$\text{for} \quad x_2 < 0, \; x_3 < 0$$

$$u_2 = \begin{cases} u_{2\min} & \text{if} \quad \dfrac{\beta}{2\eta}\dfrac{x_3}{x_2} \geqslant \varphi_{\text{mean}} \\ u_{2\max} & \text{if} \quad \dfrac{\beta}{2\eta}\dfrac{x_3}{x_2} < \varphi_{\text{mean}}. \end{cases} \qquad (15)$$

According to the above reasoning, the phase space is broken up into a series of regions, in each of which u_2 takes one or other of the values in (15). Since the distribution of signs for the function ψ_2 in the phase space is unknown, the condition (15) that arises from the maximum principle does not yield all the information needed to determine the optimal control. In order to make the law of control u_2 more precise, we need either an exact solution of the system of equations (1) and (6) with the conditions (15), or certain supplementary assumptions concerning physical considerations and some simplifications. We will consider the curves $u_1(t)$ and $u_2(t)$ in Fig. 3. We will assume that t_3 and t_4 differ by only a small amount, and that the interval between them can be neglected. This assumption considerably simplifies the synthesis. Such an assumption cannot lead to any great divergence of the process from optimal, since a small change in the excitation of the motor cannot significantly alter the trajectory for small values of the rotor current. We will therefore assume that the instants of switching t_3 and t_4 are the same. The surface l_2 can therefore be assumed to be the switching surface for u_1 and for u_2. With these assumptions, we can obtain the complete solution for the optimal control u_2. If we use (9) and (14), then the conditions (15) can be written in the form

$$u_2 = u_{2\max} \begin{cases} \text{for} \quad x_2 > 0, \; x_3 > 0, \; \psi = x_1 - f(x_2, x_3) > 0, \\ \qquad\qquad \Gamma_1 = x_3 - \dfrac{2\eta}{\beta}\varphi_{\max} x_2 > 0; \\ \text{for} \quad x_2 < 0, \; x_3 < 0, \; \psi < 0, \; \Gamma_1 < 0; \\ \text{for} \quad \psi = 0; \end{cases}$$

$$u_2 = \frac{\beta}{2\eta}\frac{x_3}{x_2} \begin{cases} \text{for} \quad x_2 > 0, \; x_3 > 0, \; \psi > 0, \quad \varphi_{\min} < \dfrac{\beta x_3}{2\eta x_2} \leqslant \varphi_{\max} \\ \text{for} \quad x_2 < 0, \; x_3 < 0, \; \psi < 0, \quad \varphi_{\min} \leqslant \dfrac{\beta x_3}{2\eta x_2} \leqslant \varphi_{\max} \end{cases}$$

$$u_2 = u_{2\min} \begin{cases} \text{for} \quad \Gamma_2 = x_3 - \dfrac{2\eta}{\beta} x_2 < 0, \quad \psi > 0; \\ \text{for} \quad \Gamma_2 > 0, \quad \psi < 0, \end{cases} \qquad (16)$$

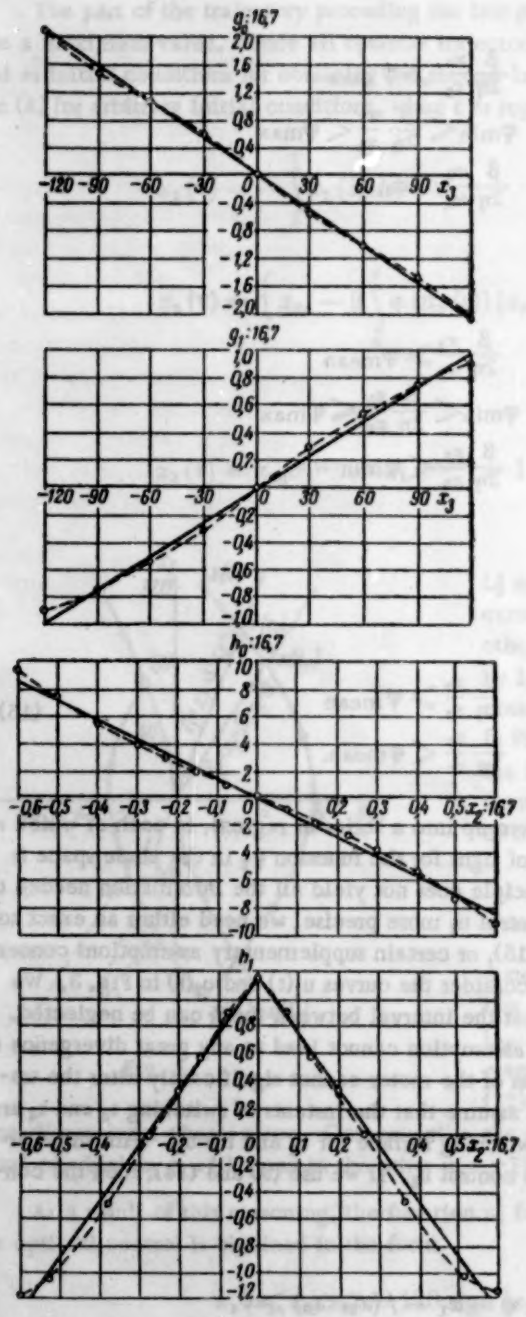

Fig. 6.

The expression for Γ_2 is obtained by replacing $\varphi_{\max}$ in Γ_1 by $\varphi_{\min}$.

The expression (16) is the analytical expression of optimal control for a function of three variables in phase space. In Fig. 5 we show the separation of the space into regions for optimal control u_2. We consider the trajectory shown in Fig. 5. Let the initial point of the motion be above the surface L_2 (the surface $\psi = 0$). At the initial instant of time, the representative point with the control $u_1 = 120$, $u_2 = u_{2\max}$ moves toward the plane Γ_1. In the sector between the planes Γ_1 and Γ_2, the control decreases with decreasing x_3, according to the relation

$$u_2 = \frac{\beta}{2\eta}\frac{x_3}{x_2}.$$

Leaving this sector, we find that the control u_2 maintains a minimum value for $u_{2\min}$ up to the time when the surface L_2 is encountered. At the point $x(t_3)$, belonging to the surface L_2, u_1 and u_2 are interchanged. The control u_1 here is changed to the maximum value with the opposite sign, while u_2 is changed to the maximum value $u_{2\max}$. In the remainder of the trajectory, on the surface L_2, the motion is on one of the trajectories of the family (12), and arrives at the origin on one of the half-curves L_1. The qualitative picture of such a transitional process is also shown in Fig. 3.

We have therefore obtained an analytical expression for the functions $u_1(x_1, x_2, x_3)$ and $u_2(x_1, x_2, x_3)$ for optimal control, as functions of the points in the phase space.

4. Realization of the Optimal Control Device

After determining the functions $u_1(x_1, x_2, x_3)$ and $u_2(x_1, x_2, x_3)$ of optimal control, we can start designing the optimal control device. It should be noted that, as a result of the synthesis, we have obtained two optimal control functions with one depending on the other. They are related through $\psi(x_1, x_2, x_3)$. We begin with a realization of the optimal control (14). The function ψ is given in terms of the variable x_1, and the function of two variables $f(x_2, x_3)$. The values of the function $f(x_2, x_3)$ have already been obtained. It is clear that, for the realization of ψ, we must first form the functional transformation from the two inputs x_2 and x_3 to an output giving the values of the function $f(x_2, x_3)$.

To obtain this functional transformation, we use a method proposed in [6]. For convenience in the realization, we expand $f(x_2, x_3)$ in a series:

$$f(x_2, x_3) = g_0(x_2) + h_0(x_3) + \sum_k \lambda_k g_k(x_2) h_k(x_3), \tag{17}$$

where $g_0(x_2)$ and $h_0(x_3)$ are obtained from the conditions

$$g_0(x_2) = \frac{1}{c-d}\int_c^d f(x_2,\ x_3)\,dx_3, \qquad h_0(x_3) = \frac{1}{a-b}\int_a^b f(x_2,\ x_3)\,dx_2; \tag{18}$$

where a, b, c, and d define the range of values of the function $f(x_2, x_3)$; λ_k, $g_k(x_2)$, and $h_k(x_3)$ are the characteristic values and normalized characteristic functions of the integral equations

$$\lambda_k g_k(x_2) = \int_a^b k_1(x_2,\ s_2)\,g_k(s_2)\,ds_2, \qquad \lambda_k h_k(x_3) = \int_c^d k_2(x_3,\ s_3)\,h_k(s_3)\,ds_3. \tag{19}$$

In the equations (19),

$$k_1(x_2,\ s_2) = \int_c^d f(x_2,\ x_3)\,f(s_2,\ x_3)\,dx_3,$$

$$k_2(x_3,\ s_3) = \int_a^b f(x_2,\ x_3)\,f(x_2,\ s_3)\,dx_2.$$

It can be proved that the series (17) for the function $f(x_2, x_3)$ converges very rapidly in the mean-square sense.* In our case, the function $f(x_2, x_3)$ can be given in tabular form, and so the integrations (18) and (19) are replaced by summations. Calculation shows that the function $f(x_2, x_3)$ can be calculated from the formula

$$f^*(x_2,\ x_3) = g_0(x_2) + h_0(x_3) + g_1(x_2)\,h_1(x_3). \tag{20}$$

with an error not greater than 4%.

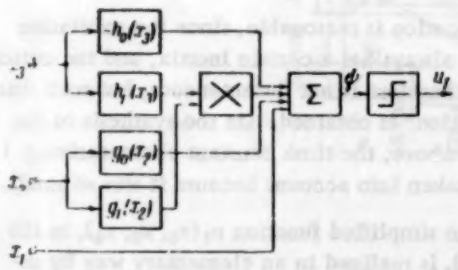

Fig. 7.

Graphs of the functions $g_0(x_2)$, $h_0(x_3)$, $g_1(x_2)$, and $h_1(x_3)$, obtained by the solution of Eqs. (18) and (19), are shown in Fig. 6. The calculated values are shown by dotted curves, the approximations by continuous straight lines. Thus, the function ψ, determining the optimal control u_1 in (14), can be expressed in the form

$$\varphi = x_1 - g_0(x_2) - h_0(x_3) - g_1(x_2)\,h_1(x_3). \tag{21}$$

The block diagram of the realization of the optimal control u_1, according to (14), is shown in Fig. 7. The signals x_1, x_2, and x_3 arrive at the input of the device. At the output of the nonlinear converter, we obtain the four functions of one variable, and then x_1, $g_0(x_2)$, and $h_0(x_3)$ are combined with the product $g_1(x_2)h_1(x_3)$ to give the function ψ. A relay element at the output finally forms the function for optimal control $u_1(x_1, x_2, x_3)$.

We now consider the realization of optimum control for the second parameter u_2 – the current in the exciting winding of the motor. We must form the analytical expression (16). It is not difficult to design a relay-contact device to give this result. Such a device, however, will be rather cumbersome, since it must contain a large number of relay elements and one divider. One of the possible designs is shown in Fig. 8. Here, E_1 and E_2 are two different voltages giving the maximum and minimum current in the anode circuit and, consequently, in the exciting winding as well. The circuit shown in Fig. 8 can be considerably simplified, if we neglect the part of the smooth variation of u_2 in the region between the planes Γ_1 and Γ_2. Let the lines Γ_1 and Γ_2 in Fig. 5 be close to one another. Then, if we assume that they coincide, the optimal control (16) can be reduced to the very simple form

$$u_2 = u_{2\max}\begin{cases}\text{for} & \psi>0, & \Gamma_1>0,\\ \text{for} & \psi<0, & \Gamma_1<0;\end{cases} \qquad u_2 = u_{2\min}\begin{cases}\text{for} & \psi>0, & \Gamma_1<0;\\ \text{for} & \psi<0, & \Gamma_1>0.\end{cases} \tag{22}$$

*This was proven by the authors. It was found that the series function $\{g_k h_k\}$ forms the best basic biorthogonal system of Fourier series from the point of view of rapidity of convergence in the mean-square sense.

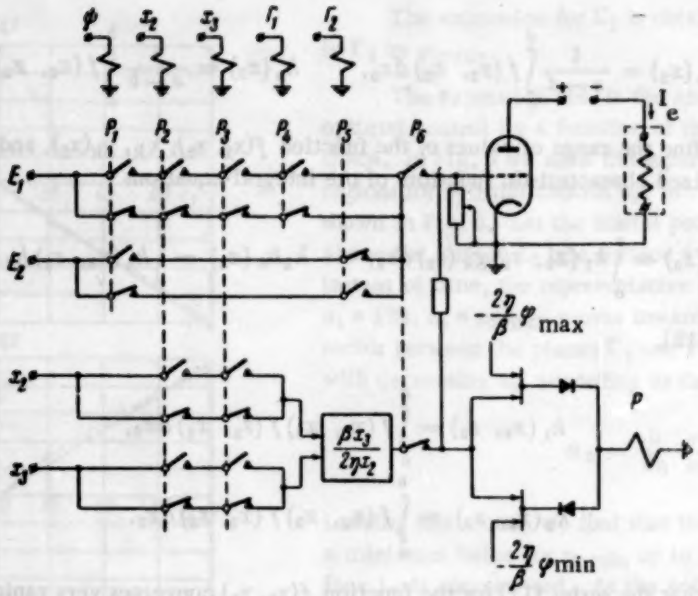

Fig. 8.

Fig. 9.

Such a simplification is reasonable, since the excitation winding of the motor always has a certain inertia, and the switching of the u_2 current therefore is not instantaneous, but such that a "natural approximation" is obtained. (In the synthesis of the system, as was shown above, the time constant characterizing this inertia was not taken into account because it was so small.)

The simplified function $u_2(x_1, x_2, x_3)$, in the form (22), is realized in an elementary way by using a logical "coincidence" unit. One of the possible schemes for forming the expression (22) is shown in Fig. 9. The output u_2 is obtained by a relay element, and so it has only two possible values. It can be either the maximum value, when the signs of the functions ψ and Γ_1 are the same, or it can have the minimum value, when these signs are different.

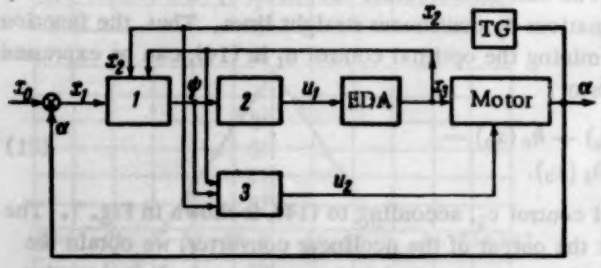

Fig. 10.

5. Description of the Servo System

The structural design, based on the above synthesis, is shown in Fig. 10. The power section consists of an EDA-12 electrodynamic amplifier and an MI-32 dc motor. In the system there are two blocks of controls, one for the main channel, the other for the channel for the exciting winding of the motor. The controlling element for the main channel 1 consists of four main elements, namely a nonlinear converter for a function of one variable, a multiplying block, a summing block, and a relay element. The functions $h_0(x_3)$, $g_0(x_2)$, and $g_1(x_2)$, as can be seen from Fig. 6, can be approximated sufficiently accurately by straight lines, and so they can be obtained from voltage dividers. The function $g_1(x_2)$ is, on the other hand, essentially nonlinear, and must be formed in the usual way by a functional converter with one input. The multiplication block is built by using nonlinear resistances (thyrites) in a system based on the expression

$$g_1 h_1 = \frac{1}{4}[(g_1 + h_1)^2 - (g_1 - h_1)^2].$$

The summation and relay characteristic 2 are obtained in an elementary way.

The control block 3 (Fig. 10) in the motor-excitation-winding channel is built up according to the design shown in Fig. 11, and forms the control law (22). The control for the excitation winding of the motor consists of

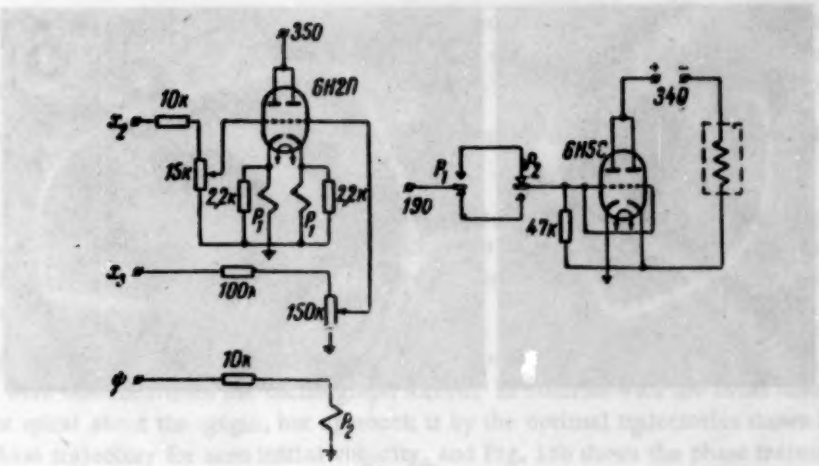

Fig. 11.

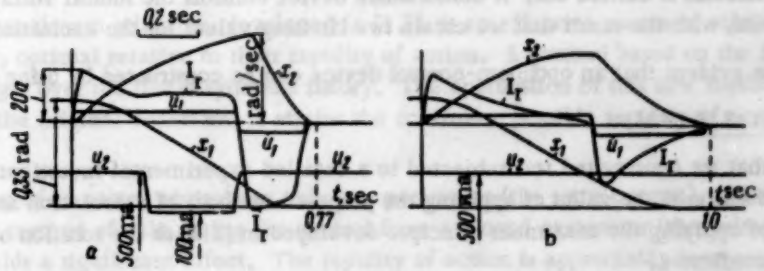

Fig. 12.

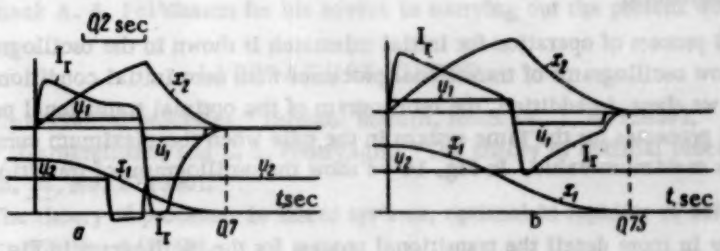

Fig. 13.

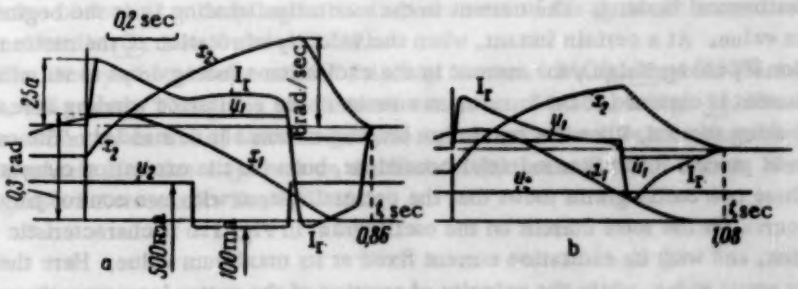

Fig. 14.

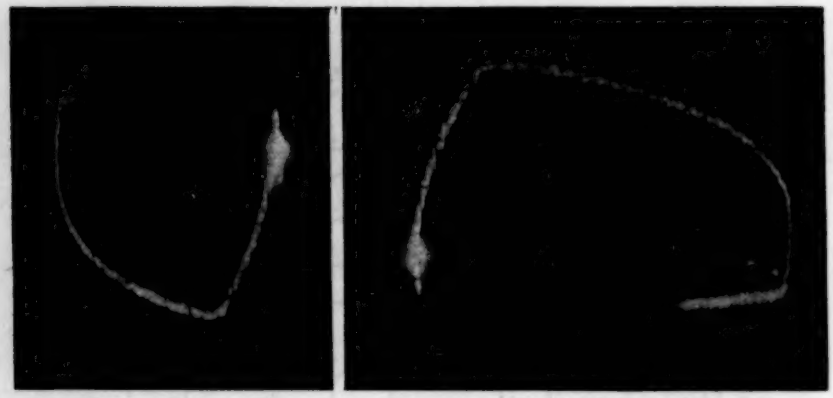

a b

Fig. 15.

two relays. The quantity Γ_1' is obtained at the relay P_1, where the summation of the two quantities x_2 and x_3 with corresponding coefficients is carried out. A coincidence device controls the shutoff voltage for a 6N5S tube in the excitation circuit, with the result that we obtain two limiting values for the excitation current.

It is therefore evident that an optimum-control device can be constructed by using simple techniques.

6. Experimental Results

The system that we constructed was subjected to a detailed experimental investigation. The results of these experiments fully confirmed the value of applying the proposed methods of calculation and principles of design. The effectiveness of applying the maximum principle developed in [1,3] to the solution of concrete, technical problems was also confirmed.

As we have already pointed out, the system that we have obtained was designed to obtain a rapid-acting annihilation of an initial mismatch, for arbitrary initial conditions of the system. Experiments were carried out with various initial conditions.

The transitional process of operation for initial mismatch is shown in the oscillograms in Figs. 12-14. In Figs. 12 and 13 we show oscillograms of transitional processes with zero initial conditions. For comparison, in each of the diagrams we show, in addition, the oscillogram of the optimal transitional process, and also the oscillogram of transitional processes for the same system in the case when the maximum current in the excitation winding of the rotor has its maximum value. In Fig. 14 we show the oscillograms of transitional processes for zero initial conditions.

We will consider in more detail the transitional process for the oscillogram in Fig. 12a, which is for the optimal transition process with zero initial conditions. The oscillogram shows that the process of operation continues without overshooting (the curve x_1). The graph of the rotation x_2 of the motor consists of clearly expressed sections of acceleration and braking. The current in the excitation winding I_e at the beginning of the process takes its maximum value. At a certain instant, when the velocity of rotation of the motor reaches its rated value (when the expression Γ_1 changes sign), the current in the excitation winding drops to its minimum value, and a high rotational moment is obtained. The maximum current in the excitation winding is reached at the instant of transition to the braking section, when the maximum braking moment is demanded. The oscillogram in Fig. 12b shows the transitional process for the same initial conditions, but with the excitation current fixed at its maximum. A comparison of these two oscillograms shows that the optimal system with two control parameters possesses great advantages. The curve for the rotor current on the oscillogram in Fig. 12b is characteristic for a motor with independent excitation, and with its excitation current fixed at its maximum value. Here the rotor current rapidly decreases to a very small value, while the velocity of rotation of the motor increases, since, for high rates of rotation, there is a high back emf. In the case of the process shown in the oscillogram in Fig. 12a, the picture differs greatly, and the rotor current, after a drop during the initial part of the acceleration, approximately maintains its rated value, and this ensures that the static load is overcome as rapidly as possible. The duration of the transitional process in the case of Fig. 12a is significantly shorter than in the case of Fig. 12b. Thus, for an initial mismatch of 0.35 radians, the process takes 0.77 sec in the first case, and 1.0 sec in the second case.

Figure 13 shows the oscillograms of transitional processes for small initial values of the mismatch. Here the effect described is less obvious, since the time of excitation current cutoff is small. For small mismatch angles, the rate of rotation of the motor does not reach values for which the second parameter is switched in.

The oscillograms in Fig. 14 show transitional processes for nonzero initial conditions. Here the same type of result can be seen.

We should mention that for small mismatch angles the system continues to operate optimally, although the second parameter is not cut in. The system we have constructed has a transitional time for eliminating small and medium mismatches, that is from $\frac{2}{3}$ to $\frac{1}{3}$ of the time required under the same conditions by the usual linear systems of the same power.

Figure 15 shows photographs of the projections of optimal trajectories on the phase plane (x_1 is the abscissa, x_2 is the ordinate) that were obtained from the oscillograph screen. In contrast with the usual linear systems, these trajectories do not spiral about the origin, but approach it by the optimal trajectories shown in Fig. 4. Figure 15a shows the phase trajectory for zero initial velocity, and Fig. 15b shows the phase trajectory for nonzero initial velocity.

SUMMARY

1. The variational maximum principle, developed in [1,3], is an effective means of solving the problem of synthesizing servo systems, optimal relative to their rapidity of action. A method based on the maximum principle has incomparable advantages over the linear synthesis theory. The application of this new method does not require the linearization of the original equations; it attains the maximum possible rapidity of action; there is no overshoot, etc.

2. The usual systems of dc motor control use only one parameter (the rotor current), and they are evidently not the best possible. Our method of calculating the control from a second parameter (the voltage in the excitation coil of the motor) yields a significant effect. The rapidity of action is appreciably increased.

3. The optimal controlling device can be constructed simply. Industrial designs of this type of control can be completely reliable, compact, and simple.

The authors wish to thank A. A. Fel'dbaum for his advice in carrying out the present work.

LITERATURE CITED

1. L. S. Pontryagin, "Optimal control processes," Uspekhi Matem. Nauk 14, 1, 85 (1959).
2. V. G. Boltyanskii, R. V. Gamkrelidze, and L. S. Pontryagin, "The theory of optimal processes," Izvest. Akad. Nauk SSSR, Ser. Matem. 24, No. 1 (1960).
3. R. V. Gamkrelidze, "The theory of processes in linear systems, optimal in rapidity of action," Izvest. Akad. Nauk SSSR, Ser. Matem. 22, No. 4 (1958).
4. A. A. Fel'dbaum, "The application of phase space in the synthesis of optimal systems," Avtomatika i Telemekhanika 16, No. 2 (1955).
5. A. Ya. Lerner, "The use of nonlinear coupling in the improvement of the dynamic properties of servo controls," Avtomatika i Telemekhanika 13, Nos. 2 and 4 (1952).
6. N. N. Krasovskii, "The theory of optimal control," Priklady Matem. i Mekh. 23, 4 (1959).
7. E. W. Pike and T. R. Silverberg, "Designing mechanical computers," Mach. Design 24, Nos. 7, 8 (1952).
8. Sung Chien, "Optimal control in a single nonlinear system," Avtomatika i Telemekhanika 21, No. 1 (1960).
9. Sung Chien, "The synthesis of optimal systems on the basis of isochrone fields," Izvest. Akad. Nauk SSSR, Otd. Tekh. n., Énergetika i Avtomatika No. 5 (1960).

All abbreviations of periodicals in the above bibliography are letter-by-letter transliterations of the abbreviations as given in the original Russian journal. *Some or all of this periodical literature may well be available in English translation.* A complete list of the cover-to-cover English translations appears at the back of this issue.

THE ESTIMATION OF SELF-OSCILLATION PARAMETERS IN NONLINEAR AUTOMATIC CONTROL SYSTEMS

V. R. Andrievskii (Leningrad)

Translated from Avtomatika i Telemekhanika, Vol. 22, No. 2, pp. 171-175, February, 1961
Original article submitted August 29, 1960

A method is described of estimating the self-oscillation parameters in nonlinear automatic-control systems in which harmonic linearization is permissible.

We will investigate a system of automatic control described by the equations with constant coefficients

$$\dot{x}_s = \sum_{k=1}^{n} a_{sk}x_k + f_s\left(\sum_{k=1}^{n} b_{sk}x_k\right) \qquad (s = 1, 2, \ldots, n). \tag{1}$$

It is often necessary to estimate the parameters of periodic regimes that can occur in the system under consideration, without the need of obtaining exact solutions. In order to save time, various methods of obtaining approximate solutions are therefore used. For example, in a very wide class of systems, it is sufficient to apply the principle of harmonic linearization. In this case, it is assumed [1,2] that, in the components of a periodic regime, all the terms of the Fourier series may be neglected except the first, so that we may use the approximation

$$x_s = a_s \sin(\omega t + \psi_s) \qquad (s = 1, 2, \ldots, n). \tag{2}$$

We also assume that higher harmonics can be neglected in the expansion of $f_s\left(\sum_{k=1}^{n} b_{sk}x_k\right)$ in a Fourier series. For simplicity in what follows, we will assume that the functions f_s are single-valued, and symmetric relative to the zero value of the argument, and that they can be approximately expressed in the form

$$f_s\left(\sum_{k+1}^{n} b_{sk}x_k\right) = q_s \sum_{k=1}^{n} b_{sk}x_k, \tag{3}$$

where the coefficients of harmonic linearization q_s are taken to be the first coefficients of the expansion of $f_s\left(\sum_{k=1}^{n} b_{sk}x_k\right)$ in a Fourier series.

Thus, (2) must coincide with certain periodic solutions of the harmonic linearization system

$$\dot{x}_s = \sum_{k=1}^{n} a_{sk}x \qquad q_s \sum_{k=1}^{n} b_{sk}x_k \tag{4}$$

or

$$\dot{x}_s = \sum_{k=1}^{n} c_{sk}x_k, \tag{4'}$$

where

$$c_{sk} = a_{sk} + q_s b_{sk} \qquad (s = 1, 2, \ldots, n).$$

The a_s and ω occurring in (2) must satisfy the condition that the characteristic determinant of the harmonically linearized system be equal to zero:

$$\| \| c_{sk} \| - j\omega E \| = 0, \tag{5}$$

where $\omega > 0$, $\|c_{sk}\|$ is the matrix of the coefficients of the system (4), and E is the unit matrix.

If we succeed in finding a set of expressions of the form (2) for which condition (5) is satisfied, and if, at the same time, ω lies in a frequency band for which the system (1) satisfies the conditions of applicability of the harmonic linearization principle (the filter condition for self-resonance), then the problem of obtaining an approximate solution for the system (1) can be assumed to be solved.

Such a determination is, as a rule, troublesome, and, in the case of a multiloop system with some nonlinear elements, often impossible in practice. This limits the possibilities of investigating nonlinear systems. A considerable decrease in the difficulty of investigating such systems can be achieved, if we do not try to find the exact values of a_s and ω, but pose the problem of estimating them approximately.

We now consider the system (4) with the condition (5). If q_s is assumed to be arbitrary, then condition (5) can be considered as the equation of the boundary of the D-division of the system (4).

We denote by U the set of points belonging to the boundary of the D-division of the system (4) in the space $\{q_1, \ldots, q_n\}$. (We should again stress the fact that the coefficients q_s are here considered to be arbitrary.) We note that each point $(q_1, \ldots, q_n) \in U$, in view of (5), corresponds to a certain frequency ω.

If the system (1) has a periodic solution that is given approximately in the form (2), and if $(q_1, \ldots, q_n)$ is the set of coefficients of the harmonic linearization corresponding to (2), then, because of (5), the condition

$$(q_1, \ldots, q_n) \in U. \tag{6}$$

must be satisfied.

To estimate the parameters a_s and ω, we must use the fact that, for the majority of cases occurring in practice, the region containing the points corresponding to the linearization coefficients (in what follows we will denote this region by Q) does not fill the whole space $\{q_1, \ldots, q_n\}$, and is usually bounded. Combining the conditions $(q_1, \ldots, q_n) \in U$, $(q_1, \ldots, q_n) \in Q$, we obtain

$$(q_1, \ldots, q_n) \in U \bigcap Q, \tag{7}$$

where $U \bigcap Q$ is the intersection of the sets U and Q. [Here each point $(q_1, \ldots, q_n)$ of the set $U \bigcap Q$ also corresponds to some frequency ω.]

For a very large class of systems, we can obtain upper and lower bounds for ω, and for at least some of the q_s, from the form of $U \bigcap Q$.

Thus, if there is a periodic regime for the system (1) which can be given approximately in the form (2), its amplitude and frequency can be estimated from these bounds.

In order that such a solution may be carried out, it is sufficient that the set $U \bigcap Q$ contain at least one point, and that this point corresponds to a frequency ω for which the conditions of applicability of the harmonic linearization method are satisfied.

It should be noted that only stable periodic regimes, usually called self-oscillation regimes, can occur in practice, and so these are the only cases that are of interest to us.

We will assume that a periodic regime for the system (1) with period T has been found:

$$x_s = \overline{x_s(t)} \qquad (s = 1, 2, \ldots, n) \tag{8}$$

The periodic solution (8) of the system (1) is called stable [3], if, for any $\epsilon > 0$, we can find a $\delta > 0$, such that, for $\rho(x_{10}, \ldots, x_{n0}) < \delta$ the inequality $\rho[x_1(t), \ldots, x_n(t)] < \epsilon$ will be satisfied for $t > 0$.

Here x_{s0} is denoted by $x_s(0)$, and ρ is the distance from the vector $(x_1, \ldots, x_n)$ to the periodic regime

$$\rho(x_1, \ldots, x_n) = inf \sqrt{\sum_{s=1}^{n} (x_s - \overline{x_s(t)})^2}, \qquad t \in [0, T].$$

Up to the present time, there are no rigorously proven criteria that can be used in practice to single out the stable, periodic solutions for systems of the usual type. In practice, the solution of this type of problem is obtained by applying certain rules that usually give reliable results. In the application of the above-described method of estimating the parameters of a periodic regime, we can use the following rule: For a point $(q_1, \ldots, q_n)$, corresponding to a stable, periodic solution, the following conditions must be satisfied: First of all, $(q_1, \ldots, q_n) \in U_0$, where U_0 is the boundary of the stable region for the system (4) in the space $\{q_1, \ldots, q_n\}$; second, for increasing amplitude a_s, the point $(q_1, \ldots, q_n)$ must be displaced toward the interior of the region of stability.

It follows from the first condition that, in estimating the self-oscillation parameters, we must not use condition (7), but must use the more stringent condition

$$(q_1, \ldots, q_n) \in U_0 \cap Q, \tag{9}$$

The second condition yields a rather effective method of singling out the unstable, periodic solutions that satisfy condition (9) from the stable solution.

The use of condition (9) for estimating the self-oscillation parameters considerably decreases the difficulties involved in such an estimate, and it also has the further advantage of making it relatively easy to estimate the influence on the self-oscillation parameters of a change in parameters for the system under consideration.

It should be noted that the condition that f_s be single-valued is not essential. In the case when this condition is not satisfied, the reasoning used remains valid but, as is known, the structure of the system (4) becomes somewhat more complex.

A generalization of the structure of the system (1) is possible. It is easy to see that everything said above also remains valid for a system of the form

$$\dot{x}_s = \sum_{k=1}^{n} a_{sk} x_k + \sum_{l=1}^{n} f_{sl}\left(\sum_{k=1}^{n} b_{slk} x_k\right) \qquad (s = 1, 2, \ldots, n).$$

In general, if a system satisfies the conditions of the applicability of the harmonic linearization principle, and if, in some way, we succeed in developing the structure of the harmonically linearized system, then, by investigating the intersection of the stability region for this system in the linearization-coefficient space with the region of possible values, we can estimate the self-oscillation parameters without the necessity of obtaining any information about equilibrium, although this information must be obtained for the direct application of the harmonic linearization principle.

We will illustrate the application of the above method of estimating the self-oscillation parameters by an example. Let a system of automatic control be described by the following system of equations:

$$\begin{aligned} &\dot{x}_1 = -375x_2, \qquad \dot{x}_2 = 0{,}266(-x_3 + x_5), \\ &\dot{x}_3 = x_4, \qquad \dot{x}_4 = 23{,}3(x_2 - x_3) - 0{,}136x_4 - 13{,}3x_5, \end{aligned} \tag{10}$$

$$\begin{aligned} &\dot{x}_5(t + 0{,}015) = f_1(\sigma_1), \qquad \dot{x}_6 = f_2(\sigma_2), \\ &\sigma_1 = 3{,}5x_3 + 0{,}7x_4 - x_5 + 20x_6, \qquad \sigma_2 = 0{,}33x_3 - 5 \cdot 10^{-5} x_1, \end{aligned}$$

where $f_i(\sigma_i)$ $(i = 1, 2)$ are the usual approximations for the static characteristics used in describing a nonlinear, insensitive, saturated element. An example of one of these functions is shown in Fig. 1, with

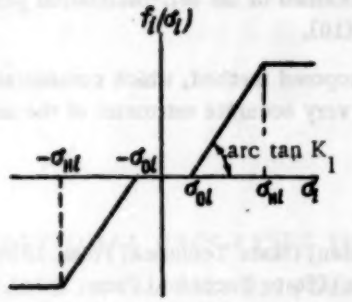

Fig. 1.

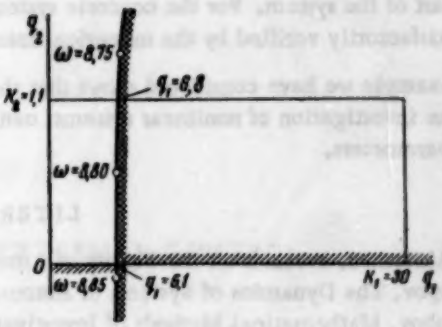

Fig. 2.

$$\sigma_{01} = 0{,}25; \quad \sigma_{H1} = 2{,}75; \quad K_1 = 30;$$
$$\sigma_{02} = 0{,}30; \quad \sigma_{H2} = 3{,}00; \quad K_2 = 1{,}1.$$

An estimate of the self-oscillation parameters that are possible in the system being investigated can, as above, be obtained from the diagram of the D-division in the plane $\{q_1, q_2\}$ for the system:

$$\begin{gathered}\dot{x}_1 = -375x_2, \quad \dot{x}_2 = 0{,}266(-x_3 + x_5)\\ \dot{x}_3 = x_4,\\ \dot{x}_4 = 23{,}3(x_2 - x_3) - 0{,}136x_4 - 13{,}3x_5,\\ \dot{x}_5(t+0{,}015) = q_1(3{,}5x_3 + 0{,}7x_4 - x_5 + 20x_6),\\ \dot{x}_6 = q_2(0{,}33x_3 - 5\cdot 10^{-3}x_1).\end{gathered} \tag{11}$$

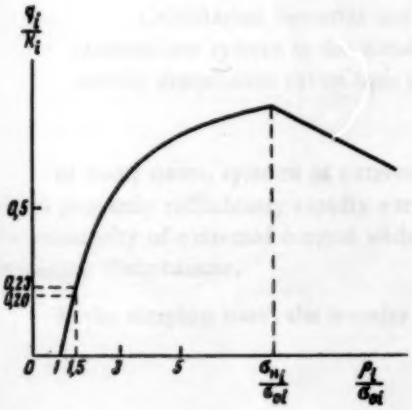

Fig. 3.

The region of stability of the system (11) is shown in Fig. 2. For using condition (9), it is necessary to know the region of possible values of the linearization coefficients Q. Figure 3, in which we show the dependence of the harmonic linearization coefficients q_i on the amplitude ρ_1 of the input signal σ_1 for an element with a characteristic of the type shown in Fig. 1, shows that $q < K_1$ in every case. Therefore, as Fig. 2 shows, the projection of the intersection of $U_0 \cap Q$ with q_1 lies in the interval (6.1, 6.8). Thus, if self-oscillations are possible in the system (10), then the amplitude of their first harmonics must satisfy

$$\frac{q_1}{K_1} \in (0{,}20;\ 0{,}23). \tag{12}$$

The circular frequency of these oscillations is thus estimated to be 8.8 sec^{-1} (1.5 cps).

It follows from Fig. 3 that two periodic solutions satisfying condition (12) are possible in principle. An application of the second condition in the rule described above for singling out stable periodic solutions shows that the solution with $\rho_1 > \sigma_{H1}$ can be discarded since, in this case, an increase in ρ_1 leads to a displacement of the point (q_1, q_2) out of the stability region.

We see from Fig. 3 that the stable, periodic solution, for which $\frac{q_1}{K_1} \in (0{,}20,\ 0{,}23)$ corresponds to an amplitude of the signal σ_1 equal to $\rho_1 = 1{,}5\sigma_{01}$. Here the amplitude x_5 will be

$$a_5 = \frac{q_1\rho_1}{\omega} \in (0{,}27,\ 0{,}31).$$

Thus, self-oscillations in the system we have considered are possible with the amplitude of x_5 equal to $a_5 \in (0{,}27,\ 0{,}31)$ and a frequency of the order of 1.5 cps. In order for such self-oscillations actually to occur, it is sufficient that this frequency be in the range of applicability of the harmonic linearization principle for the system (10). The fact that this condition is satisfied must be verified by considering the frequency characteristics of

the linear part of the system. For the concrete system (10), the estimate obtained of the self-oscillation parameters was satisfactorily verified by the numerical integration of the system (10).

The example we have considered shows that the application of the proposed method, which considerably simplifies the investigation of nonlinear systems, can, in some cases, yield very accurate estimates of the self-oscillation parameters.

LITERATURE CITED

1. M. A. Aizerman, Lectures on the Theory of Automatic Control [in Russian] (State Technical Press, 1958).
2. E. P. Popov, The Dynamics of Systems of Automatic Control [in Russian] (State Technical Press, 1954).
3. V. I. Zubov, Mathematical Methods of Investigating Systems of Automatic Control [in Russian] (Sudpromgiz, 1959).

TRANSITIONAL PROCESSES IN A SYSTEM OF EXTREMAL CONTROL WITH A DYNAMIC SENSITIVE UNIT

A. P. Yurkevich (Moscow)

Translated from Avtomatika i Telemekhanika, Vol. 22, No. 2, pp. 176-184, February, 1961
Original article submitted July 14, 1960

The distinctive features are considered of transitional processes in a system of extremal control with a memory and with a sensitive unit of dynamic type. It is shown that the mean rate of search decreases as the system approximates to the extremum of the function, and increases for any position of the executive unit, when there is an external disturbance that raises the level of the function maximum.

Calculation formulas are given for data of parameters of the steady-state motion of the commutator system in the presence of a zone of insensitivity, with delay and the effect of an outside disturbance taken into account.

In many cases, systems of extremal control are improved by the use of sensitive elements of dynamic type, which pass only sufficiently rapidly varying input signals. This makes it possible, as was shown in [1-3], to raise the sensitivity of extremal control with a memory, and to eliminate or decrease the harmful influence of low-frequency disturbances.

In the simplest case, the transfer function of the dynamic input-signal unit is

$$W_1(p) = K_t \frac{p\tau}{p\tau + 1}, \tag{1}$$

where K_t is the transfer coefficient of the unit, and τ is its time constant. The block diagram of an extremal system with such a unit, and with a noninertial object of control, is shown in Fig. 1a.

In [2,3], the question was considered of the dynamics of a system without taking into account the inertia of the object of control. In [4], a new method was proposed for the extremal control of inertial objects, which permitted a considerable improvement in the quality of the control processes. A distinctive feature of the proposed method is that, at the input of an extremal control unit, either possessing a memory or of any other type, the incident signal is a definite combination of the variation of the output signal of the object of control and its derivatives. In the particular case when the object of control is of the first order with static characteristic $y_1 = f(x)$, and with the output y_2 of the object related to y_1 by the equality

$$y_2 = y_1 \frac{K_0}{p\tau_0 + 1}, \tag{2}$$

where K_0 is a positive coefficient and τ is the time constant of the object, a signal $\underline{z}$ can arrive at the input of the extremal control unit with $\underline{z}$ the derivative of y_2, i.e., $z = py_2$ (see Fig. 1b).

Here,

$$\frac{z}{y_1} = \frac{K_0}{\tau_0} \frac{p\tau_0}{1 + p\tau_0}.$$

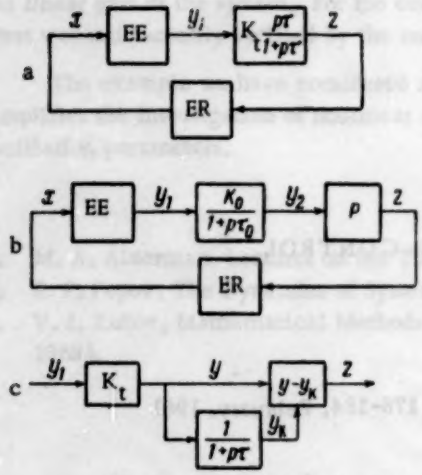

Fig. 1. Block diagram of extremal systems with dynamic transformation of the input signal. EE) Extremal element; ER) extremal control.

In this case, it is evident that the input section of the control system is, in its dynamic relationship, identical with that given above in (1). The consideration of the operation of a system with a transformed input signal of the form (1) is related not only to the case of control of a noninertial object, but also to certain cases of the control of inertial objects of the first order.

In [2,3], the motion of a system in the region of the function extremum is considered for the operation of a control without delay. It is also of interest to consider the motion of a system for large initial deviations, taking into account the instrumental delay, and we do this below.

We express the signal $\underline{z}$ as the difference of signals (Fig. 1c)

$$z = y - y_{\text{н}}. \tag{3}$$

We also have

$$y = K_t y_1, \tag{4}$$

$$y_{\text{н}} = \frac{y}{p\tau + 1}. \tag{5}$$

We note that expressions of this form describe, in some cases, real physical processes, for example in the method of dynamic transformation of the signal [1], by means of reverse coupling of the circuits of proportional and inversely proportional first-order type.

The expressions (3), (4), and (5) yield

$$W(p) = \frac{z}{y} = \frac{p\tau}{p\tau + 1}.$$

We assume that the static characteristic $f(x)$ is of parabolic form

$$y = -K_x x^2, \tag{6}$$

where $\underline{x}$ and $\underline{y}$ are coordinates with origin at the extremum point of the function.

We will also assume that the extremal control unit operates on the memory principle, has a zone of insensitivity z_{H}, and is provided with an executive unit of constant velocity, i.e., $|\dot{\underline{x}}| = V_x = \text{const}$. The motion of the executive unit is reversed each time the decrease in $\underline{z}$ reaches z_{H}.

We will consider the process of searching for the extremum of the function, with initial conditions $t = 0$, $y = y_k = y_0$. In Fig. 2 we show the process of search for the extremum of the function in the phase plane with coordinates $\underline{x}$ and $\underline{y}$, with the time also plotted in the horizontal direction.

The process of searching for the extremum proceeds in the following way. The motion starts at the point 1, and we assume that it starts in the correct direction. The value of $\underline{y}$ varies on the parabola, and the value of y_k on the corresponding curve, which is the solution of (5). We can see that the difference $y - y_k = z$ first of all increases, and then begins to decrease. At point 2, this decrease has reached z_{H}, and the system reverses. Then $\underline{y}$ rapidly decreases, while y_k continues to increase, and so $\underline{z}$ decreases very rapidly. This produces, at point 3, another reverse of the system, and the correct motion is reestablished. Similar phenomena occur at the points 4 and 5, 6 and 7, etc. We can see that, at points 2, 4, and 6, a false response is produced which slows the approximation of the system to the function's extremum. The frequency of these false responses increases as the system approaches the extremum $\underline{u}$, as can be seen from Fig. 2, and this frequency is strongly dependent on the insensitivity zone z_{H} of the control. The dotted curve II shows the variation of y_k for an insensitivity zone z_{H} half as large. We see that the number of false responses increases. If the insensitivity zone tends to zero, the number of false responses decreases indefinitely, and the search curve becomes smooth.

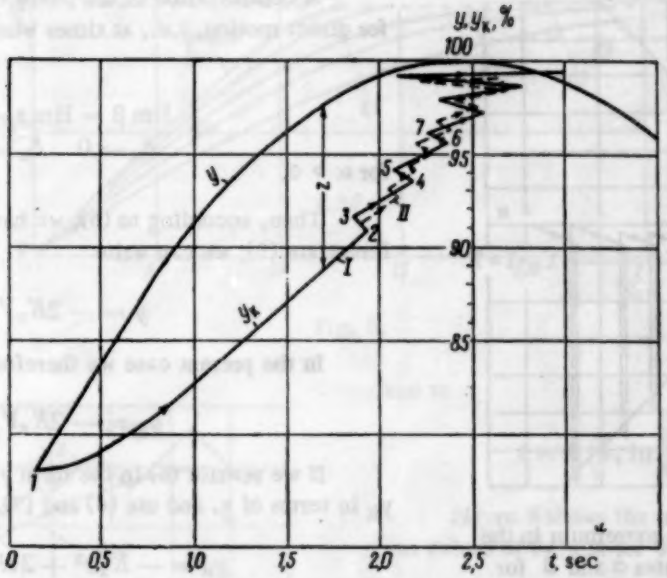

Fig. 2. The search for an extremum in the phase plane with coordinates $\underline{x}$ and $\underline{y}$ for $\nu_\tau = 0.4$, $\eta = 0.25$. I) $\delta_H = 1\%$; II) $\delta_H = 0.5\%$.

As was shown in [3], the determination of the transition-process parameters for the system, and the determination of the limiting cycles for these parameters, is facilitated by representing the motion of the system on several sheets, one on top of another, where each sheet is a phase plane, and also by using the dimensionless coordinates $\alpha = \frac{x}{V_x\tau}$ and $\beta = \frac{\dot{x}}{2K_xV_x^2\tau}$. Then, in the absence of any disturbance, the phase trajectories passing through any point α_0, β_0 of the phase plane will be exponential curves given by the equation $\beta = (\beta_0 + 1)\exp(-\Delta\alpha) - 1$, where $\Delta\alpha = \alpha - \alpha_0$.

We introduce the following notation: x_{max} for the greatest variation of $\underline{x}$, $t_c = x_{max}/V_x$, $\nu_\tau = \tau/t_c$, y_e is the value of the parameter to which the control tends for $x = 0$ in units of $\underline{y}$, and

$$\eta = \frac{K_x x_{max}^2}{y_e}, \qquad \delta_H = \frac{z_H}{y_e}.$$

The system reverses itself whenever β becomes negative and the area between the horizontal axis and the curve for β (for $\beta < 0$) reaches the negative value $S_H = \frac{\delta_H}{2\eta\nu_\tau^2}$. A discontinuous change in β of $\pm 2\alpha$ occurs at each point where there is a reverse.

Figure 3 shows the motion of the system in the α, β phase plane for the parameter values $\alpha_0 = 4$, $\beta_0 = 0$, $\delta_H = 0.2\%$, $\nu_\tau = 0.1$, $\eta = 0.5$. It is evident that a definite regime for the function-extremum search is established with relatively large direct-motion sections in the proper direction, alternated with short sections of reverse motion.

During the direct motion of this regime, the quantity β is close to zero, and during the reverse motion it is given by the straight line $\beta = -2\alpha$ (for $\alpha > 0$). A consideration of the phase trajectories $\beta(\alpha)$ also shows that, when the insensitivity zone δ_H tends to a zero range, the switchover frequency increases indefinitely, and the variation of α, corresponding to direct and reverse motion, tends to zero. Their ratio for every value of $\alpha = x/V_\alpha\tau$, however, has a definite limiting value which determines the rate at which the system approximates to the extremum of the function. We obtain $\underline{x}$ in terms of the time for the regime we are considering by assuming that δ_H tends to zero.

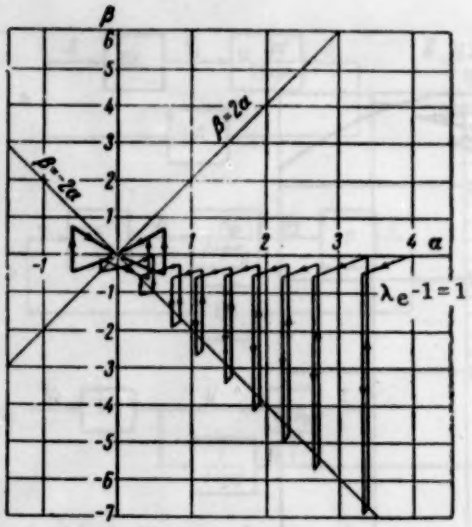

Fig. 3. The search for an extremum in the phase plane with coordinates α and β for $\nu_\tau = 0.1$, $\eta = 0.5$, $\delta_h = 0.2\%$, $\lambda_e = 0$.

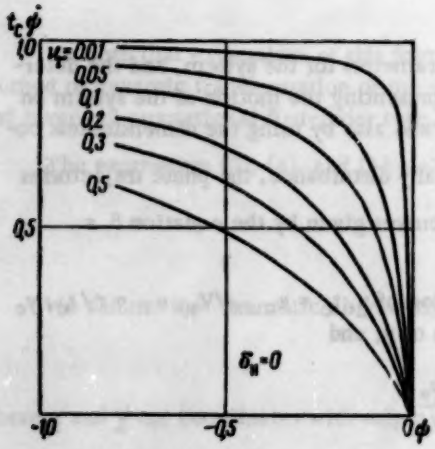

Fig. 4.

A consideration of the phase trajectories also shows that, for direct motion, i.e., at times when $\dot{\alpha} < 0$, we have

$$\lim_{\delta_н \to 0} \beta = \lim_{\delta_н \to 0} z = 0.$$

for $\alpha > 0$.

Then, according to (3), we have $\dot{y} = \dot{y}_k$. When we differentiate (6), we can write

$$\dot{y} = -2K_x V_x x.$$

In the present case we therefore obtain

$$\dot{y}_н = -2K_x V_x x. \tag{7}$$

If we rewrite (5) in the form $y_k = y - \tau\dot{y}_k$, express y and y_k in terms of x, and use (6) and (7), we get the relation

$$y_н = -K_x x^2 + 2\tau K_x V_x x. \tag{8}$$

As was said above, the function x(t) must satisfy $|\dot{x}| = V_x = \text{const}$. Therefore, in the search for the extremum for $\delta_H > 0$, the function x(t) is made up from more than one analytic function, and so $\dot{x}(t)$ is not continuous. When the transition to the sliding regime has occurred, the function x(t) becomes $x_c(t)$, and this latter function can be differentiated.

When we replace x in (8) by x_c, differentiate the result, and replace $\dot{y}_k$ by the expression (7), we obtain

$$\dot{x}_c = -\frac{V_x x_c}{\tau V_x - x_c}.$$

If we use the notation $x_c / x_{max} = \psi$, we obtain

$$\dot{\psi} = -\frac{1}{t_c}\frac{\psi}{\nu_\tau + \psi}. \tag{9}$$

The formula we have obtained gives the functional relation between the velocity of motion of the executive unit and its position in the search for the extremum of the function in a sliding regime. This relation, for various values of ν_τ, is illustrated in Fig. 4. It is evident that $\dot{\psi}$ decreases for decreasing ν_τ, i.e., for decreasing time constant τ and, in addition to this, the curves change their character somewhat. For small τ, the rate $\dot{\psi}$ in the search process for the extremum changes little, and decreases rapidly only in a small region about the function extremum. Relative to improving the quality of the transitional process, it is therefore advantageous to decrease τ. However, for $\delta_H > 0$, an excessive decrease in τ, as was shown in [2,3], results in an increase in the amplitude of the oscillations of the system about the function extremum toward the end of the search process, and so lowers the accuracy of the control.

We will determine the characteristic of the transitional process for the system in a sliding regime under the assumption that $\psi = \psi_0$ for $t = 0$. It follows from (9) that

$$dt = -t_c\left(\frac{\nu_\tau}{\psi} + 1\right)d\psi$$

Therefore,

$$t = -t_c\int_{\psi_0}^{\psi}\left(\frac{\nu_\tau}{\psi} + 1\right)d\psi,$$

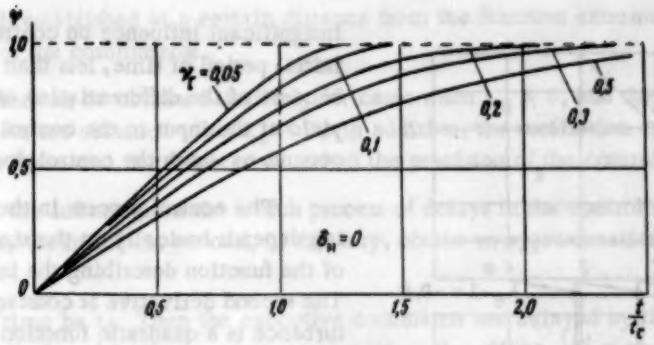

Fig. 5.

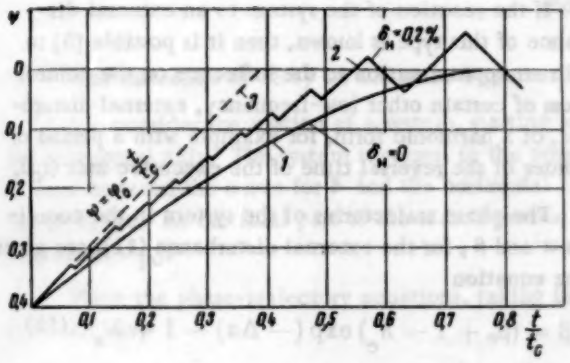

Fig. 6. Comparison of the transitional processes of system with $\nu_\tau = 0.1$. 1) Sliding regime $\delta_H = 0$); 2) in the zone of insensibility $\delta_H = 0.2\%$); 3) with constant velocity of the executive unit ($\Psi = 1/t_c$).

and so

$$t = t_c\left(\nu_\tau \ln\frac{\psi_0}{\psi} + \psi_0 - \psi\right). \qquad (10)$$

Figure 5 shows the transitional process for various values of ν_τ and for $\psi_0 = 1$.

In Fig. 6 we give a comparison of the transitional processes for $\delta_H = 0$ (Curve 1) and $\delta_h = 0.2$ % (the broken curve 2, obtained from the results obtained in describing the process shown in Fig. 3). A transitional process corresponding to $\delta_H > 0.2$ % would yield a curve lying in the region between the broken curve 2 and the straight line 3.

The distinctive feature of the system that we have pointed out – the decrease in its velocity as the function extremum is approached – can be considered to be of value, since the oscillations during the control process are decreases by it. This is true, for example, in cases when there is a dynamic, inertial unit, located between the control output and the unit with the nonlinear, extremal character.

We should note that the system we have been considering with the parameters we have used has a definite interference-rejection relative to high-frequency small-amplitude disturbances, not only for large, but also for small nonsensitivity zones of control. In fact, for a narrow zone of control insensitivity in the extremum search, if the system reverses because of the effect of interference, then its rate of approach to the extremum will be decreased. This (see Fig. 2) causes a decrease in the difference $y - y_k$, and then, according to (3), (4), and (5), at the instant when the system starts to move away from the function extremum, the rate $\dot{z} = \dot{y} - \dot{y}_k$ increases, and this increases the ratio of the useful signal to the interference.

The interference rejection of the system relative to high frequencies is also due to the fact that the real transfer function of the dynamic transformation of the input signal differs from (1), and has the form

$$W_2(p) = K_t \frac{p\tau}{(1 + p\tau)(1 + p\tau_1 + p^2\tau_2^2)}$$

because of the capacity and inductance in the electrical elements or the mass of the mechanical parts.

A device with this type of transfer function filters out the high-frequency components of the input signal, and this lowers the effect of the interference discussed above.

We will now consider the particular features of the process occurring during the function-extremum search, when low-frequency disturbances are present.

Low-frequency disturbances, which can be represented by a linear function of the time [1], only have an

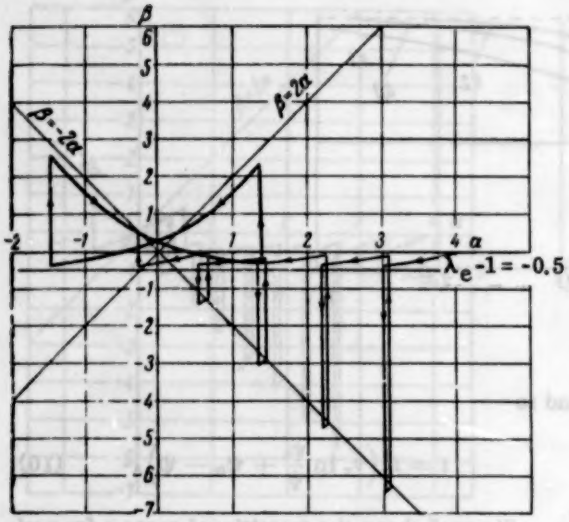

Fig. 7.

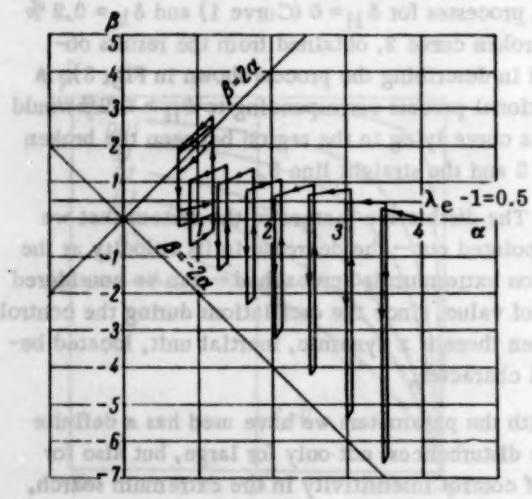

Fig. 8.

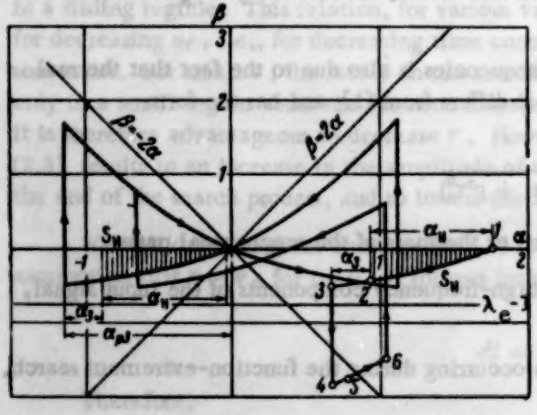

Fig. 9. Phase trajectories of a system with delay.

insignificant influence on control processes during an initial period of time, less than $(1.5\text{-}2.5)\tau$. After this, because of the differentiation of the signal $\underline{y}$ [1], they yield at the input to the control only a constant component, to which the control does not react.

The control process in the system we are considering depends basically on the size of the second derivative of the function describing the influence of the disturbance. The second derivative is constant when the external disturbance is a quadratic function of the time

$$f_e(t) = K_e t^2. \qquad (11)$$

If the reaction of the system to an external disturbance of this type is known, then it is possible [3] to obtain an approximation to the influence on the control process of certain other low-frequency, external disturbances, of a harmonic form, for example with a period of the order of the reversal time of the executive unit (t_c).

The phase trajectories of the system in the coordinates α and β, for the external disturbance (11), are given by the equation

$$\beta = (\beta_0 + 1 - \lambda_e)\exp(-\Delta\alpha) - 1 + \lambda_e \qquad (12)$$

where

$$\lambda_e = \frac{K_e}{K_x V_x^2}.$$

In Fig. 7 we show the process during the search for the function extremum for $\lambda_e = 0.5$, and with the other parameters of the system the same as in the case illustrated in Fig. 3. It is evident that the phase trajectories are characterized by fewer false responses, and so the search process proceeds more rapidly. However, the amplitude of the oscillations of the system about the extremum in the limit cycle is increased, with a corresponding decrease in control precision.

This is the type of process that occurs for $\lambda_e < 1$. If $\lambda_e \geq 1$, then the asymptotic exponent is the straight line $\beta = \lambda_e - 1$, located above the horizontal axis. In this case, after β becomes positive, the system cannot reverse for any motion of the executive unit when there is no commutator; the stability of the control system is therefore lost.

When there is a commutator that forces a reversal of the system for a definite time t_k, the system also retains its stability for $\lambda_e > 1$. In Fig. 8 we show the transitional process in a system with a commutator with $\lambda_e = 1.5$ and $t_k = 0.5\tau$, and the remaining parameters the same as in the cases shown in Figs. 3 and 7. The search process proceeds relatively rapidly with small reverse motions of the executive unit. At the end of the search

process, a limiting cycle is established at a certain distance from the function extremum. This example clearly shows the positive action of the commutator.

The phase trajectories can be obtained similarly for cases when $\lambda_e < 0$, and they show that more false responses in the search process are obtained when $\lambda_e > 0$. In addition, the oscillation amplitudes of the system in the limiting cycle are not increased, but decreased, and so the precision of the control is increased.

We now investigate the influence on the search process of delays in the control response and in the transfer of the signal to the object. As is known, we can, in this way, obtain an approximation to the inertia of the executive unit.

Let the total delay time be t_d. Then the executive commands are delayed by the time t_d for each reversal, and the executive unit is displaced by the supplementary amount α_d. Since $|\dot{x}| = \text{const}$, then $|\Delta x_d = \pm V_x t_d$, and thus,

$$\alpha_d = \pm \frac{t_d}{\tau}.$$

The influence of delay on the control process is shown in Fig. 9.

We consider the motion of a system, starting at the instant when its state is given by the point 1 located on the horizontal axis. The system reverses, in the presence of a delay, not at the point 2 corresponding to a change in area between the curve for β and the horizontal axis equal to S_H, but at the point 3, and later, not at the point 5, but at 6, etc. At the final part of the search process, a limiting cycle is established with the increased oscillation amplitude α_{pd}.

From the phase-trajectory equations, taking into account the above conditions for the switching of the system, we have

$$\exp(-\alpha_H) \cdots \alpha_H = \frac{\delta_H}{2\eta v_\tau^2 (1-\lambda_e)} + 1, \tag{13}$$

$$\frac{2\alpha_{pd}}{\exp(\alpha_{pd}) - 1} = (1-\lambda_e) \exp(-\alpha_H - \alpha_d). \tag{14}$$

In order to find α_{pd}, we determine α_H from (13), and then solve the equation (14).

We can similarly determine the parameters for steady motion of the system for the case when we have a commutator. In this case, as in the case when there is no delay, three regimes of operation of the system are possible, depending on the relation between their parameters.

If $\alpha_k = \frac{t_k}{\tau} > 2\alpha_{pd}$, then the commutator in the limiting cycle is set only for each reverse of the signal relay, and does not operate.

If

$$\alpha_H + \alpha_d < \alpha_\kappa < 2\alpha_{pd} \tag{15}$$

then there is a continuum of periodic motions. At the same time, the coordinates of the reverse points removed from the function extremum are in the range $\pm\alpha_{pd}$, where

$$\alpha_{kd} = \frac{\alpha_\kappa}{1-\exp(-\alpha_\kappa)} - 0{,}5(1-\lambda_e)[1+\exp(\alpha_\kappa)]\exp(-\alpha_H - \alpha_d). \tag{16}$$

If $\alpha_k < \alpha_H + \alpha_d$, then (16) ceases to have any meaning, and the quantity α_{kd} for the corresponding continuum of periodic motions is given by

$$\alpha_{kd} = \frac{\alpha_\kappa}{1-\exp(-\alpha_\kappa)} + 0{,}5\left[\frac{\frac{\delta_\kappa}{2\eta v_\tau^2} - (1-\lambda_e)(\alpha_\kappa - \alpha_d)}{1-\exp(-\alpha_\kappa + \alpha_d)}\right][1+\exp(-\alpha_\kappa)]. \tag{17}$$

The maximum accuracy of control, when there are external disturbances and a delay, corresponds to the optimal value of the time constant τ for the dynamic transformation of the input signal, which can be obtained by calculation, using formulas (13), (14), (16), and (17).

LITERATURE CITED

1. A. P. Yurkevich, Dynamic Converters for the Input Signal in the Case of Extremum Control, Publications of the S. Ordzhonikidze MAI No. 120 (edited by B. A. Ryabov) (Oborongiz, 1960).
2. A. P. Yurkevich, "Processes of extremal control with dynamic transformation and memory of the input signal in the presence of disturbances," Doklady Akad. Nauk SSSR 133, No. 6 (1960).
3. A. P. Yurkevich, "The dynamics of extremal-control systems with a memory in the case of low-frequency external disturbances," Izvest. Akad. Nauk SSSR, OTN, Énergetika i Avtomatika, No. 6 (1960).
4. V. V. Kazakevich, "Extremal control of inertial and unstable objects," Doklady Akad. Nauk SSSR 133, No. 4 (1960).

All abbreviations of periodicals in the above bibliography are letter-by-letter transliterations of the abbreviations as given in the original Russian journal. *Some or all of this periodical literature may well be available in English translation.* A complete list of the cover-to-cover English translations appears at the back of this issue.

LIMITING DYNAMIC CHARACTERISTICS OF POWER SERVO SYSTEM COMPONENTS. II.

G. A. Nadzhafova (Baku)

Translated from Avtomatika i Telemekhanika, Vol. 22, No. 2, pp. 185-198, February, 1961
Original article submitted July 8, 1960

In this article, we determine the dynamic characteristics of separately excited dc control mechanisms loaded by the moments of the forces of dry friction. We present the results obtained during an experimental study of the limiting characteristics of servo drives.

In the first part of this paper [1] we examined the limiting dynamic characteristics of follower servomechanism response for limited moment, speed of revolution, and armature voltage. We found the limiting response speed of such servomechanisms to the class of functions of the type $A_{glv} = A_0 + A_1 t$. We assumed that the mechanisms were loaded by inertial forces and statistical opposing moments created by the overbalancing load.

In the second part of the paper we studied the same servomechanism under the same limitations, but it had to overcome the inertial force and loading created by the moments of the dry friction forces ($J \neq 0$, $M_n = M_T \sin \omega$). The influence of the dry friction forces upon the servomechanism response speed was studied in [2,3].

The theoretical studies are outlined in [1], and also the study of the actions of a motor loaded by dry friction moments, corresponding to the ideal case: the motor is fed from an infinite power source and the inductance of the motor armature is considered infinitely small.

In actual followers, the servomechanism is not fed from an infinite power source, but from a special source whose dynamic characteristics influence the response speed of the follower.

In order to clarify the influence of the inductive circuit of the motor armature and of the time constant upon the limiting response speed of the follower, we made an experimental study of a typical follower.

As a result of the experimental study, we determined the influence of the time constants; this factor had not been taken into account in the theoretical study, but we were able to make an estimate of the limiting response speed, which took this factor into account.

1. Equation for the Isochrone Regions

Using the dimensionless variables of [1], the equation of motion of a servomechanism for the case where there is a moment due to the forces of dry friction has the form

$$\frac{d^2x}{d\tau^2} + \frac{dx}{d\tau} = u - \varphi - i_\tau \sin \quad (y + \varphi)$$

or

$$\frac{d^2x}{d\tau^2} = i_a - i_\tau \sin \quad (y + \varphi),$$

where

$$\frac{dx}{d\tau} = y.$$

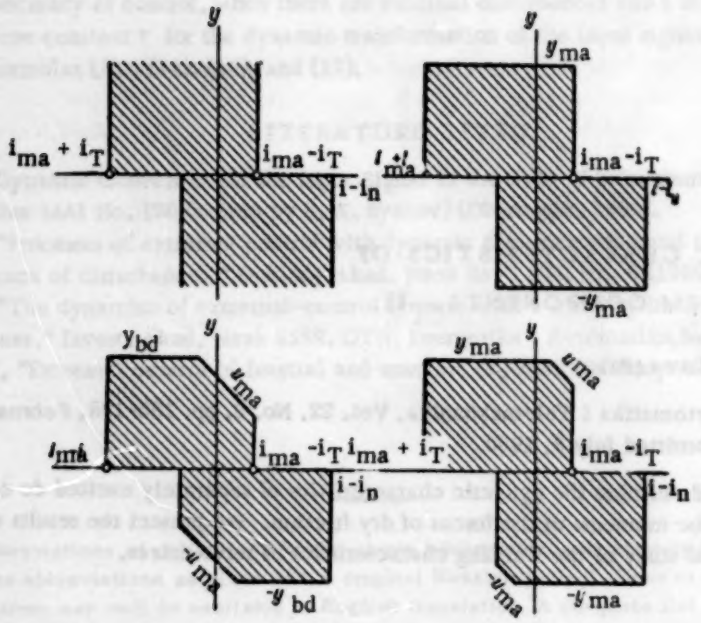

Fig. 1. Regions where motion is restricted.

The imposition of limitations upon the coordinate system, which are associated with the mechanical characteristics of the servomechanism, limit the region of allowed values to polygons for the case of limited moments and speeds; moments and voltages; and voltage, moment, and velocity; for the case where only the moments are restricted, this region is an open region (Fig. 1).

In order to evaluate the limiting response speed of the servomechanism, we will use the isochrone method [4].

During the operation of a motor loaded by the forces of dry friction, in contrast to the case considered before, the boundaries of the isochrone regions are not constructed from two equations corresponding to forward and reverse controls, but from a great number of equations which are determined not only by the controls, but also by the sign of the angular velocity.

Both for forward and reverse motion, the branches of the isochrone boundaries consist of two curve segments corresponding to the regions of initial speed differences, and are determined by the inequalities $y_0 + \varphi < 0$ and $y_0 + \varphi > 0$.

The boundaries of the isochrone regions for the case where only the moment of the motor motion is bounded are described by means of the following equations. For motion in the forward direction (or forward control law), where $y_0 + \varphi > 0$,

$$x_0 = \frac{y_0^2}{4i_{ma}} - \frac{y_0}{2}\left(1 + \frac{i_\tau}{i_{ma}}\right)\beta_* - \frac{i_{ma}^2 - i_\tau^2}{4i_{ma}}\beta^2; \quad (1)$$

where $y_0 + \varphi < 0$,

$$x_0 = \frac{y_0^2}{4i_{ma}} - \frac{y_0}{2}\left(1 - \frac{i_\tau}{i_{ma}}\right)\beta_* - \frac{i_{ma}^2 - i_\tau^2}{4i_{ma}}\beta_*^2 + \frac{i_\tau}{i_{ma}(i_{ma} + i_\tau)}(\varphi^2 + \varphi y_0). \quad (2)$$

For motion in the reverse direction (or reverse control law), where $y_0 + \varphi > 0$,

$$x_0 = -\frac{y_0^2}{4i_{ma}} - \frac{y_0}{2}\left(1 - \frac{i_\tau}{i_{ma}}\right)\beta_* + \frac{i_{ma}^2 - i_\tau^2}{4i_{ma}}\beta_*^2 + \frac{2i_\tau y_0 \varphi}{(i_{ma} - i_\tau)^2} + \frac{\varphi^2}{i_{ma} + i_\tau}; \quad (3)$$

where $y_0 + \varphi < 0$,

$$x^0 = -\frac{y_0^2}{4i_{ma}} - \frac{y_0}{2}\left(1 + \frac{i_\tau}{i_{ma}}\right)\beta + \frac{i_{ma}^2 - i_\tau^2}{4i_{ma}}\beta_*^2 - \frac{i_\tau}{i_{ma}}\varphi\beta_* + \frac{i_\tau(y_0\varphi + \varphi^2)}{i_{ma}(i_{ma} - i_\tau)}. \quad (4)$$

The boundaries of the isochrone regions for the case where the moment of the motion and the angular velocity of the motor are bounded, may be described by means of the following equations.

For motion in the forward direction, where $y_0 + \varphi > 0$,

$$x_0 = \frac{(y_0 - y_{ma})^2}{2(i_{ma} - i_\tau)} - y_{ma}\beta_* + \frac{y_{ma}^2}{2(i_{ma} + i_\tau)}; \quad (5)$$

where $y_0 + \varphi < 0$,

$$x_0 = \frac{(y_0 - y_{ma})^2}{2(i_{ma} + i_\tau)} - y_{ma}\beta_* + \frac{y_{ma}^2}{2(i_{ma} + i_\tau)} + \frac{i_\tau(\varphi^2 + 2y_{ma}\varphi)}{i_{ma}^2 - i_\tau^2}. \quad (6)$$

For motion in the reverse direction, where $y_0 + \varphi > 0$,

$$x_0 = -\frac{(y_0 + y_{ma})^2}{2(i_{ma} + i_\tau)} - \frac{y_{ma}^2}{2(i_{ma} - i_\tau)} + y_{ma}\beta_* - \frac{\varphi^2}{i_{ma} + i_\tau}; \quad (7)$$

where $y_0 + \varphi < 0$,

$$x_0 = -\frac{(y_0 + y_{ma})^2}{2(i_{ma} - i_\tau)} - \frac{y_{ma}^2}{2(i_{ma} + i_\tau)} + y_{ma}\beta_* + \frac{i_\tau(\varphi^2 - 2y_{ma}\varphi)}{i_{ma}^2 - i_\tau^2}. \quad (8)$$

The boundaries of the isochrone regions for the case where the moment of the motor motion and the voltage supplied to the armature circuit are described by the following equations.

For the direct control law, where $y_0 + \varphi > 0$,

$$x_0 = \frac{(y_0 - y_x)^2}{2(i_{ma} - i_\tau)} - y_0 + (\varphi - u_{ma} + i_\tau)\beta_* - \frac{y^2}{2(i_{ma} + i_\tau)} + \frac{(u_{ma} - \varphi + i_{ma})y}{i_{ma} + i_\tau}; \quad (9)$$

where $y_0 + \varphi < 0$,

$$x_0 = \frac{(y_0 - y_x)^2}{2(i_{ma} + i_\tau)} - \frac{(i_{ma} - i_\tau)y_0}{i_{ma} + i_\tau} + (\varphi - u_{ma} + i_\tau)\beta_* - \frac{y^2}{2(i_{ma} + i_\tau)} + \frac{(u_{ma} - \varphi + i_\tau)y}{i_{ma} + i_\tau} + \frac{i_\tau(y_x + \varphi)^2}{i_{ma}^2 - i_\tau^2} + \frac{2i_\tau\varphi}{i_{ma} + i_\tau}. \quad (10)$$

For motion in the reverse direction, where $y_0 + \varphi > 0$,

$$x_0 = -\frac{y_0^2 - y^2}{2(i_{ma} + i_\tau)} - \frac{(y_0 - y)(u_{ma} + \varphi - i_\tau)}{i_{ma} + i_\tau} + (\varphi + u_{ma} - i_\tau)\beta_* - \frac{(u_{ma} - i_{ma})^2}{2(i_{ma} - i_\tau)} - \frac{(u_{ma} - i_\tau)\varphi}{i_{ma} - i_\tau} + \varphi + y; \quad (11)$$

where $y_0 + \varphi < 0$,

$$x_0 = -\frac{y_0^2}{2(i_{ma} - i_\tau)} + \frac{y^2}{2(i_{ma} + i_\tau)} - \frac{y_0\varphi}{i_{ma} - i_\tau} - \frac{(y_0 + \varphi)(u_{ma} - i_{ma})}{i_{ma} - i_\tau} + (\varphi + u_{ma} - i_\tau)\beta_* - \frac{(i_{ma} + i_\tau)\varphi^2}{2(i_{ma} - i_\tau)^2} + \frac{(u_{ma} - i_{ma})^2}{2(i_{ma} - i_\tau)}. \quad (12)$$

For a bounded moment of motion, the boundaries of the allowed region for the voltage and angular velocity of the motor are described by the following equations.

For motion in the forward direction, where $y_0 + \varphi > 0$,

$$x_0 = \frac{(y_0 - y_x)^2}{2(i_{ma} - i_\tau)} - y_0 + \frac{(y_0 - y_x)(u - y_{ma} - \varphi - i_\tau)}{i_{ma} - i_\tau} - y_{ma}\beta_* + y_{ma} + \frac{y_{ma}^2}{2(i_{ma} + i_\tau)} + (y_{ma} - u_{ma} + \varphi + i_\tau) \ln \frac{i_{ma} - i_\tau}{u - \varphi - y_{ma} - i_\tau}; \quad (13)$$

where $y_0 + \varphi < 0$,

$$x_0 = \frac{(y_0 - y_{ma})^2}{2(i_{ma} + i_\tau)} - y_{ma}\beta_* + y_{ma} + \varphi + \frac{(u - i_{ma})(y_{ma} - u + \varphi + i_\tau)}{i_{ma} - i_\tau} + \frac{(u - i_{ma})^2}{2(i_{ma} + i_\tau)} - \frac{y_{ma}\varphi}{i_{ma} + i_\tau} - \frac{\varphi^2}{2(i_{ma} + i_\tau)} + (y_{ma} - u + \varphi + i_\tau) \ln \frac{i_{ma} - i_\tau}{u - \varphi - y_{ma} - i_\tau}. \quad (14)$$

For motion in the reverse direction, where $y_0 + \varphi > 0$,

$$x_0 = -\frac{(y_0 + y_{ma})^2}{2(i_{ma} + i_\tau)} + y_{ma}\beta_* - y_{ma} + \varphi + \frac{(u - i_{ma})(u - i_\tau + \varphi - y_{ma})}{i_{ma} - i_\tau} - \frac{(u - i_{ma})^2}{2(i_{ma} - i_\tau)} - \frac{y_{ma}\varphi}{i_{ma} + i_\tau} + \frac{\varphi^2}{2(i_{ma} - i_\tau)} + (u - i_\tau + \varphi - y_{ma}) \ln \frac{i_{ma} - i_\tau}{u - \varphi - y_{ma} - i_\tau}; \quad (15)$$

where $y_0 + \varphi < 0$,

$$x_0 = -\frac{y_0^2}{2(i_{ma} - i_\tau)} - \frac{y_{ma} y_0}{i_{ma}} - y_{ma}\beta_* \cdot \frac{y_{ma}^2}{2(i_{ma} + i_\tau)} + y_{ma}\beta_* - y_{ma} + \varphi + \frac{(u - i_{ma})(u - i_\tau + \varphi - y_{ma})}{i_{ma} - i_\tau} - \frac{(u - i_{ma})^2}{2(i_{ma} - i_\tau)} - \frac{y_{ma}\varphi}{i_{ma} - i_\tau}\left(1 + \frac{2i_\tau}{i_{ma} + i_\tau}\right) - \frac{2i_\tau^2\varphi^2}{(i_{ma} - i_\tau)^2(i_{ma} + i_\tau)} + \frac{(i_{ma} + i_\tau)\varphi^2}{2(i_{ma} - i_\tau)^2} + (u - y_{ma} - i_\tau + \varphi) \ln \frac{i_{ma} - i_\tau}{u - y_{ma} - i_\tau + \varphi}. \quad (16)$$

2. Equations of the Boundary Regions for the Various Modes of Operation

The boundaries of the time regions of the isochrones for all the cases which we have examined coincide with the times found in [1].

The boundaries of the regions for the various modes of operation, in contrast to those examined in [1], may be found from four equations.

The boundary separating the mode of operation in which only the moment is bounded from that region where two variables are bounded (moment and angular velocity) is described by means of the following equations.

For motion in the forward direction, where $y_0 + \varphi > 0$,

$$x_0 = \frac{y_0^2}{2(i_{ma} - i_\tau)} - \frac{2y_{ma}^2 i_{ma}^2}{(i_{ma} + i_\tau)^2(i_{ma} - i_\tau)} + \frac{y_{ma}^2 i_{ma}}{(i_{ma} + i_\tau)^2}; \quad (17)$$

where $y_0 + \varphi < 0$,

$$x_0 = \frac{y_0^2}{2(i_{ma} + i_\tau)} - \frac{y_{ma}^2 i_{ma}}{i_{ma}^2 - i_\tau^2} + \frac{i_\tau \varphi^2}{i_{ma}^2 - i_\tau^2}. \quad (18)$$

For motion in the reverse direction, where $y_0 + \varphi > 0$,

$$x_0 = -\frac{y_0^2}{2(i_{ma} + i_\tau)} + \frac{y_{ma}^2 i_{ma}}{i_{ma}^2 - i_\tau^2} - \frac{\varphi^2}{i_{ma} + i_\tau}; \quad (19)$$

where $y_0 + \varphi < 0$,

$$x_0 = -\frac{y_0^2}{2(i_{ma} - i_\tau)} - \frac{y_{ma}^2 i_{ma}}{i_{ma}^2 - i_\tau^2} + \frac{i_\tau \varphi^2}{i_{ma}^2 - i_\tau^2}. \quad (20)$$

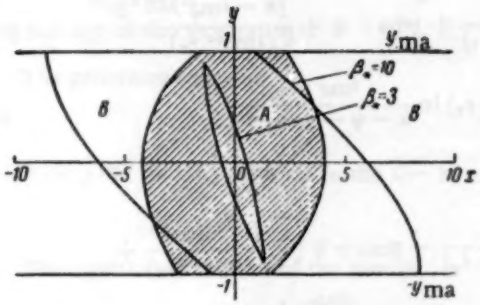

Fig. 2. Boundaries of the isochrone regions and boundaries of the regions of operation for the case where the moment and velocity are restricted ($i_{ma} = 0.25$; $i_T = 0.05$; $\varphi = 0$; $y_{ma} = 1$).

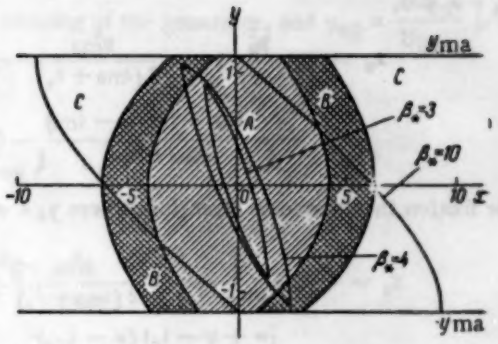

Fig. 3. Boundaries of the isochrone regions and boundaries of the regions of operation for the case where the moment, voltage, and velocity are restricted ($i_{ma} = 0.25$; $i_T = 0.05$; $\varphi = 0$; $u_{ma} = 1.25$; $y_{ma} = 1.15$).

When the servomechanism is overcoming large differences, where limitations are imposed upon three variables (moment, voltage, and velocity), as well as for the case where limitations are imposed upon two variables (moment and voltage), there are two boundary lines.

For motion in the forward direction, where $y_0 + \varphi > 0$,

$$x_0 = \frac{y_0^2 - y_x^2}{2(i_{ma} - i_T)} - \frac{y_x^2}{2(i_{ma} + i_T)}; \tag{21}$$

where $y_0 + \varphi < 0$,

$$x_0 = \frac{y_0^2}{2(i_{ma} + i_T)} - \frac{y_x^2}{2(i_{ma} - i_T)} + \frac{i_T \varphi^2}{i_{ma}^2 - i_T^2}. \tag{22}$$

For motion in the reverse direction, where $y_0 + \varphi > 0$,

$$x_0 = -\frac{y_0^2}{2(i_{ma} + i_T)} + \frac{y_x^2}{2(i_{ma} + i_T)} + \frac{(u - i_T + \varphi) y_x}{i_{ma} - i_T} - \frac{(u - i_{ma})^2}{2(i_{ma} - i_T)} - y_x + \varphi + \frac{\varphi^2}{2(i_{ma} - i_T)}; \tag{23}$$

where $y_0 + \varphi < 0$,

$$x_0 = -\frac{y_0^2}{2(i_{ma} - i_T)} + \frac{y_x^2}{2(i_{ma} + i_T)} + \frac{(u - i_T)(u - i_{ma} + \varphi)}{i_{ma} - i_T} - \frac{(u - i_{ma})^2}{2(i_{ma} - i_T)} - y_x + \frac{(i_{ma} + i_T)\varphi^2}{2(i_{ma} - i_T)^2} - \frac{2i_T^2 \varphi^2}{(i_{ma} - i_T)^2 (i_{ma} + i_T)}. \tag{24}$$

The boundary separating a region where limitations are imposed upon two variables (moment and voltage) from a region where limitations are imposed upon three variables (moment, voltage, and angular velocity) is described by means of the following equations.

For motion in the forward direction, where $y_0 + \varphi > 0$,

$$x_0 = \frac{y_0^2}{2(i_{ma} - i_T)} - \frac{y_{ma}^2}{2(i_{ma} + i_T)} - \frac{\varphi^2}{2(i_{ma} - i_T)} + y_{ma} + \varphi + \frac{(u + i_{ma})^2}{2(i_{ma} - i_T)} - \frac{(u - \varphi - i_T)(u - i_{ma})}{i_{ma} - i_T} - (u - \varphi - i_T) \ln \frac{i_{ma} - i_T}{u - \varphi - y_{ma} - i_T}, \tag{25}$$

where $y_0 + \varphi < 0$,

$$x_0 = \frac{y_0^2}{2(i_{ma}+i_\tau)} - \frac{y_{ma}^2}{2(i_{ma}+i_\tau)} - \frac{\varphi^2}{2(i_{ma}+i_\tau)} + y_{ma} + \varphi + \frac{(u-i_{ma})^2}{2(i_{ma}-i_\tau)} - \frac{(u-\varphi-i_\tau)(u-i_{ma})}{i_{ma}-i_\tau} - (u-\varphi-i_\tau)\ln\frac{i_{ma}-i_\tau}{u-\varphi-y_{ma}-i_\tau}. \quad (26)$$

For motion in the reverse direction, where $y_0 + \varphi > 0$,

$$x_0 = -\frac{y_0^2}{2(i_{ma}+i_\tau)} + \frac{y_{ma}^2}{2(i_{ma}+i_\tau)} + \frac{\varphi^2}{2(i_{ma}-i_\tau)} - y_{ma} + \varphi - \frac{(u+i_{ma})^2}{2(i_{ma}-i_\tau)} + \frac{(u+\varphi-i_\tau)(u-i_{ma})}{i_{ma}-i_\tau} + (u-i_\tau+\varphi)\ln\frac{i_{ma}-i_\tau}{u-\varphi-y_{ma}-i_\tau}; \quad (27)$$

where $y_0 + \varphi < 0$,

$$x_0 = -\frac{y_0^2}{2(i_{ma}-i_\tau)} + \frac{y_{ma}^2}{2(i_{ma}-i_\tau)} - \frac{2i_\tau^2\varphi^2}{(i_{ma}-i_\tau)^2(i_{ma}+i_\tau)} - y_{ma} + \varphi - \frac{(u-i_{ma})^2}{2(i_{ma}-i_\tau)} + \frac{(i_{ma}+i_\tau)\varphi^2}{2(i_{ma}-i_\tau)^2} + (u-i_\tau+\varphi)\ln\frac{i_{ma}-i_\tau}{u-y_{ma}-i_\tau+\varphi} \quad (28)$$

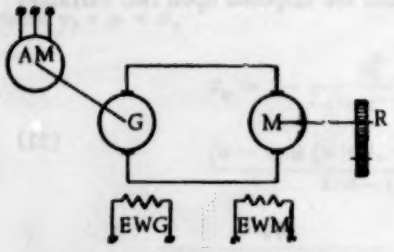

Fig. 4. Servomechanism circuit: AM) asynchronous motor; G) separately excited dc generator; M) separately excited dc motor; R) reducer, EWG) generator exciting winding; EWM) motor exciting winding.

In Figure 2 we split the phase-plane regions according to the phase trajectory for optimum operation for the case where the moment and velocity are limited. In the same figure we give examples of isochrone regions corresponding to various modes of operation.

In Fig. 3 we show the subdivision of the phase plane into regions for the case of a servomechanism which has three bounded coordinates. In the dashed region A, only the moment is limited; in the cross-hatched regions B, two coordinates are limited, for example the moment and the voltage; while in region C there are three bounded coordinates: moment, voltage, and velocity. In the same figure, we give the isochrone regions for all three cases.

3. Experimental Investigation

Experimental investigations were carried out with the aim of studying the influence of the electrical transitional processes occurring in the motor armature circuit during changes in the control voltage, and also to determine the influence of a constant excitation time for the windings of the generator, which feed the motor, upon the dynamic characteristics of the servomechanism.

The experiments were carried out using the electronic modulating device of the type IPT-5.

The circuit of the servomechanism under study is shown in Fig. 4.

The system under study is described by means of the following equations, which are written in dimensionless coordinates:

Equation for the motor-armature circuit

$$T_1 \frac{di_a}{d\tau} + i_a = u - y - \varphi, \quad (29)$$

where $T_1 = \frac{L_a}{R_a T_{bas}}$ is the time constant of the motor-armature circuit;

Equation for the exciting circuit of the generator

$$T_2 \frac{di_{eg}}{d\tau} + i_{eg} = u_{eg}, \quad (30)$$

where $T_2 = \frac{L_{eg}}{R_{eg}T_{bas}}$ is the time constant of the exciting winding of the generator, and $u_{eg} = \frac{U_{eg}}{U_{bas}}$ is the exciting voltage of the generator;

The generator equation

$$e_g = i_{eg}; \tag{31}$$

During the motor operation in the G – M circuit

$$u = e_g; \tag{32}$$

The equation of motion of the motor

$$\frac{d^2x}{d\tau^2} = i_a - i_n. \tag{33}$$

Eliminating the intermediate coordinates from Eqs. (29)-(33), and rearranging, we get the following equation for the G – M system:

$$T_1T_2\frac{d^4x}{d\tau^4} + (T_1 + T_2)\frac{d^3x}{d\tau^3} + (1 + T_2)\frac{d^2x}{d\tau^2} + \frac{dx}{d\tau} = u_{eg} - i_n - \varphi. \tag{34}$$

We studied the following particular cases of Eq. (34).

A. $T_1 = 0$, $T_2 = 0$, i.e., the motor is fed from an infinite power source, and the inductance of the armature circuit is equal to zero.

In this case, the equation takes the form

$$\frac{d^2x}{d\tau^2} + \frac{dx}{d\tau} = u - i_n \tag{34'}$$

B. $T_2 = 0$, $T_1 \neq 0$, i.e., the motor is fed from an infinite power circuit, but the inductance of the motor armature circuit is taken into account:

$$T_1\frac{d^3x}{d\tau^3} + \frac{d^2x}{d\tau^2} + \frac{dx}{d\tau} = u - i_n \tag{34''}$$

C. $T_2 \neq 0$, $T_1 \neq 0$. Equation (34) applies to this case.

We investigated the cases for $i_n = 0$, $i_n = \text{const}$, and $i_n = i_T \sin y$, where limitations were imposed*:

a) only upon the moment of the motor

$$\left|\frac{d^2x}{d\tau^2}\right| \leqslant i_{ma}$$

b) upon the moment and angular velocity of the motor

$$\left|\frac{d^2x}{d\tau^2}\right| \leqslant i_{ma} \quad \text{and} \quad \left|\frac{dx}{d\tau}\right| \leqslant y_{ma}$$

c) the moment of the motor and the voltage applied to the motor armature

$$\left|\frac{d^2x}{d\tau^2}\right| \leqslant i_{ma} \quad \text{and} \quad |u| \leqslant u_{ma}$$

d) the moment, the voltage applied to the motor armature, and the angular velocity of the motor

$$\left|\frac{d^2x}{d\tau^2}\right| \leqslant i_{ma}, \quad |u| \leqslant u_{ma} \quad \text{and} \quad \left|\frac{dx}{d\tau}\right| \leqslant y_{ma}$$

*In the experiments we assumed, for simplicity, that $\varphi = 0$.

The motor was controlled by changing the voltage applied to the motor armature for a constant excitation current. Therefore, when the motor was fed from an infinite power source, the motor was controlled by changes in the voltage u, while, in the case where the motor operated as part of the G − M circuit, the motor was controlled by changes in the voltage supplied to the exciting winding of the generator.

In our investigations we assumed that the working portion of the no-load generator characteristics was linear.

In order to evaluate the effects of the various parameters, we compared the boundaries of the isochrone regions which we obtained experimentally with those for the idealized case ($T_1 = 0$, $T_2 = 0$) (derived analytically).

The equations for the control voltage was formulated according to the equations obtained for the case $T_1 = 0$ and $T_2 = 0$. The laws of change of the controlling voltage depend upon the character of the load (further on we examine the cases where i_n = const and $i_n = i_T \sin y$), and have the following form.

For the case where only the motor moment is limited:

a) i_n = const

$$u(\tau) = \begin{cases} i_n & \text{for } \tau < 0, \\ i_{ma} + (i_{ma} - i_n)\tau & \text{for } 0 < \tau < \tau_1, \\ -i_{ma} + (i_{ma} - i_n)\tau_1 - (i_{ma} + i_n)(\tau - \tau_1) & \text{for } \tau_1 < \tau < \tau_*; \end{cases} \tag{35}$$

b) $i_n = i_T \sin y$

$$u(\tau) = \begin{cases} i_n & \text{for } \tau < 0, \\ i_{ma} + (i_{ma} - i_T)\tau & \text{for } 0 < \tau < \tau_1, \\ -i_{ma} + (i_{ma} - i_T)\tau_1 - (i_{ma} + i_T)(\tau - \tau_1) & \text{for } \tau_1 < \tau < \tau_1' \\ & \quad y = 0 \\ -i_{ma} + (i_{ma} - i_T)\tau_1 - (i_{ma} + i_T)\tau_1' - (i_{ma} - i_T)(\tau - \tau_1') & \text{for } \tau_1' < \tau < \tau \\ & \quad \text{and } y < 0. \end{cases} \tag{35'}$$

For the case where the moment and armature voltage are limited:

a) i_n = const

$$u(\tau) = \begin{cases} i_n & \text{for } \tau < 0, \\ i_{ma} + (i_{ma} - i_n)\tau & \text{for } 0 < \tau < \tau_1, \\ u_{ma} & \text{for } \tau_1 < \tau < \tau_2, \\ u_{ma} - i_{ma} - (i_{ma} + i_n\ (\tau - \tau_2) & \text{for } \tau_2 < \tau < \tau_*; \end{cases} \tag{36}$$

b) $i_n = i_T \sin y$

$$u(\tau) = \begin{cases} i_n & \text{for } \tau < 0, \\ i_{ma} + (i_{ma} - i_T)\tau & \text{for } 0 < \tau < \tau_1; \\ u_{ma} & \text{for } \tau_1 < \tau < \tau_2; \\ u_{ma} - i_{ma} - (i_{ma} + i_T)(\tau - \tau_2) & \text{for } \tau_2 < \tau < \tau_2' \\ & \quad \text{to } y = 0, \\ u_{ma} - i_{ma} - (i_{ma} + i_2)(\tau_2' - \tau_2) - (i_{ma} - i_T)(\tau - \tau_2') & \text{for } \tau_2' < \tau < \tau_* \\ & \quad \text{and } y < 0. \end{cases} \tag{36'}$$

For the case where the motor moment and velocity are bounded:

a) i_n = const

$$u(\tau) = \begin{cases} i_n & \text{for } \tau < 0, \\ i_{ma} + (i_{ma} - i_n)\tau & \text{for } 0 < \tau < \tau_1, \\ i_n + (i_{ma} - i_n)\tau_1 & \text{for } \tau_1 < \tau < \tau_2, \\ -i_{ma} - (i_{ma} + i_n)(\tau - \tau_2) & \text{for } \tau_2 < \tau < \tau_*; \end{cases} \tag{37}$$

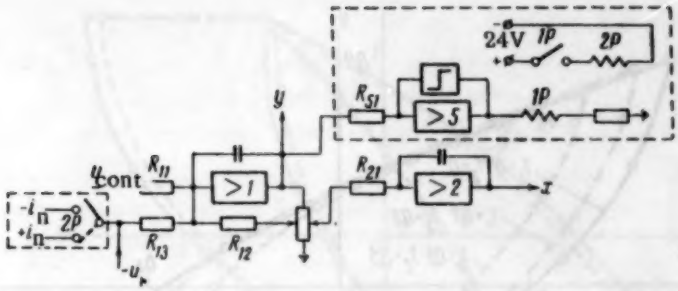

Fig. 5.

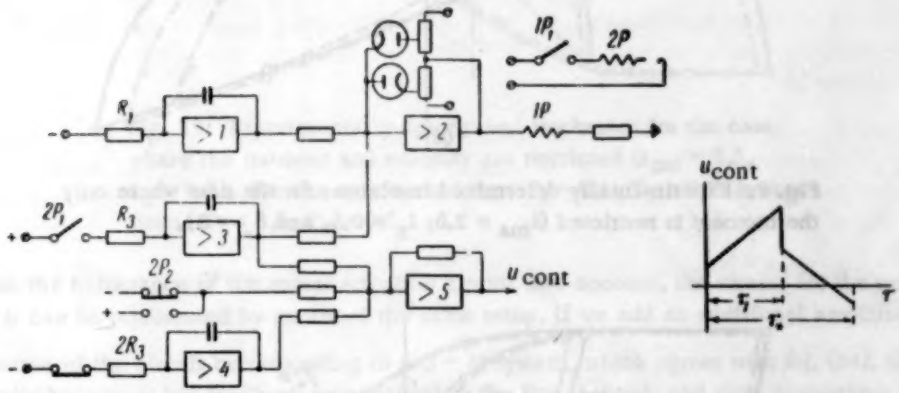

Fig. 6.

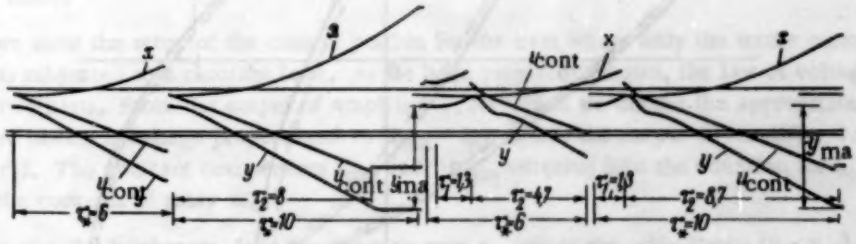

Fig. 7. Oscillograms of the changes in the control voltage, velocity, and difference angle for $i_n = i_T \sin y$, where the moment and velocity are restricted, for various isochrone times ($i_{tr} = 0.1$). Scale: $u_{cont} - 1$ mm = 4 volts; $y - 1$ mm = = 2.74 volts, and $x - 1$ mm = 5.2 volts.

b) $i_n = i_T \sin y$

$$u(\tau) = \begin{cases} i_n & \text{for } \tau < 0, \\ i_{ma} + (i_{ma} - i_\tau)\,\tau & \text{for } 0 < \tau < \tau_1, \\ i + (i_{ma} - i_\tau)\,\tau_1 & \text{for } \tau_1 < \tau < \tau_2, \\ -i_{ma} - (i_{ma} + i_\tau)(\tau - \tau_2) & \text{for } \tau_2 < \tau < \tau_2' \\ & \quad y = 0, \\ -i_{ma} - (i_{ma} + i_\tau)(\tau_2' - \tau_2) - (i_{ma} - i_\tau)(\tau - \tau_2') & \text{for } \tau_2' < \tau < \tau_c, \\ & \quad \text{and } y < 0 \end{cases} \tag{37'}$$

The case where the moment, voltage, and velocity are bounded is not of intrinsic interest, and is a limiting case when the moment and voltage are limited for large time isochrones. Therefore, this case was not investigated experimentally.

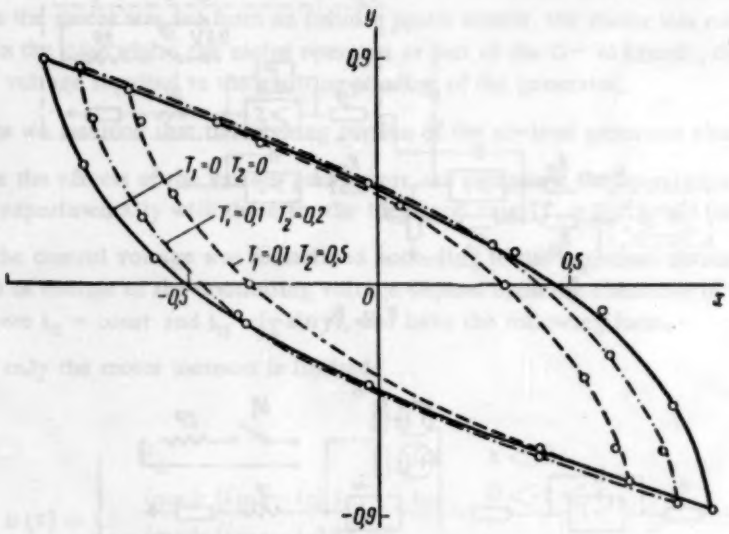

Fig. 8. Experimentally determined isochrones for the case where only the moment is restricted (i_{ma} = 2.5; i_n = 0.5, and β_* = 3).

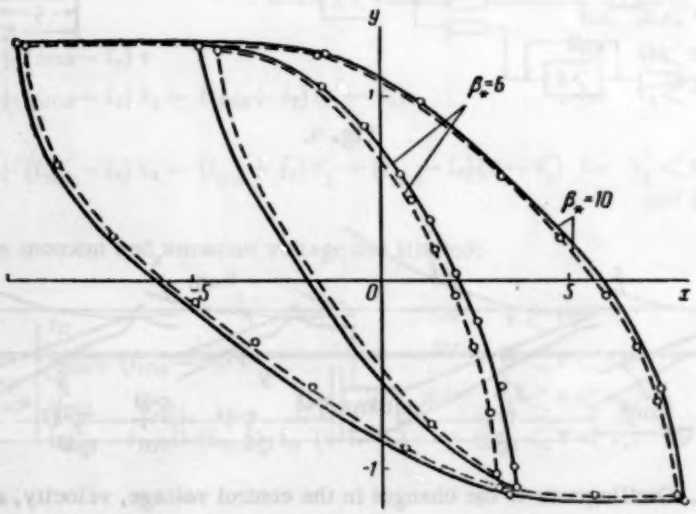

Fig. 9. Experimentally determined isochrones for the case where the moment and voltage are restricted (i_{ma} = 2.5; i_N = 0.5). For the continuous line: T_1 = 0.1, T_2 = 0.2; broken line: T_1 = 0.1, T_2 = 0.5.

4. Circuit of the Setup Involved in the Problem

In Fig. 5 we show the structure of the part of the setup which is force-modulated by an overbalanced load (i_n = const), and fed by an infinite power source for T_1 = 0.

In order to obtain the case where the motor shaft is subjected to a moment ($i_n = i_T \sin y$) due to dry friction, we use the amplifier 5 with a limiter, and relays 1P and 2P, which are used to change the sign of the load during changes in the sign of the velocity. We can change the magnitude of the load within wide limits (from 0 to i_{nom}) with the aid of resistance R_{13}. We obtain from the output of amplifier 1 a voltage corresponding to the velocity, and from the output of amplifier 2 a voltage corresponding to the value of the adjusted angle for an optimum law of change of the control voltage.

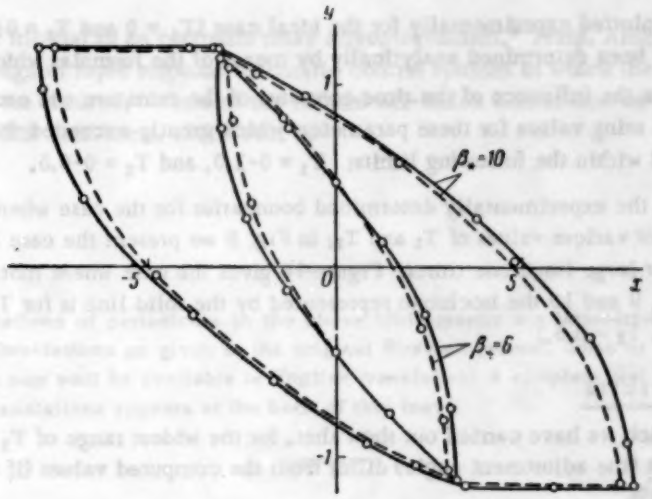

Fig. 10. Experimentally determined isochrones for the case where the moment and velocity are restricted ($i_{ma} = 2.5$, $i_n = 0.5$). For the continuous line: $T_1 = 0.1$, $T_2 = 0.2$; broken line: $T_1 = 0.1$; $T_2 = 0.5$.

If we take the inductance of the motor armature circuit into account, the circuit for the system is given by Eq. (34*), and it can be represented by means of the same setup, if we add an additional amplifier.

The structure of the circuit corresponding to a G – M system, which agrees with Eq. (34), differs from the preceding circuits because it has feedback proportional to the first, second, and third derivatives with respect to $\underline{x}$.

On the basis of the expressions obtained above, we built a model of the control parts of the optimum system. The control circuit was subject to change, the changes depending upon the number of bounded coordinates and the character of the loads.

In Fig. 6 we show the setup of the control portion for the case where only the motor moment is bounded, and the motor shaft is subjected to a constant load. As we have previously shown, the law of voltage change for this case consists of two parts. From the output of amplifier 3, for which we choose the appropriate coefficient of amplification, we obtain a voltage proportional to $(i_{ma} - i_n)$, while the output of amplifier 4 is proportional to $(i_{ma} + i_n)(\tau - \tau_1)$. The constant components i_{ma} and $-i_{ma}$, entering into the equation for u_{cont}, are obtained with the aid of the contacts of relay $2R_2$.

In order to plot the isochrones, it is necessary to vary τ_1 within the wide limits $(0 - \tau_*)$, and this we can do with the aid of a comparison circuit which uses the outputs of amplifiers 1 and 2 and a diode limiter and relays 1P and 2P. The law of change of the controlling voltage is obtained at the output of amplifier 5.

If the motor shaft experiences a moment due to the forces of dry friction, then the circuit becomes somewhat more complicated. In this case, in addition to the two intervals which occur for $i_n = \text{const}$, there is a subinterval in the course of which $u = (i_{ma} + i_T)(\tau - \tau_1')$. This part of the controlling voltage occurs when $y = 0$, and remains until the end of the process, while $y \leq 0$. In order to formulate the controlling law for this subinterval, we make use of a special amplifier which provides a voltage $u = -(i_{ma} + i_T)(\tau - \tau_1')$ for the cases where the moment, voltage, and angular velocity of the motor are limited.

As an example, we present, in Fig. 7, oscillograms* which show the changes in the controlling voltage $\underline{y}$ and $\underline{x}$ for the case where the moment and velocity are limited; for $T_1 = 0.1$, $T_2 = 0.5$, $i_{ma} = 2.5$, $i_T = 1$ for isochrone times $\beta_* = \tau_* = 0.6$ and $\beta_* = \tau_* = 1$. The following scale coefficients are used during modulation: $M_T = 0.1$, $M_x = M_y = M_u = 0.01$.

The boundaries of the isochrone regions were obtained experimentally; we determined the angle of adjustment $\underline{x}$ for various resistance moments (static or dry friction), and at various times during the transitional process.

*In motors used in follower systems $T_1 < 0.1$. The oscillograms in the figure are reduced to 1/3.

The isochrone regions, as plotted experimentally for the ideal case ($T_1 = 0$ and $T_2 = 0$), coincide perfectly with the isochrones which have been determined analytically by means of the formulas which we have derived.

In order to determine the influence of the time constants of the armature and exciting generator windings, we conducted experiments using values for these parameters which greatly exceeded those in actual systems. The time constants were varied within the following limits: $T_1 = 0\text{-}1.0$, and $T_2 = 0\text{-}0.5$.

In Fig. 8 we present the experimentally determined boundaries for the case where only the moment is limited for $\beta_* = \tau_* = 3$ for various values of T_1 and T_2; in Fig. 9 we present the case where the motor moment and voltage are limited for large isochrone times. Figure 10 gives the case where motor moment and velocity are limited. (In both Figs. 9 and 10 the isochrone represented by the solid line is for $T_1 = 0.1$, $T_2 = 0.2$; by the dashed line is for $T_1 = 0.1$, $T_2 = 0.5$.)

5. Experimental Results

The experiments which we have carried out show that, for the widest range of T_1 (0-1.0), the velocity $\underline{y}$ and angular displacement $\underline{x}$ (the adjustment angle) differ from the computed values (if we neglect the armature inductance) by less than 10%.

The electrical transitional processes in the exciting winding influence the operation of the optimum system and, consequently, the estimate of the possible limiting time required for the transitional processes for the case where the difference between the angles is small, i.e., for sufficiently small times $\beta_* < 2$ (the $\underline{x}$ and $\underline{y}$ errors are approximately 25%).

The errors are the result of neglecting the time constants T_1 and T_2, and increase as T_1 and T_2 and the load on the motor shaft increase.

For $\beta_* > 3$, the error does not exceed 10%. Since the voltage and velocity limitations become effective after a time $\beta_* > 3$ then, for a limited moment and voltage, the absolute values of the errors in the moments and velocities for $\underline{y}$ and $\underline{x}$ are less than 10%.

SUMMARY

1. The equations which we have obtained for the isochrones and the region boundaries permit us to evaluate the response speed of an electrical servomechanism loaded by the moments of dry friction. Examining the regions of initial differences and technical requirements, it is not difficult to choose the required servomechanism, or to verify whether a given servomechanism will function satisfactorily with respect to speed of response.

2. The investigation which we have carried out has shown that, during the projection of electrical constant-current, separately excited servo-follower systems we can estimate, with sufficient accuracy, the limiting possibilities of the system from the boundaries of the isochrone regions for the ideal case ($T_1 = 0$ and $T_2 = 0$).

3. In the synthesis of a control with optimum response speed, we may use the point of intersection of the equations of lines which represent the ideal case. This permits us to simplify the control circuit considerably without introducing any basic (significant) errors.

4. Where the motor is fed from an electronics rectifier, the errors will be much lower than for the G – M system, since the rectifier constants are small compared with G – M time constant.

5. There were large errors in $\underline{y}$ and $\underline{x}$ (about 25%) during the processes involved in correcting small errors. Since it is of importance to have a servomechanism with a rapid response for cases where there are large errors, errors in the velocity $\underline{y}$ and adjustment angle $\underline{x}$ in an actual optimum control system do not have a practical meaning.

LITERATURE CITED

1. G. A. Nadzhafova, "The maximum dynamic characteristic values of servomechanism components of servo systems. I," Avtomatika i Telemekhanika 21, No. 7 (1960).
2. R. A. Velershtein and A. A. Fel'dbaum, "The development with the aid of an electronic model of systems which are close to optimum systems," Avtomatika i Telemekhanika 19, No. 9 (1958).

3. T. M. Stout, "Effects of friction in an optimum relay servomechanism," Trans. AIEE 72, Pt. II (1953).
4. A. Ya. Lerner, "The design of rapid response automatic control systems in which the values of the coordinates of the regulated object are limited," Works of the Second All-Union Conference on the Theory of Automatic Regulation [in Russian] (AN SSSR Press, 1955) Vol. 2.

All abbreviations of periodicals in the above bibliography are letter-by-letter transliterations of the abbreviations as given in the original Russian journal. *Some or all of this periodical literature may well be available in English translation.* A complete list of the cover-to-cover English translations appears at the back of this issue.

ELEMENTS AND UNITS OF A DIGITAL COMPUTER ONE-CYCLE PARALLEL ARITHMETIC DEVICE WHICH USES FERRITE TRANSISTOR CELLS

M. I. Petrukhin (Leningrad)

Translated from Avtomatika i Telemekhanika, Vol. 22, No. 2, pp. 199-208, February, 1961
Original article submitted January 22, 1960

In this paper we examine some of the principles involved in the design of one-cycle ferrite transistor cell circuits such as delay elements, unsymmetrical output triggers, shift registers, and cumulative adders for a parallel arithmetic device.

Switching circuits which use ferrite transistor cells (FT-cells) possess a series of advantages over circuits built of static potential triggers. This is due to the less rigorous requirements which may be imposed upon transistors. The use of FT-cells results in a significant improvement of the reliability of digital computers (DC).

FT-cell circuits, in contrast to potential pulse circuits, possess a series of properties which are the result of the following properties of FT-cells:

a) there are no control potentials at the outputs of the memory cells;

b) a pulse appears at the output of the memory cell only during the time when the core, which has a rectangular hysteresis loop, changes over from one stable magnetic state to the other;

c) the information stored in the cell is "erased" after it has been transmitted to another circuit element.

In the majority of cases, the FT-cell circuit is constructed so that information is transmitted from one group of cells to the other by means of pulse action. Double and multiple cycle circuits are slower than single-cycle systems. The devices which must be used to direct the operation of such circuits are much more complex.

In the following we will examine some of the principles of circuit construction of the elements and units of a single-cycle parallel digital computer (AC) DC which uses FT-cells. The parameters of various types of cells used in particular applications are determined in each case by the characteristics of the transistors and ferrites used. The circuit design depends upon the mutual relations between the parameters of the elements of which the circuit is to be constructed. Therefore, in the following, we will emphasize the necessity of observing the relationships between the circuit parameters; the specific circuits studied in this article are presented as illustrations of this principle.

1. Computer Elements

Time Delay Elements

The time delay elements used were the so-called self-excited FT-cells. They operate in the manner outlined below. In the self-excited cell shown in Fig. 1 there is a degree of positive feedback between the transistor collector and base circuits, i.e., there are more turns in the collector (w_k) and base (w_b) windings than in the usual FT-cell.

If the initial state of the ferrite is the $+B_r$ ($-B_r$) state, then the pulse will change the cell induction from $+B_r$ ($-B_r$) to $-B_m$. During the process, an emf will be induced in the transistor base winding which prevents the transistor from acting as a closed switch. After the passage of the input pulse (i.e., after the trailing edge has passed), the core induction changes from $-B_m$ to $-B_r$, and an emf is induced in the base winding which unlocks

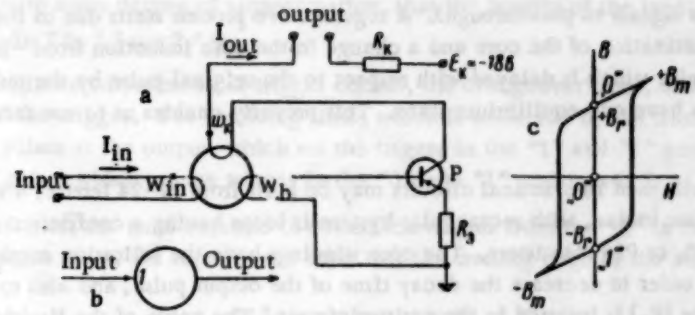

Fig. 1. Self-excited ferrite-transistor cell: a) circuit schematic; b) block diagram; c) ferrite hysteresis loop.

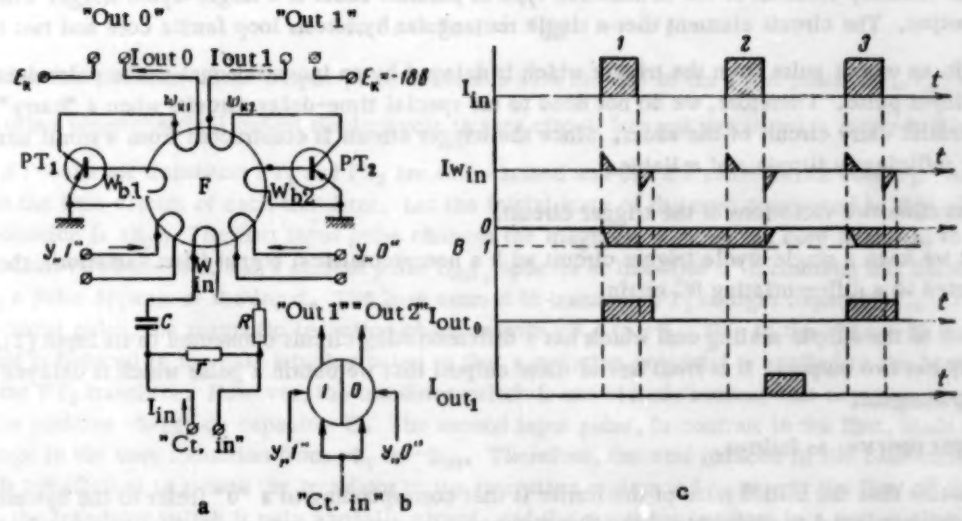

Fig. 2. Single-cycle trigger with an unsymmetrical output (first variation): a) circuit schematic; b) block diagram; c) sequential diagram. $w_{b1} = w_{b2} = 8$; $w_{к1} = w_{к2} = 12$; $w_{in} = 12$; r = 56 ohms, C = 6800 picafarads.

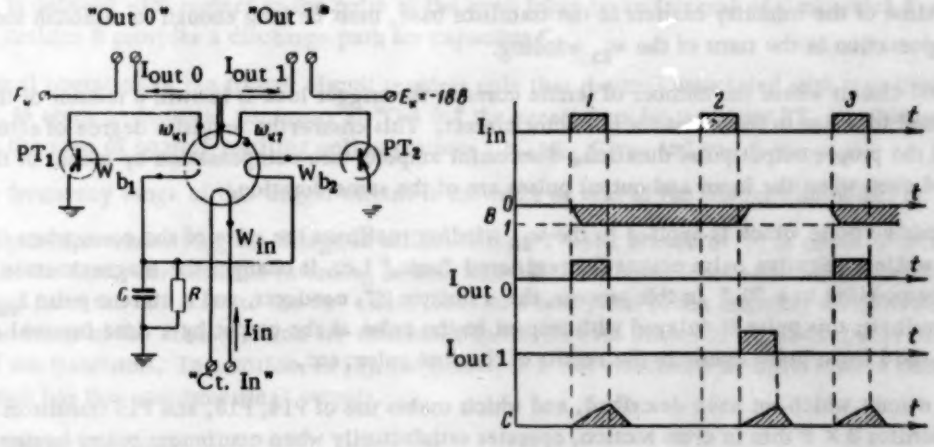

Fig. 3. Single-cycle trigger with an unsymmetrical output (second variation): a) circuit schematic; b) sequential diagram. $w_{к1} = 12$; $w_{b1} = 8$; $w_{к2} = 18$; $w_{b2} = 12$, $w_{in} = 8$.

the transistor (this permits signals to pass through). A regenerative process starts due to the strong positive feedback leading to the magnetization of the core and a change in the core induction from $-B_r$ to $+B_m$. We obtain, at the output, a current pulse which is delayed with respect to the original pulse by the pulse-duration interval. The self-excited FT-cells have one equilibrium state. This property enables us to use these cells as time-delay elements.

The self-excited cells used in practical circuits may be built from PP-24 ferrite, 4 × 2.5 mm in size, or from K-132 ferrite, 3 × 2 mm in size, with rectangular hysteresis loops having a coefficient of linearity $\alpha \leq 0.8$, and may use type P14, P15, or P16 transistors. The core windings have the following number of turns: $w_k = 18$, $w_b = 12$, and $w_{in} = 8$. In order to decrease the decay time of the output pulse, and also to improve the circuit stability, a 10-ohm resistor (R_e) is inserted in the emitter circuit. The value of the limiting resistor R_k depends upon the number of cells (which constitute the load) that are included in the output circuit of the given cell.

Trigger with Unsymmetrical Output

The basic memory element of the cumulative type of parallel adder is a single-cycle trigger with an unsymmetrical output. The circuit element uses a single rectangular hysteresis loop ferrite core and two transistors.

We obtain an output pulse from the trigger which is delayed by an interval equal to the pulse duration with respect to the input pulse. Therefore, we do not need to use special time-delay circuits when a "carry" unit is fed into the parallel carry circuit of the adder. Since the trigger circuit is constructed from a small number of elements, it is sufficiently simple and reliable.

Let us examine two variations of the trigger circuit.

In Fig. 2 we have a single-cycle trigger circuit with a nonsymmetrical output (first variation), the trigger input is connected to a differentiating RC chain.

In contrast to the simple scaling cell which has a differentiating circuit connected to its input [1], the circuit under study has two outputs. It is from one of these outputs that we obtain a pulse which is delayed with respect to the input signal.

The trigger operates as follows.

Let us assume that the initial state of the ferrite is that corresponding to a "0" (refer to the hysteresis loop of Fig. 1b and the sequential diagram Fig. 2b). The first pulse (positive) that is applied to the winding w_{in} applies ampere-turns to the core, which change the core magnetization from $+B_r$ to $-B_r$, i.e., to the state corresponding to a "1." At the time of remagnetization, the transistor PT_1 switch provides a closed path and a current pulse I_{out_0} appears at "Out 0." The NI of the second (negative) pulse are compensated for by the NI in the w_{k1} winding due to the current I_{out}. The duration of the I_{out_0} pulse, which, when the transistor is saturated, is determined by the dispersion time of the minority carriers in the transistor base, must be long enough to establish successful ampere-turn compensation in the turns of the w_{in} winding.

In a practical circuit where the number of ferrite cores in the trigger load is known, a resistor of the order of 100 ohms is added in series in the transistor collector circuit. This ensures the requisite degree of saturation of the transistor, and the proper output pulse duration. Successful ampere-turn compensation by means of the w_{in} winding is assured even when the input and output pulses are of the same duration.

The next positive pulse which is applied to the w_{in} winding reaffirms the state of the core, when the core is indicating a "1," while a negative pulse counts the registered "unit," i.e., it changes the magnetic state of the ferrite to that corresponding to a "0." In this process, the transistor PT_2 conducts, and a current pulse I_{out_1} appears at the "Out 1" terminals; this pulse is delayed with respect to the pulse at the output by a time interval equal to its duration. The third input pulse confirms the results of the first pulse, etc.

The trigger circuit which we have described, and which makes use of P14, P15, and P16 transistors and K-132 and BT-5 ferrites 3 × 2 mm in cross section, operates satisfactorily when continuous pulses having a frequency of 300-350 kilocycles are applied to the input. We may omit resistor R, since, in a practical circuit, its role is taken by the input resistance of the ferrite, looking into the w_{in} winding. In order to increase the circuit stability and the slope of the trailing edge of the output pulse, a 3-5 ohm resistor is placed in the transistor emitter circuit; this creates an automatic positive voltage shift in the transistor base circuit. This resistor is not shown in the diagram.

We may assume, with some degree of approximation, that the lengths of the input and output pulses are the same for all FT-cells, i.e., $\tau_{in} = \tau_{out} = \tau_i$.

We must note that, in an unsymmetrical trigger circuit, the changeover time, as well as the resolving time, depend upon the state of the trigger. The resolving time, which is measured by the minimum interval between two consecutive output pulses at the output, which set the trigger in the "1" and "0" positions, is equal to τ_i, while that between two pulses which set the trigger in the "0" and "1" positions is $2\tau_i$.

In an analogous manner, the time required to switch the trigger from the "1" to the zero state is measured from the time that the pulse enters the input to the time that the trailing edge of the pulse leaves the output,

$$\tau_{sw\ 0} = \tau_{out} + \tau_{dt_0} = \tau_i + \tau_{dt_0}$$

where τ_{dt_0} is the time involved when the trigger switches from a "0" to a "1."

The time required for the trigger to switch from a "1" to a "0":

$$\tau_{sw\ 1} = \tau_{out} + \tau_{dt_1} = 2\tau_i$$

if we consider that the start of the output pulse coincides with the end of the input pulse, i.e., $\tau_{dt_1} = \tau_{in} = \tau_i$.

The other unsymmetrical output single-cycle trigger circuit (second variation) is shown in Fig. 3.

The FT-cells for transistors PT_1 and PT_2 are self-excited and use the same ferrite core F_1. An RC chain is common to the base circuit of each transistor. Let the initial state of the core correspond to that of a "0" (the residual induction is $+B_r$). The first input pulse changes the magnetic state of the core from $+B_r$ to $-B_m$. Meanwhile, transistor PT_1 conducts, and a current pulse I_{out_0} appears at the "Out 0" terminals; this coincides with the time when a pulse appears at the input. The base current in transistor PT_1 charges capacitor C. At the conclusion of the input pulse, the magnetic induction changes from $-B_m$ to $-B_r$. Due to the change in magnetic induction, an emf is induced in the base winding poled so that a negative potential is applied to the base; this tends to switch on the PT_2 transistor. However, the transistor switch is not closed, because this negative potential is opposed by the positive charge on capacitor C. The second input pulse, in contrast to the first, leads to an insignificant change in the core induction from $-B_r$ to $-B_m$. Therefore, the emf induced in the base circuit of transistor PT_1 is insufficient to switch the transistor to the saturation region and to permit the flow of collector current. Therefore, the transistor switch is only partially closed, and the transistor operates in a region close to that which would result in a flow of collector current and an error pulse appears at the "Out 0" terminals of the trigger. However, the base current of transistor PT_1 is not large enough to charge the capacitor to a voltage high enough to compensate for the change in the core induction from $-B_m$ to $-B_r$, caused by the trailing edge of the input pulse. As a result, the cell and transistor PT_2 are self-excited, and a current pulse I_{out_1} appears at the "Out 1" terminals. This pulse is delayed with respect to the pulse at the even input by an interval of time which is equal to the pulse duration. Resistor R provides a discharge path for capacitor C.

Normal operation of the trigger circuit requires only that the cell associated with transistor PT_2 operate. Therefore, in order to decrease the errors at "Out 0," the parameters for transistor PT_1 are those which are usually chosen for the case of nonself-exciting cell operation, i.e., $w_{k1} < w_{k2}$ and $w_{b1} < w_{b2}$.

The frequency range of this trigger circuit is the same as that of the trigger circuit of Fig. 2.

The principle underlying the design of self-exciting FT-cells is used in [2] in order to obtain scale counters. However, in the latter circuits, the retarding action, associated with self-excitation, which results after the core has switched from the "0" state to the "1" state, leads to a resorption of the minority carriers which had accumulated in the bases of the diodes, which are connected in the forward direction in parallel with the base-emitter circuits of the transistors. In addition, in [2], the principle is not associated with the idea of designing a trigger circuit which has two unsymmetrical outputs.

Composite FT-Cells

Usually the process of reading out the information stored in the FT-cells is associated with the emission of a pulse to the external circuit. Very often circuits are used which do not require that a pulse be sent out simultaneously with the reading of a "1," which has been stored in the ferrite core. In these cases, it is convenient to use a so-called composite FT-cell.

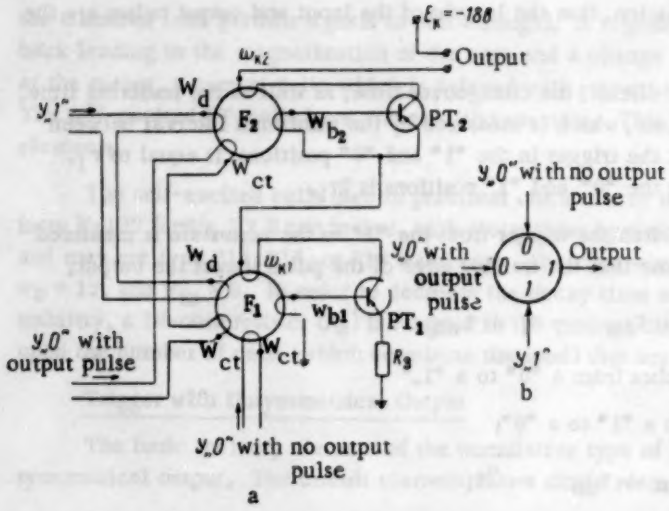

Fig. 4. Composite FT-cell: a) circuit schematic; b) block diagram. T_1) and T_2) P14 transistors, $w_{k1} = w_{k2} = 12$, $w_{b1} = w_{b2} = 8$, $w_{ct} = w_d = 8$.

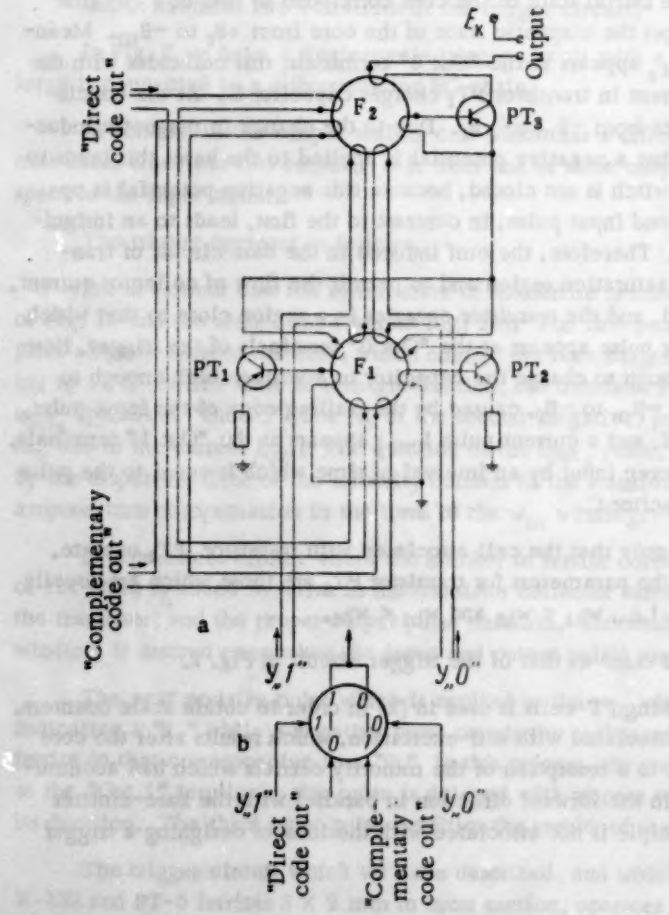

Fig. 5. Cell for transmitting the information in the direct or reverse code: a) schematic diagram; b) block diagram.

The composite FT-cell (Fig. 4) consists of two series-connected simple cells. Ferrite F_1 is the basic memory cell, and ferrite F_2 is the auxiliary cell.

In order to register a "1" (Y"1"), an input pulse must be received simultaneously by the cores. The counting (reading out) of the "1" (Y "0") may or may not be associated with the appearance of an output pulse at the output of the composite cell.

Let us examine a composite FT-cell which we use for reading out digits in either the direct or complementary code, from the registers or the adder.

The basic circuit of such a cell is shown in Fig. 5. Windings associated with the base and collector circuits of transistors PT_1 and PT_2 are placed on core F_1. A "0" or a "1" is stored (written) in the cell when a pulse is fed either to input Y"0" or input Y"1."

Let us assume that a "1" is registered in the cell; this corresponds to a negative induction in both cases. Then, when a control pulse is applied to the terminals labelled "Direct Code Readout," the magnetic state of both cores is reversed simultaneously, the transistor switches PT_1 and PT_3 are closed, and a pulse corresponding to a "1" appears at the circuit output. If a control pulse is applied to the terminals labelled "Complementary Code Output," only the magnetization of core F_2 is reversed. The "0" is read out in a similar manner (either in the direct or complementary code).

2. Arithmetic Computer Blocks

Shift Register

The schematic of a single-cycle shift register [3] for one digit (on the left) is presented in Fig. 6.

The following cells are provided in the register for each digit: FT_{pk} – composite FT-cells which are used to receive, remember, and store the parallel number code; FT_{zk} – self-excited cells which serve to delay the pulses by the time corresponding to a "unit" shift in response to the application of a shift pulse to the "Shift" input; and the FT_{Bk} – composite cells used to transmit, in either the direct or complementary code, the number stored in the register to the other parts of the DC.

The code is written in the FT_{pk} cell at the same time that it is received by the basic register memory cell FT_{Bk}.

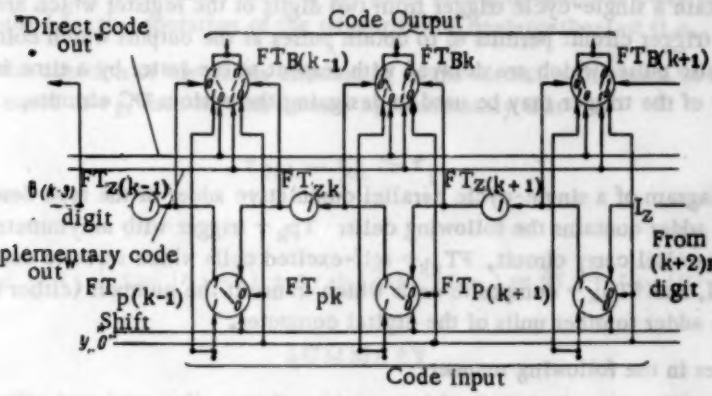

Fig. 6.

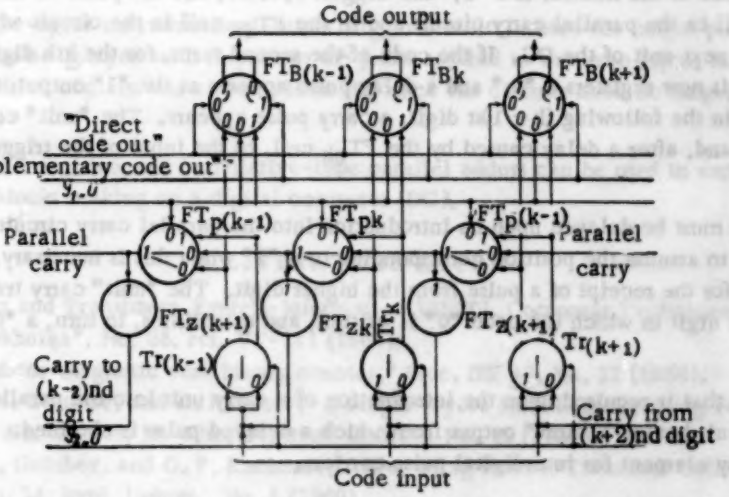

Fig. 7.

The code shift is actuated when the control unit applies a pulse to the "Shift" terminals. This involves the simultaneous counting of the "units" by those digits of the register in which they had been stored.

The impulses at the output of the FT_{pk} cells enter the FT_{zk} cells (here they are delayed by a time interval equal to the pulse duration), and they set up a "0" on the FT_{Bk} for the same digit of the register.

Upon its release from the FT_{zk} cell, the pulse, as in the case when a "1" is written, enters the $FT_{p(k-1)}$ cell of the neighboring digit, and shifts the number on the digit-register to the left, as in the $FT_{B(k-1)}$ cell which "follows" the code which is registered in the basic cells of the corresponding digit of the register.

If we make an approximation and assume that all impulses are of the same length, and neglect the delay caused by the operating time of the FT_{pk} cells, then the FT_{zk} cells delay the pulse by a time interval equal to the duration of the pulse applied to the "shift" terminals, i.e., the minimum necessary time delay is obtained by the normal register operation when a pulse is applied to the "Shift" terminals. This type of circuit gives us a register which functions more rapidly than one using the double-cycle principle.

When a control pulse is applied to the "Direct Complementary Code Output," the number stored in the register is transmitted to other parts of the computer. A code can only be sent out by the register one time. If the register must transmit the same code many times, then supplementary cells (which are self-excited) must also be used to regenerate the code.

Practical single-cycle registers using P14-P16 transistors and 3 × 2 mm ferrite cores, operate with shift pulses having a frequency of 200-250 kilocycles.

We can easily obtain a single-cycle trigger from two digits of the register which are connected to each other in a ring. This type of trigger circuit permits us to obtain pulses at the outputs which coincide with pulses arriving at the even input, and also pulses which are delayed with respect to the latter by a time interval equal to the pulse duration. This property of the trigger may be used in designing the various DC circuits.

Adder

The functional diagram of a single-cycle parallel cumulative adder of the type described in [4] is given in Fig. 7. One unit of the adder contains the following cells: Tp_k – trigger with unsymmetrical output, FT_{pk} – composite cells in the parallel carry circuit, FT_{zk} – self-excited cells which serve to delay the pulses during the interdigital carry period, and FT_{Bk} – composite cells which transmit the numbers (either in the direct or complementary code) from the adder to other units of the digital computer.

The adder operates in the following manner.

We will assume that all digits of the register are set to the "0" position. The code of the first term which is received from the control element (input register) is applied to the even inputs of the triggers Tp_k. For those digits for which the code of the number is a "1," the triggers operate, and the pulse at the "0" trigger input writes a "1" in the FT_{pk} cell in the parallel carry circuit and in the FT_{Bk} cell in the circuit which transmits the code from the adder to the next unit of the DC. If the code of the second term, for the kth digit, is also a "1," then the trigger for this digit now registers a "0," and a delay pulse appears at the "1" output; this counts a "1" on the FT_{pk} cell, and thus, in the following $(k-1)$st digit, a carry pulse appears. The "unit" carry is applied to the parallel carry circuit and, after a delay caused by the FT_{zk} cell, to the input of the trigger associated with the $(k-1)$st digit.

The carry pulse must be delayed upon its introduction into the parallel carry circuit in order to enable the FT_{pk} cell of the digit to assume the position corresponding to a "1" when this is necessary, and to thus prepare the parallel carry circuit for the receipt of a pulse from the higher digit. The "unit" carry travels through the parallel carry circuit up to the digit in which the code "0" is written, and establishes, in turn, a "0" in the triggers of all the higher digits.

Thus, the delay that is required upon the introduction of a carry unit into the parallel carry circuit is assured by a trigger circuit having a "unit" output from which a delayed pulse is obtained. The self-excited cell fills the role of a delay element for interdigital pulse carriers.

The code is transmitted from the adder by means of the FT_{Bk} cells when control pulses are applied to the "Direct Complementary Code Output."

The adder is set to a "0" in the following manner. A "0" pulse is applied to the Y_1"0" terminal, the FT_{pk} and FT_{Bk} cells are set to the "0" position, and after a delay which assures the proper operation of the controls in the self-excited cells, it is applied to the Y_2"0" terminals setting the Tp_k trigger in the null position.

We will now determine the maximum time taken by the adder to add two numbers; the time will be measured from the moment that the second term enters the adder input (the first term is already in the adder), to the time when the adder finishes obtaining the sum. For an n digit adder, this time is determined by the time required for the carry pulse to travel from the highest (nth) digit to the lowest (first) digit in the parallel carry circuit. Thus, assuming that the first term consists of all 1's except for the first digit, and the second term consists of a 1 in the highest digit. In determining the maximum time required for the addition, we must take account of the fact that the time required for the operation (switchover) of the trigger associated with the second digit when the trigger is in the "1" position is greater than the time required for the operation (switchover) of the trigger for the first (i.e., lowest) digit, which is in the "0" state. Therefore, the conclusion of the addition process coincides with the conclusion of the transitional processes in the second digit of the adder. If we take this into account, the maximum time required for the summation is determined by the formula

$$T_{s\,max} = \tau_{dt1} + \tau_{dp}\,(n-1) + \tau_{di} + (\tau_{sw1} - \tau_{dp}),$$

where τ_{dt1} is the time delay due to the operating time of the trigger circuit for the highest digit during the transition from the position corresponding to a "1" to the position corresponding to a "0," τ_{dp} is the time delay due to the time required for the pulse to travel along the parallel carry circuit for one digit (in the FT_{pk} cell), n is the

number of digits in the adder, τ_{di} is the delay time of the pulse during interdigital carry (delay in the FT_{zk} cell), and τ_{sw1} is the time required for the operation of the trigger in the next-to-the-last (i.e., the second) digit.

If we assume that the duration of the pulses circulating in the circuit is the same at the inputs and outputs to all the elements, and equal to τ_i, then we can assume approximately that

$$\tau_{dt1} = \tau_{di} \approx \tau_i.$$

Consequently,

$$T_{s\,max} = \tau_i + \tau_{dp}\,(n-1) + \tau_i + (2\tau_i - \tau_{dp}) = 4\tau_i + \tau_{dp}\,(n-2).$$

SUMMARY

1. Self-excited ferrite transistor cells may be widely used in digital-computer circuits. Their use leads to rapid-acting, single-cycle circuits for the basic elements and blocks of the parallel arithmetic devices of digital computers. These circuits require a minimum amount of components.*

2. The use of single-cycle unsymmetrical-output trigger circuits, where the output pulse obtained at one of the trigger outputs must be delayed with respect to the pulse applied to the even input, leads to circuit simplification and to circuits which contain less circuit elements, since the circuits need no longer include supplementary delay elements.

3. Single-cycle shift registers and cumulative-type parallel adders can be used in various fast-acting circuits for the arithmetic blocks making up a digital computer (DC).

LITERATURE CITED

1. Counters Using Cores and Transistors, Express-Information VINITI, Computer Techniques Series (seriyz "Vychislitel'naya tekhnika", No. 35, ref. VT-141 (1957).
2. H. R. Irons, "A transistor-magnetic core binary counter," Proc. IRE 46, No. 12 (1958).
3. M. I. Petrukhin, L. A. Golubev, and D. P. Losev, A Single-Cycle Shift Register Using Ferrite-Transistor Cells, Author's Certificate No. 122949, kl. 42m, 14, Byul. isobret., No. 19 (1959).
4. M. I. Petrukin, L. A. Golubev, and G. F. Kucherov, Adder Using Ferrite-Transistor Cells, Author's Certificate No. 127864, kl. 42m, 14, Byul. isobret., No. 8 (1960).

*By the number of components in a circuit we mean the number of basic (or their equivalent in cost, dimensions, or other indices) elements in a circuit. In the given case, the transistor is the basic circuit element.

ELECTRONIC DECODING AND CODING FUNCTION GENERATORS

V. B. Smolov (Leningrad)

Translated from Avtomatika i Telemekhanika, Vol. 22, No. 2, pp. 209-215, February, 1961
Original article submitted October 10, 1960

This article describes digital-analog computers which can be used for the functional decoding of digital information and the functional coding of analog information. It also presents the calculations used in the design of these computers.

1. In the theory of automatic devices, linear electrical coding and decoding computers which transform digital information N into analog form (voltages, currents), and vice-versa, according to the functions

$$U = K_U N, \tag{1}$$

$$N = K_N U, \tag{2}$$

where K_U and K_N are scale factors, are well known [1,2].

However, in a series of cases where decoding and coding computers have been used in various automatic systems, it is necessary to decode and code according to the functions

$$U = K_U \Phi(N), \tag{3}$$

$$N = K_N F(U). \tag{4}$$

It is obvious that the problem may be solved by the use of linear decoding and coding computers in conjunction with a computer which has the characteristics $U_{out} = F(U_{in})$ – a continuous type computer; $N_{out} = \Phi(N_{out})$ – a discrete (digital) computer.

Since, in the given case, the required functional transformation can be performed by a digital computer while analog computers serve only in the linear processing of the information, the setup for a functional decoder and coder becomes more complex. Therefore, it is undoubtedly of great interest to design a so-called functional decoding and coding generator which, in its operating principles, is a continuously operating discrete type of computer, and which possesses characteristics of the type (3) and (4).

This paper is devoted to the examination of one of the possible methods of building a functional decoding and coding generator [3,4].

2. An electronic functional decoder automatically transforms digital information N_1, usually provided in the form of a parallel double (paired) code, as an output voltage U_2 obtained according to Eq. (3).

As a result of the discrete form of the input information N_1, the voltage U_2 has a stepwise character (Fig. 1), and the magnitude of the step ΔU, in contrast to the linear coding generator, is represented here as a function of N_1:

$$\Delta U = f(N_1).$$

In the design of functional decoding generators, we may make use of piecewise-linear, piecewise-stepped, piecewise-nonlinear, and smooth approximating functions (3) [5,6]; however, we will examine the piecewise-

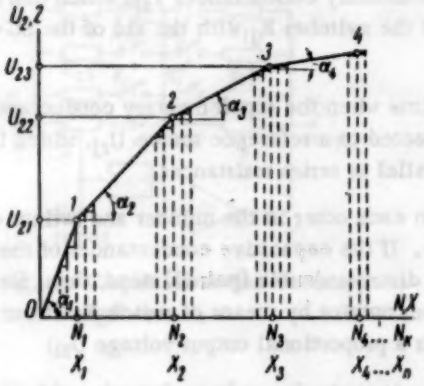

Fig. 1. Piecewise-linear approximating function for discrete argument.

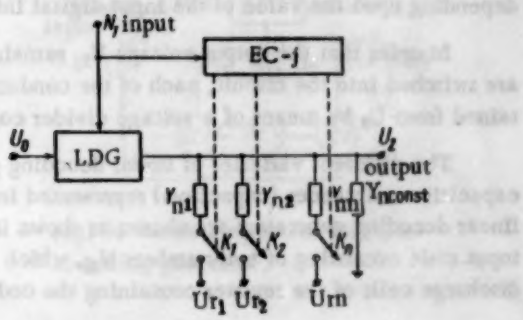

Fig. 2. Block diagram of decoding function generator.

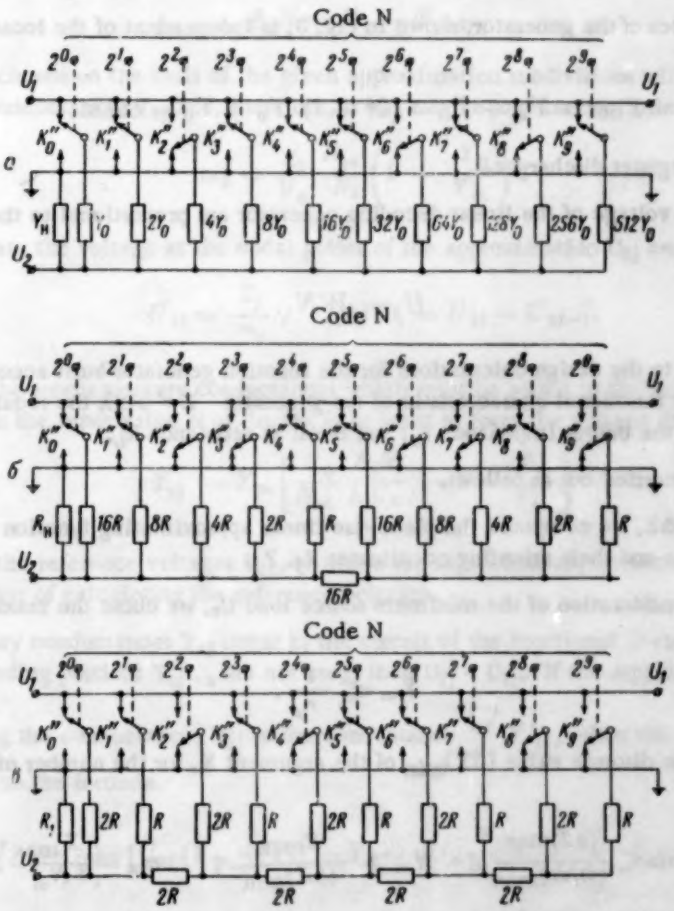

Fig. 3. Linear decoding generator with constant output resistance.

linear method of approximation, since this leads to the simplest design. As we see from Fig. 1, in this method the output voltage has a stepwise character, but within each linear subdivision j the magnitude remains constant.

A functional decoding generator operating on the basis of a piecewise-linear approximation must operate as a voltage divider. We can use the circuit of Fig. 2, which contains a linear decoding generator with constant output resistance LDG, and electronic commutator EC-j containing a number of segments equal to the number of

subdivisions used in the approximation, and a group of constant supplementary conductances Y_{sj}, which can be connected to the output of the linear decoding generator by means of the switches K_j with the aid of the EC-j, depending upon the value of the input digital information.

In order that the output voltage U_{zj} remain unchanged at the time when the supplementary conductances Y_{sj} are switched into the circuit, each of the conductances must be connected to a reference source U_{rj}, which is obtained from U_0 by means of a voltage divider composed of either parallel or series resistances.

The different varieties of linear decoding generators differ from each other in the number and ratings of the capacitive reactances (capacitors) represented in Figs. 3a, 3b, and 3c. If the capacitive conductances of these linear decoding generators are chosen as shown in Fig. 3 by means of discrete double (paired) steps, then, for any input code consisting of two numbers N_{1i}, which is placed into the commutator by means of switch K_i^* from the discharge cells of the register containing the code number N_1, there is a proportional output voltage U_{zi}:

$$U_{zi} = U_0 \frac{N_{1i}}{N_m} = U_0 \frac{Y_i}{Y_m},$$

where Y_m is the maximum generator conductance, and N_m is the maximum value of the digital information.

The output conductance of the generator, shown in Fig. 3, is independent of the location of the switch K_i^*, and is given by

$$Y_{out} = Y_m + Y_n = (2^n - 1)\ Y_0 + Y_n = \text{const},$$

where n is the number of register discharges.

Changes in the input voltage of the linear decoding generator are proportional to the argument W, and are given by

$$U_2 \equiv WN_1.$$

3. The basic factors in the design calculations for the function generator built according to the scheme delineated in Fig. 2 are the functional characteristic of the generator $Z = \Phi(x)$, the required decoding precision ΔZ, the source voltage U_0, the output impedance r_u, and the load resistance R_L.

The calculation was carried out as follows.

a) For a given error ΔZ, we computed the piecewise-linear approximating function Z, determined the number of linear increments and their orienting coordinates X_j, Z_j.

b) Based upon the consideration of the minimum source load U_0, we chose the maximum generator conductance

$$Y_m \ll \frac{1}{r_u}.$$

c) We determined the discrete value $(\Delta X)_{min}$ of the argument X, for the number of divisions N_m and the argument range m_x:

$$(\Delta X)_{min} \leqslant \frac{(\Delta Z)_{max}}{(dz/dx)_{max}}, \qquad N_m \geqslant \frac{X_{max}}{(\Delta X)_{min}}, \qquad m_x = \frac{X_{max}}{N_m},$$

such that N_m must satisfy the entire range of m_x.

d) We calculate the value of the argument based upon the scale

$$N_j = \frac{X_j}{m_x}.$$

e) The codes for the N_j are written out, and a scheme for the electronic commutator EC-j, containing the simple logic cells "and" or "or", is worked out. We can determine the abscissas N_j within the given error limits ΔZ, so that the number codes between N_j and N_{j+1} would have a common group of discharge states.

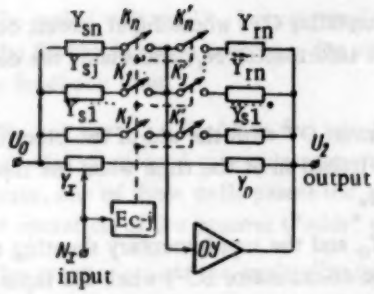

Fig. 4. Circuit of active decoding function generator.

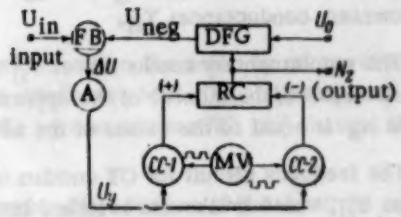

Fig. 5. Block diagram of functional coding generator.

f) After the values of the abscissas N_j are more precisely determined, we can recalculate the ordinates Z_j of the subdivision used in the approximation.

g) For each subdivision, we calculate the increments of the abscissas

$$\Delta_j N = N_j - N_{j-1}.$$

h) The Z scale is chosen on the basis of the given approximation subdivisions without taking into consideration the supplementary conductances Y_{sj} and, therefore, it has a large angular coefficient

$$m_z = \frac{Z_1}{U_0}\frac{N_m}{N_1}\left(1 + \frac{Y_n}{Y_m}\right).$$

i) We then calculate the voltage at the nodal points of the approximation U_{2j} and the increments $\Delta_j U_2$:

$$U_{2j} = \frac{Z_j}{m_z}, \qquad \Delta_j U_2 = U_{2j} - U_{2j-1}.$$

j) We determine the supplementary conductances which must be added to the output of the linear decoding generator when we obtain the input value N of the (N_{j+1})st input to form the voltage divider for each subdivision

$$Y_{sj} = Y_m\left[\frac{U_0}{N_m}\frac{\Delta_j N}{\Delta_j U_2} - 1 - \frac{Y_n}{Y_m}\right].$$

k) We determine the reference voltages U_{rj}, to which the supplementary conductance Y_{sj} must be added; there are two possible ways of calculating the reference voltages.

If the supplementary conductances Y_{sj} occur in the circuit of the functional decoding generator, and the conductances of the preceding portions Y_{sj-1} are not used, then $U_{rj} = U_{2j}$. If the supplementary conductances Y_{sj} are formed by connecting the conductances Y'_{sj} to the conductance $\sum_1^{j-1} Y'_{si}$, then the reference voltages U_{rj} are computed according to the formula

$$U_{rj} = \frac{1}{Y'_s}\left[U_{2j}(Y_m + Y_{sj} + Y_n) - U_0\frac{N_j}{N_m}Y_m - \sum_{i=1}^{i=j-1} U_{ri}\,Y'_{si}\right],$$

where

$$Y'_{sj} = Y_{sj} - Y_{sj-1}.$$

l) The threshold circuit is computed in order to establish the voltages U_{rj}.

4. If the functional decoding generator must operate under a low resistance or alternating load, then its circuit is calculated by means of the active principle (Fig. 4) [4].

An active functional decoding generator contains an operational amplifier OY, whose input circuit consists of a digital conductance Y_X, which changes proportionately to the digital information N_X, and shunts the constant supplementary conductances Y_{sj}.

The supplementary conductances Y_{sj} are connected to the input circuit OY with the aid of the electronic commutator EC-j, the number of the approximation subdivisions being switched in at the time when the input is equal to N_X is equal to the values of the abscissas of the N_{Xj} subdivisions.

The feedback circuit for OY consists of the constant conductance Y_0 and the supplementary shunting conductance Y_{sj}, which is likewise switched into the circuit by the electronic commutator EC-j when the input reaches the value N_{Xj}.

If Y_m, the maximum digital conductance, is proportional to the maximum input digital information N_{Xm}, then the incremental conductance ΔY_X of the amplifier input circuit is equal to Y_m/N_{Xm} per unit digit, and the corresponding incremental increase in the output voltage $|\Delta U_2|_{\Delta N=1}$ is given as:

$$[\Delta U_2]_{\Delta N=1} = U_1 \frac{Y_m}{N_{xm}} \frac{1}{Y_0 + Y_{0j}}. \tag{5}$$

This increase in the output voltage of the active functional decoding generator circuit must be equal to the unit incremental voltage $|\Delta U_2|_{bd}$ shown on the graph of the piecewise-linear approximation of the given function $U_2 = F(N_X)$:

$$[\Delta U_2]_{bd} = \frac{\Delta U_{2j}}{\Delta N_{xj}} = \frac{Y_m}{N_{xm}} \frac{\Delta U_{2j}}{\Delta Y_{xj}}. \tag{6}$$

Equating (5) and (6), we get

$$Y_0 + Y_{0j} = \Delta_j Y_x \frac{U_0}{\Delta U_{2j}}. \tag{7}$$

The initial ordinate U_{2j} of the jth linear subdivision, as determined from the approximation curve, is obtained in the circuit of Fig. 4 by simultaneously switching in the supplementary conductances Y_{rj} and Y_{sj} to the corresponding amplifier circuits. In this process, the relation

$$U_{2j} = U_0 \frac{Y_{xj} + Y_{sj}}{Y_0 + Y_{rj}}. \tag{8}$$

must be satisfied.

From Eqs. (7) and (8) we can determine the values of the supplementary conductances Y_{rj} and Y_{sj}, which will give the piecewise-linear approximation of the given function of the digital argument $U_2 = F(N_X)$. In this process, the amplifier output voltage will vary within the limits of the jth subdivision of the linear approximation according to the equation

$$U_2 = U_0 \frac{Y_x + Y_{sj}}{Y_0 + Y_{rj}}.$$

One of the features of the active decoding function generator is the absence of a special voltage divider circuit for the provision of reference voltages.

We can also obtain nonmonotonic functions either by using a more complex circuit for the generator by introducing additional operational amplifiers, or by using an operational amplifier with a differential input cascade, as in the diode function generators used in modulators [7].

5. Coding function generators realizing the dependence (4) can be built using open or closed loop systems.

In the first case, we obtain functional coding by the use in the coding generator of special masks, together with an electron-beam tube [8]. However, the disadvantages associated with this method (the complexity of the setup and the presence of errors or uncertainties) limits their use in automatic regulation and control systems.

The block diagram of a closed-loop functional coding generator is shown in Fig. 5 [1,8]; it represents an electronic pulsed follower system, which includes in its feedback loop the functional decoding generator which we have previously examined.

The coded voltage U_{in} is compared with the output voltage of the functional decoding generator U_{neg} within the FB block which computes the error. The error voltage $\Delta U = U_{in} - U_{neg}$ is amplified by the amplifier A in the feedback loop.

The voltage $U_y = K_A \Delta U$ is fed into the cells CC-1 and CC-2 simultaneously; the cells, by means of a second input, are also connected to a pulse generator, such as a free-running multivibrator MV. Depending upon the sign of the error, one of these cells passes the multivibrator (MV) pulses to the reverse counter RC, and changes the mode of operation of the counter ("adds" or "subtracts").

The counter counts the multivibrator pulses until we reach the number N_Z which establishes, at the output of the functional decoding generator, the voltage

$$U_{\text{neg}} = U_0 \Phi \left[\frac{N_z}{N_m} \right],$$

which assures the balance of the expression

$$U_{\text{in}} - U_0 \Phi \left[\frac{N_z}{N_m} \right] \approx 0.$$

It is obvious that since U_{neg} follows U_{in}, the functional coding generator generates the function $F(U_{in})$ if the decoding generator in the feedback loop has the characteristic

$$F \left[\Phi \left(\frac{N_z}{N_m} \right) \right] = U_{\text{in}}.$$

LITERATURE CITED

1. Notes on Analog-Digital Conversion Techniques (edited by A. Susskind) (The Technology Press, Massachusetts Institute of Technology, 1957).
2. A. A. Fel'dbaum, Computers Used in Automatic Systems [in Russian] (Fizmatgiz, 1959).
3. V. B. Smolov, Digital-Analog Function Generators [in Russian] Author's Notice No. 645818/16, Nov. 30, 1959.
4. V. B. Smolov, Active Decoding Function Generator [in Russian] Author's Notice No. 670336/26, June 17, 1960.
5. B. D. Smith, "Coding by feedback methods," Proc. IRE, No. 8 (1953).
6. R. N. Hofheimer and K. E. Perry, "Digital-analog function generators," Trans. IRE 1-7, No. 2 (1958).
7. B. Ya. Kogan, Electronically Modulated Devices and their Use in the Study of Automatic Control Systems [in Russian] (Fizmatgiz, 1959).
8. M. Klein, G. Morgan, and M. Aronson, Digital Techniques Used in Computation and Control [Russian translation] (IL, 1960).

DETERMINATION OF THE REQUIRED MEASURING FREQUENCY FOR DISCRETE CONTROL

É. L. Itskovich (Moscow)

Translated from Avtomatika i Telemekhanika, Vol. 22, No. 2, pp. 216-223, February, 1961
Original article submitted July 11, 1960

We examine the method of calculating the required measuring frequency for the discrete control of technological objects.

The required frequency is determined from the statistical characteristics of the value to be controlled. In the absence of the necessary initial data, the required frequency is determined by means of special experiments. As an example, the technique described is used to calculate the measuring frequency of some concrete values during discrete automatic and manual control.

The expanding use of general control systems, measuring devices with digital outputs, and devices which test and analyze objects by means of tests which are made at discrete time intervals, present us with the problem of determining the proper frequency at which these measurements are to be made.

The question of how to choose the requisite measuring frequency faces the investigator who is trying to conduct an automatic study of the properties of a technological object. In this case, the first step usually consists of the study of a series of manual measurements of the physicochemical indices of the object during various operating conditions.

An increase in the sampling (measuring) frequency of a discrete control system leads to increased complexity of construction of the system, while the use of manual controls leads to increased effort due to the work associated with the handling and analysis of test probes. A decrease in the measuring frequency can lead to a lack of results as far as the operation of the discrete control system is concerned, since it may be impossible to measure the changes in the controlled value with the necessary precision.

In this paper, we examine the class of controlled values which are random stationary time functions. The values (properties) which belong to this class are characterized as technological objects which are subjected to continuous processes. Under the actual conditions of production, the technological objects are subject to irregularities (perturbations) which are random functions of time. This is the reason why all the indices characterizing the processes occurring in objects also have a random character. At the same time, in objects subject to continuous processes, involving changes in properties (or magnitudes) which are controlled by periodic examinations, the variations in these values consist of bounded oscillations about a mean value, i.e., these magnitudes have a steady-state or stationary value.

The following factors must be taken into account in the control of continuous technological processes:

1) the initial data available for the solution of the problem;

2) the character of the approximation curve to be used in the discrete control of the process;

3) the required precision in making the measurement; this depends upon the influence of changes in the magnitude of the measured values upon the controlled process.

1. In the determination of the required measuring frequency we meet, in practice, two cases. The two

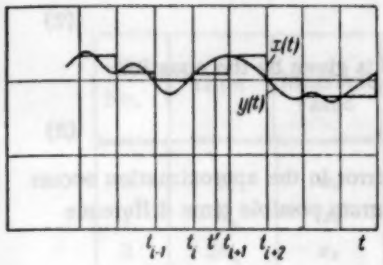

Fig. 1

cases depend upon the initial data. For the case where there is a transition from continuous to discrete control, we use the values of the changes in magnitude with time to determine the necessary initial data. In view of the fact that the magnitudes under consideration are random functions of time, the analysis of these values by means of the correlator and spectrograph permits us to determine their statistical characteristics: correlation function and spectral density. These characteristics contain the initial data required for the computation of the necessary measurement frequency. In the case of the development of a discrete control system or a manual method of measuring magnitudes for which we do not have values that were obtained during continuous automatic control, initial data regarding the indices of the magnitudes (values) being measured are absent. In this case, the requisite measuring frequency must be determined as a result of trial experiments.

2. In the practically applied discrete control of technological processes, the approximation curve x(t) of the function of time y(t), which is being measured, has a stepwise character (Fig. 1). In this case, at any given time we judge the value of the function by the value it had during the last sampling. The value of the magnitude y(t'), which we are measuring at any given time t', which lies within the interval $t_i \leq t' < t_{i+1}$, is taken to be equal to the value measured at time t_i. At the next measuring point t_{i+1}, the value of the magnitude x(t) changes discontinuously by the amount $\Delta x_i = x(t_{i+1}) - x(t_i)$, and remains at this value up to the point t_{i+2}, at which time the next measurement is made. Therefore, the choice of the necessary measuring frequency must take into account the errors arising in a stepwise approximation to the magnitude being measured.

3. The requirements which must be satisfied during the measurement of the controlled magnitude of technological objects can be divided into two groups. In the first group we place those magnitudes which may not even be allowed to deviate from the norm, even as a single momentary occurrence. Such deviation may lead in the aggregate to a trouble condition. For example, in the control of a coal-gas mill with predrying, the temperature of the gases in the pipe behind the mill must be kept at a sufficiently high level, and yet must not exceed a fixed value to prevent explosion of the coal-gas mixture. During the control of such a property we cannot fail to note any change which occurs, even if it takes place extremely rarely. Therefore, we must choose the frequency of such changes in such a manner that we can satisfy the necessity of obtaining a precise determination of the value of this quantity at any time.

The second group of properties, indices of technological processes, are those where a single (unit) transitory fluctuation does not affect the mode of operation of the object. In the control of such objects it is important to know not so much their momentary values, as their average values over a certain time interval, i.e., their tendency to change with time. For example, the dampness of the raw materials entering into a rotary cement baking oven influences the course of the process occurring in the stove; however, due to the mixture of large masses of material in the oven, only sufficiently protracted changes in the dampness of the raw materials have a significant effect. For this group of properties the measuring frequency must be chosen according to an averaged (for example, root-mean-square) value of the changes in magnitude with time.

We show below methods for determining the necessary measuring frequency for the indicated groups.

In the discrete control of the properties belonging to the first group, we set a maximum allowable value for the measured error obtained at any time. This value is determined on the basis of the technological requirements for the control and regulation of this process. The maximum allowable error δ consists of the maximum error in the discrete measurement δ_d, plus the maximum approximation error δ_a in the interval between the measurements, i.e.,

$$\delta = \delta_d + \delta_a. \tag{1}$$

Taking into account the stepwise character of the approximation curve x(t), we can determine the error in the approximation as the error involved in interpolation according to Lagrange's formula. The degree n of the polynomial used in the interpolation is smaller by 1 than the number of points involved in the interpolation and, in this case, it is equal to zero. Practically, in such an approximation, we are extrapolating from one measuring point t_i to the next measuring point t_{i+1}:

$$x(t') = x(t_i) \quad \text{for} \quad t_i \leqslant t' < t_{i+1}. \tag{2}$$

According to Lagrange's formula, the error in the approximation for n = 0 is given by the equation

$$y(t) - x(t) = y'(t')(t - t_i), \tag{3}$$

where t' is the value of the argument in the interval t_i to t_{i+1}. The maximum error in the approximation occurs for the maximum value of the derivative of the desired function and for a maximum possible time difference which occurs at the point preceding the next measuring point t_{i+1}.

Thus,

$$\delta_a = |y'_{\max}(t)| h_1, \tag{4}$$

where $h_I = t_{i+1} - t_i$ is the time interval between measurements.

Using Eq. (1) and the relationship connecting the measuring frequency (N_I) with the time interval between the measurements, we get:

$$N_I = \frac{|y'_{\max}(t)|}{\delta - \delta_d}. \tag{5}$$

The maximum value of the derivative of the random stationary function y(t) can be found from C. N. Bernstein's inequality [1], which holds for functions which are bounded according to a model, and have a spectral density with a finite cutoff frequency:

$$|y^{(k)}_{\max}(t)| \leqslant \omega_c^k |y_{\max}(t)| \quad (k = 0, 1, 2, \ldots). \tag{6}$$

Here $y_{max}(t)$ is the maximum value of the function y(t), $y^{(k)}_{max}(t)$ is the maximum value of the kth derivative of the function y(t), and $\omega_c = 2\pi f_c$ is the cutoff frequency of the spectral density of the function y(t).

The functions which are being investigated in this paper practically always have a bounded frequency spectrum, inasmuch as their values are characterized by technological processes, and the measuring frequency is bounded by the inertia of the objects being studied. Assuming, without loss of generality, that the probability function y(t) is centered (i.e., its mathematical probability is equal to zero), and substituting (6) at k = 1 into (5), we obtain the inequality

$$N_I \leqslant \frac{\omega_c |y_{\max}(t)|}{\delta - \delta_d}. \tag{7}$$

Inequality (7) permits us to estimate the necessary measuring frequency for magnitudes (values) in the first group for a prescribed maximum error in measurement, the cutoff frequency of the spectral density for the desired function, and the maximum possible deviation of the desired function from its mean value.

For example, the necessary measurement frequency for a maximum relative error in the approximation

$$\varepsilon_a = \frac{\delta - \delta_d}{|y_{\max}(t)|} = 0{,}1$$

can be obtained as a function of the cutoff frequency* by means of the following inequality:

$$N_I \leqslant 60 f_c.$$

*In order that we may obtain an approximation for the measured function at the close of the experiment, for the case where the values of the measurements taken at the various discrete times are known, we usually use the linear approximation; in this case the neighboring measurement points are connected by straight lines. V. N. Khlinstrunova [2] shows that, in this case, the necessary discrete measuring frequency is determined from the following expression:

$$N_{II} = \sqrt{\frac{|y''_{\max}(t)|}{8(\delta - \delta_d)}}. \tag{a}$$

Line No.	Time	Measured value	Deviations in the measurements with time					
			$h_в$		$2h_в$		$3h_в$	
0	0	x_0						
1	$h_в$	x_1	Δ_{10}	Δ^2_{10}				
2	$2h_в$	x_2	Δ_{21}	Δ^2_{21}	Δ_{20}	Δ^2_{20}		
3	$3h_в$	x_3	Δ_{32}	Δ^2_{32}	Δ_{31}	Δ^2_{31}	Δ_{30}	Δ^2_{30}
4	$4h_в$	x_4	Δ_{43}	Δ^2_{43}	Δ_{42}	Δ^2_{42}	Δ_{41}	Δ^2_{41}
...	...	...	...	...	...	...	...	...
$n-1$	$(n-1)h_в$	x_{n-1}	$\Delta_{(n-1)(n-2)}$	$\Delta^2_{(n-1)(n-2)}$	$\Delta_{(n-1)(n-3)}$	$\Delta^2_{(n-1)(n-3)}$	$\Delta_{(n-1)(n-4)}$	$\Delta^2_{(n-1)(n-4)}$
n	$nh_в$	x_n	$\Delta_{n(n-1)}$	$\Delta^2_{n(n-1)}$	$\Delta_{n(n-2)}$	$\Delta^2_{n(n-2)}$	$\Delta_{n(n-3)}$	$\Delta^2_{n(n-3)}$
Estimates of the standard deviation			$\sigma^*_{1h_в}$		$\sigma^*_{2h_в}$		$\sigma^*_{3h_в}$	

Expression (7) can be used to evaluate the necessary measurement frequency only for preliminary continuous control of the desired value. For the majority of the controlled magnitudes in the first group, where a basic change can lead to a trouble situation, these magnitudes are subject in practice to continuous control. In the case where initial data are not available regarding the controlled magnitude, in order to choose the trial measuring frequency, we substitute the directed values of the cutoff frequency for the object in the formula (7), and the formula gives us the value of the magnitude and the half-value of the expected maximum variation of this value. The chosen trial frequency must, in any case, be greater than the required one, inasmuch as we take for the parameters ω_c and $|y_{max}(t)|$ their maximum possible values. After the choice of the trial frequency, we make measurements using the frequency in order to determine the true initial data. The lengthiness of the experiment is due to the necessity of obtaining sufficiently accurate reflections of the changes in magnitude with time.

As far as discrete control of a magnitude or a property is concerned, for properties belonging to the second group, we may make use of less rigorous estimates of the changes in the value of the property with time, namely, instead of using the maximum allowed error at a given time, we may use the root-mean-square error.

Let us assume that, on the basis of the technological requirements for regulation and control of a process, the root-mean-square error of the measurements obtained is σ; this consists of the root-mean-square errors involved in the approximation and the actual measurement. For a given approximation, the maximum value of the root-mean-square error will occur at a time h_{II} after each measurement (h_{II} is the time between successive measurements, and equals the root-mean-square deviation of the measured magnitude during the time h_{II}:

$$\sigma = \sqrt{M\{[y(t+h_{II}) - y(t)]^2\}}, \tag{8}$$

where M is the mathematical expectation.

Inasmuch as the value of y(t) is determined by the measuring device, formula (8) takes into account not only the changes in the magnitude of the value being measured, but also the errors made by the measuring device.

Substituting inequality (6) for k = 2, into the above expression, we get

$$N_{II} < \frac{\omega_c}{2}\sqrt{\frac{|y_{max}(t)|}{2(\delta - \delta_d)}}. \tag{b}$$

Formula (b) gives us an estimate of the necessary measuring frequency where a linear approximation is to be used. The value obtained for the necessary measuring frequency using a linear approximation is much lower than that obtained with a stepwise approximation. Thus, for $\epsilon_a = 0.1$, $N_{II} \leq 7 f_c$, i.e., the necessary measuring frequency is now decreased 10 times.

Removing the brackets, and taking account of the fact that

$$R_y(0) = M[y^2(t)] = M[y^2(t + h_{II})], \qquad R_y(h_{II}) = M[y(t)\, y(t + h_{II})],$$

where $R_y(\tau)$ denotes the value of the correlation function for the process y(t) at the point τ, we get

$$\sigma = \sqrt{2[R_y(0) - R_y(h_{II})]},$$

therefore,

$$R_y(h_{II}) = R_y(0) - \frac{\sigma^2}{2}. \tag{9}$$

Given the allowed value of σ, and computing the value of the correlation function from the available continuous data for the magnitude being measured, we get the value of $R_y(h_{II})$ from formula (9). Making use of the curve for the correlation function, we find the value of the abscissa h_{II} from the ordinate of the curve $R_y(h_{II})$. The necessary measuring frequency can then be determined from the formula

$$N_{II} = \frac{1}{h_{II}}. \tag{10}$$

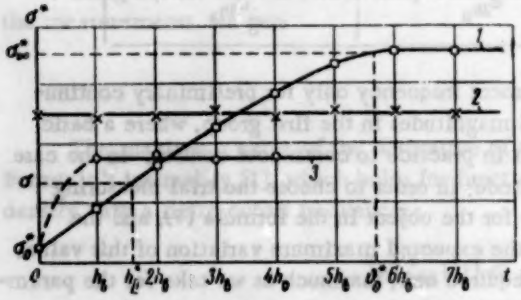

Fig. 2.

However, we can rarely use formulas (9) and (10), inasmuch as the magnitudes, which belong to the second group, are, in the majority of cases, qualitative indices, and usually are not under the preliminary continuous automatic control which is necessary for the determination of the correlation function of the magnitude (value) which is being measured. In the absence of initial data regarding the controlled value we should, in order to calculate the necessary measuring frequency, perform an experiment which consists of from 20-30 measurements with an arbitrary time interval between the measurements, h_B. The data obtained as a result of this experiment are written down in a table, and then the indicated operations are performed upon them.

In the table, $\Delta_i(i-k) = x_i - x_{i-k}$

$$\sigma^*_{kh_B} = \sqrt{\frac{\sum_{i=k}^{n} \Delta^2_{i(i-k)}}{n-(k-1)}}, \tag{11}$$

where i is used to designate the row number, and k the column number of the table.

We have now determined the root-mean-square deviations of the magnitude for the case where the time interval is h_B. In order to determine the necessary measuring frequency, we now plot the values of $\sigma^* = f(h_B)$ on a graph, and draw a smooth curve through them. In Fig. 2 we show several possible curves which we might obtain as a result of calculations based upon our experimental results.

The point σ^* at t = 0 on all the curves corresponds to the root-mean-square error of the measuring device, determined in the usual manner. The remaining points are obtained from the data in the table.

Curve 1 corresponds to the case where the interval h_B, chosen arbitrarily, was considerably smaller than the total drop of the correlation function. There is a significant connection between consecutive (neighboring) measurements, and the root-mean-square deviation is constantly increasing from the value of the root-mean-square error in the measurement (at t = 0) to the constant (steady) value (at $t = \vartheta^*_0$). For $t \geq \vartheta^*_0$, there is no connection between neighboring measurements and, therefore, over this portion of the curve, the root-mean-square deviation has a constant value.†

† It follows that the value ϑ^*_0 also evaluates the time required for the complete descent of the correlation function of the given magnitude.

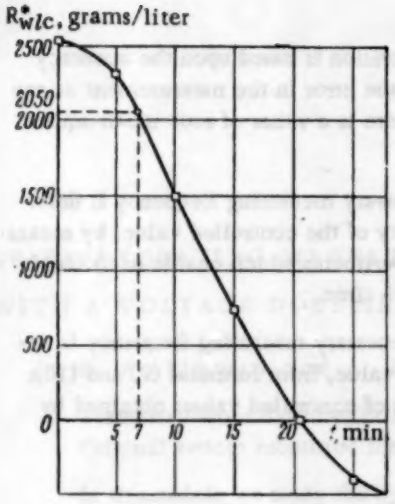

Fig. 3.

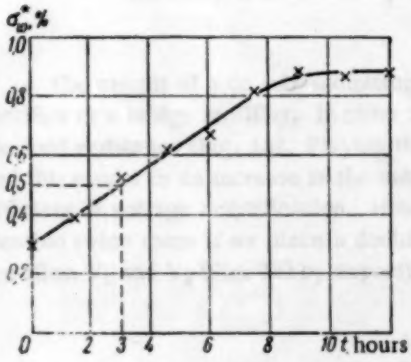

Fig. 4.

For any possible given σ lying between σ^*_δ and σ^*_∞, the evaluation of the time interval between neighboring measurements h^*_{II} or the evaluation of the necessary measuring frequency N^*_{II}, is made using Curve 1.

If necessary, the frequency thus obtained can be made more accurate by making further measurements at the computed frequency N^*_{II}. In order to do this, after making 20-30 measurements one should verify the root-mean-square error which we have obtained [formula (11) for k = 1] and, if there is a significant difference between the permissible and obtained errors, the measuring frequency should be changed accordingly.

Curve 2 occurs when the extent of the changes in magnitude is equal to, or less than, the error of the measuring device (or method). In this case, we cannot use the chosen device or method to measure the magnitude in question.

Finally, we obtain Curve 3 where the arbitrarily chosen interval h_B exceeds the time required for a complete drop in the correlation function. Besides this, all the points except σ^*_δ lie on a horizontal line. In order to obtain the necessary measuring frequency in this case, one should drastically decrease the time interval and repeat the initial experiment again.

Examples

We now give examples of the application of this method to the determination of the measuring frequency of two qualitative indices of a revolving cement heating oven.

1. The measurement of the basic qualitative index of the operation of the oven – the weight of a liter of clinkers – is made by a discrete measuring device. The choice of the necessary operating cycle of the device was based upon the known correlation function for the weight of a liter of clinkers. This function is shown in Fig. 3. The allowed root-mean-square (standard) deviation was σ = 30 grams per liter, the error in the measuring device was 10 grams per liter.

Using formula (9), we find the value of $R^*_{wlc}(h)$:

$$R^*_{wlc}(h_{II}) = 2500 - \frac{(30)^2}{2} = 2050 \text{ g/l}$$

we find the abscissa corresponding to the ordinate which we have just determined from the curve of the correlation function,

$$h_{II} = 7 \text{ min.}$$

This value determines the necessary role of operation of the device.

2. Measurements of the most important perturbing factor – the dampness of the raw materials entering the oven – were carried out manually by laboratory drying in a definite setup. The root-mean-square (standard) deviation for this method of measurement was 0.3%. The allowed root-mean-square (standard deviation) error in determining the dampness of the raw materials at any given time must, according to the technological chart, be not more than 0.5%. On the basis of 30 measurements of the dampness $\underline{w}$, taken with an arbitrarily chosen time interval between measurements of 90 minutes, we constructed a table, made the required calculations, and plotted the graph of the changes σ^*_w versus time (Fig. 4). We then obtained the value of the necessary time interval between measurements, h^*_{II} = 3 hours, directly from the graph.

SUMMARY

1. The values to be measured may be divided into two groups. This division is based upon the accuracy with which these measurements must be made. For values in the first group, the error in the measurement at any time cannot exceed a set maximum error. For values in the second group, there is a value of root-mean-square error set for the measurement.

2. For the case of discrete control of values in the first group, the necessary measuring frequency is determined: a) in the case where there is a definite cutoff frequency for the density of the controlled value, by means of formula (7); b) in the absence of initial data by means of special trial experiments which enable us to obtain a sufficiently accurate picture of the changes in the controlled magnitude with time.

3. For the case of discrete control of values in the second group, the necessary measuring frequency is determined: a) where there is a definite correlation function for the controlled value, from formulas (9) and (10); b) in the case where there are no initial data, by a special analysis of a series of controlled values obtained by trial measurements made at an arbitrary time interval (see table).

LITERATURE CITED

1. N. I. Akhiezer, Lectures on Approximation Theory [in Russian] (Gostekhizdat, 1947).
2. V. N. Khlistunov, "On the approximation errors involved in discrete methods of measurement," Priborostroenie, No. 5 (1960).

SELF-SATURATING MAGNETIC AMPLIFIER WITH A VOLTAGE DOUBLING CIRCUIT*

R. A. Lipman and A. I. Moskalev (Moscow)

Translated from Avtomatika i Telemekhanika, Vol. 22, No. 2, pp. 224-230, February, 1961
Original article submitted June 18, 1960

In this article we study the operation of a self-saturating dc magnetic amplifier (MA) with a voltage doubling circuit. The use of this MA permits a considerable increase in the output voltage, coefficient of amplification, and the range of the dynamic input-output characteristics of the amplifier.

An analysis of the steady-state operation of the circuit for the case of forced saturation is given.

The circuit of a dc self-saturating magnetic amplifier (MA) usually contains either a differential transformer rectifier or a bridge rectifier. In order to smooth out the output voltage, a capacitive shunt is often placed across the load resistance (Fig. 1a). Playing the role of a filter, the use of the shunt capacitor rectifies the amplitude, and this results in an increase in the output voltage of the amplifier. There is a corresponding increase in the coefficient of voltage amplification. However, we increase the output voltage and the voltage coefficient of amplification twice more if we place a doubling rectifier in the amplifier circuit. In order to do this, we replace the rectifiers V_3 and V_4 (Fig. 1a) by capacitors C_1 and C_2 (Fig. 1b).

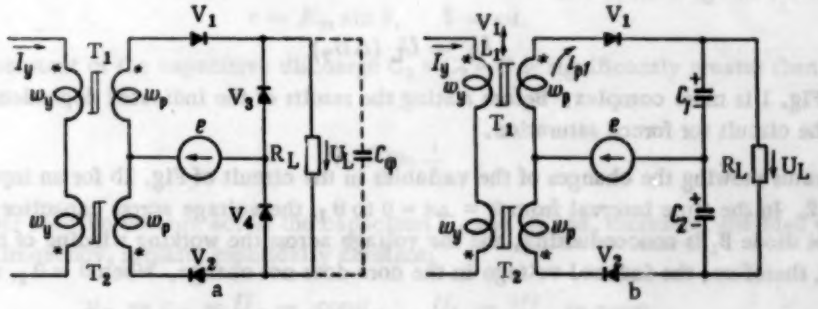

Fig. 1. Self-saturating dc magnetic amplifier: a) using a bridge rectifier; b) using a voltage doubler rectifier.

For low-power amplifiers which are not used over their entire operating range during warmup (for example, "operational" amplifiers), this increase in the output voltage (power) does not require an increase in the transformer parameters. The transition from the circuit of Fig. 1a to the circuit of Fig. 1b permits us to substantially increase the coefficient of amplification and the level of output voltage of the MA, while keeping the same dimensions, transformer parameters, and a constant input voltage.

In spite of its indicated advantages, the MA circuit of Fig. 1b has not been described in the literature; not in any of the well-known monographs devoted to MA. The authors knows of only one paper [1] in which the

*Paper presented at the Seminar on Contactless Magnetic Elements at the IAT, AN SSSR, April 27, 1960.

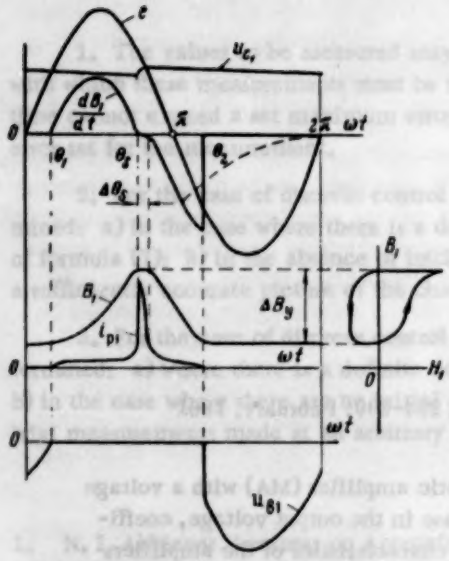

Fig. 2.

circuit of Fig. 1b has been mentioned. However, this paper does not even contain a qualitative analysis of the circuit. The absence of such an analysis hinders the introduction and practical use of this amplifier.

We present below a theoretical analysis of the operation of the circuit of Fig. 1b for forced saturation.

For the circuit of Fig. 1a (neglecting the filter capacity) there is a very simple connection between the mean value of the load voltage U_L and the total change in the core inductance, due to the control signal ΔB_y.

$$U_L = \frac{R_L}{R_L + r_p}[E - 2f w_p S_c \Delta B_y]. \qquad (1)$$

The dependence of ΔB_y upon the control current for forced saturation is determined by the core demagnetization curve which can be easily determined experimentally [2]:

$$\Delta B_y = \Delta B_y(H_y), \quad H_y = \frac{I_y w_c}{l_c}. \qquad (2)$$

In the following, E is the mean value of the source emf, f is the frequency, w_p and w_y are the number of turns in the working and control windings, respectively, S_c and l_c are the cross section and length of the mean line of force of the magnetic circuit of the choke, H_y is the intensity of the control field, I_y is the control current, R_L is the load resistance, r_p is the sum of the active resistances of the working winding, the forward resistance of the diodes, and the internal resistance of the source, the so-called amplifier output resistance.

Equations (1) and (2) determine the input-output characteristics of the amplifier whose circuit is shown in Fig. 1a for forced saturation. If we permit some error, they may also be used for the case of self-saturation. However, for the amplifier which uses a doubler circuit (Fig. 1b), Eq. (1) is incorrect. The dependence of the output voltage upon the total change in inductance

$$U_L = U_L(\Delta B_y) \qquad (3)$$

for the circuit of Fig. 1 is more complex. Before stating the results of the indicated dependence, let us examine the operation of the circuit for forced saturation.

Linear diagrams showing the changes of the variables in the circuit of Fig. 1b for an input-voltage period are shown in Fig. 2. In the time interval from $\theta = \omega t = 0$ to θ_1, the voltage across capacitor C_1 exceeds the emf of the source. The diode B_1 is nonconducting, and the voltage across the working winding of transformer T_1 is equal to zero and, therefore, the induced voltage in the core does not change. When $\theta = \theta_1$, and

$$e = e(\theta_1) = u_{C_1}, \qquad (4)$$

the diode V_1 conducts, and voltage across the transformer is equal to the difference between the emf of the source and the voltage across the capacitor C_1. The rate of change of the inductance in the core T_1 will be equal to

$$w_p S_c \frac{dB_1}{dt} = e - u_{C_1} - i_{p_1} r_p \approx e - u_{C_1} \qquad (5)$$

(we can neglect the voltage drop across the resistance r_p due to the magnetizing current when the core is not saturated). As a result, the inductance will increase, and the change in the magnetic state of the core will follow the ascending branch of the frequency cycle (Fig. 2).

At time $\theta = \theta_s$, the core T_1 becomes saturated, and the inductive component of the voltage drop across the working winding falls to nearly zero, and the capacitor C_1 is therefore connected to the voltage source e which has a small active resistance r_p. As a result, there is a rapid precharge of the capacitor C_1 to a voltage of approximately $e(\theta_s)$; this is accompanied by a pulse of charging current within the contour of the working winding.

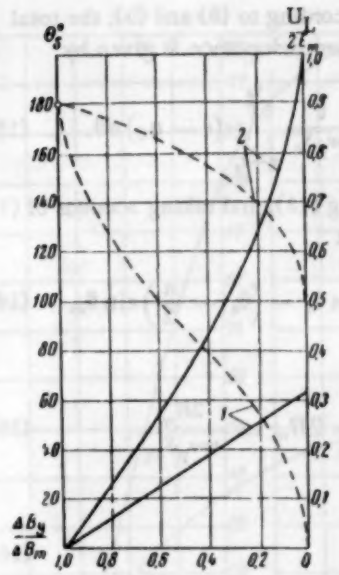

Fig. 3. The relative change in amplifier output voltage (solid line) and angle of saturation (broken line) plotted as functions of the relative change in inductance: 1) for the circuit of Fig. 1a; 2) for the circuit of Fig. 1b.

At the end of the precharge ($\theta = \theta_3 + \Delta\theta_3$), when the value of the current in the working winding T_1 becomes sufficiently small, the core is no longer saturated, and the inductance V_1 starts to decrease due to the action of the controlling field. The diode V_1 remains in the conducting state. Therefore, the rate of change of inductance is again determined by Eq. (5). The changes in the magnetic state of the core follow the descending branch of the frequency cycle, and this determines the law of change of the coil field intensity.

For $\theta = \theta_2$, when the core-field intensity becomes equal to the intensity of the controlling field

$$H_1(\theta_2) = H_y, \tag{6}$$

the current in the working winding becomes zero. The diode V_1 becomes open-circuited, and the demagnetization of the core T_1 ceases ($dB_1/dt = 0$). In actual cases we also note a decrease in the induction after the diode V_1 becomes nonconducting; this is due to the eddy currents and magnetic viscosity.

The character of the changes in the rate of change of induction in this case are shown by the broken line in Fig. 2 [2]. In all cases, the area of the negative half-wave of the curve giving the rate of change of inductance remains equal to the area of the positive half-wave. Therefore, open-circuiting of the diode V_1 takes place somewhat sooner when eddy currents are present.

We wish to determine the function $U_N = U_N(\Delta B_y)$ under the following conditions.

1. The input emf is sinusoidal:

$$e = E_m \sin\theta, \quad \theta = \omega t. \tag{7}$$

2. The time constant of the capacitive discharge $C_1 = C_2 = C$ is significantly greater than the period of the source voltage,

$$R_L C \gg \frac{1}{f} \tag{8}$$

We can consider that the voltage across the capacitors C_1 and C_2 and, therefore, the load voltage over a period of the source frequency, remains practically constant:

$$u_{C_1} = u_{C_2} = U_C = \text{const}, \quad U_L = 2U_C = \text{const}. \tag{9}$$

3. The time constant of the capacitive charge, for capacitors C_1 and C_2, where the choke is saturated, is much less than the period of the input voltage

$$r_p C \ll \frac{1}{f} \tag{10}$$

The duration of the charge is given by $\Delta\theta_3$ (Fig. 2), during this interval the core remains saturated; also it is small when compared with the period and, therefore, we can assume (approximately) that the capacitor is charged up to a voltage

$$u_{C_1} = u_{C_2} = U_C = E_m \sin\theta_3. \tag{11}$$

It follows from (4), (7), (9), and (11) that

$$\theta_1 = \pi - \theta_3. \tag{12}$$

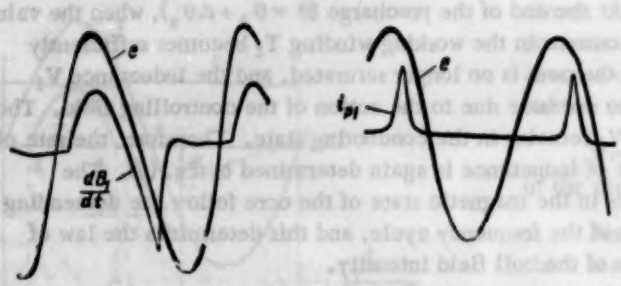

Fig. 4. Oscillograms of the changes in the variables for the circuit of Fig. 1b: e—supply voltage; dB/dt — rate of change of inductance (voltage across the measuring winding of the choke); i_{p1} — current in the working winding.

Then, according to (5) and (9), the total charge in the core inductance is given by

$$\Delta B_y = \frac{1}{\omega w_p S_c} \int_{\pi-\theta_s}^{\theta_s} (e - u_C)\, d\theta. \qquad (13)$$

Integrating (13), and taking account of (7) and (11), we get

$$\frac{\Delta B_y}{\Delta B_m} = -\cos\theta_s - \left(\theta_s - \frac{\pi}{2}\right)\sin\theta_s, \qquad (14)$$

where

$$\Delta B_m = 2B_m = \frac{2E_m}{\omega w_p S_c}. \qquad (15)$$

The load voltage according to (9) and (11) is equal to

$$\frac{U_L}{E_m} = 2\sin\theta_s. \qquad (16)$$

Expressions (14) and (16) determine the desired expression for the load voltage as a function of the change of inductance in the core. In Fig. 3, we have plotted the functions $\theta_s = \theta_s(\Delta B_y)$ and $U_L = U_L(\Delta B_y)$. These functions have been calculated according to formulas (14) and (16); for purposes of comparison, we have also plotted the corresponding curves for Fig. 1a (which does not contain a filter capacitance).

We wish to note that, in the circuit which we are studying, the angle of saturation changes from $\theta_s = \pi$ (no-load operation of the amplifier) to $\theta_s = \pi/2$ (maximum possible transmission), while, in the usual circuits (for example Fig. 1a, $C_\varphi = 0$), the angle of saturation varies from π to 0.

The curve $U_L = U_L(\Delta B_y)$ shown in Fig. 3, together with the core demagnetization curve $\Delta B_y = \Delta B_y(H_y)$ determines the amplifier input-output characteristics: $U_L = U_L(H_y)$, $H_y = I_y w_y / l_c$.

We will determine the differential coefficient of amplification of the amplifier as the ratio of the increase in load voltage to the increase in control current

$$k = \frac{\Delta U_L}{\Delta I_y}. \qquad (17)$$

Using Eqs. (2) and (14)-(16), we get

$$k = m\omega\mu_y \frac{w_y w_p S_c}{l_c}, \qquad (18)$$

where

$$\mu_y = \frac{\partial \Delta B_y}{\partial H_y} \qquad (19)$$

is the differential slope of the demagnetization curve,

$$m = \frac{\partial U_L / 2E_m}{\partial \Delta B_y / \Delta B_m} = \frac{1}{\theta_s - \frac{\pi}{2}} \qquad (20)$$

is the differential slope of the curve $U_L/2E_m = f(\Delta B_y/\Delta B_m)$, shown in Fig. 3; m increases monotonically with an increase in output voltage. For the no-load case ($\theta_s = \pi$) $m = \frac{2}{\pi} = 0.637$; for maximum transmission $\left(\theta_s \to \frac{\pi}{2}\right)$ $m \to \infty$. For the intermediate portion of the input-output characteristics, $m \approx 0.8$.

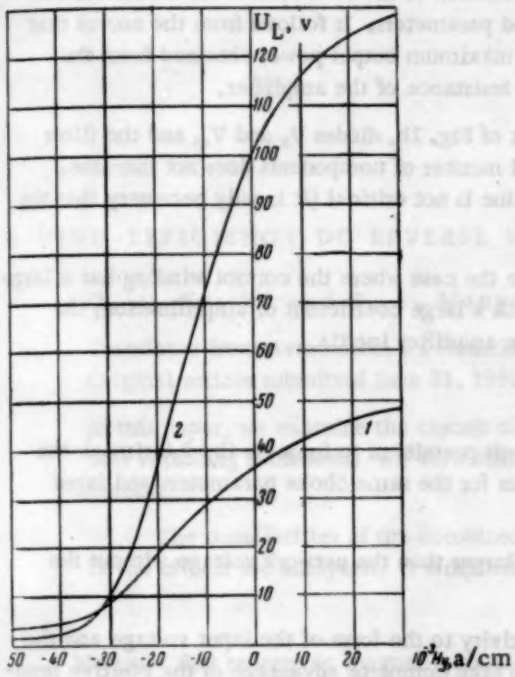

Fig. 5. Load voltage as a function of the magnetic field intensity for the circuit of Fig. 1a (Curve 1) and Fig. 1b (Curve 2).

Equation (18) also holds for the circuit of Fig. 1a (for $C_\varphi = 0$); however, here, m is constant; according to (1), $m = 1/\pi \approx 0.32$. Thus, the circuit of Fig. 1b provides an increase in the differential coefficient of amplification over the intermediate (central portion) of the input-output characteristics, which is 2.5 times greater than that for the circuit of Fig. 1a. The maximum value of the inverse voltage across the diodes of Fig. 1b, as in the circuit of Fig. 1a, is equal to the load voltage.

In Fig. 4 we show the oscillograms of the input voltage, the voltage across the measuring winding of the choke, and the current in the working winding taken for the circuit of Fig. 1b for the case of forced saturation (the circuit parameters are: core OL-35/40-7-0.05-79 HM, $w_p = 1000$, $E_m = 80\sqrt{2}$ volts, $f = 2400$ cycles, $R_L = 2$ kiloohms, $C = 1\,\mu f$). The oscillograms show good qualitative agreement with the theoretical curves of Fig. 2.

In Fig. 5 we plot the output voltage as a function of the control field for circuits 1a and 1b for the choke parameters, input voltage, and load resistance given above.

It follows from Fig. 5 that the transition from the circuit of Fig. 1a (without the filter capacity) to the circuit of Fig. 1b for the same choke parameters and input voltage leads to an increase in the output voltage level and the slope of the linear portion of the input-output parameters of 2.6 times.

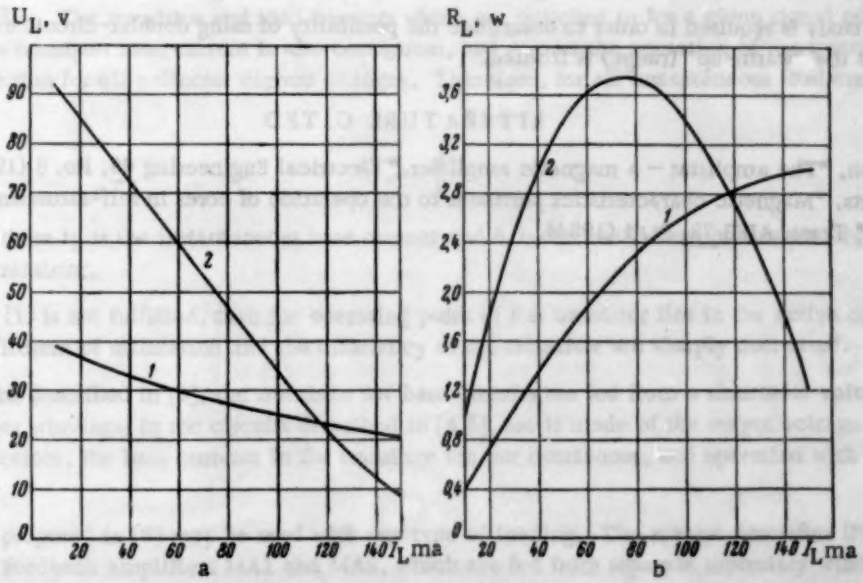

Fig. 6. a) External characteristics of the amplifier for $H_y = 0$. b) Load power as a function of load current for $H_y = 0$: 1) for the circuit of Fig. 1a; 2) for the circuit of Fig. 1b.

The characteristics of the circuit of Fig. 1b also have a significantly greater working range, due to the increase in the maximum output voltage and to the somewhat decreased no-load voltage. The latter is due to the fact that, in the presence of the capacitor (Fig. 1b), the equivalent load resistance to the no-load current is less than for the case of a purely active load (pure reactance).

In Figs. 6a and 6b we plot the load voltage and power as a function of the load current for a constant control signal for the circuits of Figs. 1a and 1b for the above-indicated parameters. It follows from the curves that the transition to the doubler circuit permits a basic increase in the maximum output power obtained from the choke, even though it leads to an increase in the equivalent output resistance of the amplifier.

During the transition from the circuit of Fig. 1a to the circuit of Fig. 1b, diodes V_3 and V_4, and the filter capacity C_φ, are replaced by capacitors C_1 and C_2. Thus, the total number of components does not increase. Capacitors C_1 and C_2 may be electrolytic capacitors, since their value is not critical [it is only necessary that we satisfy condition (8)].

Experimental investigation of the dynamics has shown that, in the case where the control winding has a large time constant (as compared to the period), i.e., for an amplifier with a large coefficient of amplification, the transition to a doubler circuit leads to practically no increase in the amplifier inertia.

SUMMARY

Building a MA which has a voltage doubler in the output circuit permits us to increase (by 2.5 times) the slope and working range of the amplifier input-output characteristics for the same choke parameters and input voltage.

The circuit also permits us to obtain a load voltage which is larger than the network voltage without the transformer.

The disadvantages of the circuit consist of its increased sensitivity to the form of the input voltage and the magnitude of the input resistance of the source voltage. In order to take complete advantage of the positive properties of the circuit with the voltage doubler, the internal resistance of the input must be sufficiently small. The application of input current pulses for a limited source power can lead to distortion of the input voltage and, in some cases, this is not permissible.

One of the applications where the advantages of the circuit of Fig. 1b are made use of more completely is the "operational" magnetic amplifier.

A special study is required in order to determine the possibility of using doubler-circuit magnetic "power" amplifiers where the "warm-up" (range) is limited.

LITERATURE CITED

1. R. E. Morgan, "The amplistat – a magnetic amplifier," Electrical Engineering 68, No. 8 (1949).
2. R. W. Roberts, "Magnetic characteristics pertinent to the operation of cores in self-saturating magnetic amplifiers," Trans. AIEE 73, Pt. 1 (1954).

A HIGH-EFFICIENCY DC REVERSE MAGNETIC AMPLIFIER

O. A. Kossov and E. A. Manychkina (Moscow)

Translated from Avtomatika i Telemekhanika, Vol. 22, No. 2, pp. 231-237, February, 1961
Original article submitted June 21, 1960

In this paper, we examine the circuit of a high-efficiency reverse dc magnetic amplifier which uses switching transistors. We show that the amplifier may operate under inductive (complex) loading.

The peculiarities of the combined usage of magnetic amplifiers and switching transistors in the circuit are analyzed. A simplified calculating technique and experimental data are given.

We know that reverse dc magnetic amplifiers (MA) have a low coefficient of useful output (low efficiency) due to the effect of shunt diodes which are included in the load [1]. As a rule, the reverse MA operate with an inductive (complex) load (exciting windings of electrical generators, clutches, relays, etc.). Lately, several proposed dc reverse output magnetic amplifier circuits have been proposed which have high efficiency. These circuits contain switching transistors (SW) which permit us to subdivide the power circuits of nonreverse MA into circuits with common loads [2-5]. We can easily convince ourselves that the circuits which we have examined [3-5] cannot operate under inductive loading. Actually, for a definite angle of saturation of the MA cores, we get a constant conductivity. The transistor and load currents which are switched in for a given signal polarity flow uninterruptedly. The transistor base current is also continuous, and assures the operation of the transistor switch SW in the saturation region for all collector current changes. Therefore, for all instantaneous load currents i_L, the condition

$$i_b \geqslant \frac{i_L}{\beta} \qquad (1)$$

must be satisfied where i_b is the instantaneous base current and β is the coefficient of current amplification of the common emitter transistor.

If condition (1) is not fulfilled, then the operating point of the transistor lies in the active or breakdown region, and the coefficient of utilization and the efficiency of the transistor are sharply decreased.

In the circuits described in [3], the transistor SW base circuits are fed from a sinusoidal voltage source through separate transformer windings; in the circuits described in [4,5], use is made of the output voltage of a magnetic amplifier and, therefore, the base currents in the transistor are not continuous, and operation with inductive loads is ineffective.

The circuit proposed in [2] may be used with any type of loading. The reverse amplifier (Fig. 1) consists of two nonreverse feedback amplifiers MA1 and MA2, which are fed from separate secondary windings of the transformer T_c. The output of each MA is connected to the load through the emitter-collector of common emitter switching transistors T_1 and T_2. The transistors are switched on in such a manner that, for separate MA operation, the output voltage has different polarities. The control winding of each amplifier is connected in series with the emitter-base junction of its transistor. The control circuits of the nonreverse amplifiers and switches are connected in parallel and lead to a common output for the push-pull amplifier. With the aid of the phase-shift winding, the operating points of the MA are shifted to the region of minimum load current.

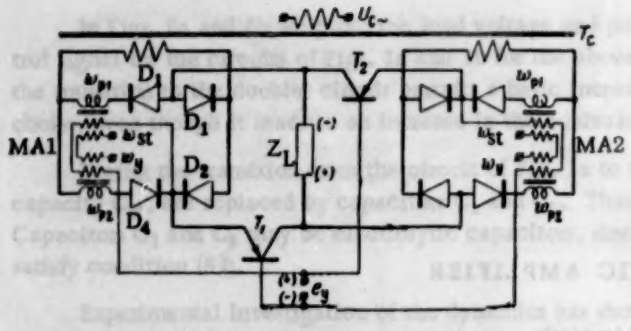

Fig. 1. Circuit of a dc reverse magnetic amplifier with switching transistors.

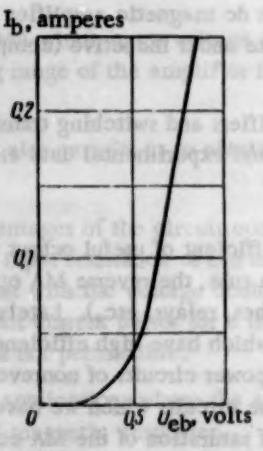

Fig. 2. A plot of the function $I_b = f(U_{eb})$ for the P4B transistor.

When a signal e_y of the polarity indicated in Fig. 1 is applied to the amplifier, then the control circuit of MA2 will be open-circuited due to the fact that the emitter-base junction of transistor T_2 is biased in the reverse direction (the switch is open), and the output of the amplifier will be disconnected from the T_2 power circuit. Thus, MA2 does not participate in the operation of the circuit. Since the emitter-base junction of T_1 is biased in the forward direction, a current flows in the control winding of MA1 which regulates the angle of saturation of the cores, and the amplifier output is connected to the load through the emitter-collector junction of transistor T_1. The load current and base current of transistor T_1 increase as the control current increases, and this results in saturation of the transistor.

When the polarity of signal e_y is changed, MA1, T_1, and MA2, T_2 interchange their mode of operation.

Let us consider the peculiarities of the combined operation of a transistor and magnetic amplifier in such a circuit.

1. Inasmuch as the transistor input circuit is nonlinear (see characteristic plotted in Fig. 2), it may substantially affect the input-output characteristics of the magnetic amplifier if the maximum value of the input signal $e_{y\,max}$ is not large. However, due to the presence of a no-load current in the nonreverse magnetic amplifier, and the significant increase in β for small collector currents, we can disregard the influence of the nonlinearity of the transistor input circuit for values of $e_{y\,max} \approx 2.5$-3 volts.

2. The inclusion of the control winding in the transistor control-circuit affects the breakdown voltage of the SW. We know that an increase in the active-base resistance of a common emitter transistor significantly decreases the breakdown voltage U_{bd}. However, the presence of a reverse bias across the output of the transistor hinders the decrease of the U_{bd}. In Fig. 3 we plot the breakdown voltage U_{bd} as a function of the transistor base resistance for various values of reverse-base potential U_b for the P4B transistor. We see from the graph that, for $e_{y\,max} \approx 3$ volts, and a MA control-winding resistance of not more than 200 ohms, we can use a SW in circuits where the amplitude of the applied voltage is equal to the maximum possible transistor collector voltage.

3. The presence of a no-load MA current forces the SW to operate in the active region for small values of the control signal. This determines the necessity for a manifold change in the output current of a nonreverse MA:

$$k_I = \frac{I_L}{I_{L\,min}} \geqslant 10 - 15. \qquad (2)$$

In the latter formula, I_L is the value of the load current for maximum output, and $I_{L\,min}$ is the value of load current for minimum output. This ensures linearization of the amplifier characteristics in the vicinity of the null.

4. The relatively small value of β for present-day transistors does not permit us to use magnetic amplifiers with large coefficients of current amplification.

5. The operation of the magnetic amplifier control circuit is of the greatest interest to us, since it determines the state of the transistor-base circuit. Let us examine Fig. 4, in which we plot the basic variables which

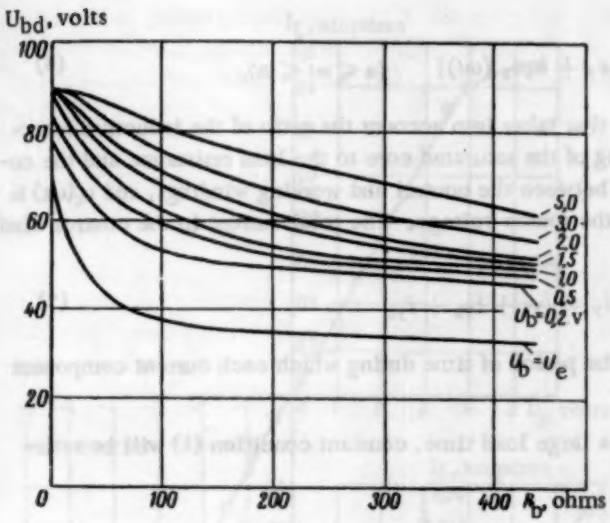

Fig. 3.

characterize the operation of the nonreverse magnetic amplifier: the circuit voltage $U_{c\sim}$; the voltage applied to the load U_L; the load current i_L; the current (ac) in the windings of the MA, i_{p1} and i_{p2}; the diode currents, which constitute a shunting circuit, i_{d1} and i_{d2}; and the control current i_y (for easier reading of the graphs, the scale for the current i_y has been considerably increased).

In [1] an analysis is made of the operation of a dc magnetic amplifier with an internal feedback loop. An ideal hysteresis loop and zero resistance in the control circuit is assumed.

For the power circuit, the results of this analysis will be exact for the case where the control circuit resistance is not equal to zero and the hysteresis loop has a finite slope in the saturation region. However, in the ideal case, the character of the changes in the control circuit differs significantly from those described in [1]. In the ideal magnetic amplifier, the current in the control winding flows only during the excitation period, and it is given by:

$$i_y = I_c = \frac{H_c l_{av}}{w_y} = \text{const} \quad (0 < \omega t < \alpha), \tag{3}$$

where H_c is the coercive force, l_{av} is the mean length of the magnetic lines of force, and w_y is the number of turns in the control winding. During the saturation interval, $\alpha \leq \omega t \leq \pi$, the current in the control winding is equal to zero.

In the actual magnetic amplifier there is a continuous current flow. The working half-period of the core can be divided into two parts: the excitation interval $0 \leq \omega t \leq \alpha$ and the saturation interval $\alpha \leq \omega t \leq \pi$. For the case of inductive loading, we must set aside, during the excitation period, a commutation interval $0 < \omega t < \gamma$, during which the load current is commutated from the working winding to the circuit of diodes D_1 and D_2.

As in the ideal case, a component of the current, i_y, as determined by Eq. (3),

$$i_{y1} = I_c \quad (0 < \omega t < \alpha). \tag{4}$$

flows through the control winding of the MA.

During the commutation interval we add to this the component resulting from current changes in the working winding of the saturated core due to the slope of the hysteresis loop in the saturation region, and from the interaction with the control winding

$$i_{y2} = \frac{k_1 L_s}{r_y} \frac{di_{ps}}{dt} \quad (0 < \omega t < \gamma), \tag{5}$$

where k_1 is the coefficient which takes into account the mutual inductance and the coefficient of transformation between the control and working windings, L_s is the inductance of the working winding when the core is saturated, and i_{ps} is the current in the working winding of the saturated core.

Since, in the actual amplifier, the control-circuit resistance is not equal to zero, the value of e_y is also not equal to zero, and during the saturation interval a component of current which is proportional to the signal voltage flows through the control winding.

In addition, the finite value of the inductive reactance of the working winding of the saturated core of the MA, and the presence of a magnetic connection with the control winding, result in a transformation of the even harmonics in the control circuit. As a result, the current in the control winding during the saturation interval is given by:

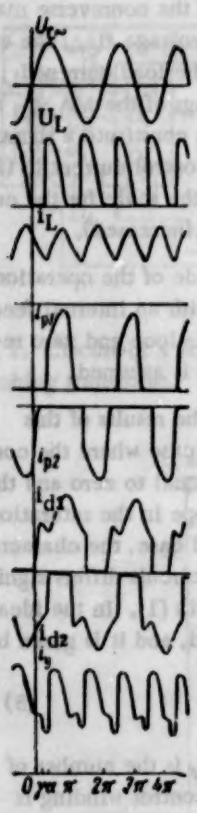

Fig. 4.

$$i_{y3} = \frac{1}{r_y}[e_y + k_2 u_s(\omega t)] \qquad (\alpha < \omega t < \pi), \tag{6}$$

where k_2 is the coefficient that takes into account the ratio of the inductive reactance of the working winding of the saturated core to the load resistance and the coefficient of transformation between the control and working windings, and $u_s(\omega t)$ is the instantaneous value of the source voltage. The total current in the control winding is given by

$$i_y = i_{y1} + i_{y2} + i_{y3} \tag{7}$$

where we take account of the period of time during which each current component flows.

It is obvious that for a large load time, constant condition (1) will be satisfied if

$$i_{y1} = I_c \geqslant \frac{I_L}{\beta} \tag{8}$$

and

$$\frac{e_{y.max}}{r_y} \approx I_y \geqslant \frac{I_L}{\beta}. \tag{9}$$

For the case of operation with an active resistance, where we take the transformation of even harmonics into consideration, relation (1) will be satisfied for a MA with saturated cores if

$$\frac{e_{y.max}}{r_y} \approx I_y \geqslant 2\frac{I_L}{\beta}. \tag{9'}$$

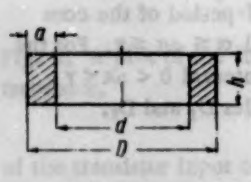

Fig. 5.

In the given circuit we cannot include a parallel load capacitance in order to smooth out the current pulsations. Thus, the specification of the simultaneous use of a MA and a SW for the circuit under consideration imposes three limitations upon the projected nonreverse magnetic amplifier, which have a significant effect upon the changes in the output current: relatively low input resistance, and limitations of the coefficients of current and voltage amplification.

The question of an increase in efficiency usually arises where significant load power is involved. In this case, the circuit as a rule consists of an output cascade with an intermediate amplifier; this permits us to easily overcome the above-indicated disadvantages associated with the choice of the output cascade.

If the output cascade amplifiers have toroidal cores which have rectangular hysteresis loops, then we can make use of simple relations in our calculations.

Assuming that we know the amplifier output power P_L and current I_L (voltage U_L) for the maximum signal, then we will also know the magnetic flux density B_s and the magnetizing force H_c for the chosen magnetic material. We must determine the core dimensions (Fig. 5) and winding parameters of a single-cycle magnetic amplifier. When the magnetic circuits have the optimum toroidal geometry, the following relations must be satisfied [6]:

$$\varkappa = \frac{D}{d} = 1,2 - 1,4, \qquad \frac{h}{a} = \frac{2h}{D-d} \approx 2. \tag{10}$$

The losses in the magnetic amplifier power circuit amount to 10-20%, and depend upon the output voltage, amplifier power, and the supply frequency. Therefore, the voltage of the transformer secondary windings is equal to:

$$U_2 = \frac{U_L}{\eta} \approx (1,1 - 1,2)\,U_L \tag{11}$$

where η is the coefficient of useful output of the nonreverse MA.

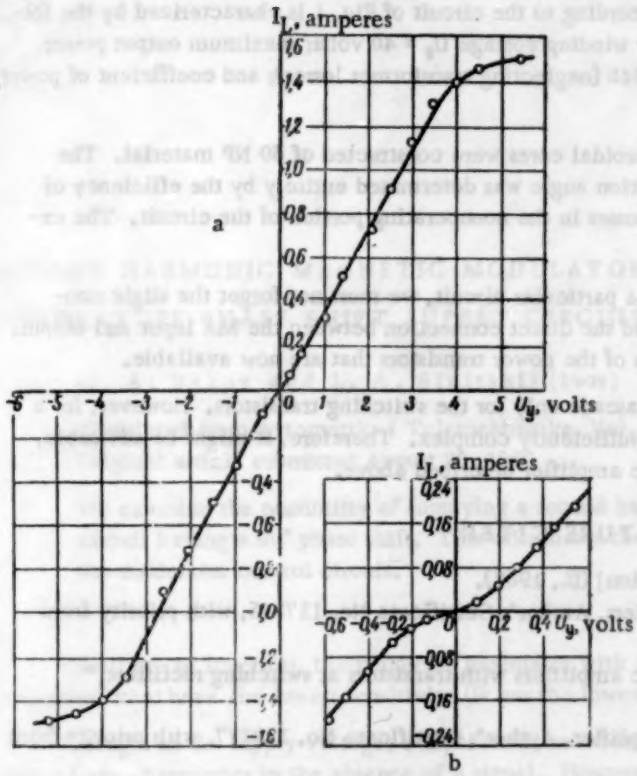

Fig. 6. Experimental static characteristic of the reverse MA.

In magnetic amplifiers with feedback loops, 10-15% of the window area is filled with control and phase-shift windings. Then the window area filled by the ac winding is given by:

$$S_{o\sim} = 0{,}85\frac{\pi d^2}{4} = \frac{I_L w_p}{2k_3\Delta}, \qquad (12)$$

where Δ is the permissible current density, and $k_3 \approx 0{,}25$ is the coefficient of utilization of the copper.

The cross section area of the steel core is given by the relation

$$S_{st} = \frac{\pi(D^2-d^2)}{4}hk_{su} = \frac{\pi d^2(\varkappa^2-1)}{4}hk_{su}, \qquad (13)$$

where k_{su} is the coefficient of steel utilization.

In order to obtain sharper changes in the load current of a single-cycle amplifier, the number of turns should be determined by means of the formula:

$$U_s = 4.44 w_p f B_s S_{st} 10^{-8}. \qquad (14)$$

From (12)-(14) we get

$$d = \sqrt[4]{0{,}215\frac{P_L\cdot 10^8}{\eta k_3 k_{su}\Delta f B_s h}}. \qquad (15)$$

Using the customary meaning of h for ribbon-type material, we can find the value of d which satisfies condition (10). We then find the number of turns in the ac winding from formula (12), and the magnetic circuit cross section for the given load current and desired value of Δ. Having determined the mean length of the magnetic line of force from the formula

$$l_{av} = \pi d\frac{1+\varkappa}{2}, \qquad (16)$$

we can find the number of turns in the control winding from (3).

Having chosen the switching transistor on the basis of the requisite load current and voltage (the load current and voltage amplitudes), and having determined β, we can find the value of the control winding resistance from (9), bearing in mind that $e_{y\,max} \geq 3$ volts. Knowing the resistance of, and the number of turns in the control winding, we can determine the wire diameter. We then verify the control winding design using the allowed current density, and determine the number of turns and the wire diameter of the phase-shift winding and verify the phase-shift between the windings. It is necessary that the switching transistor and the magnetic amplifier operate harmoniously, so that we obtain the desired coefficient of current amplification. In order to do this, the amplifier circuit is modified, a shunt resistance is added in the power circuit in parallel with the diodes.

In order to decrease the dimensions of the supply transformer, we feed both magnetic amplifiers from a single secondary winding.

We also verified the design in which the transistor and magnetic amplifier control circuits are connected in parallel. In this case, agreement between the MA and SW characteristics is not required, but the coefficient of amplification is decreased, and there is less linearity in the vicinity of the null.

A sample experimental amplifier constructed according to the circuit of Fig. 1 is characterized by the following data: circuit voltage U_c = 220 volts; secondary winding voltage U_s = 40 volts; maximum output power P_L = 35 watts; efficiency, for maximum signal, η = 0.845 (neglecting transformer losses); and coefficient of power amplification over the linear portion k_p = 300.

The P4D transistors were used as SW. The MA toroidal cores were constructed of 50 NP material. The amplifier efficiency over the entire range of the saturation angle was determined entirely by the efficiency of the single-loop amplifier. There were practically no losses in the nonoperating portion of the circuit. The experimental amplifier characteristic is given in Fig. 6.

If we are considering the use of the amplifier in a particular circuit, we must not forget the slight nonlinearity of the amplifier in the vicinity of the null, and the direct connection between the MA input and output. The load power is limited by the maximum parameters of the power transistors that are now available.

Lately there is a tendency to provide an output cascade only for the switching transistors. However, for a dc reverse output, a purely semiconductor amplifier is sufficiently complex. Therefore, it might be advisable, in a series of cases, to use the high efficiency magnetic amplifier described above.

LITERATURE CITED

1. G. F. Storm, Magnetic Amplifiers [Russian translation] (IL, 1957).
2. O. A. Kossov, Double Cycle DC Magnetic Amplifiers, Author's Certificate No. 117345, with priority from March 3, 1958.
3. A. G. Milnes, "High efficiency push-pull magnetic amplifiers with transistors as switching rectifiers," Comm. and Electronics, No. 37 (July, 1958).
4. M. A. Rozenblat, Double-Cycle DC Magnetic Amplifier, Author's Certificate No. 122777, with priority from March 26, 1959.
5. M. A. Rozenblat and G. V. Subbotina, "The use of transistors to improve the efficiency of reverse dc magnetic amplifiers," Avtomatika i Telemekhanika 20, No. 9 (1959).
6. N. P. Vasil'eva, O. A. Sedykh, and M. A. Boyarchenkov, Magnetic Amplifier Design [in Russian] (Gosénergoizdat, 1959).

All abbreviations of periodicals in the above bibliography are letter-by-letter transliterations of the abbreviations as given in the original Russian journal. *Some or all of this periodical literature may well be available in English translation.* A complete list of the cover-to-cover English translations appears at the back of this issue.

SECOND HARMONIC MAGNETIC MODULATOR WITH A QUADRATURE PHASE SHIFT SUPPLY CIRCUIT

M. A. Rakov and L. A. Sinitskii (Lvov)

Translated from Avtomatika i Telemekhanika, Vol. 22, No. 2, pp. 238-242, February, 1961
Original article submitted August 30, 1960

We examine the possibility of supplying a second harmonic magnetic modulator from a supply circuit having a 90° phase shift. This eliminates the need for filters in the exciting circuit and the modulator control circuit.

Of all dc-ac inverters, the magnetic modulator with a second harmonic output (frequency doubler magnetic amplifier) must have the lowest sensitivity (it has the lowest sensitivity threshold) [1].

Changes in the supply voltage, temperature, or second harmonic core parameters do not result in the appearance of even harmonics in the absence of a signal. However, a second harmonic modulator has a series of defects, the most serious of which is the necessity of using a series of auxiliary elements in order to ensure the requisite sensitivity, which complicate the modulator circuit and lead to a worsening of some of the modulator characteristics. These elements are the filters which appear in all three modulator circuits – the control circuit, the exciting circuit, and the output circuit. Each filter performs a definite function in the modulator circuit. It is necessary to use a second harmonic cutout filter in the control winding in order to prevent short-circuiting of the second harmonic emf induced in the control winding by the low impedance of the signal source which, in the majority of cases, is of low ohmage. We must have a filter in the exciting circuit in order to remove the second harmonic emf which is always present in the supply emf. The use of frequency sensitive elements, such as filters, makes the modulator characteristics frequency-sensitive. The construction of the filters becomes extremely complex when the filter is fed from a supply which has a low-frequency stability; this is often the case in practice.

Therefore, the logical question arises regarding the design of a second harmonic magnetic modulator for which there are no filters in the control and exciting circuits. It is obvious that, in such a modulator, even harmonics of the emf will not be induced in the control winding, and the presence of even harmonics in the supply emf will not lead to the appearance of a parasitic signal in the output circuit. We can accomplish all this by supplying the second harmonic from a quadrature circuit.

If we feed each of the exciting windings of the modulator from a separate supply, and each supply voltage is shifted by 90° with respect to the voltage of the other supply, thus, by including half of the control winding, we can obtain mutual cancellation of the second harmonic emf in the signal circuit. However, this does not assure compensation for the odd harmonics of the emf in the control windings and the output. We can compensate for the odd harmonics by increasing to four the number of cores used, and by using separate winding halves, as shown in Fig. 1 [2,3]. As we see from the figure, the control and output windings are connected, so that there is a bucking connection with respect to the first harmonic for each pair of cores; the second harmonic is only induced in the output winding, and is not shorted in the control circuit.

Up to the present time, we have not been successful in obtaining reliable and sufficiently simple voltage supplies which provide a 90° phase shift between two voltages, and which are independent of frequency variations. This problem may be solved by using the principle of frequency division. We know that the most easily achieved phase shift between two electrical voltages is 180°. If we transform each of two 180° phase-shifted voltages by means of identical frequency dividers into half-frequency voltages, then there will be a 90° phase shift between the two resulting voltages.

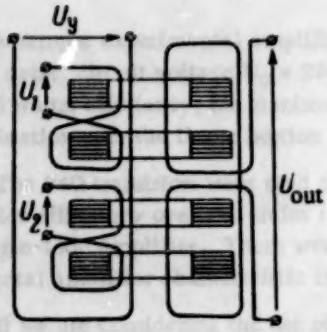

Fig. 1. Mode of connection of the windings of a second harmonic modulator which is fed from a supply having a quadrature phase shift.

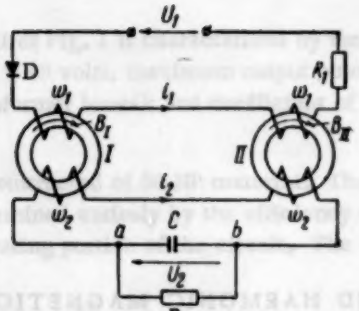

Fig. 2. Magnetic frequency divider. w_1 = 500 turns, w_2 = 2000 turns, permalloy core 79HM, S = = 0.05 cm^2.

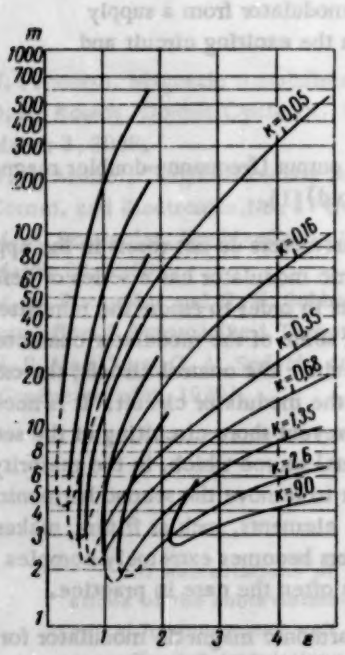

Fig. 3. Regions of stable divider operation.

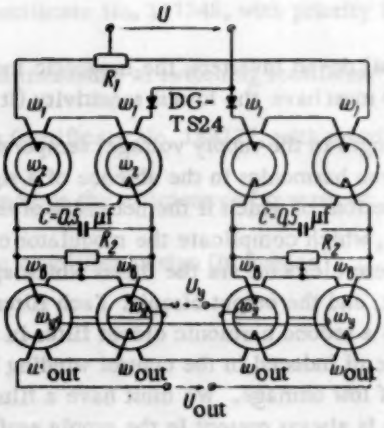

Fig. 4. Circuit for 90° phase shift modulator supply. w_1 = 500 turns, w_2 = 1500 turns, w_B = 500 turns, w_y = = 2500 turns, w_{out} = 1500 turns, core 79 HM, S = 0.05 cm^2.

We wish to note that, in the frequency division process, the phase of each of the new voltages is not uniquely determined. In the case in which we are interested, the one where the frequency is cut in half, then, depending upon the conditions involved in the frequency division process, it is possible to obtain two stable operating states in which one of the voltages is shifted by 180° with respect to the other [4]. In the case of two voltages, there are four possible results of the process which can be reduced to two basic variations, in each of which the voltages which lead and lag by 90° change places. This generally undesirable property does not exist when a double frequency output magnetic modulator is used, since a change in phase of the exciting current by 180° does not affect the phase of the second harmonic voltage (as a result of the properties of the 180° phase shift during frequency doubling, the phase angle becomes 360°).

Magnetic frequency dividers are among the simplest and most dependable frequency dividers [5,6]. We use as our magnetic modulator supply a magnetic frequency divider with a diode in the exciting winding (Fig. 2), which has the advantage that it does not require a separate dc source. The equations describing the frequency divider are of the form:

$$w_1 S \left(\frac{dB_I}{dt} + \frac{dB_{II}}{dt} \right) + R_1 i_1 + U(i_1) = U_1(t), \quad (1)$$

$$U_2 = w_2 S \left(\frac{dB_{II}}{dt} - \frac{dB_I}{dt} \right), \tag{2}$$

$$i_2 = C \frac{dU_2}{dt} + \frac{U_2}{R_L}, \tag{3}$$

$$H_I = \frac{i_1 w_1 + i_2 w_2}{l}, \qquad H_{II} = \frac{i_1 w_1 - i_2 w_2}{l}, \tag{4}$$

$$B = B(H). \tag{5}$$

In these equations, B_I, B_{II} and H_I, H_{II} are the values of magnetic flux density and field intensity in cores I and II, respectively; S is the area of transverse core cross section; $U = U(i_1)$ is the equation of the volt-ampere characteristic of the diode; l is the mean length of the magnetic lines of force in the core, and $B = B(H)$ is the equation of the magnetization curve of the core material.

In the following we will assume an ideal diode volt-ampere characteristic and an ideal magnetization curve for the core material.

As a result of the nonlinearity of the functions $U(i_1)$ and $B(H)$, it is extremely difficult to solve the system of Eqs. (1)-(5), even with the assumed simplifications. Therefore, in order to establish the boundaries of the stable operating region of the frequency divider, and to choose the optimum mode of operation, a careful experimental determination was made of those regions for which there was stable and reproducible operation of the frequency divider.

In order to present the experimental results in a generalized manner, the relations obtained are expressed in terms of dimensionless parameters which are obtained by putting Eqs. (1)-(5) in dimensionless form.

Introducing the new variables

$$\theta = \omega t, \quad y_2 = \frac{U_2}{\omega w_2 S B_s}, \quad b_I = \frac{B_I}{B_s}, \quad b_{II} = \frac{B_{II}}{B_s},$$

$$j_1 = \frac{i_1 R_1}{\omega w_1 S B_s}, \quad j_2 = \frac{i_2 R_L}{\omega w_2 S B_s},$$

where B_s is the magnetic flux density, it is not difficult to write the original system of equations in the form

$$\frac{db_I}{d\theta} + \frac{db_{II}}{d\theta} + j_1 + U(j_1) = \varepsilon \sin\theta, \tag{6}$$

$$y_2 = \frac{db_{II}}{d\theta} - \frac{db_I}{d\theta}, \tag{7}$$

$$j_2 = m \frac{dy_2}{d\theta} + y_2, \tag{8}$$

$$b_I = b(j_1 - k j_2), \tag{9}$$

$$b_{II} = b(j_1 + k j_2), \tag{10}$$

where b(j) is the equation of the core magnetization curve in dimensionless coordinates.

In the newly obtained system of Eqs. (6)-(10), we introduce two substitutions

$$\varepsilon = \frac{U_{1m}}{w_1 S \omega B_s},$$

$$k = \frac{R_1 w_2^2}{R_L w_1^2}, \qquad m = \omega R_L C.$$

With the assumptions which we have made regarding the ideal volt-ampere characteristic of the diode and the ideal magnetization curve for the core material, the dimensionless parameters ϵ, k, and m completely determine the operation of the frequency divider.

In Fig. 3 we plot the regions for which there is stable and reproducible operation of the frequency divider in terms of ϵ and $\underline{m}$. These regions correspond to varying values of $\underline{k}$. Each region of stable operation is included between two boundaries. The left boundary is indicated by a thick, and the right by a thin line. These regions were obtained by a generalization based upon experimental study of the operation of the magnetic frequency divider.

For the frequency divider under study, we easily obtain the relations

$$\frac{U_{\max}}{U_{\min}} \approx 3, \quad \frac{\omega_{\max}}{\omega_{\min}} \approx 10,$$

where U_{max}, U_{min} and ω_{max}, ω_{min} correspond to the upper and lower voltage and frequency limits of the values for which the frequency divider operates stably, and its operation can be reproduced.

The basic advantage of the frequency divider is the fact that the curve of its output voltage does not contain even harmonics. It is especially important to take note of the fact that this is independent of the shape of the voltage curve of the source of supply.

Therefore, the use of the frequency divider in the input circuit permits us to substantially lower our requirements regarding the shape of the input voltage curve, and to omit all filters from the input circuit.

A magnetic modulator with a double frequency output and fed from an exciting circuit, which is a frequency divider, is transformed essentially to a modulator with an output at the fundamental frequency which, at the same time, preserves the basic advantages possessed by second harmonic modulators – high zero-level stability. In particular, we are not longer faced with a series of difficulties in using this modulator in automatic control and regulation circuits where the output is fed to two-phase asynchronous motors. The application in such circuits of the usual second harmonic modulator would require the use of a special frequency doubler to feed the exciting winding of the motor.

As a result of the elimination of filters from the modulator control and excitation circuits, its characteristics become frequency independent over a wide frequency range, and this allows us to greatly lower the requirements placed upon the supply.

When the customary supply circuit was used to feed the magnetic modulator, successful operation for variations in frequency was obtained in the case where inductive filters were used. This led to either a large increase in the size of the entire setup, or to a decrease in the coefficient of amplification of the modulator. Actually, in order that there be no basic decrease in the coefficient of amplification of the modulator where there is an inductive filter in the signal circuit, it is necessary that the filter inductance be 2-3 times lower than the corresponding values for the modulator signal winding. In this case, the dimensions of the choke equal, or even exceed, those of the modulator.

The facts outlined above give us the basis for coming to the conclusion that it is very desirable to use a double frequency modulator which is fed from two quadrature voltages in various applications and, in particular, in those cases where the frequency of the source of supply is subject to frequency variations and the shape of the input voltage differs significantly from that of a sine wave.

The complete circuit of a modulator fed from a quadrature phase shift circuit is shown in Fig. 4. For the indicated winding and core data, the coefficient of voltage amplification of the modulator was 600, and the value of the deviation was zero over a wide temperature range (0 to 50°C), and for a variation of ± 10% in the external voltage, and an input power of the order of 10^{-13} watts.

LITERATURE CITED

1. M. A. Rozenblat, "The bases of construction of magnetic amplifiers with low-sensitivity thresholds," Avtomatika i Telemekhanika 17, No. 1 (1956).
2. M. A. Rozenblat, Magnetic Amplifiers [in Russian] (Soviet Radio, 1960).
3. W. Krämer, Patent No. 931541 (1955).
4. T. Khayasi, Forced Oscillations in Nonlinear Systems [Russian translation] (IL, 1957).
5. L. A. Bessonov, Self-Oscillations in Iron Core Electrical Circuits [in Russian] (Gosenergoizdat, 1953).
6. K. G. Mityushkin, "Magnetic frequency dividers," Collection: Works of the VNIIÉ, Issue 7 [in Russian] (Gosenergoizdat, 1958).

THE USE OF MAGNETIC AMPLIFIERS FOR IMPEDANCE MEASUREMENTS BY MEANS OF MAGNETICALLY COUPLED CIRCUITS

O. G. Malkina (Moscow)

Translated from Avtomatika i Telemekhanika, Vol. 22, No. 2, pp. 243-249, February, 1961
Original article submitted August 1, 1960

This article briefly presents the advantages and the essence of a new method for measuring the impedance components (R and X). It is shown how the method of magnetically coupled circuits can be used for practical measurements.

The method of magnetically coupled circuits [1] makes it possible independently to measure either of the impedance components (R or X). This simplifies laboratory measurements, and facilitates the design of automatic control devices for various industrial processes.

In designing data transmitters for the regulation or automatic control of any industrial process, as well as for feeding automatic control signals to balancing components, it is often necessary that each control signal be a well-defined function of only one impedance component.

There are two different basic procedures for the separate measurement of impedance components in using the bridge method.

1. The first method consists in using circuits where the bridge diagonal voltages are decomposed into two components, and where two zero phase-detecting indicators (ZPDI) are used with subsequent signal amplification (the amplifiers are sometimes mounted ahead of ZPDI).

2. The other method consists in using circuits where the control voltage is obtained by means of separate balancing indicators. Additional phase-shifting iterated networks are connected to the bridges, and two voltages, which are tapped off different points of the bridge circuits and the phase-shifting iterated networks, are fed to the indicators. Either amplitude-differential or phase-differential indicators are used as the indicating instruments. The output signals are amplified by means of amplifiers.

Only magnetic amplifiers are necessary for such measurements if the method of magnetically coupled circuits is used, which makes it possible to design vibration-resistant and shock-resistant measuring instruments.

This measurement method provides the possibility of combining the measuring device with a contactless control device in a single unit. The method is suitable for measuring small resistances on higher frequencies.

It is known from the literature [2] that the provision of automatic balancing in bridge circuits is difficult if they are fed from sources with higher frequencies, which is the reason why balancing components, necessary for this purpose, are still not available at the present time. In [2], it is indicated that the resistance moment value must satisfy special requirements in automatic bridge balancing – it is necessary that the rheochords have small and uniformly distributed resistance moments. The use of ordinary rheochords on higher frequencies involves difficulties due to the parasitic reactances of rheochords.

Ordinary rheochords can be used in automatic impedance measurements by means of the method of magnetically coupled circuits, since the balancing, in this case, can be secured by changing the rheochord resistance in the dc circuit.

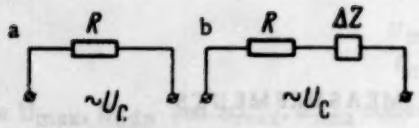

Fig. 1.

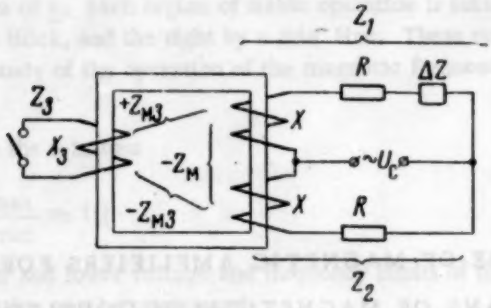

Fig. 2.

This measurement method is based on changes in the current – in its amplitude, average, or acting value – which are caused by the connection of the impedance to be measured to the measuring circuit.

In the measurement variants considered below, the difference between the rectified currents in two circuits is used; one of these circuits contains the resistance R (Fig. 1a), and the other circuit, besides this resistance R, also has the impedance ΔZ to be measured (Fig. 1b).

The constant component of the difference between the two rectified currents is, in this case, equal to the difference between the average values of the alternating currents, i.e., it is proportional to the current-value variation.

The current-magnitude variation in measuring small impedances ΔZ for which

$$\Delta R \ll R, \quad \Delta X \ll R, \tag{1}$$

is proportional to the resistance ΔR, since

$$|R + \Delta Z| = \sqrt{(R + \Delta R)^2 + \Delta X^2} \approx R + \Delta R$$

and

$$\Delta I = |\dot{I}_2| - |\dot{I}_1| \approx \frac{|\dot{U}_c|}{R} - \frac{|\dot{U}_c|}{R + \Delta R} = |\dot{I}_1| \frac{\Delta R}{R}.$$

For measuring the current-magnitude changes due to the reactance ΔX (in using circuits with the same R and R + ΔZ resistances), negative magnetic coupling is introduced between the currents in the circuits. For this purpose, two identical windings are wound on a single magnetic circuit in such a manner that the circuit currents create an opposing magnetic-circuit magnetization.

Circuits with such magnetically coupled windings are shown in Fig. 2.

The windings with negative magnetic coupling are connected to the measuring circuits in ΔX measurements, as well as in ΔR measurements. In order to prevent current changes due to the reactance ΔX in measuring ΔR, an additional winding, which is shorted during ΔR measurements, is wound on the magnetic circuit.

In the absence of the impedance to be measured (ΔZ = 0), and if no dispersion is present, the currents in such circuits will remain equal to

$$\dot{I}_1 = I_2 = \frac{\dot{U}_c}{R}. \tag{2}$$

if the shorted winding is provided, as well as in the case where it is not.

The connection of the small resistance to be measured will cause a small change in the circuit currents, which can be determined by simultaneously solving the following equations:

$$\dot{U}_c = \dot{I}_1 Z_1 - \dot{I}_2 Z_M + \dot{I}_3 Z_{M3}, \quad U_c = I_2 Z_2 - \dot{I}_1 Z_M - \dot{I} Z_{3M3}, \tag{3}$$
$$0 = \dot{I}_3 Z_3 + \dot{I}_1 Z_{M3} - \dot{I}_2 Z_{M3}.$$

Hence, for $Z_1 = Z_2 + \Delta Z$,

$$\dot{I}_2 = \dot{I}_1 \left[1 + \frac{\Delta Z}{Z_2 + Z_M - \frac{2Z_{M3}^2}{Z_3}} \right]. \tag{4}$$

If the additional winding is shorted ($r_3 = 0$) then, in the absence of dispersion,

$$\dot{I}_2 = \dot{I}_1 \left[1 + \frac{\Delta R + j\Delta X}{R + jX + jX - \frac{2j^2 X X_3}{jX_3}} \right] = \dot{I}_1 \left[1 + \frac{\Delta R}{R} + j\frac{\Delta X}{R} \right].$$

If the small resistances are to be measured, the difference between the absolute values of the currents, equal to

$$\Delta I = |\dot{I}_2| - |\dot{I}_1| \approx |\dot{I}_1| \frac{\Delta R}{R}, \tag{5}$$

will, for all practical purposes, depend only on the magnitude of pure resistance ΔR.

If the additional winding is open, i.e., if $Z_3 = r_3 + jX_3 = \infty$, the current $\dot{I}_2$ is equal to

$$\dot{I}_2 = \dot{I}_1 \left[1 + \frac{\Delta R + j\Delta X}{R + j2X} \right] = \dot{I}_1 \left[1 + \frac{\Delta R R + \Delta X 2X}{R^2 + 4X^2} + j\frac{\Delta X R - \Delta R 2X}{R^2 + 4X^2} \right].$$

If inequality (1) is satisfied, the terms containing ΔR and ΔX in the last expression will be much smaller than 1, and the current difference will be equal to

$$\Delta I = |\dot{I}_2| - |\dot{I}_1| \approx |\dot{I}_1| \frac{\Delta R R + \Delta X 2X}{R^2 + 4X^2}. \tag{6}$$

The difference between current changes in the presence, and in the absence, of the shorted winding is used in measurements.

In the presence of the shorted winding, the current change caused by the impedance ΔZ to be measured is compensated by the change ΔR in the circuit resistance R.

After the resistances of both measuring circuits have been equalized, the disconnection of the shorted winding will cause another change in the currents. Since, in this case, there is no difference between the resistances of the circuits [as ΔR in Eq. (6) is equal to zero, it will be compensated by the change in resistance R], the new current change will depend only on the magnitude of reactance ΔX. This new change in circuit currents can also be compensated by changing the circuit resistance R, i.e., it can be compensated by a new unbalanced state of the circuit resistances, which is specially introduced for this purpose. The unbalancing of the circuit resistances must cause an opposite change in the current magnitudes in order that the total current variation be equal to zero [see Eq. (6)].

The value of reactance ΔX can be determined with respect to the new change in the circuit resistance, since ΔX will be proportional to this change. This change will be equal to

$$-\Delta R_1 \approx \Delta X \frac{2X}{R}. \tag{7}$$

The minus sign indicates the nature of the change in the basic measuring-circuit resistance: it decreases for inductive ΔX, and increases for capacitive ΔX.

In the circuits considered below, the small value of the constant component of the difference between the two rectified currents passing through the control windings is directly amplified by a magnetic amplifier.

Figure 3 shows a variant of the simplest single-ended magnetic amplifier, which is controlled by the difference between two rectified currents.

If identical cores with identical magnetic characteristics are used in the W_r and W_c windings, the induced emf is equal to zero, due to the opposition of equal magnetic fluxes. Therefore, the shorting of either of the W_r and W_c windings will not cause a change in the load current I_l.

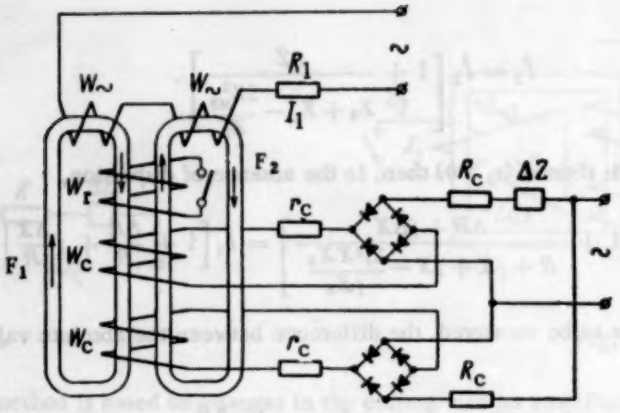

Fig. 3.

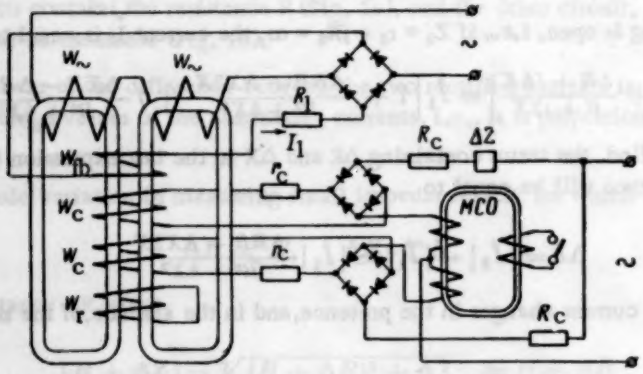

Fig. 4. Circuit of a single-ended magnetic amplifier for impedance measurements.

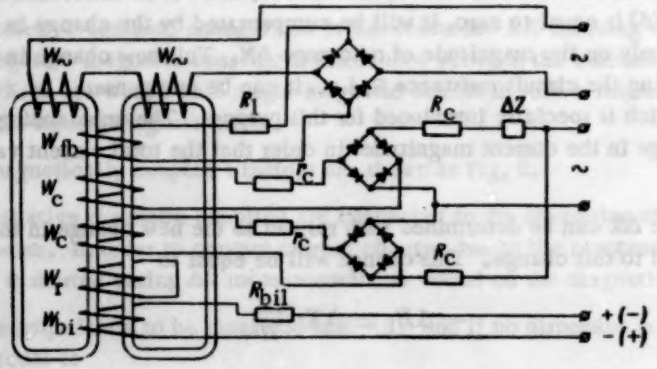

Fig. 5.

The load current will change only due to the constant component of the difference between the rectified currents in the control windings.

The W_c windings, which are wound on a common magnetic circuit, are magnetically coupled, and they have a certain inductance.

It was shown in [3] that the connection of magnetically coupled windings to the output of rectifier bridges can be used for impedance measurements. In this case, if the winding W_r is shorted, the constant component of the rectified control-current difference will depend on the resistive component ΔR of the impedance to be

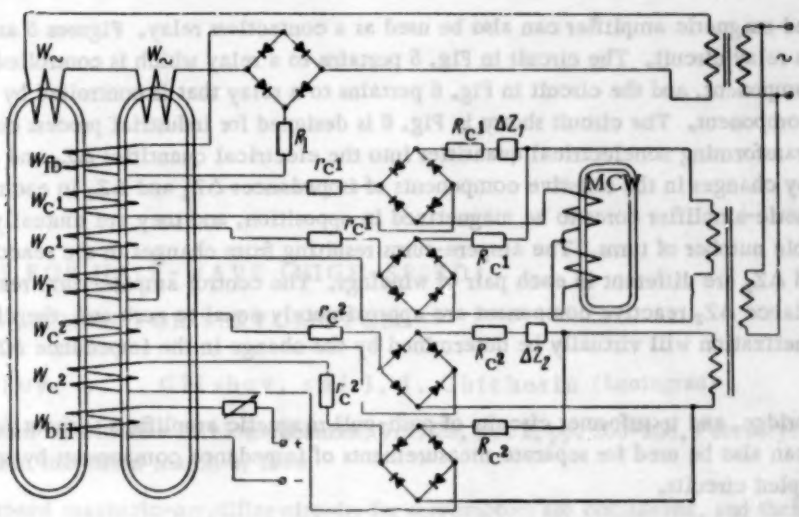

Fig. 6.

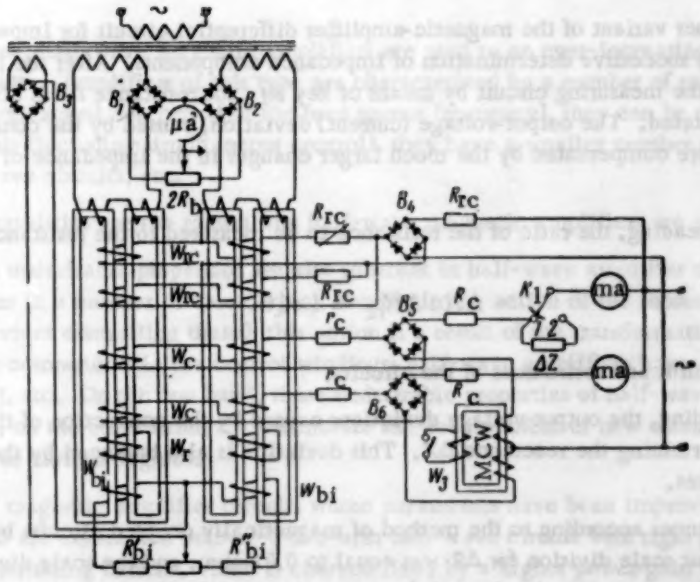

Fig. 7. Differential circuit of a push-pull magnetic amplifier for impedance measurements.

measured and, if the winding W_r is open, it will depend on the magnitude of ΔX, as well as on the magnitude of the introduced resistance unbalance ΔR.

The simultaneous magnetization of the cores by several magnetic fields with different frequencies will affect the inductance of the W_c windings, and cause the appearance in these windings of an emf with the even harmonics of the magnetic-amplifier feed frequency. The appearance of even-harmonic currents is undesirable because they distort the sinusoidal shape of the control alternating current – the measuring-circuit current.

In order to eliminate the control-current distortions caused by even-harmonic currents, the W_r winding must be shorted in ΔR measurements, as well as in ΔX measurements. In this case, the separate measurement of ΔR and ΔX can be secured by means of additional magnetically coupled windings (MCW), by connecting them to the ac circuit, as is shown in Fig. 4. The circuit in Fig. 4 has a feedback winding, which is used for a larger gain, as well as for the purpose of distinguishing between the polarities of the current difference to be amplified. In this case, the change in the amplified-signal polarity will cause an opposite change in the magnetic-amplifier load current.

Such amplifiers can have load characteristics similar to that shown in Figs. 7 and 8 in [4].

A single-ended magnetic amplifier can also be used as a contactless relay. Figures 5 and 6 show two variants of a contactless relay circuit. The circuit in Fig. 5 pertains to a relay which is controlled by varying the impedance resistive component, and the circuit in Fig. 6 pertains to a relay that is controlled by the impedance inductive-reactance component. The circuit shown in Fig. 6 is designed for industrial process control by means of two converters for transforming nonelectrical quantities into the electrical quantities ΔZ_1 and ΔZ_2. The current differences caused by changes in the resistive components of impedances ΔZ_1 and ΔZ_2 in each control-winding pair cause the magnetic-amplifier cores to be magnetized in opposition, and they are mutually completely compensated for a suitable number of turns. The ampere-turns resulting from changes in the reactive components of impedances ΔZ_1 and ΔZ_2 are different in each pair of windings. The control ampere-turns resulting from the change in the impedance ΔZ_2 reactive component are approximately equal to zero and, therefore, the magnetic-amplifier core magnetization will virtually be determined by the change in the impedance ΔZ_1 reactive component.

Differential, bridge, and transformer circuits of push-pull magnetic amplifiers without feedback, and with external feedback, can also be used for separate measurements of impedance components by means of the method of magnetically coupled circuits.

Paper [1] is concerned with an impedance-measurement variant employing a differential circuit with push-pull magnetic amplifiers, where the magnetic-amplifier control windings are used as the magnetically coupled windings.

Figure 7 shows another variant of the magnetic-amplifier differential circuit for impedance measurements. This circuit is designed for successive determination of impedance components. After the impedance ΔZ to be measured is connected to the measuring circuit by means of key K_1, the resistance ΔR is always determined first, while the W_3 winding is shorted. The output-voltage (current) deviation, caused by the connection of the impedance to be measured, is here compensated by the much larger changes in the impedance of the compensation winding W_{rc}.

For convenience in reading, the ratio of the resistance to be measured to the resistance to be varied was made to be

$$\Delta R : \Delta R_{rc} = 1 : 10$$

by a suitable selection of turns and resistances of the circuits.

For the open W_3 winding, the output-voltage deviations caused by the connection of the resistance to be measured are used for determining the reactance ΔX. This deviation is also balanced by the change in the compensation-winding resistances.

In measuring impedances according to the method of magnetically coupled circuits by means of the circuit shown in Fig. 7, the smallest scale division for ΔR was equal to 0.01 ohm, and the scale division for ΔX was equal to 0.1 mm. In this case, the measuring circuits and the magnetic-amplifier load windings were fed from a single 1000-cps feed source.

The magnetic amplifiers were made of laminated toroidal cores, for which the 79 NM alloy was used. A type-167311 multirange galvanometer with a luminous indicator was used as the magnetic-amplifier load.

Push-pull, as well as single-ended magnetic-amplifier circuits, can be used as contactless control relays with different characteristics.

There is a great variety of magnetic-amplifier circuits, which provides for a large scope of application of this measurement method in combination with various data transmitters.

LITERATURE CITED

1. O. G. Malkina, "Impedance measurements on audio frequencies by using the method of magnetically coupled circuits," Izmeritel'naya Tekhnika, No. 6 (1959).
2. V. Yu. Kneller, Alternating-Current Bridges with Two-Parameter Automatic Balancing. Thesis [in Russian] (IAT AN SSSR, 1959).
3. O.G. Malkina, "Rectifier bridges with magnetically coupled output loads," Avtomatika i Telemekhanika 20, No. 5 (1959).
4. M. A. Rozenblat, Magnetic Amplifiers [in Russian] (Soviet Radio Press, 1956).

SOME CIRCUITS FOR HALF-WAVE (HIGH-SPEED) MAGNETIC AMPLIFIERS FOR SERVOMOTORS

V. G. Leskov, A. I. Chizhov, and I. I. Chicherin (Leningrad)

Translated from Avtomatika i Telemekhanika, Vol. 22, No. 2, pp. 250-258, February, 1961
Original article submitted March 4, 1960

Three high-speed magnetic-amplifier circuits for servomotors are considered, and their properties are noted. The article provides data and the results of tests that were performed in using the proposed magnetic-amplifier circuits for an ac servomotor.

At the present time, half-wave magnetic amplifiers are used to an ever-increasing extent in automatic control and regulation circuits. Amplifiers of this type are characterized by a number of specific properties: Their inertia is low (it does not exceed one period of the feed source frequency), they can be controlled by dc, ac, and half-wave current signals (including simultaneous control), they have a smaller number of circuit elements in comparison with full-wave circuits, etc.

The above characteristics are the reason why half-wave magnetic amplifiers are used to such a great extent.

However, certain undesirable properties are also inherent in half-wave amplifier circuits. For instance, nondirectional action occurs in a number of cases, which consists in the action of the subsequent stages on the preceding stages (or on the devices controlling them); this action is a result of the transformation of the basic-frequency emf or of the harmonic components in the control windings; half-wave amplifiers have a relatively low power amplification factor [1], etc. On the one hand, these undesirable properties of half-wave magnetic amplifiers restrict their scope and, on the other hand, they stimulate the development of new circuits that would be free from the above deficiencies to various degrees.

Three half-wave magnetic amplifier circuits whose parameters have been improved in comparison with those of the available circuits are considered below: a two-arm half-wave circuit with rigid positive capacitive feedback with respect to alternating current, which is characterized by a higher power-gain value, and two two-arm half-wave amplifier circuits, which are characterized by a high q factor, and by their improved detecting properties (a better action directivity).

The Two-Arm Half-Wave Magnetic Amplifier with Rigid Positive Capacitive Feedback with Respect to Alternating Current

The amplifier circuit, which is shown in Fig. 1a, consists of a so-called half-wave bridge amplifier, which differs from the known circuits by the presence of rigid positive capacitive feedback with respect to alternating current, which makes it possible considerably to improve the stage-amplification factor.

Basic Circuit Elements

The choke is made of toroidal laminated cores with windings. Permalloy N79M4, 0.1-mm thick, is used as the core material. D_1-D_4 denote germanium-type D2V diodes.

Figure 1b shows another variant of this circuit, which differs from the first variant by a smaller number of diodes and working windings $W_{\sim}$.

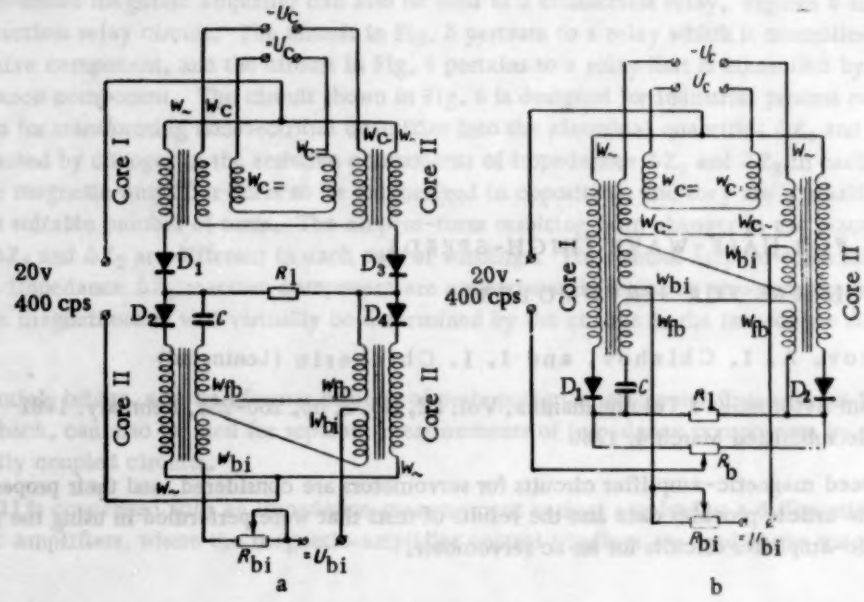

Fig. 1.

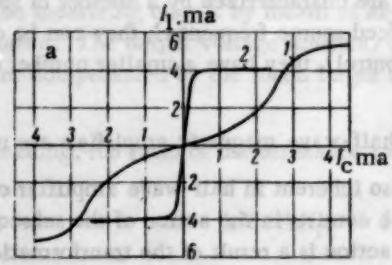

Fig. 2.

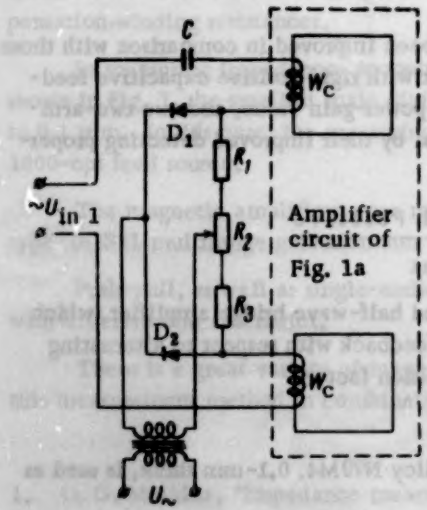

Fig. 3.

The amplifier operates in the following manner. If there is no signal at the input, a half-wave rectified current passes through each working winding $W_{\sim}$ of the cores I and II. The constant component of this current creates the feedback field, whose direction is invariable in each of the cores. In this, the amplifier load current is equal to zero. If an ac or dc current signal is present in one of the amplifier control windings $W_{c\sim}$ or $W_{c=}$, one of the cores becomes magnetized, and the other demagnetized, as a result of which an amplified half-wave rectified current will pass through the load.

The variable component $\frac{U_{max}}{2}$ sin ωt of the output-voltage basic frequency is fed to the positive-feedback winding W_{fb} through capacitor C. In this, the current arising in the circuit of the feedback windings creates additional ampere-turns whose sign is identical to the sign of the control ampere-turns (which is secured by a suitable connection of the W_{fb} windings). It should be noted that this method of introducing positive feedback is especially efficient in the case where the inductive load is considerable. In particular, by a suitable choice of the C value and the number of turns in the W_{fb} winding, the feedback-factor value can be increase to a value $K_{fb} > 1$, i.e., the stage can operate as a relay. In this case, the relay

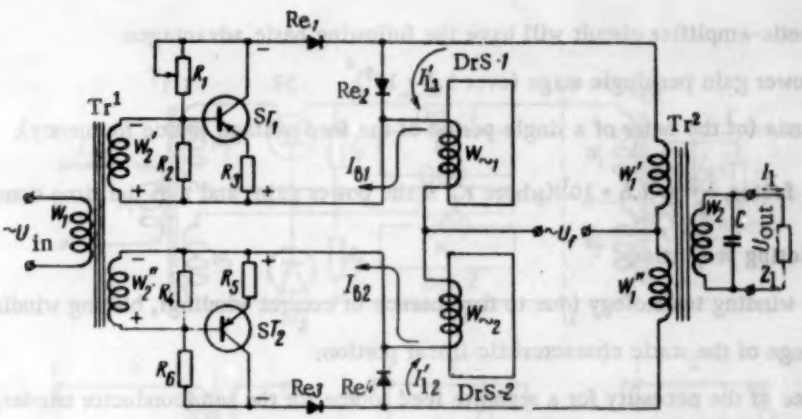

Fig. 4.

insensitivity zone can be regulated within certain limits by means of the R_{bi} resistor in the biasing circuit.

The amplifier and the relay static characteristics are given in Figs. 2a and 2b, respectively, while Curve 1 in Fig. 2a corresponds to the absence of positive capacitive feedback, and Curve 2 corresponds to the presence of rigid positive capacitive feedback.

The circuit under consideration can be used as an input or intermediate low-power stage in servomotor amplifiers and, for $K_{fb} > 1$, it can be used as a relay in approximate-reading circuits of two-reading servomotors and as a contactless relay in automatic-control relay systems.

Another interesting characteristic of the magnetic-amplifier circuit under consideration should be mentioned. If it is used with the half-wave phase-detecting rectifier whose circuit is shown in Fig. 3 (the circuit was proposed by V. G. Baranovskii); due to the possibility of simultaneously controlling half-wave circuits by means of dc and ac currents, it is possible to obtain an amplifier-output voltage whose one component is proportional to the input signal, and the other is proportional to the rate of change of the constant component of the phase-detecting rectifier input voltage.

In a number of cases, the above property of this circuit makes it possible to simplify, to a considerable extent, the entire servomotor circuit.

Two-Arm Half-Wave Magnetic Amplifiers with a High q Factor

As is known, the basic problem of magnetic-amplifier control consists in changing the core magnetic state by varying the magnetic field constant component.

In magnetic amplifiers with positive feedback, this problem can be solved by varying the current magnitude and direction in the control windings, or by varying the positive-feedback magnitude by changing the rectification factor of the feedback rectifiers.

Experiments indicate that the second method provides wide opportunities of designing magnetic-amplifier circuits of much better quality in comparison with the circuits already available. This is especially true of half-wave magnetic amplifiers with small inertia.

In practice, the essence of the second method consists in shunting the feedback rectifiers by means of variable and controllable resistors, and in changing the magnitude of this variable resistance in correspondence with the intensity of the input signal to be amplified.

Various devices, in particular electronic tubes, thyratrons, semiconductor triodes, etc., can apparently be used as such variable and controllable resistors. Semiconductor triodes, which would, in this case, constitute integral parts of the magnetic amplifiers, should be preferred.

Figure 4 shows the circuit of a high-speed, two-arm (push-pull) magnetic power amplifier with an ac output, which is controlled by varying the internal-feedback magnitude by means of semiconductor triodes that, in turn, regulate the rectification factor of the internal-feedback rectifiers.

Such a magnetic-amplifier circuit will have the following basic advantages:

1) a large power gain per single stage (over $1.5 \cdot 10^5$);

2) a low inertia (of the order of a single period of the feed-voltage source frequency);

3) a large $\frac{q}{}$ factor, $\frac{K_p}{\tau} \approx 7.5 \cdot 10^7$ (where K_p is the power gain, and τ is the time constant);

4) good detecting properties;

5) a simpler winding technology (due to the absence of control windings, biasing windings, etc.);

6) a wide range of the static characteristic linear portion;

7) the absence of the necessity for a separate feed source for the semiconductor triodes;

8) the possibility of tapping off large power from the same cores by using the entire core opening area only for the working winding.

As follows from Fig. 4, the amplifier circuit under consideration consists of a four-arm ac bridge, two arms of which consist of DrS-1 and DrS-2 differential-control saturable reactors with internal positive feedback, which is secured by rectifiers Re_2 and Re_4, respectively; the other two arms consist of the Tr2 transformer windings. The feed voltage U_f is connected to the bridge diagonal (between the common points of the adjacent arms), and the load impedance Z_l is connected to the secondary winding of the balancing transformer Tr2. The saturable reactors are controlled by shunting the Re_2 and Re_4 rectifiers by means of semiconductor triodes ST_1 and ST_2.

It is known [2] that, if ac voltage is fed to the crystal-triode collector circuit, the collector current will flow in both directions, and a strong reverse influence of the collector circuit on the emitter circuit will be observed. The connection of rectifiers Re_1 and Re_3 to the collector circuit results in the fact that the collector current can flow only in one direction.

By means of resistors R_1-R_6, the operating point on the linear portions of the triode characteristics is determined, and the stabilization of their operating temperature conditions is secured. The current intensity I_b (the initial operating point on the semiconductor triode characteristic) is chosen in such a manner that the initial current value $I_l^{\prime}$ approximately corresponds to the middle of the characteristic linear portion $I_l = \varphi(I_b)$, where I_l is the current passing through the bridge arms when the feed voltage "plus" is applied to the common point of the transformer Tr2 windings, and I_b denotes the same for the case where the feed voltage "plus" is applied to the common point of the chokes.

In the absence of input signals, the bridge balancing with respect to the feed-voltage first harmonic is effected by means of resistor R_1. The circuit differential control is secured by the fact that the input signal with frequency f is fed to the base of one semiconductor triode in step with the collector voltage, and to the base of the other semiconductor triode in phase opposition to the collector voltage. When the input signal is supplied, the I_{b1} current increases, and the I_{b2} current decreases (see Fig. 4). Correspondingly, the I_{l1} current decreases, and the I_{l2} current increases, and a voltage with a certain given phase arises in the load. If the input-signal phase is changed by 180°, the pattern of the described effects will be reversed.

The Tr1 transformer serves for the phase-opposition feed of the input signal to the semiconductor triodes, and for matching the signal data transmitter with the input resistance of the semiconductor triodes. The connection polarities of the Re_1-Re_4 rectifiers shown in Fig. 4 are those specified for p – n – p semiconductor triodes. The connection polarities for n – p – n semiconductor triodes must be reversed.

The basic data concerning the stage constructed on the basis of the circuit shown in Fig. 4 are the following: Tr1 is a toroidal transformer with a core made of 50NP material (strip thickness 0.05 mm); Tr2 is a three-leg transformer with a core made of E44 material (plate thickness 0.2 mm); DrS-1 and DrS-2 are reactors with toroidal cores made of KhVP material (thickness 0.08 mm).

In the absence of input signals, $I_{l1}^{\prime} = I_{l2}^{\prime} = 0.325$ amp, $I_{b1} = I_{b2} = 0.001$ amp, $U_{\sim} = 110$ volts, $f = 500$ cps.

If input signals are supplied, $U_{in} = 0.5$ volts, $i_{in} = 0.0002$ amp, $I_{l1}^{\prime} = 0.15$ amp, $I_{l2}^{\prime} = 0.5$ amp, $I_{b2} = 0.0005$ amp, $I_{b1} = 0.0015$ amp, $U_{out} = 100$ volts, $I_l = 0.15$ amp.

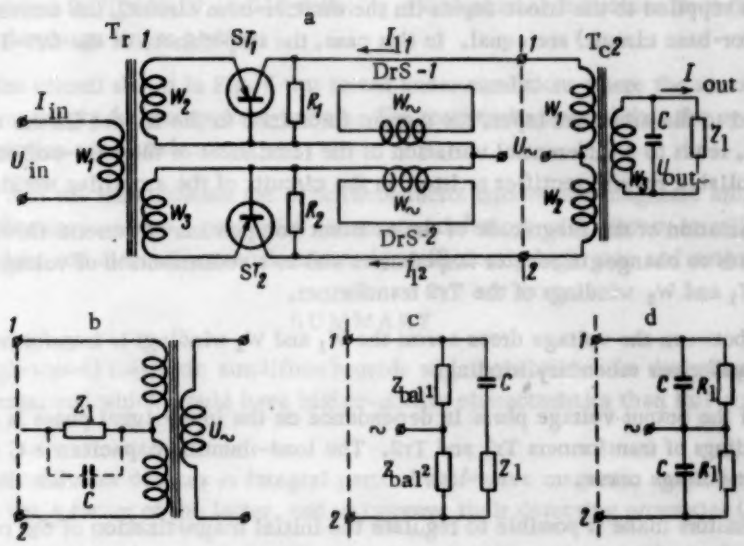

Fig. 5.

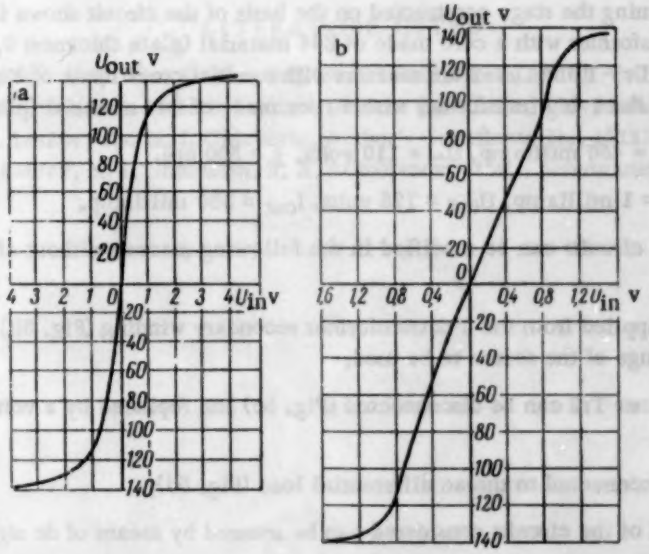

Fig. 6.

The circuit shown in Fig. 5a is a result of further improvement of the above-considered two-arm half-wave magnetic power amplifier. As can be seen from the figure, this circuit differs from the circuit considered above by the fact that the feedback rectifiers have been eliminated. Their functions, and the functions of the variable control resistors, are simultaneously performed by semiconductor triodes, which are connected to a circuit with a common base. In other respects, the circuit in Fig. 5a is basically the same as the circuit in Fig. 4; it also consists of a four-arm ac bridge, whose two arms consist of differential-control saturable reactors DrS-1 and DrS-2, the working windings of which are connected in series to triodes ST_1 and ST_2. The other two arms consist of the identical windings W_1 and W_2 of the Tr2 transformer.

The detecting properties of the collector-base junction of each of the triodes secures the flow of half-wave rectified currents through the $W_\sim$ windings of the DrS-1 and DrS-2 reactors in the direction of the low triode resistance, i.e., from the collector to the base. The magnitudes of these currents determine the magnetic state of the cores and the impedance of each of the reactors.

If no signals are supplied to the triode inputs (in the emitter-base circuit), the currents flowing through the triodes (in the collector-base circuit) are equal. In this case, the impedances of the DrS-1 and DrS-2 reactors are also equal.

If signals are fed to the amplifier input, the current intensities in the triodes (in the emitter-base circuit) change which, in turn, leads to a differential variation of the resistances of the base-collector junctions, which play the role of controllable reverse rectifier resistors in the circuits of the amplifier working windings.

The resulting variation of the magnitude of the constant components of currents flowing through the reactor $W_{\sim}$ windings leads to changes in reactor impedances and to a redistribution of voltage-drop values across the reactors and the W_1 and W_2 windings of the Tr2 transformer.

The difference between the voltage drops across the W_1 and W_2 windings is transformed into load Z_l, which is connected to the transformer secondary winding.

The variation of the output-voltage phase in dependence on the input-signal phase is secured by a suitable connection of the windings of transformers Tr1 and Tr2. The load-shunting capacitance C serves for correcting the shape of the output-voltage curve.

The R_1 and R_2 resistors make it possible to regulate the initial magnetization of the reactors (for $U_{in} = 0$), and to eliminate the spread of the triode and reactor characteristics. A more flexible method for solving this problem is that of selecting the operating points on the triode characteristics by supplying a negative bias to the bases of the triodes with respect to the emitters.

The basic data concerning the stage constructed on the basis of the circuit shown in Fig. 5a are the following: Tr1 is a three-leg transformer with a core made of É44 material (plate thickness 0.2 mm), ST_1 and ST_2 are germanium P-201V triodes, DrS-1 and DrS-2 are reactors with toroidal cores made of KhVP material (strip thickness 0.08 mm), and Tr2 is a three-leg transformer with a core made of É44 material (plate thickness 0.2 mm).

For $U_{in} = 0$, $I_{l1} = I_{l2} = 450$ milliamp, $U_{\sim} = 110$ volts, $f = 500$ cps.

For $U_{in} = 1$ volt, $I_{in} = 1$ milliamp, $U_{out} = 125$ volts, $I_{out} = 380$ milliamp.

The above-considered circuits can be modified in the following manner without affecting their basic advantages:

a) The feed can be supplied from the Tr2 transformer secondary winding (Fig. 5b), which makes it possible to widen the feed-voltage range of the source to be used;

b) the output transformer Tr2 can be disconnected (Fig. 5c) and replaced by a voltage divider ($Z_{bal\,1}$ and $Z_{bal\,2}$);

c) the output can be connected to the ac differential load (Fig. 5d);

d) differential control of the circuits considered can be secured by means of dc signals.

The high qualities of the circuits under consideration were confirmed in experiments. Thus, in particular, the first circuit amplification factors with respect to power, voltage, and current attained values of the order of $K_p = 150{,}000$, $K_u = 200$, and $K_i = 750$, respectively, while the following values were obtained for the second circuit: $K_p = 45{,}000$, $K_u = 120$, and $K_i = 375$.

The q factors for the first and second circuit, respectively, were

$$\frac{K_{p_1}}{\tau_1} = 7{,}5 \cdot 10^7 \ \text{sec}^{-1}; \qquad \frac{K_{p_2}}{\tau_2} = 2{,}25 \cdot 10^7 \ \text{sec}^{-1}.$$

The experimental data indicate that the qualities of the circuit shown in Fig. 4 are higher than that of the circuit of Fig. 5a.

An investigation of the inertia of the above two circuits yielded $T_1 = 0{,}002$ sec for the first-circuit time constant and $T_2 = 0{,}002$ sec for the second-circuit time constant.

The static characteristic of the amplifier based on the circuit of Fig. 4 is shown in Fig. 6a (the control winding of an ADP-123 motor was used as the amplifier load), and the static characteristic of the amplifier based on

the circuit of Fig. 5a is shown in Fig. 6b ($U_{\sim}$ = 110 volts; Z_l = 320 ohms). It is clear from the figures that the characteristics have a rather large linear portion.

The operation of the circuit shown in Fig. 4 was tested under conditions where the surrounding temperature, the voltage, and the power-supply frequency were varied. The test results showed that the operating stability of the circuit under consideration was satisfactory.

It should be noted that the simultaneous use of semiconductor triodes and magnetic amplifiers makes it possible to design amplifier devices whose properties are most satisfactory with respect to reliability, operating speed, and minimum weight and dimensions requirements for sufficiently high gain and output-power values.

SUMMARY

1. Half-wave (high-speed) magnetic amplifiers provide wide possibilities for designing circuits which would satisfy various requirements, and which would have higher-quality characteristics than full-wave magnetic-amplifier circuits.

2. The use of semiconductor devices as integral parts of half-wave magnetic amplifiers makes it possible to considerably improve the $\underline{q}$ factor of the latter, and to improve their detecting properties (action directivity).

3. The two-arm half-wave magnetic amplifiers which we developed and constructed made it possible to obtain a $\underline{q}$ factor value of the order of $(2.0\text{-}7.0) \cdot 10^7$ sec^{-1} for a single stage, and a time constant equal to T = = 0.002 sec.

LITERATURE CITED

1. M. A. Rozenblat, Magnetic Amplifiers [in Russian] (Soviet Radio Press, 1956).
2. Yu. I. Konev, Crystal Triodes in Automatic Control Devices [in Russian] (Soviet Radio Press, 1957).
3. V. K. Artem'ev, V. G. Leskov, and N. I. Chicherin, Author's Certificate No. 111155, November 19, 1957.
4. D. V. Vasil'ev, V. A. Fateev, N. I. Chicherin, B. A. Mitrofanov, et al., Servomotor Design [in Russian] (Sudpromgiz, 1958).

THE PULSE FEED OF MEASURING-BRIDGE CIRCUITS WITH SEMICONDUCTOR RESISTORS IN TWO-POSITION TEMPERATURE CONTROL DEVICES

V. F. Bakhmut-skii, I. I. Vinshtein, and S. E. Sas (Lvov)

Translated from Avtomatika i Telemekhanika, Vol. 22, No. 2, pp. 259-262, February, 1961
Original article submitted April 5, 1960

The thermal regime of a semiconductor thermoresistor under pulse-feed conditions is considered here. The power gain at the output of a measuring bridge circuit in comparison with the case of continuous feed, is estimated. General recommendations regarding the pulse feed of measuring circuits with thermoresistors in temperature position control devices are provided.

In ordinary two-position temperature control systems, the time interval between two successive regulator actuations lies within the interval from units to tens of minutes, while the output relay actuation time is 10^{-3} to 10^{-1} sec for electromagnetic relays, and 10^{-6} to 10^{-5} sec for electronic relays. Under these conditions, continuous feed of measuring circuits with semiconductor thermoresistors (STR) is not necessary. In principle, the feed can be provided periodically in pulses whose duration is sufficient for the output relay actuation. If we consider the fact that, in the case of continuous feed, the electrical energy dissipated in STR is wasted on heating STR, and that, under pulse-feed conditions, the energy in STR is dissipated during a very short interval of time, the pulse power can be considerably increased without exceeding the assigned STR overheating value, which is determined by the assigned regulation accuracy. The corresponding power gain at the measuring-circuit output, in comparison with the case of continuous feed, makes it possible to simplify the amplifying device to a considerable extent, or to eliminate it completely.

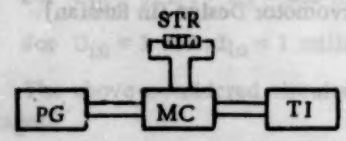

Under pulse-feed conditions, the measuring circuit can be loaded with any element having two stable states: a polarized relay, a magnetostatic trigger, an electronic trigger, etc., can be used. In this, if an electronic trigger is used, because of its fast action, the pulses can be directly formed from industrial-frequency voltage by means of the well-known methods used in pulse techniques [1]. Mechanical and bimetal time relays, time relays with indirect-heating STR [2], relays with filamentless thyratrons [3], etc., can be used for the periodic switching of the pulse-shaping elements. In this, the pulse repetition period must be shorter than the time during which the object temperature changes by a magnitude equal to the assigned regulation zone. By the term regulation zone, we here understand a temperature interval within which the object temperature changes in cycles when the regulator is switched on.

The figure shows the block diagram of a regulator with a pulse-fed measuring circuit with STR, where PG is the pulse generator, MC is the measuring circuit, and TI is the two-position indicator.

Let us consider the STR thermal regime under pulse-feed conditions.

Let the power dissipated in STR change according to the law

$$p(t)=\begin{cases} P & \text{for } n(t_p+t_i)\leqslant t\leqslant n(t_p+t_i)+t_i, \\ 0 & \text{for } n(t_p+t_i)+t_i\leqslant t\leqslant (n+1)(t_p+t_i), \end{cases} \quad (1)$$

where $n = 0, 1, 2, \ldots$, t_i is the pulse time, t_p is the pause time, and P is the pulse power value.

The heat-balance equation will be written thus:

$$mc\,dT + ks\,(T - \theta)\,dt = p\,(t)\,dt, \tag{2}$$

where m is the STR mass, c is the specific heat, k is the heat transfer coefficient, s is the STR surface area, T is the STR temperature (we assume that there is no temperature gradient throughout the STR volume), and θ is the surrounding medium temperature.

By introducing in (2) the notation $\frac{mc}{ks} = \tau$ (the STR time constant) and $\frac{1}{mc} = \sigma$, and by substituting p(t) from (1), we can rewrite (2) thus:

$$\begin{aligned} &\frac{dT}{dt} + \frac{1}{\tau}T = \frac{1}{\tau}\theta + \sigma P \quad \text{for} \quad n(t_p + t_i) \leqslant t \leqslant n(t_p + t_i) + t_1 \\ &\frac{dT}{dt} + \frac{1}{\tau}T = \frac{1}{\tau}\theta \quad \text{for} \quad n(t_p + t_i) + t_1 \leqslant t \leqslant (n+1)(t_p + t_i). \end{aligned} \tag{3}$$

We shall denote by $T^{(1)}_{n+1}$ the solution of Eq. (3) for the (n + 1)th pulse, and by $T^{(2)}_{n+1}$ the solution for the (n + 1)th pause. The general solution will be obtained by the fitting method. As a result, we obtain

$$T^{(1)}_{n+1} = \theta + \sigma\tau P - \sigma\tau P\,\frac{\exp\frac{t_p + t_i}{\tau} - \exp\frac{t_i}{\tau} + \left(\exp\frac{t_i}{\tau} - 1\right)\alpha^{(1)}_n}{\exp\frac{t_p + t_i}{\tau} - 1}\exp\left(-\frac{t_1}{\tau}\right), \tag{4}$$

$$T^{(2)}_{n+1} = \theta + \sigma\tau P\,\frac{\left(\exp\frac{t_p}{\tau} - 1\right)\left(\exp\frac{t_i}{\tau} + \alpha^{(2)}_n\right)}{\exp\frac{t_p + t_i}{\tau} - 1}\exp\left(-\frac{t_2}{\tau}\right) \tag{5}$$

where $\alpha^{(1)}_n \to 0$, $\alpha^{(2)}_n \to 0$ for $n \to \infty$; t_1 varies within the $[0, t_i]$ interval, and t_2 varies within the $[0, t_p]$ interval. For steady-state conditions ($n \to \infty$), we obtain:

$$T^{(1)}_{\infty} = \theta + \sigma\tau P - \sigma\tau P\,\frac{\exp\frac{t_p + t_i}{\tau} - \exp\frac{t_i}{\tau}}{\exp\frac{t_p + t_i}{\tau} - 1}\exp\left(-\frac{t_1}{\tau}\right), \tag{6}$$

$$T^{(2)}_{\infty} = \theta + \sigma\tau P\,\frac{\exp\frac{t_p}{\tau}\left(\exp\frac{t_i}{\tau} - 1\right)}{\exp\frac{t_p + t_i}{\tau} - 1}\exp\left(-\frac{t_2}{\tau}\right). \tag{7}$$

From (7), we find the maximum steady-state overheating (for $t_2 = 0$):

$$\Delta T_{\max} = \sigma\tau P\,\frac{\exp\frac{t_p}{\tau}\left(\exp\frac{t_i}{\tau} - 1\right)}{\exp\frac{t_p + t_i}{\tau} - 1}. \tag{8}$$

It is necessary that

$$(\Delta T_{\max})_{all} = (\Delta T_0)_{all} = \sigma\tau\,(P_0)_{all} \tag{9}$$

where $(\Delta T_{max})_{all}$ is the maximum allowable overheating under pulse-feed conditions, $(\Delta T_0)_{all}$ is the maximum allowable overheating under continuous feed conditions, and $(P_0)_{all}$ is the maximum allowable power under continuous feed conditions. By substituting (9) in (8), we obtain the gain in power that is dissipated by STR (or, which is the same, the power gain at the measuring bridge circuit output):

$$N = \frac{(P)_{all}}{(P_0)_{all}} = \frac{\exp \frac{t_p + t_i}{\tau} - 1}{\exp \frac{t_p}{\tau} \left(\exp \frac{t_i}{\tau} - 1 \right)} \qquad (10)$$

Equation (10) indicates that the power gain under pulse-feed conditions, in comparison with continuous feed, is determined by two parameters: t_p/τ and t_i/τ. For $t_p/\tau = 0$ (the case of continuous feed), N = 1, and no gain is obtained. As t_p/τ increases and t_i/τ decreases, the gain becomes larger. However, it should be noted that there is an upper limit for t_p/τ, as well as a lower limit for t_i/τ. The lower limit of t_i and, correspondingly, of t_i/τ, is determined by the indicator actuation time. The upper limit of t_p and, correspondingly, of t_p/τ, is determined by the rate of change in the object temperature. Since t_p is the time during which the circuit does not follow the changes in the STR resistance (temperature), and the time of the STR reaction to temperature changes in the object is of the order of τ, a t_p value of the order of τ, i.e., a t_p/τ value of the order of unity, can be accepted. It can be readily seen that the power gain N is of the order of the time constant to the pulse-time ratio. Actually, from (10), we have $N \approx 0.6(\tau/t_i)$ for $t_p/\tau = 1$. With an increase in the t_p/τ ratio, the value of N rapidly tends to τ/t_i; even for $t_p/\tau = 3$, $N \approx 0.95(\tau/t_i)$. In practice, we can choose a t_p/τ value which is even considerably lower than unity. In the latter case, as can be readily seen from (10), $N \approx \frac{t_p + t_i}{t_i}$, i.e., the power gain is equal to the duty ratio.

In conclusion, we shall consider some additional advantages of pulse feed.

1. In estimating the power gain at the measuring-circuit output, it was assumed that the maximum allowable STR overheating under pulse-feed conditions (equal to the maximum allowable STR overheating under continuous-feed conditions) was determined on the basis of the assigned measurement accuracy, and that it was not taken into account in calibrating the measuring circuit. This STR thermal regime can be forced by further increasing the pulse power under the condition that the corresponding STR overheating is taken into account in calibrating the measuring circuit. This will make it possible to increase, to a considerable extent, the power gain at the measuring-circuit output in comparison with the value given in (10). It is obvious that the STR overheating under forced conditions can be taken into account only if the overheating is steady, i.e., only if the character of the medium to be controlled, and its motion velocity with respect to STR, are constant.

2. The above pertains to STR and measuring-bridge circuits. However, all that has been said can be readily applied to cases where wire resistance thermometers and differential measuring circuits are used.

3. The feed pulses can be nonrectangular; in this case, the calculations are performed with respect to the effective pulse power value.

4. Two-position control has been treated here. However, pulse feed of measuring circuits with thermoresistors can be used with equal success in three-position temperature regulators, as well as in temperature signalization and safety devices.

5. If there are several points to be controlled in a single system, pulse feed can be supplied from a common high-power pulse generator (or from a generator of the same power if a bypass device is available). In this case, a single pulse generator would replace the amplification units, the number of which is proportional to the number of the points to be controlled.

LITERATURE CITED

1. M. M. Aizinov, Transient Processes in Radio Device Components [in Russian] (Sea Transport Press, 1955).
2. N. P. Udalov, On the Application of Thermally Controlled Semiconductor Resistors in Timing Devices, Thesis [in Russian] (MAI, 1952).
3. L. N. Korablev, New Applications of Cold-Cathode Tubes in Pulse Equipment [in Russian] (AN SSSR Press, 1956).

NEW DEVELOPMENTS CONCERNING HIGH-FREQUENCY REMOTE-CONTROL CHANNELS

Ya. L. Bykhovskii, R. A. Izrailev, G. V. Mikutskii,

V. S. Skital'tsev, and V. B. Sokolov (Moscow)

Translated from Avtomatika i Telemekhanika, Vol. 22, No. 2, pp. 263-270, February, 1961
Original article submitted May 7, 1960

The present paper describes the work performed at the All-Union Scientific-Research Institute of Electrical Power Engineering in the field of high-frequency remote-control channels. Among the devices considered in detail here are the audio equipment with semiconductor components for remote-control channels, new combined equipment for telephone communications, and remote control for use with electrical power transmission-line conductors, and equipment for the transmission of switchoff signals (remote disconnection) and the remote transmission of the industrial-frequency voltage phase angle for devices controlling the excitation of hydraulic generators. Block diagrams of the above equipment are considered, and the results of laboratory tests are provided.

1. Audio Equipment for Remote-Control Channels (TMT-P)

Modern equipment for remote-control channels must have the following properties: It must have maximum flexibility in utilization, small power consumption, and small weight and dimensions, while being highly reliable at the same time. The equipment must be suitable for the connection of contact, as well as contactless, remote-control devices of different types.

In connection with these requirements, and on the basis of the experience gained in the utilization of TMT, TMT-M, etc., devices, new remote-control channel equipment with semiconductor TMT-P devices have been developed at the Institute of Electrical Power Engineering in collaboration with industrial enterprises. This equipment is designed for the multiplexing of wire networks in the 400 to 3200 cps range, or for the multiplexing of high-frequency channels in electrical power transmission lines, radio lines, and wire communication lines.

In the 400-3200 cps range, up to 16 simplex, or seven duplex, channels can be provided in a single circuit. The equipment can be used for the transmission of code pulses at a rate of up to 50 bands, as well as in ac remote measurement frequency systems where the frequency changes from 23 to 50 cps. The frequency scale of the channels is the same as that of the telegraphic equipment TT 12/16, and the remote-control channel equipment with TMT-M electronic tubes, i.e.,

$$f_n = 450 + 180\,(n - 1),$$

where n is the channel number from 1 to 16; the transmission bandwidth of each channel is approximately equal to 140 cps. For a better noise stability and a better control stability in time, the transmission is based on the method of narrow-band frequency modulation with an index approximately equal to 1.

The main difference between the TMT-P equipment and the previously used remote-control channel devices consists in the fact that the electronic tubes have been replaced by semiconductor triodes, and that the channel transmitters and receivers have been constructed as self-contained units with separate electrical feed and measurement units. The transmitters, as well as the receivers, can be used without group devices. The most important practical requirements have thereby been satisfied, and wide possibilities for a versatile arrangement of transmitters and receivers for any frequency at the equipment mounting post have been provided.

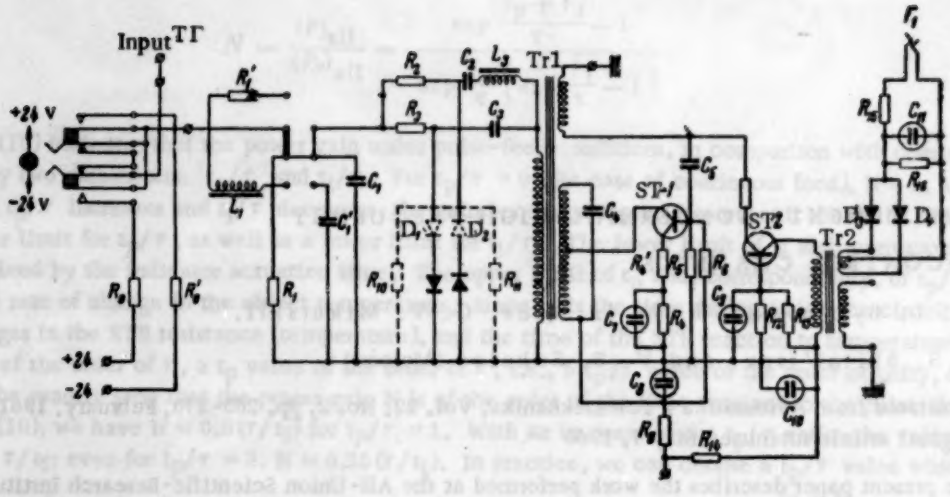

Fig. 1.

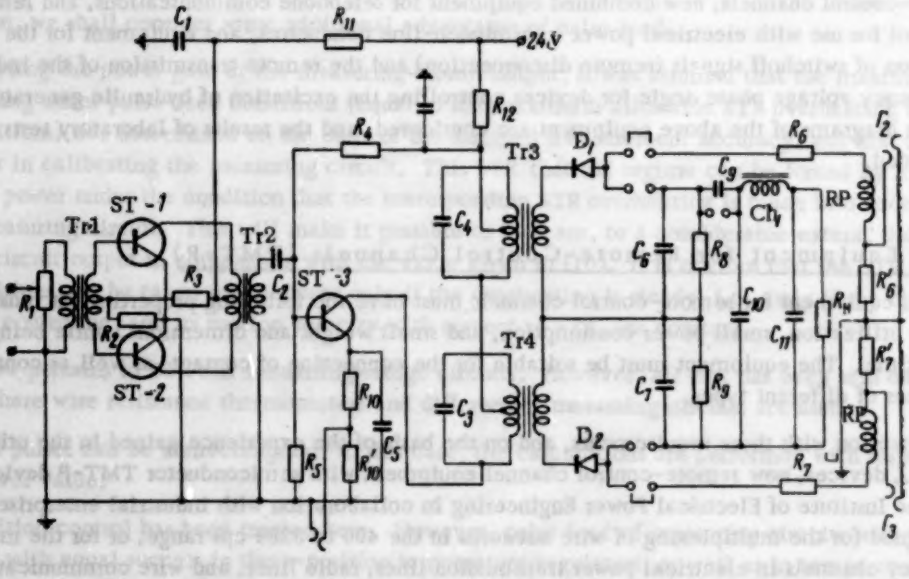

Fig. 2.

For duplex operation with a single circuit, a mounting plate with a differential system is available.

The channel overlapping attenuation in simplex operation amounts to approximately 5 nepers. This corresponds to a distance of over 1500 km for a bronze circuit, or to a distance of approximately 150 km for a steel circuit. In duplex operation, the overlapping attenuation is approximately over 4 nepers, i.e., it is approximately higher by 1 neper than that encountered in using the TMT-M equipment.

The increase in overlapping attenuation can be explained by the fact that the generator is provided with a separate output amplifier, which secures a level of up to +1.5 nepers beyond the transmitter filter.

In order to cover an even greater channel attenuation, an intermediate amplifier can be used, which would secure an output level of up to +3.5 nepers for a harmonic coefficient less than or equal to 0.25%, and a power amplification factor approximately equal to 50,000.

The wiring diagram of the TMT-P transmitter (without the terminal amplifier stage and the output filter) is shown in Fig. 1.

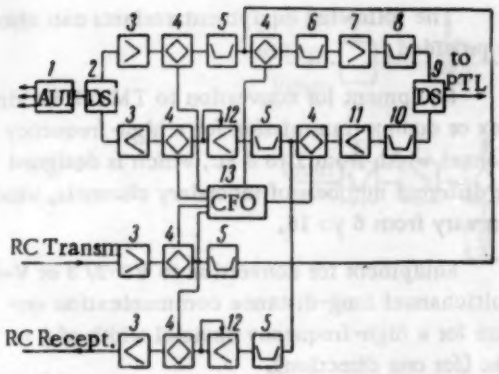

Fig. 3. Block diagram of the high-frequency equipment for a single telephone channel and 12 remote-control channels: 1) automation devices; 2) differential system; 3) low-frequency amplifier; 4) toroidal transducer; 5) intermediate-frequency filter; 6) high-frequency band filter; 7) high-power amplifier; 8) linear filter; 9) high-frequency differential system; 10) receiver-input filter; 11) high-frequency amplifier; 12) intermediate-frequency amplifier with automatic volume control; 13) carrier-frequency oscillator.

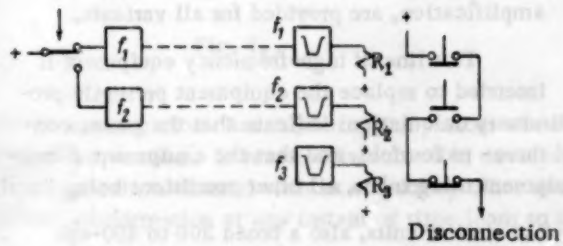

Fig. 4.

Frequency modulation in the audio channels is secured by connecting in parallel to the generator LC-circuit a capacitance or inductance through the control diodes, and supplying the signal voltage to them. A voltage of 4 volts for a transmitter input resistance of not less than 2 kohms is sufficient for the transmitter modulation.

The receiver is based on an ordinary circuit with a push-pull limiter and a two-circuit discriminator. Provisions have been made for the connection of any remote measurement or remote-control device with relay contact, as well as contactless inputs. A simplified TMT-P receiver circuit (without the input filter and the first amplifier stages) is shown in Fig. 2.

A voltage of over 4 volts for a resistance of 1600 ohms is secured at the output of the receiver designed for the connection of contactless remote-control devices. The switch to semiconductor devices, and the use of small-size components, have drastically reduced the equipment dimensions. Therefore, not six (as in the tube variant of the TMT-M equipment), but 16 transmitters or receivers, together with the intermediate amplifier mounting plates or a differential system plate, can be mounted on a stand 2.5 m high.

The feed-power reduction by a factor of about 20 in comparison with the tube equipment constitutes an advantage of the semiconductor variant of the equipment. The maximum feed-power consumption in operation with 16 receivers does not exceed 60 watts.

The stabilization of the triode operating conditions secures stable equipment operation for temperature changes from +5° to +45°.

The industrial production of this equipment is presently being organized.

2. High-Frequency Equipment with New Components for Telephone Communications and Remote Control

The high-frequency equipment with the newly developed units for telephone communications and remote control is designed for organizing telephone communication and remote-control channels and, in certain cases, also relay protection and system automation channels in medium- and high-voltage power-transmission lines.

The equipment is based on semiconductor triodes and miniature resistors, capacitors, and induction coils. Electronic tubes can be temporarily used in the transmitter high-power amplifiers, since the production of high-frequency semiconductor triodes for powers of the order of tens of watts has not yet been organized.

The equipment design in the form of self-contained units provides the possibility of various modifications with different numbers of telephony and remote-control channels. Transmission is effected according to the single-frequency sideband system (SSB) in the range from 40 to 300-500 kc.

A bandwidth of 4.5-5.0 kc (for one transmission direction) contains one telephone channel and 12 remote-control channels (Fig. 3), or two telephone channels and four remote-control and telephone channels.

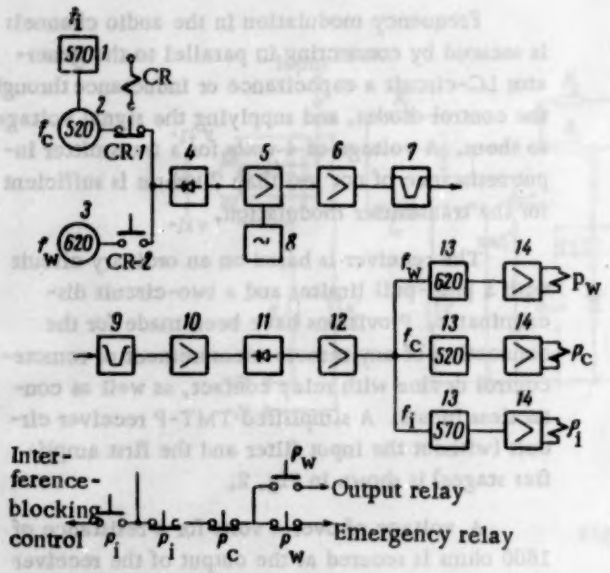

Fig. 5. Block diagram of the remote-disconnection device: 1) 570-cps resonator; 2) tuning-fork 520-cps oscillator; 3) tuning-fork 620-cps oscillator; 4) manipulator stage; 5) controlled stage; 6) power amplifier; 7) transmitter linear filter; 8) master oscillator; 9) receiver-input filter; 10) high-frequency amplifier; 11) detector with automatic cutoff regulation; 12) low-frequency amplifier; 13) tuning-fork filters; 14) amplifiers.

The following equipment variants can also be provided.

Equipment for conversion to TMT-P for simplex or duplex transmission for a high-frequency channel width from 1 to 3 kc, which is designed for different numbers of secondary channels, which can vary from 6 yo 16.

Equipment for conversion to VS-2/3 or V-3 multichannel long-distance communication systems for a high-frequency channel width of 5 or 9 kc (for one direction).

Equipment for telephone communications along lines with branches for a single 2-kc band for both directions.

Equipment designed for a single telephone channel, one to three remote-control and telephone channels, and a channel for remote cyclic measurement transmission (RM) with a high-frequency channel width of 2.5-3.5 kc (for one direction).

Along with terminal equipment, universal intermediate amplifiers, which provide the possibility of frequency inversion or shifting, or direct amplification, are provided for all variants.

This line of high-frequency equipment is intended to replace the equipment presently produced, and also to satisfy a number of new requirements. Preliminary calculations indicate that the power consumption of the recently developed equipment will be reduced three- to fourfold, and that the equipment dimensions will be reduced two- to threefold in comparison with equipment using tubes, all other conditions being equal.

Along with the ordinary 140-cps channel based on TMT-P or similar units, also a broad 300 to 400-cps channel for remote cyclic measurement systems will be provided.

The carrier frequencies to be supplied to the converters will be stabilized. Quartz resonators for the same frequency (for instance, 60 kc) will be used in carrier-frequency oscillators independently of the adjustment of the equipment and of the division and multiplication device for producing all the necessary frequencies. These measures will simplify the problem of ordering quartz resonators in the mass production of the equipment, whose tuning frequencies can vary to a great extent within the 40-500 kc range.

Telephone automation will provide connection to the automatic telephone communications system, as well as to individual subscribers. Automation devices with telephone relays are presently available; however, work on the switch to contactless elements is now in progress.

In organizing the industrial production of the equipment, requirements with respect to the electric-feed standardization should be taken into account; the electric feed should be designed for 127/220 volt alternating current, as well as for 24-, 48-, and 60-volt direct current. The possibility of mounting the equipment in unheated rooms in unserviced substations should also be provided.

3. Remote Disconnection Channels

In the utilization of power systems, the necessity of remote transmission of decision (in particular, disconnecting) automation and protection signals is sometimes encountered. A substation without switches on the high-voltage side can serve as an example. In the case of transformer damage in such substations (for instance, during the gaseous protection action), the high-voltage switch on the opposite side of the line must open the circuit.

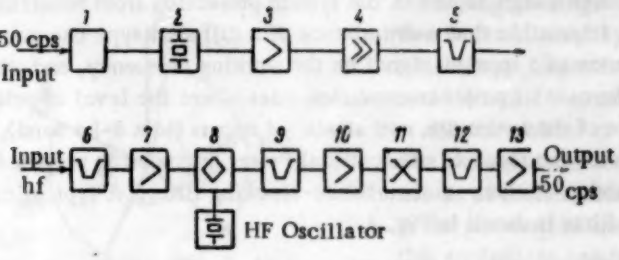

Fig. 6.

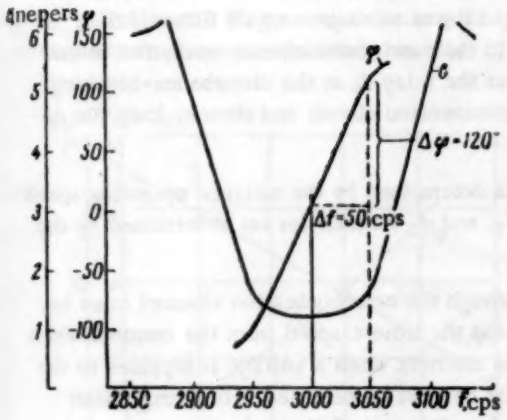

Fig. 7.

The experience gained in utilizing affiliated power systems often indicates the necessity of using special devices for the transmission of disconnecting signals. Such devices will doubtless be widely used in the near future. These devices are termed remote disconnection devices.

Remote disconnection channels, in combination with power transmission lines (PTL) and radio, are widely used abroad for the protection of substations without switches on the high-voltage side, as well as for accelerating the operation of remote protective devices in the second zone.

The basic requirements that remote disconnection channels must satisfy are reliability and fast action. The reliability of remote disconnection channels must be much greater than that of high-frequency protection channels. This is explained by the fact that, in the case of high-frequency protection, the reception of a spurious signal through the communication channel, during the periods when the protective device itself is not actuated, does not lead to spurious operation. In remote disconnection devices, the apparatus control operation is performed through the communication channel without control by other devices (without a trigger unit). Therefore, the reception of spurious information at any instant of time leads to spurious operation of the controlled apparatus.

As a rule, the operating speed of remote disconnection channels can be lower than that of high-frequency protection channels. However, it must not exceed 0.05-0.1 sec in a number of cases.

The possibility of transmitting remote disconnection signals along power-transmission lines is not so obvious as in the case of protection signals. Protection channels can be realized in the power-transmission lines to be protected since, if the line is out of order, there is no necessity for transmitting signals through it. In certain cases, remote disconnection channels must be kept open, regardless of the state of repair of the line between the objects. In such cases, it is desirable to double the high-frequency channels in power-transmission lines by using another type of communication (radio, conductors, or cables). At the same time, it should be noted that, if the electric power-transmission line insulation is damaged, the necessity of transmitting disconnecting signals is sometimes eliminated (for instance, in protecting substations without switches on the high-voltage side). Moreover, damage to power-transmission lines is not often accompanied by the high-frequency channel breakdown. In the majority of cases where the power-transmission line is damaged, the high-frequency channel through this line does not break down if the line is not grounded for repair. However, even in this case, the channel interruption can be avoided by using grounding stoppers.

It follows from what has been said above that, in most cases, remote disconnection channels can be organized along power-transmission line wires connecting transmission and receiving points.

Two-frequency coding seems to be suitable for the transmission of remote disconnection signals. Voltage with one (control) frequency is continuously transmitted through the communication channel. When the disconnection command is transmitted, the voltage with this frequency is removed, and a voltage with another (working) frequency is supplied. If the high-frequency channel breaks down, the control-frequency voltage vanishes at the receiving point, and the disconnection circuits must be blocked.

Such an arrangement secures a high degree of the system protection from receiving spurious disconnection commands. However, it is not impossible that a disturbance of a different type can occur, namely, a disturbance which would cause the appearance of a spurious signal on the working frequency, and which would suppress the control-frequency signal. In the case of power-transmission lines where the level of pulse disturbances in commutation operations, or in the case of short-circuits, can attain +4 nepers (in a 5-kc band), such a possibility must be taken into account. Therefore, the Institute of Electrical Power Engineering proposed to supplement the two-frequency arrangement with another device – a disturbance-blocking filter. A typical circuit of a remote disconnection device with such a filter is shown in Fig. 4.

At the transmitting end, the circuit has two oscillators with the control frequency f_1 and the working frequency f_2, respectively. The receiving end is provided with three filters, each of which has a relay connected to its output. The filter which is tuned to the f_3 frequency serves for blocking pulse disturbances. The pulse disturbance that appears at the receiver input will act approximately to the same degree on all filters if their tuning frequencies do not greatly differ from each other. Therefore, in the case of disturbance-actuation of the relay R_2 at the working-frequency filter output, it is most probable that the relay R_3 at the disturbance-blocking filter output will be actuated. The contacts of this relay open the disconnection circuit and thereby keep the device inoperative during the disturbance action.

The maximum allowable transmission bandwidth of the filters is determined by the assigned operating speed of the remote disconnection device. The intervals between the f_1, f_2, and f_3 frequencies are determined by the selective properties of the filters used.

As was indicated above, the total time of signal transmission through the communication channel must be of the order of 50-60 μsec. By the total transmission time we understand the time elapsed from the moment when the contacts of the control relay at the transmitting end close until the moment when a voltage is supplied to the relay at the receiving end. On the basis of this, it was decided that the devices be provided with narrow-band electromechanical FNIIE filters with a transmission band of 20 cps, and an interval of 50 cps between the nearest frequencies [1]. Two types of remote disconnection devices have been developed at the Institute of Electrical Power Engineering. The first device is designed for operation with a preferred high-frequency channel. Its block diagram is shown in Fig. 5.

The high-frequency transmitter is continuously manipulated by the 520-cps control voltage. For transmitting the disconnection command, the 520-cps oscillator is disconnected from the manipulator, and a 620-cps oscillator is connected to it. Both oscillators operate continuously, and the commutation of the manipulator from one oscillator to another is performed by means of the control relay contacts. The receiving end is provided with three filters and three relays in correspondence with the circuit shown in Fig. 4. The tuning frequency of the disturbance-blocking filter is 570 cps; this frequency is located between the control and the working frequency. Signalization of channel damage (vanishing of the control frequency in the absence of the working frequency), and signalization of the disturbance-blocking relay actuation, have been provided. The signal transmission time is 50 μsec.

The device was put in operation on a 400-kv line in January, 1959, and was connected for switchoff action in February of the same year. The device has transmitted disconnection commands several times. No spurious operation has occurred, and no disturbance-blocking relay actuations have been observed.

The second device is designed for the transmission of signals through a physical circuit, or for ultrasonic multiplexing of high-frequency telephone channels. Frequencies in the 2600-3000 cps range are used for transmission. The block diagram of the device is similar to that shown in Fig. 4. The device is based on semiconductor components.

A specimen of this device was mounted in March, 1960, on a 400-kv line. The ultrasonic range of a combined ÉPO-3 high-frequency communication apparatus is used for transmission.

4. Channels for Remote Phase Transmission

Control by means of the voltage phase at the system central point provides promising possibilities for efficient regulation of hydraulic-generator operating conditions. In this, the voltage phase is transmitted through a communication channel to the regulator location. A device for remote phase transmission, which operates through the preferred high-frequency channel in a power-transmission line, has been developed at the Institute of Electrical

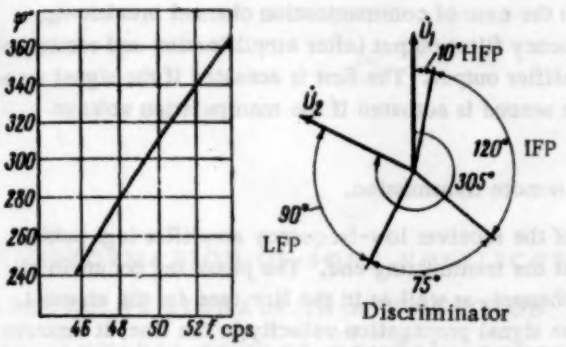

Fig. 8. The vector diagram and the frequency response of the remote phase transmission channel.

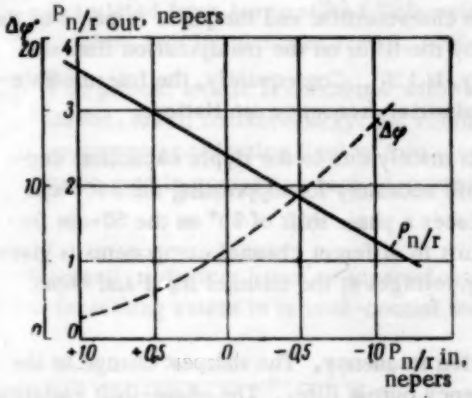

Fig. 9. Interference ratio at the input and output of the remote phase transmission device receiver.

Power Engineering. The preferred channel selection is determined by the requirement for higher reliability. In particular, the channel must not break down if the voltage for the specific purposes at the transmitter or receiver location vanishes. The possibility of remote phase transmission by means of multichannel equipment is not excluded if the problem of inertialess feed reservation for this equipment can be solved.

The block diagram of the remote phase transmission device is shown in Fig. 6.

The transmitter contains a controllable oscillator with frequency quartz-stabilization, a two-stage amplifier-limiter 3, a power amplifier 4, and an output linear differential-bridge filter 5. Inertialess frequency manipulation of the master oscillator 2, by means of industrial-frequency voltage, the phase of which is to be transmitted, is effected in the transmitter.

Single-frequency conversion is used in the receiver; it contains a high-frequency amplifier 7, with a high-frequency filter 6, a frequency converter 8, an intermediate-frequency filter 9, a limiter, a frequency detector (discriminator) 11, a filter 12, and an industrial-frequency amplifier 13.

The degree of protection from disturbances of a system with frequency manipulation depends on the modulation index. If it is necessary to secure a high degree of interference suppression for a comparatively large signal-to-noise ratio at the receiver output, a large modulation index, i.e., a large frequency deviation, is used. In this, the intermediate-frequency filter transmission band must be large. If the device is to operate under conditions where the signal-to-noise ratio at the receiver input is small, the noise voltage at the frequency detector can have a value comparable to that of the signal voltage, and the detector is then controlled by the noise frequency instead of the signal frequency, which leads to a sharp increase in signal distortion. Therefore, in operation under strong interference conditions, the system with the best interference protection will be that which allows the minimum transmission bandwidth of the intermediate-frequency filter. For any modulation type except the signal sideband modulation, the minimum transmission band of the intermediate-frequency filter is equal to the double frequency of the modulating signal. In frequency manipulation, this condition will be satisfied for a modulation index somewhat smaller than unity.

Deviation is effected directly in the oscillator with frequency quartz-stabilization by means of connecting in series a sufficiently large inductance to the quartz resonator. The inductance is regulated by means of a reactance tube.

A bandwidth of 100 cps, i.e., the minimum possible bandwidth, was chosen for the intermediate-frequency filter in the receiver. An intermediate frequency of 3000 cps was chosen, so that selectivity in the image channel could be readily secured by means of the high-frequency filter.

As usual, the discriminator is based on two resonance circuits, which are detuned in different directions with respect to the intermediate frequency. A somewhat distorted industrial-frequency voltage is obtained at the discriminator output. The shape of this voltage is corrected by means of an industrial-frequency filter at the discriminator output. A 10-cps (45-55 cps) filter transmission band is used. After passing through the filter, the industrial-frequency voltage is amplified by means of a low-frequency amplifier.

Two relays are provided for deactivating the device in the case of communication channel breakdown. Voltage to one relay is supplied from the intermediate-frequency filter output (after amplification and rectification), and the other relay is fed from the low-frequency amplifier output. The first is actuated if the signal transmitted through the high-frequency channel vanishes, and the second is actuated if the manipulation voltage vanishes.

Let us briefly consider the phase distortions caused by remote transmission.

The industrial-frequency voltage phase at the output of the receiver low-frequency amplifier lags behind the phase of the industrial-frequency manipulating voltage at the transmitting end. The phase lag occurs in all selective components entering the transmitter and receiver channel, as well as in the line used for the channel. The phase shift in the line is caused by the finite value of the signal propagation velocity in the line; it amounts to 6° per 100 km of line.

The phase lag in the selective devices (filters) is equal to the phase shift between the carrier and the manipulation first-side frequency, i.e., it is determined by the transmission frequency (in this case, 50 cps), and by the steepness of the filter phase response. Figure 7 shows the attenuation characteristic and the phase response of the receiver intermediate-frequency filter. The phase shift introduced by the filter on the manipulation first-side frequency, in comparison with the phase shift on the carrier frequency, is 120°. Consequently, the intermediate-frequency filter introduces a phase lage of 120° in the transmitted industrial-frequency oscillations.

A considerable phase shift occurs in the discriminator, which is mainly due to the ripple capacitors connected in parallel to the discriminator load. The ripple capacitors are necessary for suppressing the 3000-cps voltage at the discriminator output. The low-frequency filter introduces a phase shift of 90° on the 50-cps frequency. The vector diagram showing the transmitted-signal phase shift in different channel components is given in Fig. 8. The resulting phase shift between the industrial-frequency voltages at the channel input and ouput amounts to approximately 300°.

The phase-shift magnitude depends on the transmitted oscillation frequency. The sharpest change in the phase shift in dependence on frequency takes place in the low-frequency output filter. The phase-shift variation in the output filter, which is constructed as a series resonance circuit, is determined by the expression

$$\Delta f = \frac{360}{\pi \Delta f_{pass}} \text{ deg/cps}$$

where Δf_{pass} is the filter passband.

For Δf_{pass} = 10 cps, the phase shift is 11°30' if the frequency changes by 1 cps. Actually, the variation of the transmitted oscillation phase amounts to 15° per cps. The additional 3°30' are due to the effect of other filters in the circuit, especially of the intermediate-frequency filter.

The reliability of the interference rejection of the developed equipment was laboratory-tested. Measurements of additional phase errors, caused by the action of smooth interferences on the receiver, were performed.

Figure 9 shows the dependence of the difference between the signal and the interference levels at the receiver output on such a difference at the input. The same figure shows the dependence of the maximum instantaneous deviation of the transmitted oscillation phase on the difference between the signal and the interference levels at the receiver input, which was measured in the 2000-cps band. It is obvious from this graph that the system is very well protected from smooth interferences.

LITERATURE CITED

1. Application of Electromechanical Components in Equipment for Remote Control and Communications Channels. VNIIÉ Information Material, No. 38 [in Russian] (Gosénergoizdat, 1959).

TRANSFORMATION OF SOME NONELECTRICAL QUANTITIES INTO ELECTRICAL SIGNALS IN APPLICATION TO CONTACTLESS REMOTE-CONTROL DEVICES

M. V. Kadzharov (Tbilisi)

Translated from Avtomatika i Telemekhanika, Vol. 22, No. 2, pp. 271-273, February, 1961
Original article submitted June 1, 1960

The present article is concerned with the transformation of some nonelectrical quantities, for instance, level, radiant energy, the volume of some friable materials, and the pressure and level of noncurrent-conducting liquids, into electrical signals suitable for remote transmission, which are to be used in contactless remote-control devices based on ferrite-diode cells.

Contactless devices based on square-loop (SL) magnetic elements and semiconductor devices are used to an ever-increasing extent in remote-control techniques. In connection with this, the development of primary nonelectrical quantity converters with semiconductor devices for application in contactless remote-control (RC), remote-signalization (RS), and remote-measurement (RM) devices, is of definite interest.

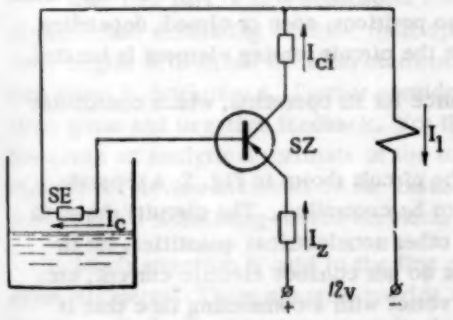

Fig. 1.

Figure 1 shows the circuit of a converter with a relay characteristic. A semiconductor triode is used as the circuit amplifier. The control circuit in this arrangement is the feedback circuit, which includes a controllable resistor SE (sensing element). A resistor with a constant resistance of the order of 100 kohms can be used as the sensing element. A very small current I_c in the control circuit, which is caused by the leakage current through the sensing element when the latter is immersed in water, causes the appearance of a negative potential on the triode base with respect to the emitter, due to which the triode opens, and the current I_l in the working collector circuit sharply increases. A pilot lamp, or the winding of an electromagnetic relay, can be connected to the working collector circuit. The device has very small dimensions, it uses a small amount of power, and it is very simple to make and operate.

An experimental model of this device was mounted on one of the mechanical irrigation control units for regulating the water level in the tank of the pump station in Tbilisi.

The above-described level-data transmitter circuit can be used without any modification as a converter of a nonelectrical quantity to be measured – level, pressure head, or radiant energy – into an auxiliary electrical quantity suitable for transmission over a certain distance. For this purpose, the above circuit can be directly connected to the output-load winding of an element of the pulse distributor, as is shown in Fig. 2.

Instead of the pilot lamp of the electromagnetic-relay winding, the control winding W_c of a linear unit element (LUE) is connected to the working collector circuit.

During the pulse-distributor operation, a pulse appears in the load winding W_l in the corresponding cycle of the motion winding W_m. If the sensing element is in air, the triode is closed, the LUE control winding W_c is

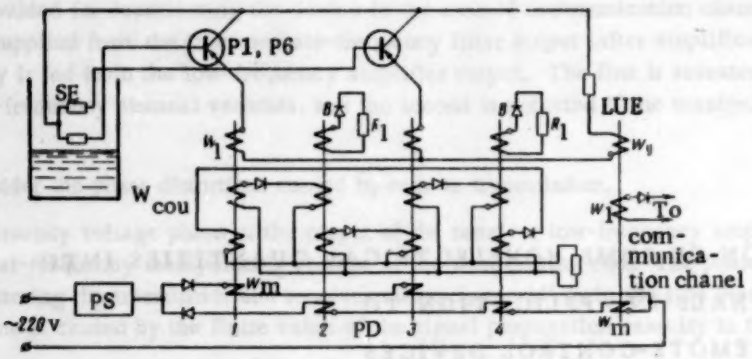

Fig. 2. PD – Push-pull pulse distributor with ferrite-diode cells; PS – pulse shaper; W_{cou} – distributor coupling winding.

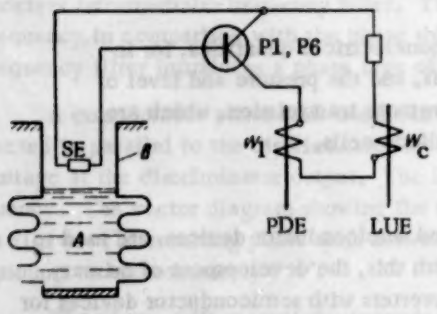

Fig. 3. PDE – Pulse-distributor element; LUE – linear-unit element.

deenergized, and no signal is fed to the communication channel. As soon as the sensing element is immersed in water, the triode opens, and a pulse, which is supplied by the distributor element, appears in the LUE control winding W_c. Under the action of the magnetomotive force of this pulse, the magnetic polarity of LUE is reversed (preconditioning).

Due to the next pulse in the motion winding W_m, the LUE magnetic state will be changed (actuation), and a pulse, which is to be transmitted through the communication channel, appears in the LUE load winding W_l. It is obvious that the converter circuit operates as a trigger, i.e., it dwells for long periods of time in one of the two positions; open or closed, depending on the medium in which the circuit-sensing element is located.

The converter amplifier circuit does not require a separate feed source for its operation, which constitutes an important advantage.

Low-power P1 or P6 triodes are used in the circuit. According to the circuit shown in Fig. 2, a separate converter circuit and one distributor element are required for each point to be controlled. The circuits shown in Figs. 1 and 2 can be used for the transformation into electrical signals of other nonelectrical quantities, for instance volume of some friable materials, pressure and level of liquids that do not conduct electric current, etc. For this purpose, the converter arrangement should be supplemented by a vessel with a connecting tube that is readily deformable under the action of gravity or pressure.

Figure 3 shows the diagram of such a device. The readily deformable vessel A is filled with water, and the sensing element is installed in the connecting tube B at the required height.

In the case of volume determination, the vessel will change its initial shape due to the friable-material weight, and the vessel volume will be reduced, due to which the water level in tube B will rise. As soon as the sensing element is immersed in water, the converter circuit is actuated.

If this device is used for controlling the level of a noncurrent-conducting liquid, the water level in tube B changes as soon as vessel A is deformed, due to the hydrostatic pressure of the liquid in which it is immersed.

The described indirect method for volume determination can also be used in grain and other storage spaces, on construction sites, for controlling the filling of coal or rock bins, and especially in those cases where direct weighing is difficult.

In those cases where the primary variable quantity is a radiant-energy source, a photocell can be used as the sensing element in the circuit of Fig. 2 and, in dependence on the photocell illumination, the converter triode circuit will be closed or open.

The principle of remote transmission of the above quantities is based on the circuit shown in Fig. 2. Work on the pulse-code method for signal transmission by means of the circuit of Fig. 2 is in progress.

REVIEWS AND BIBLIOGRAPHY

REVIEW OF B. YA. KOGAN'S BOOK "ELECTRONIC SIMULATING DEVICES AND THEIR APPLICATION IN INVESTIGATING AUTOMATIC CONTROL SYSTEMS" (FIZMATGIZ, 1959)

M. N. Babushkin, S. Ya. Berezin, and A. A. Birshtein

Translated from Avtomatika i Telemekhanika, Vol. 22, No. 2, pp. 274-275, February, 1961

Electronic simulating devices are presently used to a great extent in many fields of science and technology. They have gained especially widespread application in the investigation and design of automatic control systems. A great amount of experience in utilizing them has already been accumulated. However, until recently, the domestic literature did not comprise books which would treat, in sufficient detail, the various problems connected with the construction, design, and utilization of electronic simulating devices for solving different problems.

The book reviewed here is the first of its kind, where the problems pertaining to the investigation of automatic control systems are considered in great detail. The book consists of two parts.

The first part, which constitutes the main portion of the book (309 pages), is devoted to the basic elements of electronic simulating devices, their operating principles, structural characteristics, and design methods. The study begins with linear decision elements of various types, which are compared and analyzed, and whose application scope is determined. Further considerations are devoted mainly to decision elements with dc amplifiers with large gains and negative feedback. For these elements, the author has determined the basic sources of error, and has given an analytical estimate of the total error, which makes it possible to determine the effect of the parameters of the device elements on the mathematical-operations accuracy. From this point of view, the basic component of all simulating-device elements – the electronic dc amplifier – is then considered.

Much attention is paid in the first part (152 pages) to functional converters, which are based mainly on diode elements. These chapters provide a large amount of generalized and systematized material concerning the basic diode element types used in simulating-device units; also, a finalized theory of these elements is given. A number of variants of universal functional converters, multipliers, and dividers are also considered.

This section ends with a brief description of auxiliary devices for electronic mockups.

The second section (114 pages) is devoted mainly to methodological problems connected with the application of electronic simulators for the investigation of automatic control systems. The first part of this section is concerned with the general problems of preparation, programming, and solution of equations, which is then followed by a consideration of the particularities encountered in simulating linear, as well as nonlinear, automatic control systems.

The appendices provide the technical characteristics of some domestic and foreign-made devices.

Thus, a considerable number of problems is analyzed in this book. Besides a generalization of the domestic and foreign experience gained in the design and utilization of electronic simulating devices, the book presents a number of original theoretical and structural developments contributed by the author (problems in the theory and design of diode functional converters, an analysis of decision-element errors, etc.), as well as a number of original developments elaborated under his guidance at IAT AN SSSR. The basic material in the book is appropriately illustrated by examples. However, it is difficult to avoid deficiencies in a first book of this kind.

Among the basic shortcomings, the following can be mentioned.

1. No consideration whatever has been given in the book to problems connected with the operation of simulating devices in combination with actual equipment, although they are important in investigating automatic control systems.

2. Very little attention is paid to electromechanical elements, which are widely used in modern electronic simulating devices.

3. Unfortunately, in the section devoted to methodology, the author did not make full use of the valuable material published by him in the periodical literature.

4. One cannot always agree with the author on the question concerning the organization of the material. In particular, from our point of view, it would be more logical to consider the design of units for multiplication by constant and variable factors, lag units, etc., in the first section instead of in the second, as was done in the book.

As for the first two shortcomings, they can obviously be explained by the limited space and the main purpose of the book where, according to the author's intention, only electronic elements are considered.

At the same time, it should be noted that this book greatly exceeds its scope as defined by the author in the title and the preface. The broad and detailed material presentation makes this book valuable and useful not only in designing and investigating automatic control systems, but also in solving other scientificotechnical problems by means of electronic simulating devices and, especially, in designing electronic analog computers.

Generally speaking, the book deserves the greatest praise, and its publication should be welcomed, since it will be of great help to specialistsengaged in work on electronic simulating devices, and will promote a more diversified application of electronic simulating devices in various fields of science and technology.

At the present time, the book reviewed here is being widely used as a text book at the Naval Academy of the Order of Lenin.

LIST OF DOMESTIC PAPERS ON THE THEORY OF RELAY CIRCUITS AND FINAL AUTOMATIC DEVICES FOR 1959

V. D. Kazakov and O. P. Kuznetsov

Translated from Avtomatika i Telemekhanika, Vol. 22, No. 2, pp. 275-277, February, 1961

1. I. Ya. Aksenov, Yu. Ya. Bazilevskii, and R. R. Vasil'ev, "The second international cybernetics congress," Problemy Kibernetiki 2, 311-319 (1959).
2. A. A. Arkhangel'skaya, V. G. Lazarev, and V. N. Roginskii, "A machine for the synthesis of contact circuits," Problemy Peredachi Informatsii,No. 1, 41-52 (1959).
3. Yu. L. Vasil'ev, "Minimal contact circuits for Boolean functions of four variables," Doklady Akad. Nauk SSSR 127, 2, 242-245 (1959).
4. N. P. Vasil'eva and N. O. Prokhorov, "Magnetic logical elements for automatic control circuits," Avtomatika i Telemekhanika 20, 12, 1647-1658 (1959).
5. M. A. Gavrilov, "Minimization of Boolean functions characterizing relay circuits," Avtomatika i Telemekhanika 20, 9, 1217-1238 (1959).
6. V. N. Grebenshchikov, "Seminar on technical contributions to mathematical logic," Avtomatika i Telemekhanika 20, No. 1 (1959).
7. I. S. Danilyuk, "Problems in synthesizing relay circuits for fixing and commutation," Avtomatika i Telemekhanika 20, No. 3 (1959).

8. V. F. D'yachenko and V. G. Lazarev, "Application of the algebra of logic for the analysis and synthesis of relay-contact circuits in telephony," Collection: Logical Investigations [in Russian] (1959) pp. 450-463.
9. V. F. D'yachenko, "A method of analyzing complex relay-contact circuits," Avtomatika i Telemekhanika 20, 10, 1417-1425 (1959).
10. Yu. I. Zhuravlev, "On the construction of minimum disjunctive normal forms for logic-algebra functions," Doklady Akad. Nauk SSSR 126, 2, 263-266 (1959).
11. A. D. Zakrevskii, "An operator method for synthesizing algorithmic systems," Izvest. Vyssh. Ucheb. Zaved., No. 2, 306-315 (1959).
12. A. D. Zakrevskii, "A method for synthesizing functionally stable automatic devices," Doklady Akad. Nauk SSSR 129, 4, 729-731 (1959).
13. Ya. G. Koblents, "Design and analysis of single-cycle logical magnetic and trigger commutation circuits," Élektrosvyaz', March, 73-81 (1959).
14. N. E. Kobrinskii and B. A. Trakhtenbrot, "On the development of a general theory of logical nets," Collection: Logical Investigations [in Russian] (1959) pp. 352-378.
15. L. N. Korolev, "On the switching function of the device for table scanning," Doklady Akad. Nauk SSSR 125, 482-484 (1959).
16. R. E. Krichevskii, "On the realization of functions by means of superpositions," Problemy Kibernetiki, No. 2, 123-138 (1959).
17. R. E. Krichevskii, "On the complexity of the realization of functions by means of superpositions," Doklady Akad. Nauk SSSR 126, 6, 1195 (1959).
18. V. G. Lazarev, "A method for determining the number of relays necessary for designing a relay-contact circuit according to the assigned operating conditions," Problemy Peredachi Informatsii, No. 1, 53-71 (1959).
19. V. G. Lazarev and Yu. L. Sagalovich, "The commutator of the machine for synthesizing contact circuits," Problemy Peredachi Informatsii, No. 4, 124-132 (1959).
20. Logical Investigations. Collection of Articles [in Russian] (AN SSSR Press, 1959).
21. O. B. Lupanov, "On the asymptotic determination of the number of graphs with n edges", Doklady Akad. Nauk SSSR 126, 3, 498 (1959).
22. O. B. Lupanov, "On the asymptotic determination of the complexity of formulas representing logic-algebra functions," Doklady Akad. Nauk SSSR 128, 3, 464 (1959).
23. T. L. Maistrova, "Equivalence of relay circuits with respect to action," Problemy Peredachi Informatsii, No. 4, 96-114 (1959).
24. V. M. Mikheev, "On multiplicity sets containing the greatest number of Boolean vectors that cannot be compared in pairs," Problemy Kibernetiki No. 2, 69-72 (1959).
25. I. S. Morosanov and P. I. Chinaev, "Conference on the theory and application of discrete automatic systems," Avtomatika i Telemekhanika 20, No. 1 (1959).
26. G. K. Moskatov, "List of domestic papers on the theory of relay circuits and final automatic devices for 1958," Avtomatika i Telemekhanika 20, 8, 1148 (1959).
27. V. L. Murskii, "On equivalent transformations of contact circuits," Doklady Akad. Nauk SSSR 127, 2, 262-265 (1959).
28. É. I. Nechiporuk, "On transformations of contact-rectifier circuits," Vestnik LGU (Mathematics, Mechanics, and Astronomy), No. 13, 148 (1959).
29. P. P. Parkhomenko, "Analysis of relay circuits by means of machines," Avtomatika i Telemekhanika 20, 4, 486-497 (1959).
30. G. N. Povarov, "Logic and automation," Collection: Logical Investigations [in Russian] (1959) pp. 300-310 Bibl. 91 title.
31. G. N. Povarov, "On the logical synthesis of electronic computer and control circuits," Collection: Logical Investigations [in Russian] (1959) pp. 406-413.
32. G. N. Povarov, "Mathematical and logical investigation of the synthesis of contact circuits with a single input and k outputs," Collection: Logical Investigations [in Russian] (1959) pp. 379-403.
33. G. N. Povarov, "On the structural theory of communication networks," Problemy Peredachi Informatsii, No. 1, 126-140 (1959).
34. G. N. Povarov, "Absolutely rigid Markov nets in independent relay-contact circuits and similar determined systems," Problemy Peredachi Informatsii, No. 4, 85-95 (1959).
35. G. N. Povarov, "Investigation of ordered contact circuits," Problemy Peredachi Informatsii, No. 4, 133-139 (1959).

36. B. M. Rakov, "Logical synthesis of relay-action circuits with resistors and contacts," Collection: Logical Investigations [in Russian] (1959) pp. 429-432.
37. B. I. Rameev and Yu. A. Shreider, "Analysis and synthesis of certain contactless discrete-action circuits," Avtomatika i Telemekhanika 20, No. 1 (1959).
38. V. N. Roginskii, "A graphical method for designing multipole contact circuits," Problemy Peredachi Informatsii, No. 1, 5-40 (1959).
39. V. N. Roginskii, Fundamentals of Structural Synthesis of Relay Control Circuits [in Russian] (AN SSSR Press, 1959) p. 167.
40. V. N. Roginskii, "Operation of relay circuits during transient periods," Avtomatika i Telemekhanika 20, 10, 1409-1416 (1959).
41. Yu. L. Sagalovich, "On the group invariance of Boolean functions," Uspekhi Matem. Nauk 14, 6, 191-195 (1959).
42. Yu. L. Sagalovich, "On limiting the number of contact-circuit variants," Problemy Peredachi Informatsii, No. 4, 115-123 (1959).
43. Yu. L. Sagalovich, Review of the Book "Logical Investigations" (AN SSSR Institute of Philosophy, AN SSSR Press, Moscow, 1959), Avtomatika i Telemekhanika 20, 11, 1544-1545 (1959).
44. A. D. Talantsev, "On the analysis and synthesis of some electrical circuits by means of special logical operators," Avtomatika i Telemekhanika 20, 7, 898-907 (1959).
45. A. D. Talantsev, "On the analysis of potential-pulse systems by means of special transition operators," Doklady Akad. Nauk SSSR 127, 2, 320-324 (1959).
46. B. A. Trakhtenbrot, "Asymptotic determination of the complexity of logical nets with memory," Doklady Akad. Nauk SSSR 127, 2, 281-284 (1959).
47. N. A. Filippov, "A graphical method for the time analysis of relay-contact circuit operation," AN Kirg. SSR Press, Natural and Tech. Sci. Sect. Publication 1, 4, 47-51 (1959).
48. A. D. Kharkevich, "On commutation circuits and their logical essence," Collection: Logical Investigations [in Russian] (1959) pp. 415-428.
49. M. L. Tsetlin and L. M. Shekhtman, "Push-pull ferrotransistor circuits and the algebraic method of their synthesis," Problemy Kibernetiki, No. 2, 139-180 (1959).
50. V. I. Shestakov, "Simulation of operations of the calculus of propositions by means of relay-contact circuits," Collection: Logical Investigations [in Russian] (1959) pp. 315-351.
51. V. I. Shestakov, "The perforated-card method of synthesizing multicycle-multiposition relay systems," Avtomatika i Telemekhanika 20, 11, 1496-1506 (1959).
52. A. N. Yurasov, "Analytical synthesis of multicycle circuits by means of connection formulas," Collection: Logical Investigations [in Russian] (1959) pp. 442-449.
53. S. V. Yablonskii, "On the impossibility of eliminating the surplus of all functions from P_2 in solving certain circuit-theory problems," Doklady Akad. Nauk SSSR 124, No. 1 (1959).
54. S. V. Yablonskii, "Basic cybernetics concepts," Problemy Kibernetiki, No. 2, 7-38 (1959).
55. S. V. Yablonskii, "On algorithmic difficulties in the synthesis of minimal contact circuits," Problemy Kibernetiki, No. 2, 75-122 (1959).

All abbreviations of periodicals in the above bibliography are letter-by-letter transliterations of the abbreviations as given in the original Russian journal. *Some or all of this periodical literature may well be available in English translation.* A complete list of the cover-to-cover English translations appears at the back of this issue.

LIST OF FOREIGN LITERATURE ON MAGNETIC COMPONENTS WHICH ARE USED IN AUTOMATION, REMOTE CONTROL, AND COMPUTER TECHNIQUES FOR 1959

Translated from Avtomatika i Telemekhanika, Vol. 22, No. 2, pp. 277-291, February, 1961

1. General Problems. Terminology, Bibliography, Standardization, etc.

1. M. Ikeda, "Standard for magnetic materials and their testing," Ohm. Electr. Mag. 45, 8, 194-196 (1958) [in Japanese].
2. L. Lewin, Monographs published individually this month, J. IEE 5, 52, 245 (April, 1959).
3. 1957 Magnetic Amplifier Bibliography (AIEE Committee Report) Commun. and Electronics, No. 40, pp. 1051-1057 (January, 1959).
4. "Magnetic amplifier conference stresses applications," Elec. Manufacturing 64, 6, 149-151 (Fig. 6) (1959).
5. M. Mamon, "One from Russia," Control Engng., No. 10, 208-209 (1959) (Communication concerning the book Magnetic Amplifier Design by N. P. Vasil'eva, O. A. Sedykh, and M. A. Boyarchenkov).
6. W. L. Morgan, "Bibliography of digital magnetic circuits and materials," Trans. IRE on Elec. Computers EC-8, No. 2, 143-158 (1959).
7. "Proposed standard test codes for magnetic amplifiers," Trans. AIEE 78, 453-546; Commun. and Electronics, No. 44, 453-456 (1959) [Annotated Index of Radio Electronics Literature 3, ref. No. 1155 (1960)[in Russian].
8. "Recommended symbols for magnetic-amplifier papers," A Report, Commun. and Electronics, No. 45, 519-521 (1959) bibl. 1.
9. T. B. Rymer, "Summerized proceedings of a conference on solid-state memory and switching devices," Brit. J. Appl. Phys. 10, No. 4, 153-158 (Fig. 7) (1959) bibl. 12.
10. "Special technical conference on nonlinear magnetics and magnetic amplifiers, Washington, D. C., Sept. 23-25, 1959," AIEE (1959) p. 383, Fig. 297, Table 15, Bibl. 191.
11. Tashiro, "Survey of magnetic-amplifier patents," Ohm. Electr. Mag. 45, No. 8, 115-119 (1958) [in Japanese].
12. "Translation of Soviet 'Magnetic Amplifiers'," Elec. Engng. 78, 7, 771 (1959) [Communication on the decision of the AIEE Subcommittee on Magnetic Amplifiers concerning the translation of M. A. Rozenblat's book Magnetic Amplifiers, with short review].

2. Ferromagnetic Materials. Cores

a) Magnetic Materials

13. E. Albers-Schoenberg, "Ferrites," J. Am. Ceram. Soc. 41, 11, Pt. 2, 484-489 (1958)["Ferrites," Elektrotekhnika Abstr. J., No. 1, 860 (1960)].
14. W. Arrott, "New developments in magnetic materials and applications," Elec. Manufacturing 63, No. 2, 56-67 (1959) (Fig. 21, Table 9).
15. F. Berlinghoff, Neuere Entwicklung der Ferrite. ETZ. Ausg. A 1959, Bd. 80. No. 17, pp. 600-605 [Russian translation: GPNTB, No. 1240 (1960). New Ferrite Developments].
16. R. Roll, Metallische Magnetwerkstoffe und Kernformen in der Nachrichtentechnik, ETZ, Ausg. A 1959 No. 17, pp. 582-587 [Metallic magnetic materials and core types in communication techniques].
17. A. Boltax, "Behavior of semiconductor and magnetic materials in radiation environment," Elec. Manufacturing 63, 3, 90-95 (1959) (Fig. 10, Bibl. 9).
18. J. C. Betts, "Hysteresis torque limits lifted with new magnetic alloy," Elec. Manufacturing 63, 3, 101-104 (1959) (Fig. 6).
19. B. R. Budny, "A new 'square loop' ferrite and its potential fields of application", Proc. 1959 Electron. Compon. Conf., Philadelphia, Pa., S. J. 1959, pp. 122-127. [Russian translation: Express Information: Vychisl. Tekhnika, No. 18 (1960)].

20. S. Chikazumi, "Contemporary investigations of magnetic materials in the U.S.A.," Om. Denki Zassi (Ohm. Electr. Mag.), 45, No. 8, 18-21 (1958) [in Japanese].
21. W. Dabrowski and T. Postupolski, Zastosowanie ferrytów w technice teletransmisji przewodowej.– Przeglad Telekomunikacyjny, 31, No. 8-9, 252-267 (1958), Fig. 11, Table 4. [Application of ferrites in wire communication techniques].
22. M. Destrade, Que sont – ferrites? – Ingrs automob. 32, No. 5, 325-334 (1959) [What are ferrites?]
23. C. Durrante, Contribution à l'étude du basculement d'un noyau ferromagnétique alimenté par une source parfaite de tension.– C. R. Acad. Sc. 248, No. 24, 3412-3414 (1959). [Contribution to the study of magnetic polarity reversal in Ferromagnetic cores fed by an ideal voltage source].
24. G. Economos, A guide to ferromagnetic ceramics. Part 2. Square loop ferrites, microwave ferrites, permanent magnet ceramics. Mater. Design Engng. 48, No. 4, 109-114 (1958) [Elektrotekhnika Abstr. J., 6 (1960), ref. 1, 1491.]
25. H. Fahlenbrach, Magnetische Werkstoffe.– Techn. Mitt. Krupp. 17, 95-99 (1959). [Magnetic Materials].
26. Le Ferrite, matériaux-clé de l'électronique.– Telonde, No. 3, 4-13 (1958). [Ferrites as key materials in electronics].
27. G. Finke, Metallische, weichmagnetische Werkstoffe für die Elektrotechnik.– Elektro-Anz., 1959, Bd. 12, Nr. 39-40. SS. 403-405. [Russian translation: Express Information: Elektrotekhnika, 6 (1960) No. 32. Metallic magnetically soft materials in electrical engineering].
28. J. Górski, Ferrytowe rdzenie litowo-cynkowe w. cz.– Przeglad Telekomunikacyjny, 1958, R. 31, No. 8-9, s. 248-249, rys. 4. [Lithium-zinc ferrite cores].
29. C. Hack and H. Reiner, Rechteckferrite und die Prüfung ihrer Speichereigenschaften.– Nachrichtentechn. Z., 1958. Bd. 11, Nr. 7, SS. 360-369. [Elektrotekhnika Abstr. J., 5, ref. 1. 1189 (1960). Square-loop ferrites and the testing of their properties as memory devices].
30. W. Haken and C. Haza-Radlitz, Ferritkörper mit temperaturunabhängigen gyromagnetischen Eigenschaften.– Arch. Elektr. Übertragung, 1959, Apr., Bd. 13, Nr. 4, SS. 157-160, Fig. 4, Bibl. 5. [Ferrite cores whose gyromagnetic properties are independent of temperature].
31. G. Heilbardt and H. Staeblein, Zwei Beispiele de Weiterentwicklung von weichmagnetischen Werkstoffen.– ETZ, Ausg. A, 1959, Nr. 17, SS. 570-576. [Two examples of the development of magnetically soft materials].
32. F. Hengelhaupt, Die Verlustziffer von Transformatorenblechen bei Mittelfrequenz.– Deutsche Elektrotechnik, 1959, Bd. 13, SS. 93-99. [Losses in transformer steel at intermediate frequencies].
33. A. A. Hirsch, Double hysteresis loops in ferromagnetic crystals.– J. Phys. et Radium, 1959, vol. 20, No. 2-3, pp. 262-263.
34. L. Hroudny, Teplotni kompensace kovových práskových ferromagnetických materiálu.– Slaboproudý Obzor, 1959, Cerven, R. 20, No. 6, s. 349-353, rys. 9, bibl. 3. [Temperature compensation of metallic powder ferromagnetic materials].
35. A.C. Hudson and E. J. Stevens, Data on ferrite core materials.– Electronic Engng, 1958, vol. 30, No. 370, pp. 718-719, Bibl. 2.
36. S. Ikeuchi, "Modern development of materials with high initial permeability and saturation induction and their magnetic characteristics," Om. Denki Zassi, Ohm. Electr. Mag., 1958, vol. 45, No. 8, pp. 34-51 [in Japanese].
37. T. Karasawa, "Ferrites and Magnetostriction," Om Denki Zassi, Ohm. Electr. Mag., 1958, vol. 45, No. 8, pp. 55-60 [in Japanese].
38. N. Kawai and H. Nakamura, "Ferrite-based magnetic materials," Om. Denki Zassi, Ohm. Electr. Mag., 1958, vol. 45, No. 8, pp. 61-66 [in Japanese].
39. D. Köhler, Der Frequenz- und Temperaturgang der komplexen Permeabilität hochpermeabler Ferrite.– Arch. Elektr. Übertragung, 1959, Bd. 13, 1, Nr. 1, SS. 1-12, Fig. 18, Bibl. 36. [Frequency and temperature characteristics of the complex permeability of high-permeability ferrites].
40. M. Kornetzki, Perminvarferrite.– ETZ, Ausg. A, 1959, Bd. 80, Nr. 17, SS. 605-609 [Russian translation: GPNTB, No. 1241 (1960). Perminvar Ferrites.]
41. J. Król, Urzadzenie do szybkiego automatycznego zapisu zmian przenikalnosci magnetycznej materialow magnetycznych w funkcji temperatury.– Przeglad Telekomunikacyjny, 1958, R. 31, No. 8-9, s. 250-251, rys. 5. [Recording of magnetic permeability variations in dependence on temperature].
42. H. A. Lewis and J. E. Mitch, Effects of environment on the magnetic properties of toroidal cores.– Proc. C.M.A., 1959, Washington, AIEE, 1959, pp. 347-357, Fig. 9, Table 4.
43. Magnetic materials.– Toshiba Rev., 1958, vol. 13, No. 4, pp. 451-461 [in Japanese].
44. K. Mihara, "Modern developments of square-loop materials and their magnetic properties," Om. Denki Zassi, Ohm. Electr. Mag., 1958, vol. 45, No. 8, pp. 42-48 [in Japanese].

45. T. Moriwaki, Y. Shimazu, J. Futami, T. Nakajima, T. Kabota, and T. Oda, "Modern magnetic materials and their role in the development of the communications industry," Om. Denki Zassi, Ohm. Electr. Mag., 1958, vol. 45, No. 8, pp. 89-110 [in Japanese].
46. Neue weichmagnetische Werkstoffe und ihre Anwendung.– VDI-Z, 1959, Bd. 101, Nr. 20, S. 816 [New magnetically soft materials and their application].
47. W. M. Overn and V. J. Korkowski, Study of the residual states of ferrite cores in computer memory operation.– J. Appl. Phys., 1959, Suppl. to vol. 30, No. 4, pp. 52S-53S, Fig. 1, Bibl. 1.
48. M. Pasnak and R. H. Lundsten, Effects of high temperature on magnetic properties of core materials.– J. Appl. Phys., 1959, Suppl. to vol. 30, No. 4, pp. 107S-108S.
49. F. Pawlek, Zukunftsaussichten für die Entwichlung magnetischer Werkstoffe.– ETZ, Ausg. A, 1959, Nr. 17, SS. 651-655 [Future prospects for the development of magnetic materials].
50. A. Pierrot, J. Lescroel, B. Grabowski, and C. Guillaud, Perfectionnements aux matériaux ferromagnétiques à cycle d'hystérésis rectangulaire. [Improvement of square-loop ferromagnetic materials].
51. H. Reinboth, Technologue und Anwendung magnetischer Werkstoffe.– Berlin (Technik), 1958, S. 379. [Technology and application of magnetic materials].
52. C. E. Richards, Some recent developments in magnetic alloys.– IRE Trans. and Component Parts, 1959, vol. CP-6, No. 2, pp. 119-122, Bibl. 6.
53. L. Ruess, Über die Richtungsabhängigkeit magnetischer Eigenschaften von Elektroblechen und ihre Messung.– ETZ, Ausg. A, 1959, Nr. 17, SS. 588-592 [Anistropy of the electrical steel magnetic properties and their measurement].
54. E. I. Salrovitz, G. C. Bailey, and A. I. Schindler, Effect of neutron irradiation on the Curie temperature of a variety of ferrites.– J. Appl. Phys., 1958, vol. 29, No. 12, pp. 1747-1748, Fig. 2.
55. A. Schinkmann, Herstellung und Weiterentwicklung weichmagnetischer Ferrite.– Nachrichtentechnik, 1959, Bd. 9, Nr. 9, SS. 392-395, Fig. 11, Bibl. 4 [Production and further development of magnetically soft ferrites].
56. W. L. Shevel, Observations of rotational switching in ferrites. J. Res. and Development, 1959, vol. 3, No. 1, pp. 93-95, Bibl. 4.
57. J. Shichiyo, "Magnetic materials," Denki Tsushin Gakkai Zassi, J. Inst. Electr. Commun. Engrs. Japan, 1958, vol. 41, No. 4, pp. 443-447 [in Japanese].
58. G. Sideris, Soft magnets for amplifiers. (Choice of magnetic amplifier core materials broadens as new square-loop and high-permeability alloys are added to the old stand-bys.)– Elektronics, 1959, vol. 32, No. 6, p. 55, Table 2.
59. P. U. Sukhadia, Applications of ferrites.– Radio Serv., 1958, vol. 20, No. 4, pp. 11-15, 18.
60. K. Takahashi, "Modern developments of magnetic materials and their characteristics. Silicone steel sheets and strips, Om. Denki Zassi, Ohm. Electr. Mag., 1958, vol. 45, No. 8, pp. 22-23 [in Japanese].
61. K. Takahashi, "Table of magnetic material properties," Om. Denki Zassi, Ohm. Electr. Mag., 1958, vol. 45, No. 8, pp. 208-216 [in Japanese].
62. R. Wadas, Wlasności ferrytów Mg–Mn i Mg–Zn–Mn o prostokatnej petli histerezy.– Przeglad Telekomunikacyjny, 1959, I, No. 1, s. 14-1, Bibl. 11. [Properties of Mg–Mn and Mg–Zn–Mn ferrites with rectangular hysteresis loops].
63. M. Wakai, "Modern magnetic materials and their application," Om. Denki Zassi, Ohm. Electr. Mag., 1958, vol. 45, No. 8, p. 17.

b) Magnetization Processes and the Dynamic Characteristics of Ferromagnetic Materials

64. A. Arrott, and J. E. Goldman, Fundamentals of Ferromagnetism.– El. Manufacturing, 1959, March, vol. 63, No. 3, pp. 109-140, Fig. 47, Bibl. 6.
65. L. F. Bates, H. Clow, D. J. Craik, and P. M. Griffiths, Magnetization processes in a polycrystalline manganese zinc ferrite.– Proc. Phys. Soc., 1958, vol. 72, No. 2, pp. 224-232.
66. E. M. Bradley and M. Prutton, Magnetization reversal by rotation and wall motion in thin films of nickel-iron alloys.– J. Electronics and Control, 1959, vol. 6, No. 1, Series 1, pp. 81-96, Fig. 11, Bibl. 7.
67. E. W. Lee, A. G. Troughton, and D. R. Callaby, Eddy current losses in 65/35 nickel-iron.– Proc. Phys. Soc., 1959, vol. 73, No. 1, pp. 133-136.
68. L. Neel, Repétition des cycles d'hystérésis.– Colloq. nat. magnetisme commémoratif oeuvre Pierre Weiss. Strasbourg, 9-10 juill. 1957. Paris, SNRS, 1958, pp. 75-77, Bibl. 5. [Elektrotekhnika Abstr. J., 5, ref. 1. 1176 (1960). Hysteresis loop creep].
69. K. Sixtus, Die Rolle der magnetischem Nachwirkung in den Werkstoffen der Technik.– ETZ, Ausg. A, 1959, Nr. 17, SS.565-570. [The role of magnetic aftereffect in technological materials].

70. J. Sommer, Zkresleni hysteresni křivky působením vířivých proudů.– Sb. vedec. prací Vysoké školy Bánske Ostrave, 1958, R. 4, No. 6, s. 581-585. [Hysteresis loop distortion due to eddy currents].

c) Core Design and Production Technology

71. H. Brechna, Einfluss von Form und Bauart der Transformator–Eisenkörper auf die Ummagnetisierungsverluste.– Scientia Electr., 1959, Bd.5, Nr. 1, SS. 1-18. [Effect of the shape and structure of transformer cores on magnetization reversal losses].

72. Design Parameters of Ferrite Magnetic Amplifiers.– Military Systems Design, 1959, vol. 3, No. 3, pp. 146-147, Fig. 3.

73. H. Fuohse, Kernwerkstoffe und Kernbauformen für magnetische Verstärker.– VDI, 1959, Bd. 101, Nr. 9, SS. 341-342. [Design of and materials for magnetic amplifier cores].

74. J. P. Jones, Magnetic core assembly. US Pat., Class 336-65, No. 2823360, February 11, 1958. [Elektrotekhnika Abstr. J., 15, ref. 32255 (1959)].

75. T. Karasawa, "Magnetic core characteristics and their application," Erekutoronikusu, 1959, vol. 4, No. 3, pp. 265-274, Fig. 22.

76. T. Lindstrom, Electromagnet Copper-to-iron ratio for optimal design.– El. Manufacturing, 1959, vol. 63, No.3, pp. 105-107, Fig. 2.

77. Memory windings may be printed.– Electronics, 1959, vol. 32, No. 25, pp. 86, 88, 89. [Russian translation: Express Information: Vychisl. Tekhn. (Computer Techniques), 3, 12 (1960).

78. E. Miyazawa and S. Tyoda, Design methods for magnetic amplifiers using V-type lamination cores.– Denki Shikense Iho, Bull. Electrotechn. Lab., 1959, vol. 23, No. 1, pp. 503-516, 555.

79. E. Miyazawa and L. T. Chang, "Effect of toroidal core dimensions on the maximum power output of magnetic amplifiers," Denki Shikense Iho, Bull. Electrotechn. Lab., 1958, vol. 22, No. 7, pp. 525-530, 558.

80. A. a.o. Okamoto, "Magnetic amplifier design," Erekutoronikusu, 1959, vol. 4, No. 1, pp. 20-28, Fig. 17, Bibl. 7 [in Japanese].

80a. Perfectionnements aux bobinages électriques.– French Pat., Class H 01 d, H 03 f, No. 1166717; November 14, 1958. [Improvement of coil design].

81. J. Sakurai, "New magnetic cores and their application," Om. Denki Zassi, Ohm. Electr. Mag., 1958, vol. 45, No. 2, pp. 284-286, Fig. 16 [Elektrotekhnika Abstr. J., 4, 3179, part I (1960); see Elektrotekhnika Abstr. J., 3, 8076 (1958) (in Japanese)].

82. C. L. Snyder, Producing high-performance low-cost magnetic memory cores for an expanding digital computer market.– Computers and Automat., 1959, vol. 8, No. 3, pp. 9-11.

83. Specifying bobbin cores for digital circuits.– El. Manufacturing, 1959, vol. 63, No. 5, pp. 182-184; Fig. 3.

84. K. Weigelt, Konstruktive Massnahamen bei der Einführung der Kaltgewalzten Bleche.– Deutsche Elektrotechnik, 1959, Bd. 13, Nr. 3, SS. 84-86. [Design characteristics in the application of cold-rolled transformer sheet steel].

3. General Problems in the Theory of Nonlinear Magnetic Circuits

85. F. Dahlgren and R. Ladziński, Self-sustained modulations in transductor circuits.– Arch. automat. i telemech., 1958, vol. 3, No. 1-2, 37-57. [Elektrotekhnika Abstr. J., 18, 108 (1959)].

86. R. H. Dennard, Behavior of the ferroresonant series circuit containing a square-loop reactor.– Commun. and Electronics, 1959, January, No. 40, pp. 903-911, Fig. 17, Bibl. 8.

87. Ferromagnetism without ferromagnetic element.– Bull. Labs. Rec., 1958, vol. 36, No. 8, p. 303.

88. H. L. Goldstein, Observation of transients in the series connected saturable reactor with high-impedance control source.– Commun. and Electronics, 1959, No. 45, pp. 521-526, Fig. 19, Bibl. 11.

89. G. E. Kelly, The ferroresonant circuit.– Commun. and Electronics, 1959, January, No. 40, pp. 843-848, Fig. 8, Bibl. 10. Discussion p. 1061-1062.

90. H. W. Lord, An equivalent circuit for transformers in which nonlinear effects are present.– Commun. and Electronics, 1959, No. 45, pp. 580-586, Fig. 18, Bibl. 3.

91. G. Mellgren, Magnetisk spänningstabilisator.– Swedish Pat., Class 21c, 67/70, No. 156892; November 13, 1956. [Ferroresonant voltage stabilizer].

92. N. Nandon, "Parametric phenomena," Erekutoronikusu, 1959, vol. 4, No. 11, pp. 1178-1190, Fig. 15, Bibl. 9 [in Japanese].

93. K. M. Poole and P. K. Tien, A ferromagnetic resonance frequency converter.– Pire, 1958, vol. 46, No. 6, pp. 1387-1396, Fig. 9, Bibl. 11.

94. H. Rabl, Ein Resonanzphänomen bei magnetfeldgetemperten Perminvarferriten.– Z. angew. Phys., 1959, Bd.11, Nr. 2, SS. 57-63, Bibl. 18. [On a resonance phenomenon in thermomagnetically treated Perminvar ferrites].
95. A. A. Read and A. V. Pohm, Magnetic film parametric amplifiers.– Proc. NEC, 1959, October 12-14, Chicago, vol. 15, pp. 65-78, Fig. 10, Bibl. 10.
96. Régulateurs automatiques de tension à ferrorésonance.– Rabioconstr. et dépanneur, 1959, N 143, pp. 270-271. [Elektrotekhnika Abstr. J., ref. 4, 2929 (1960). Ferroresonance automatic voltage stabilizers].
97. J. Snieber, La résonance ferromagnétique dans les ferrites polycristallines.– Arch. sci., 1958, vol. 11, Fasc. spéc., p. 116. [Ferromagnetic resonance in polycrystalline ferrites].

4. Magnetic Amplifiers. Theory, Circuits, and Design

a) Books, Monographs, and Dissertations

98. G. M. Attura, Magnetic amplifier engineering.– McGraw-Hill book company, Inc., 1959, p. 220, Fig. 201, Bibl. 56.

b) Single-Cycle Magnetic Amplifiers

99. F. H. Belsey, Improvements relating to control means for magnetic amplifiers.–[The use of carbon stubs as control elements in high-speed magnetic amplifiers].
100. G. Biorci and D. Pescetti, Some consequences of the analytical theory of the ferromagnetic hysteresis.–J. phys. et radium, 1959, vol. 20, No. 2-3, pp. 233-236, Bibl. 2.
101. H. C. Bourne and J. T. Salihi, Analysis of series-connected saturable reactor with capacitive loading and finite control resistance by use of difference equations.– Commun. and Electronics, 1959, No. 45, Fig. 12, Bibl. 6.
102. D.A. Brown, Approximate methods for calculating the behavior of square loop magnetic cores in circuits.– Electronic Engng, 1959, vol. 31, No. 377, pp. 408-411, Bibl. 4.
103. M. Cambornac, Perfectionnements aux amplificateurs à courant continu.– French Pat., Class H03f, No.1165743; October 28, 1958. [Improvements of dc amplifier circuits].
104. M. C. Creusere, Magnetic amplifier.– US Pat., Class 235-61, No. 2810519; October 22, 1957.
105. C. M. Davis, Biasing means for selfsaturating magnetic amplifier.– US Pat., Class 179-171, No. 2839617, June 17, 1958.
106. G. H. Dewitz, Magnetic amplifier.– US Pat., Class 179-171, No. 2812389; November 5, 1957.
107. J. P. Eckert, Bipolar output carrier magnetic amplifier.– US Pat., Class 307-89, No. 2808520, October 1, 1957.
108. J. A. Fingerett and F. A. Hill, Magnetic amplifier.– US Pat., Class 323-89, No. 2827608; March 18, 1958. [Elektrotekhnika Abstr. J., 4, ref. 4, 2974 (1960)].
109. L. A.Finzi and J. J. Suozzi, On feedback in magnetic amplifiers. Commun. and Electronics, 1959, I–No. 40 (I), pp. 1019-1030, Fig. 4, Bibl. 5, discussion, pp. 1030-1031; II–No. 42 (3), pp. 136-140, Fig. 3, Bibl. 6, Appendix 2.
110. S. Frankenthal, Analysis of magnetic amplifiers using a resistive-reactor model.– Proc. C. M. A., 1959, Washington, AIEE, 1959, pp. 86-102, Fig. 16, Table I, Bibl. 7.
111. F. Gasparini and L. Merigliano, Trasduttori amperometrici in regime permanente.– Elettrotechnica, 1959, vol. 46, No. 4, pp. 238-249, Fig. 10. [Elektrotekhnika Abstr. J., 4, ref. 4, 2919 (1960). Magnetic current amplifiers].
112. K. Horada, "Magnetic amplifiers with feedback with respect to even harmonics," Denki Gakkai Zassi, J. Inst. Electr. Engrs, Japan, 1958, vol. 78, No. 3, pp. 335-346 [in Japanese].
113. K. E. Hardieck, Theretische und experimentalle Untersuchungen der stationären Vorgänge in magnetischen Verstärkern.– Forschungsber. Wirtsch.- und Verkshrsminister. Nordrhein Westfalen, 1958, Nr. 596, S. 74. [Elektrotekhnika Abstr. J., 2, ref. 4, 920 (1960). Theoretical and experimental investigations of steady-state phenomena in magnetic amplifiers].
114. C. E. Hardies and R. L. Van Allen, Self-regulation in magnetic-transistor amplifiers.– Proc. C.M.A., 1959, Washington, pp. 196-203, Fig. 8, Bibl. 2.
115. R. M. Hubbard, Temperature compensated magnetic amplifier.– US Pat., Class 179-171, No. 2841656; July 1, 1958.
116. G. L. G. Jeans, Improvements in ore relating to transductor arrangements.– Brit. Pat., Class 40(4), No.787987; December 19, 1957.
117. W. Jentsch, Gleichstromverstärker mit vormagnetisierten Drosseln.– French Pat, Class $21a^2$ 18/08, No.1012328; January 9, 1958. [Elektrotekhnika Abstr. J., 24, ref. 50142 (1959). A dc amplifier with saturable reactors].
118. P. R. Johanessen, Analysis of magnetic amplifier.– El. Engng, 1959, vol. 78, No. 10, pp. 1002-1003.

119. P. R. Johanessen, Analysis of magnetic amplifiers without diodes.– Commun. and Electronics, 1959, No. 45, pp. 471-485, Fig. 13, Bibl. 4.
120. P. R. Johanessen, Analysis of magnetic amplifiers with diodes.– Commun. and Electronics, 1959, No. 45, pp. 485-504, Fig. 25, No. 5.
121. I. Johansen, The winding capacitances in magnetic amplifiers.– Proc. C. M. A., 1958, Washington, AIEE, 1959, pp. 369-383, Fig. 12, Bibl. 2; Commun. and Electronics, 1958, No. 45, pp. 702-707, Fig. 12, Bibl. 2.
122. K. A. Key, Improvements in and relating to magnetic amplifiers.– Brit. Pat., Class 40(9), No. 818057; August 12, 1959.
123. K. A. Key, Improvements in and relating to magnetic amplifiers.– Brit. Pat., Class 40(9), No. 823693, November 18, 1959.
124. H. W. Kunnes, High speed magnetic amplifier.– US Pat., Class 307-106, No. 2820156, January 14, 1958. [Elektrotekhnika Abstr. J., 4, ref. 4, 2969 (1960)].
125. Fen Li, Heat calculation of magnetic amplifier with III-type cores.– J. of the Harbin Polytechnical Institute, 1959, No. 4 (No.22), pp. 127-136, Fig. 7, Bibl. 6.
126. E. W. Manteuffel, Time response constant and transfer function of magnetic amplifiers.– Proc. C. M. A., 1959, Washington, AIEE, 1959, pp. 47-71, Fig. 17, Bibl. 2.
127. H. F. McKenney and W. T. Keating, High gain magnetic amplifier.– US Pat., Class 179-171, No. 2878327; March 17, 1959.
128. E. Miyazawa, "Magnetic amplifier design methods," Otomeshion (Automation), 1959, vol. 4, No. 7, pp. 24-29, Fig. 9 [in Japanese].
129. K. Murakami and T. Kikuchi, Graphical circuit analysis of the full-wave magnetic amplifier control characteristics affected by control-circuit resistance.– Commun. and Electronics, 1959, No. 45, pp. 526-530, Fig. 15, Bibl. 9.
130. K. Murakami and T. Kikuchi, Graphical circuit analysis of the full-wave magnetic amplifier with square-loop core materials.– 1958, vol. 78, No. 841 (10), pp. 1288-1293, Fig. 15, Bibl. 14.
131. K. C. Parton, Improvements in or relating to magnetic amplifier arrangements.– Brit. Pat., Class 40(4), No. 753363; July 25, 1956.
132. R. Peterson, Magnetic amplifier with condenser discharge control circuit.– US Pat., Class 323-63, No. 2850696; September 2, 1958.
133. E. Pio, Determination graphique de la caractéristique d'utilisation d'un amplificateur magnétique.– C. R. Acad. Sc., 1959, vol. 248, No. 13, pp. 1960-1961. [Graphical determination of magnetic amplifier characteristics].
134. E. Pio, Théorie des amplificateurs magnétiques à autosaturation.– Bulletin de la Société Française des Electriciens, 1959, vol. 9, No. 101, pp. 256-264. [Theory of self-saturating magnetic amplifiers].
135. T. J. Pula, Volt-second transfer efficiency in fast-response magnetic amplifiers. Par N 2/R and Control.– Commun. and Electronics, 1959, No. 40, pp. 861-867, Fig. 5, Bibl. 17.
136. T. J. Pula, G. E. Lynn, and J. E. Ringelman, Volt-second transfer efficiency in fast-response magnetic amplifiers. Part II: N 2/R as a design parameter.– Commun. and Electronics, 1959, No. 41, pp. 8-11, Fig. 6, Bibl. 6.
137. J. F. Ringelman and F. G. Timmel, Magnetic amplifier maximum output control.– US Pat., Class 307-88, No. 2862112; November 25, 1958.
138. A. B. Rosenstein, The transactor: A self-saturated transformer.– Trans. Amer. IEE, P. I. (Commun. and Electronics), 1958, vol. 77, pp. 129-141, Bibl. 11.
139. B. Rossi, H. S. Sack, R. T. Beyer, and G. H. Miller, Magnetic amplifier. (June 26, 1946). – US Pat. Class 179-171, No. 2831929; April 22, 1958.
140. N. A. Ruggles and P. Real, Correlation of magnetic amplifier performance with core characteristics.– Proc. C. M. A., 1959, Washington, AIEE, 1959, pp. 324-339, Fig. 10, Table 9, Bibl. 2, Appendix 2.
141. Y. Sakurai, "A ferrite magnetic amplifier," Erekutoronikusu, 1958, vol. 3, No. 11, pp. 1140-1144 [in Japanese].
142. Y. Sakurai, and E. Itikawa, Core characteristics and control characteristics in self-saturating magnetic amplifier with ferrite core.– Denki Gakkai Zassi, 1958, vol. 78, No. 843(12), pp. 1580-1584, Fig. 13, Bibl. 9.
143. K. L. Sanders, Minimum time delay magnetic amplifier (North American Aviation, Inc.), October 14, 1952.– US Pat., Class 323-89, No. 2820943, January 21, 1958.
144. W. Schilling, Die Steuerverfahren beim spanungssteuernden Transduktor.– ETZ-A, 1959, Bd. 80, Nr. 3, SS. 83-87, Fig. 8, Bibl. 6. [Control of magnetic amplifiers for voltage regulation].
145. Guang-ming Shen, A method of deriving transfer functions for magnetic amplifiers.– Scientia Sinica, 1959, vol. 8, No. 2, pp. 183-195.

146. J. Sherlock, The flux resetting magnetic amplifier.– El. Energy, 1959, vol. 3, No. 1, pp. 2-10, Fig. 23.
147. G. Sichling, Magnetverstärker in Selbstsättigungschaltung.– West Germany Pat., Class 21a², 18/08, No. 1026362, September 4, 1958. [Elektrotekhnika Abstr. J., 4, ref. 4, 2972 (1960). Self-saturating magnetic amplifier].
148. S. Sonoda, "Magnetic amplifier time constant," Kenkyu Zitsuyuka Kokoku, Electr. Commun. Lab. Techn. J., 1958, vol. 7, No. 7, pp. 599-606 [in Japanese].
149. S. Sonoda, Time Constant of Magnetic Amplifier.– Reports Electr. Comm. Lab., 1958, August, vol. 6, No. 8, pp. 299-302, Fig. 3.
150. Ti-tjen Sye, "Effect of some factors on magnetic amplifier properties," Tzurtunghua, 1959, vol. 2, No. 8, pp. 283-292, Fig. 12, Bibl. 3 [in Chinese].
151. K. Szacka, "Certain characteristics of voltage-controlled magnetic amplifiers." – Arch. automat. i telemech., 1958, vol. 3, No. 4, pp. 260-261.
152. Tashiro, "Improvement of magnetic amplifiers," Otomeshion, 1959, vol. 4, No. 7, pp. 36-40, Fig. 14, Bibl. 22 [in Japanese].
153. Transformateur à transducteur.– French Pat., Class HO21 HO1h, No. 1168783, December 16, 1958. [Transformer with magnetization].
154. Tung Shing-hwang, "Investigation of transient processes in magnetic power amplifiers," Tzuhtunghua, Automation, 1958, vol. 1, No. 2, pp. 64-72 [in Chinese].
155. E. W. VanWinkle, Magnetic amplifier.– US Pat., Class 323-89, No. 2883613; April 21, 1959.
156. M. Wengryn, Transistor driven magnetic amplifier.– US Pat., Class 318-207, No. 2885619; May 7, 1959.
157. J. Werner, Das dynamische Verhalten des magnetischen Verstärkers.– AEG–Mitt., 1959, Bd. 49, Nr. 8-9, SS. 353-361. [Russian translation: Express Information: Pribory i Elementy Promyshlennoi Avtomatiki (Industrial Automation Devices and Components), 12, 90 (1960). Magnetic amplifier dynamic characteristics].
158. H. H. Woodson, A mathematical model for a magnetic amplifier reactor core.– Proc. C. M. A., 1959, Washington, AIEE, 1959, pp. 72-85, Fig. 11, Bibl. 24.

c) Push-Pull Amplifiers

159. J. Eckert, Forcible reversion of magnetic amplifiers.– US Pat., Class 307-88, No. 2792507; May 14, 1957.
160. K. Fuchs, Magnetverstärker zur richtungs–und amplitudenabhängigen Steuerung des Ausgangsstromes.– West Germany Pat., Class 21a², 18/08, No. 1031354; November 13, 1958. [Elektrotekhnika Abstr. J., 4, 4, 2971 (1960). Magnetic amplifier for directional and amplitude control of output currents].
161. L. M. Germain, Low drift magnetic amplifier.– US Pat., Class 179-171, No. 2884493; April 28, 1959.
162. H. Herz, A. A. Sterk, and H. A. Goldsmith, (Magnetic Amplifiers, Inc.) Packaged magnetic amplifier. (November 21, 1951).– US Pat., Class 179-171, No. 2849544; August 26, 1958.
163. H. Iinuma, "Magnetic amplifier for weak signals. Application of weak currents in magnetic amplifiers," Erekutoronikusu, 1959, vol. 4, No. 1, pp. 8-19, Fig. 15 [in Japanese].
164. Low-level 60-cps magnetic amplifiers.– El. Manufacturing, 1959, vol. 63, No. 2, p. 274.
165. Magnetic D-C amplifier is drift free.– Electronics, 1959, vol. 32, No. 16, p. 62.
166. L. N. Rowley and J. L. Hennessy, (Sperry Rand Corp.) Magnetic amplifier circuit. August 19, 1954.– US Pat., Class 323-89, No. 2858503, October 28, 1958. [Circuit of a push-pull magnetic amplifier with biasing by means of shunting the internal feedback rectifiers].
167. W. Schilling, Spannungssteuerung und magnetische Kennlinie des Zweiweg-Transduktors mit Gleichspannungsausgang.– ETZ.–A, 1959, Bd. 80, Nr. 23, SS. 817-822. [Voltage control and the magnetic characteristics of push-pull magnetic amplifiers with a dc output].
168. W. Schilling, Spannungssteuerung und magnetische Kennlinie des Zweiweg-Transduktors mit Wechselspannungsausgang.– ETZ.–A, 1959, Mai, Bd. 80, Nr. 9, SS. 269-273, Fig. 8, Bibl. 8. [Voltage control and the magnetic characteristics of push-pull magnetic amplifiers with an ac output].
169. N. L. Schmitz and T. Bernstein, Reversible-polarity D-C power amplifier using magnetic–amplifier–controlled switched transistors.– Commun. and Electronics, 1959, January, No. 40, Fig. 7, Bibl. 5.
170. S. D. Warner, High-gain magnetic amplifier in bridge circuit.– El. Manufacturing, 1959, vol. 64, No. 3, pp. 114, 116, and 177, Fig. 7, Bibl. 5.

d) Multistage Magnetic Amplifiers

171. H. W. Collins, Capacitively coupled magnetic amplifiers.– Commun. and Electronics, 1959, No. 45, pp. 707-712, Fig. 7, Bibl. 5.

172. F. H. Guth, (Thompson Products, Inc.) Magnetic amplifier.– US Pat., Class 323-89, No. 2831159; April 15, 1958.
173. R. M. Hubbard, Shunt-coupled magnetic amplifier circuits.– Commun. and Electronics, 1959, No. 42, pp. 124-131. [Russian translation: Express Information: Industrial Automation Devices and Components, 1, 1-3 (1960)].
174. W. Keating, Magnetic amplifier circuit.– US Pat., Class 323-89, No. 28200191; January 14, 1958. [Elektrotekhnika Abstr. J., 5, ref. 4, 4029 (1960)].
175. H. Kind, Frequenzgänge mehrstufiger Magnetverstärker mit Rückführungen.– Regelungstechnik, 1959, Bd. 7, Nr. 3, SS. 86-89. [Frequency characteristics of multistage magnetic amplifiers with feedback].
176. W. McMurray, Elimination of coupling problems in multi-stage magnetic amplifiers.– Proc. C.M.A., 1959, Washington, AIEE, 1959, pp. 116-129, Fig. 10, Bibl. 9.

e) Multiphase Magnetic Amplifiers

177. H. F. Storm and C. W. Flairty, Theory of three-phase bridge magnetic amplifier. Part I: Steady-state.– Proc. CMA, 1959, Washington, AIEE, 1959, pp. 5-46, Fig. 24, Bibl. 17.

f) High-Frequency Magnetic Amplifiers

178. G. H. Dewitz, Magnetic amplifier.– US Pat., Class 179-171, No. 2820109; January 14, 1958. [Elektrotekhnika Abstr. J., 5, ref. 4, 4030 (1960)].
179. Y. Sakurai, "Application of high-frequency magnetic amplifiers," Otomeshion, 1959, vol. 4, No. 7, pp. 10-14, Fig. 24 [in Japanese].

5. Magnetic Amplifiers. Application

a) General Application Problems

180. J. Albin, Circuits à noyaux magnétiques saturables.– French Pat., Class 12.3, No. 1150418; January 13, 1958. [Elektrotekhnika Abstr. J., 4, ref. 4, 2966 (1960). Circuits with saturable cores].
181. G. Arbinger, Magnetische Verstärker und ihr Einsatz für die Steuerung und Regelung in Hüttenwerken.– E. and M., 1959, Nr. 23, SS. 579-583. [Magnetic amplifiers and their application for the control and regulation of metallurgical processes].
182. N. J. Behne, H. C. Diener, and J. R. Erbe, Static control provides blast furnace automation.–Iron and Steel Engr, 1959, vol. 36, No. 2, pp. 127-138.
183. T. W. Carreyett, The magnetic-amplifier applied to voice-frequency ringers.– Brit. Commun. and Electronics, 1959, v. 6, No. I, pp. 16-18.
184. A. D. Cawdery and H. T. Carden, Application of magnetic amplifiers to engineering problems.– Brit. Commun. and Electronics. 1959. v. 6. No. 3, pp. 180-184.
185. P. L. Cerato, Gli amplificatori magnetici, I.– Elettrificazione, 1958, n. II, Elettr. industr. ed energia nucleare, t. 2, n. 11, pp. 167-171, Fig. 9. [Elektrotekhnika Abstra. J., 2, ref. 4, 917 (1960). Magnetic amplifiers].
186. G. Conti and E. Ferraboschi, Un moderno sistema di regolazione ad amplificazione magnetronica nell'automazione dell'industria siderurgica.– Strum. e automaz., 1959, v. 7, n. 3, pp. 105-123, Fig. 19, Bibl. 8. [Elektrotekhnika Abstr. J., 1, ref. 4, 486 (1960). A modern control system with magnetic amplifiers for metallurgical automation].
187. S. Davis, Magnetic amplifiers for servo systems.– Electronics, 1959, March 13, v. 32, No. 11, pp. 134-135.
188. W. K. Dillon, Magnetische Kleinverstärker als Schaltungselemente.– Bull. As. Suisse Electriciens, 1859, Bd. 50, III, Nr. 7, SS. 341-348, Bibl. 10.
189. H. Have, Improvements relating to electro-magnetic control devices.– Brit. Pat., Class 38(2), 38(4), 40(4), No. 742487; December 30, 1955.
190. F. J. Hierholzer, Linear power amplifiers using dynistors or trinistors.– Commun. and Electronics, 1959, v. I, No. 40, pp. 892-898.
191. T. Hioki and Y. Onuma, "Comparison between magnetic and electronic amplifiers in automatic lines," Erekutoronikusu, 1959, v. 4, No. 1, pp. 33-40, Fig. 15 [in Japanese].
192. W. F. Horton, S. J. Reisman, R. O. Decker, and R. A. Ramey, Magnetic amplifier for control purpose.– US Pat., Class 323-89, No. 2792547; May 14, 1957.
193. Hu Tshu-ding, "Magnetic amplifiers (1, 2, 3, 4, and 5)," Teng Shihchieh, 1959, v. 13, No. 6, pp. 369-370, No. 7, pp. 433-434; No. 8, pp. 499-500; No. 9, pp. 558-560; No. 11, pp. 671-673 [in Chinese].
194. M. Ito, K. Yamagishi, K. Fijiki, T. Mackawa, H. Kobayashi, F. Hamaoka, and M. Kamura, "Magnetic amplifier application. New devices," Om. Denki Zassi, Ohm. Electr. Mag., 1958, v. 45, No. 8, pp. 137-155 [in Japanese].

195. A. Kavabuti, "Control of industrial processes by means of magnetic amplifiers," Shinko Denki, 1958, No. 6, pp. 36-41 [in Japanese].
196. H. Kobayashi, "Various rectifier types for magnetic amplifiers," Otomeshion, 1959, v. 4, No. 7, pp. 30-35, Fig. 14 [in Japanese].
197. A. Köhler, Trunsduktorn som reglerförstärkare. Elektrotechn. tidsskr., 1958, v. 71, No. 19-20, pp. 253-259, Fig. 16. [Magnetic amplifiers in control systems].
198. K. Kühnert, Le rôle des amplificateurs magnetiques dans le contrôle industriel.— Instrum. et labs, 1958, No. 5, pp. 9-18, Fig. 20. [The role of magnetic amplifiers in industrial automation].
199. K. Kurogawa, "Interference-protection of magnetic amplifiers," Otomeshion, 1959, v. 4, No. 7, pp. 21-23, Fig. 6 [in Japanese].
200. A. Lang, Bedeutung der Transduktortechnik für die Mess-Steuerungs- und Regelungstechnik.— AEG-Mitt., 1959, Bd. 49, Nr. 8-9, SS. 329-333. [Russian translation: Express Information: Automatic Control of Industrial Processes, 14, 63 (1960). Significance of magnetic components in measurement, control, and regulation techniques].
201. H. G. Lott, Schaltungen des Transduktorverstärkers.— AEG-Mitt., 1959, Bd. 49, Nr. 8-9, SS. 437-442. [Russian translation: Express Information: Automatic Control of Industrial Processes, 18, 82 (1960). Magnetic amplifier circuits].
202. Magnetic amplifiers.— Control, 1959, v. 2, No. 8, p. 110. Pullin and Co., Ltd. Advertisement.
203. Magnetic amplifier has varied missile uses.— Missiles and Rockets, 1959, v. 5, No. 8, pp. 44, 47. [A magnetic amplifier for rockets with output power from 0 to 2000 w].
204. Magnetic amplifier is new on-off type.— Missiles and Rockets, 1959, v. 5, No. 23, p. 76. [A small-size magnetic amplifier].
205. Magnetic output amplifier.— Brit. Commun. and Electronics, 1959, v. 6, No. 4, p. 63.
206. M. Mesarović, Magnetski pojačivač kao elemenat automatizacije.— Tesla, 1958, v. 5, No. 4, pp. 21-24. [Magnetic amplifiers as automation components].
207. N. P. Milligan, The magnetic circuit—the key to successful applications of the Hall effect.— Proc. C. M. A., 1959, Washington, AIEE, 1959, pp. 256-267, Fig. 10, Table 1, Bibl. 5.
208. E. Miyazawa, "Magnetic amplifier application," Otomeshion, Automation, 1959, v. 4, No. 5, pp. 17-22, Fig. 10 [in Japanese].
209. E. Miyazawa, "Magnetic amplifier application. Basic characteristics of magnetic amplifier application," Om. Denki Zassi, Ohm. Electr. Mag., 1958, v. 45, No. 8, pp. 130-136 [in Japanese].
210. A. Mogi, "Magnetic amplifier application. Introduction," Om. Denki Zassi, Ohm. Electr. Mag., 1958, v. 45, No. 8, pp. 120-124 [in Japanese].
211. O. Nishino, "Modern trends in magnetic amplifier design," Otomeshion, 1959, v. 4, No. 7, pp. 8-9, Bibl. 4 [in Japanese].
212. S. Oshima, S. Watanabe, and H. Enomoto, "The demand for new analog memory devices," Denki Kagaku, 1959, v. 9, No. 9, pp. 10-12, Fig. 5 [in Japanese].
213. Z. Oyama, "Magnetic amplifiers in automatic control systems," Otomeshion, 1959, v. 4, No. 7, pp. 15-20, Fig. 12, Bibl. 3 [in Japanese].
214. I. Romano, Principes des amplificateurs magnetiques.— Rev. gén. électr., 1958, v. 67, No. 4, pp. 233-244. [Magnetic amplifier operating principles].
215. Y. Sakurai, "Magnetic amplifier applications. Industrial applications," Om. Denki Zassi, Ohm. Electr. Mag., 1958, v. 45, No. 8, pp. 124-130 [in Japanese].
216. Y. Sakurai, "Magnetic amplifier types and their characteristics," Otomeshion, Automation, 1958, v. 3, No. 8, pp. 8-15 [in Japanese].
217. K. L. Shrider and P. W. Pfaff, Saturable reactor control circuit.— US Pat., Class 323-39, No. 2809342; October 8, 1957. [Elektrotekhnika Abstr. J., 24, ref. 50200 (1959)].
218. P. Sirven, Les amplificateurs magnétiques.— Electricien, 1958, t. 86, No. 1978, pp. 106-109, Fig. 4. [Magnetic amplifiers].
219. R. W. Spencer and T. H. Bonn, Stabilized amplifier devices.— US Pat., Class 307-88, No. 2830197, April 8, 1958. [Elektrotekhnika Abstr. J., 4, ref. 4,2973 (1960)].
220. L. W. Stammerjohn, Magnetic amplifiers.— US Pat., Class 318-207, No. 2843813, July 15, 1958. [Elektrotekhnika Abstr. J., 4, ref. 4,2970 (1960)].
221. H. Tanaka, "Investigations of magnetic amplifiers," Waseda Daigaku Daigakuin Kogaku Kenkyu Iho, Synop. Engng Papers. Grad School Sci. and Engng. Waseda Univ., 1958, No. 7, pp. 179-180. [Elektrotekhnika Abstr. J., 4, ref. 4,2914 (1960)].

222. The transductor—a modern control device.— Australian Machinery, 1959, v. 12, No. 125, pp. 35-38, Fig. 1.
223. J. Wetzger, Vacantieleergang over roterende en stationaire magnetische versterkers. VI. Wirkungsweise und Anwendung des Magnetverstärkers.— Ingenieur (Nederl.), 1958, Bd. 70, Nr. 6, E. 21-E. 26. [Mashinostroenie (Machine Construction) Abstr. J., 5, 1, ref. 1492 (1960). Operating principle of magnetic amplifiers and their application].
224. C. C. Whitehead, How magnetic amplifier controls transconductance.— Electronics, 1959, v. 32, No. 46, pp. 84-87.
225. C. C. Whitehead, "Variable-M" – magnetic amplifier.— Wireless World, 1959, No. 5.

b) Servomotor and Electrical Machine Application

226. F. W. Alexanderson, Magnetic amplifier motor control system.— US Pat., Class 318-298, No. 2844779; July 22, 1958.
227. L. S. Bryson and R. J. Truscott, Servo amplifiers for the navy.— Part I — Control, 1959, v. 2, No. 10. Part 11— Control, 1959, v. 2, No. 11, pp. 82-88, Fig. 17.
228. S. B. Cohen, Servo system using a magnetic amplifier mixer. (Sperry Rand Corp.) (November 14, 1952).— US Pat., Class 318-30, No. 2832019; April 22, 1958.
229. C. Giot, Regulation de vitesse d'un moteur asynchrone par amplificateur magnetique.— Revue "E", 1959, v. 2, No. 10, pp. 268-276. [Induction motor speed regulation by means of magnetic amplifiers].
230. F. Hamaoka, A. Imaide, and E. Ono, "A magnetic amplifier for servomotors," Mitsubishi Danki, 1958, v. 32, No. 5, pp. 500-506 [in Japanese].
231. B. Hamel, Procédé et dispositif de commande d'un moteur a courant continu pour les deux sens de marche par amplificateurs magnétiques.— French Pat., Class 12.5, No. 1140671; August 15, 1957 [Elektrotekhnika Abstr. J., 2, ref. 3,722P (1960) A reversive control circuit with magnetic amplifiers for dc motors].
232. T. Ito, "Braking control by means of relay-type magnetic amplifiers," Shinko Denki, 1958, No. 6, pp. 26-35 [in Japanese].
233. F. Kümmel, Verhalten von Magnetverstärkern bei Motorbelastung.— Elektrotechnica Z. A., 1959, Bd. 80, Nr. 11, SS. 344-349. [Russian translation: Express Information: Elektrotekhnika, 39, 226-227 (1959). Magnetic amplifier operation with motor load].
234. W. Neumann and J. Wetzger, Magnetverstärker.— Elektrotechnik, 1959, Bd. 41E, Nr. 3, SS. 81-85. [Magnetic amplifiers and their application in electric drive regulation systems].
235. J. Paulik, Použitie magnetických zosilňovačov pri automatickom riadení tažných strojov.— Strojnoelektrotechn. časop., 1958, R. 9, No. 5, SS. 275-283. [Application of magnetic amplifiers for lifting machine control].
236. E. C Rhyne, System for controlling induction motors by saturable reactors and coordinately controlled resistors.— US Pat., Class 318-214, No. 2793338; May 21, 1957.
237. W. R. Seegmiller, Reversible D-C shunt motor drive using magnetic amplifier and controlled rectifiers.— Proc. NEC, 1958, pp. 898-904, Fig. 12, Bibl. 2.
238. J. F. Szablya, Torque and speed control of induction motors using saturable reactors.— Power Apparatus and Systems, 1959, No. 40, pp. 1676-1682, Fig. 14.
239. D. E. Villers, Magnetic amplifiers in the control of motor drives.— Automat. Progress, 1959, v. 4, No. 11, November, pp. 360-363.
240. M. Weinstein, Integrating servo mechanism.— US Pat., Class 318-327, No. 2825861; March 4, 1958. [Elektrotekhnika Abstr. J., 1, ref, 4.258 (1960)].
241. M. Wendt and R. Lappe, Antriebsregelungen mit magnetischen Verstärkern.— Elektrie; 1959, Bd. 3, Nr. 7, SS. 255-256. [Drive control with magnetic amplifiers].
242. L. Werner, Elements of reactor-controlled reversible induction-motor drive.— Applic. and Ind., 1959, No. 42, pp. 106-115, Fig. 13.

c) Application for Regulators and Current and Voltage Stabilizers

243. AEG Transduktorgeregelte Spannungskonstanthalter.— ETZ, Ausg. A., 1959, Bd. 80, Nr. 5, A 15. [Russian translation: Express Information: Elektrotekhnika, 5, 99 (1959). Voltage stabilizer with a magnetic amplifier].
244. E. S. L. Beale and A. H. Morser, Improvements in and relating to the stabilization of alternating voltages.— Brit. Pat., Class 38(4), 40(6), No. 751730: July 4, 1956. [Elektrotekhnika Abstr. J., 2, ref. 4,953 (1960)].
245. R. R. Berghoff, Voltage stabilizing system.— US Pat., Class 323-61, No. 2825024; February 25, 1958.
246. M. Duma and W. Roisman, Stabilizatoare de tensiume alternativa cu amplificatoare magnetice si electronice.— Automat. si electron., 1958, v. 2, n. 5, p. 204-212 [Elektrotekhnika Abstr. J., 4, ref. 4. 2927 (1960). AC voltage stabilizers with magnetic and electronic amplifiers.]

247. H. A. Engle, Voltage regulating system.– US Pat., Class 323-21, No. 2808559, October 1, 1957.

248. E. Flötenmeyer, Ein elektronisch-magnetischer Spannungsregler mit Regeldiode.– Ind.– Anz., 1958, Bd. 80, Nr. 88, SS. 1331-1332. [Elektrotekhnika Abstr. J., 23, ref. 48092 (1959). Electronic-magnetic voltage regulator with a controllable diode].

249. W. A. Geyger, Automatic regulators with self-balancing magnetic amplifiers.– Commun. and Electronics, 1959, No. 44, pp. 433-438, Bibl. 9. [Annotated radio electronics literature index, 3, ref. 1154 (1960) – in Russian].

250. R. Hahn, Der Einsatz von Konstantspannungs–Generatoren.– Siemens – Zeitschrift, 1959, Januar, Bd. 33, Nr. 1, SS. 31-38. [Utilization of stabilized-voltage generators].

251. A. C. Halter, Control system utilizing magnetic amplifier for reference voltage. (Allis-Chalmers Manufacturing Co., November 18, 1953). US Pat., No. 2752545; June 26, 1956.

252. L. R. Hetzler, Magnetic amplifier voltage regulator.– US Pat., Class 322-28, No. 2886765; May 12, 1959.

253. A high-speed transistor magnetic amplifier for a servo drive.– Automat. Progress, 1959, v. 4, No. 11, pp. 364-365, 378, Fig. 4, Bibl. 5. [Translation of the article by V. S. Volodin, E. D. Larin, M. A. Rozenblat, and G. V. Subbotina from the journal Avtomatika i Telemekhanika 20, 3, 323-330 (1959)].

254. H. Howe, Improvements in and relating to voltage stabilization devices for A.C. circuits.– Brit. Pat., Class 38 (2), 38(4), No. 742513; December 30, 1955.

255. J. Krušek and B. Dudàš, Teorie noveho stabilizàtoru proudu pracujiciho na principu transduktoru.– Slaboproudý Obzor, 1959, R. 20, N. 4, s. 212-216, rys. 8, Bibl. 5. [Theory of new current stabilizers based on the transducer principle].

256. J. Krušek, B. Dudàš, and J. Hejda, Transduktorový stabilizátor proudu pro regulační účely.– Automatizace, 1959, Cerven., v. 11, No. 6, s. 161-163, rys. 6, Bibl. 4. [Current stabilizers with magnetic amplifiers for regulation purposes].

257. The magnetic A.C. voltage regulators with all the trumps-sorensen.– Brit. Commun. and Electronics, 1959, v. 6, No. 4, p. 58.

258. Magnetic amplifier voltage regulation.– El. Revue, 1958, v. 163, No. 25, pp. 1123-1126, Fig. 7.

259. R. G. Martin, Improvements, relating to electric stabilizing circuits suitable for use in servo system.– Brit. Pat., Class 38(4), No. 791314; February 26, 1958. [Elektrotekhnika Abstr. J., 23, ref. 48101 (1959)].

260. W. J. McDaniel and T. L. Tanner, High-voltage magnetically regulated D-C supply.– Proc. NEC, 1958, v. 14, pp. 905-912, Fig. 8, Bibl. 7.

261. R. D. Pettit, Improvements in regulating circuits utilizing saturable reactors.– Brit. Pat., Class 38(4), A6B No. 753321; July 25, 1956.

262. D. S. Ridler and R. Grimmond, Improvements in or relating to circuit arrangements for producing substantially constant currents.– Brit. Pat., Class 40(4), No. 791905; March 12, 1958.

263. A. Rogojan and E. Pop, Analiza unor scheme de stabilizator de tensiune cu amplificatori magnetici.– Bul. stiint. si tehn. Inst. politehn. Timisoara, 1958, v. 3, pp. 117-123. [Analysis of some voltage stabilizer circuits with magnetic amplifiers].

264. S. Sapira, Stabilizator de tensiune alternativa reglat cu amplificatoare magnetice.– Automat. si electron., 1958, v. 1, n. 4, pp. 148-153. [Elektrotekhnika Abstr. J., 4, ref. 4,2928 (1960). AC voltage stabilizer using a magnetic amplifier for regulation].

265. N. Silver, Voltage regulator.– US Pat., Class 321-19, No. 2810877; October 22, 1957.

266. Stabilisateur de tension alternative réglé a l'aide d'amplificateurs magnétiques.– Monit. Profess. Electr., 1959, v. 14, No. 36, pp. 27, 29, 30. [Russian translation: Express Information: Elektrotekhnika, 27 (1959). AC voltage stabilizer controlled by magnetic amplifiers].

267. A. A. Sterk, Voltage regulator.– US Pat., Class 323-66, No. 2816263; December 10, 1957. [Elektrotekhnika Abstr. J., 23, ref. 48050 (1959)].

268. T. Tongo, "Automatic voltage stabilizers with magnetic amplifiers," Denki Keisan, 1958, v. 26, No. 12, pp. 2231-2233 [in Japanese].

269. A. H. B. Walker and K. G. King, Improvements relating to voltage current regulators.– Brit. Pat., Class 38(4), 40(4), No. 782684; September 11, 1957. [Elektrotekhnika Abstr. J., 3, ref. 4,1917 (1960)].

270. O. Werner, Einrichtung zur Regelung der Spannung von über magnetische Verstärker gespeisten Verbrauchern auf einen konstanten Wert und zur Begrenzung des Verbraucherstormes durch Spannungsabsenkung.– West Germany Pat., Class 21 c, 67/70, No. 1018516, April 10, 1958. [Elektrotekhnika Abstr. J., 33, ref. 48048 (1959). A device for regulating the voltage and limiting the current of a load fed through a magnetic amplifier].

d) Application for Measuring Instruments

271. K. Bielański, Transduktorowe przekladniki pradowe pradu stalego.– Pomiary, Automatyka, Kontrola, 1959, No. 6, s. 220-225, rys. 17, Bibl. 4. [Measuring dc transformers].

272. W. A. Geyger, Magnetic-amplifier-operated ink recorders.– Commun. and Electronics, 1958, No. 38, pp. 457-471, Bibl. 43.
273. W. A. Geyger, A miniaturized D-C instrument transformer.– Proc. C.M.A., 1959, Washington, AIEE, 1959, pp. 130-153, Fig. 22, Bibl. 30.
274. M. H. Goosey and A. C. Lapsley, Magnetic amplifiers aid D-C measurement.– Electronics, Eng. Edition, 1958, v. 31, No. 51, pp. 98-99.
275. W. E. Nesbitt, Obtaining optimum performance from a magnetic thermocouple amplifier.– IRE Trans. Industr. Electronics, 1958, No. 6, pp. 101-114, Fig. 9, Bibl. 3.
276. H. G. Smith, The place of magnetic amplifiers and kindred magnetic devices in instrumentation.– J. Electronics and Control, 1959, I. Series, v. VI, No. 5, pp. 436-453. [Russian translation: Express Information, PPA, 5, 28 (1960)].
277. E. W. Yetter, Magnetic measuring system. (Leeds and Northrup Co.)– US Pat., Class 324-43, No. 2755434; July 17, 1956.

e) Application for Decision Amplifiers

278. I. Danylshuk and D. Katz, Magnetic amplifier binary-to-analog conversion.– Proc. C.M.A., 1959, Washington; AIEE, 1959, pp. 306-312, Fig. 6, Bibl. 3.
279. W. A. Geyger, Multiplying circuit uses magnetic amplifiers.– Electronics, 1959, v. 39, No. 2, pp. 58-59.
280. L. W. Langley, Saturable-core oscillator integrates gas-flow data.– Electronics, 1959, v. 32, No. 4, pp. 36-37.
281. W. B. McLean and J. A. Crawford, Magnetic integrator.– US Pat., Class 317-149, No. 2822511; February 4, 1958.
282. K. Noriyoshi, Flux controlling type adder.– Repts Electr. Commun. Lab., 1958, v. 6, No. 12, pp. 468-475, Fig. 11.
283. E. W. Yetter, Magnetic device for addition and abstraction.– US Pat., Class 235-61, No. 2819018; January 7, 1958. [Elektrotekhnika Abstr. J., 4, ref. 4,3233 (1960)].

f) Other Applications

284. A. O. Adams, Magnetic amplifier operated relays.– Electronic Inds., 1958, v. 17, No. 12, pp. 72-74, 153. [Elektrotekhnika Abstr. J., 4, ref. 4.2919. Russian translation: Express Information, Vychisl Tekhn. (Computer techniques), 25, 97-98 (1959). Magnetic amplifier operated relays for aircraft and guided missiles].
285. J. W. Butler, New uses of static magnetic components in protective circuits.– Control Eng., 1959, v. 6, No. 11, pp. 135-138. [Annotated radio electronics literature index, 3, ref. 2053 (1960) – in Russian].
286. H. Hecht and P. G. Graff, Servo system with magnetic rate-taking.– US Pat., Class 318-489, No. 2812487; November 5, 1957. [Elektrotekhnika Abstr. J., 23, ref. 48099 (1959)].
287. A. Kalnitz, Using magnetic circuits to pulse radar sets.– Electronics, 1959, v. 32, No. 27.
288. K. H. Lakkey, A review of protective gear practice in Great Britain.– El. Energy, 1957, No. 13, 14.
289. R. Marenesi and G. Ruffino, Transduttore e commutatore magnetico per registrazioni oscillografiche.– Elettrotechnica, 1959, v. 46, No. 8, pp. 466-473, Fig. 9. [Russian translation: Express Information, Elektrotekhnika, 48 (1959). Magnetic amplifier for oscillographic recording].
290. E. Ono, "Application of contactless relays," Otomeshion, Automation, 1959, v. 4, No. 6, pp. 52-58 [in Japanese].
291. Y. Onoda and T. Imao, "Accurate current regulation in mercury rectifiers for powerful magnetic field generators by means of magnetic amplifiers," Erekutoronikusu, 1959, v. 4, No. 1, pp. 41-46, Fig. 12 [in Japanese].
292. S. Oshima, S. Watanabe, and H. Enomoto, "Analog memory devices based on magnetic cores," Denshi Kagaku, 1959, v. 9, No. 9, pp. 16-22, Fig. 19 [in Japanese].
293. S. Oshima, S. Watanabe, and H. Enomoto, "Magnetic analog memories," Denshi Kagaku, 1959, v. 9, No. 8, pp. 13-15, Fig. 7 [in Japanese].
294. S. Oshima, S. Watanabe, and H. Enomoto, "Application of analog magnetic core materials," Denshi Kagaku, 1959, v. 9, No. 9, pp. 23-24, Fig. 5 [in Japanese].
295. J. H. Porter, Pulse sorting with transistors and ferrites.– Electronics, 1959, May 15, v. 32, No. 20, pp. 64-65.
296. A. W. Pratt, Transistor-magnetic control circuits for aircraft electric systems.– Commun. and Electronics, 1959, v. 45, pp. 643-650, Fig. 12.
297. D. A. Ramsay, Improvements in or relating to magnetic amplifiers.– Brit. Pat., Class 38(4), 40(9), No. 800594; August 27, 1958. [Elektrotekhnika Abstr. J., 3, ref. 4,1905 (1960)].
298. T. Yosida, "Automatic light signal device "Magnetact" with magnetic amplifiers," Erekutoronikusu, 1959, v. 4, No. 2, p. 179, Fig. 2 [in Japanese].

EVENTS

SEMINAR ON TECHNICAL CONTRIBUTIONS TO MATHEMATICAL LOGIC (1959-1960)*

V. P. Goncharov

Translated from Avtomatika i Telemekhanika, Vol. 22, No.2, pp. 292-294, February, 1961

Since Autumn, 1959, the Seminar on Technical Contributions to Mathematical Logic continued its work under V. I. Shestakov's direction. Among the Seminar participants were lecturers, scientific workers, and engineers from a number of scientific-research institutes and colleges, including the Institute of Automation and Remote Control of the Academy of Sciences of the USSR, the Laboratory for Communication Systems of the Academy of Sciences of the USSR, the Applied Mathematics Department of the Academy of Sciences of the USSR, and the Moscow State University. In all, seventeen sessions were held, where sixteen reports were heard and discussed.

The report by V. I. Shestakov, entitled "Analog mockups of control systems" (February 26 and March 4, 1960), was devoted to the mathematical simulation of analog control systems. As was mentioned by M. L. Tsetlin, the heart operation served as a prototype for these mockups. This report has been published [Doklady Akad. Nauk SSSR 131, No. 6 (1960)].

In his report, "On technical logic problems," which was presented May 20, 1960, G. N. Povarov gave a detailed presentation of the technical logic concept, which was closely related to his article, "Logic in the service of automation and technical progress" [Voprosy Filosofii, No. 10 (1959)]. According to the author's opinion, technical logic is concerned with logical relations between phenomena in technical systems and, especially, in discrete determined systems. Functional theories of discrete determined systems have a preeminently logical character (logical analysis, logical synthesis, and logical programming of relay circuits, automatic computers, etc.). Moreover, technical logic is concerned with the simulation of logical processes (logic techniques – logical machines, etc.). The tool of technical logic is the mathematical (symbolic) logic calculus in the broad sense, which can be considered partly as ideography and partly as logical mathematics in contrast to the logic of mathematics or mathematical logic in the narrow sense (the theory of mathematical proofs, theory of the foundation of mathematics, etc.); mathematical logic and technical logic have useful points in common; however, generally speaking, they are independent of each other.

On June 23, 1960, Zemanek (Austria) reported on his paper, "Solution of logical equations" [the contents of this paper have already been presented by V. P. Goncharov at the Seminar session held on May 29, 1959; see Avtomatika i Telemekhanika 21, No. 1 (1960)]. In discussing this report, M. L. Tsetlin remarked that the method of writing the solutions of equations in terms of Boolean algebra, which was proposed by Zemanek, can be widely used in synthesizing circuits with feedback. V. I. Shestakov noted that Zemanek's suggestion to use the symbol "!" for denoting the impossibility of obtaining a solution is an important innovation; the introduction of this sign makes it possible to write any solution of a logical equation.

The reports by I. L. Oifa, A. D. Zakrevskii, Yu. L. Sagalovich, A. D. Talantsev, and O. P. Kuznetsov, and two (of three) reports by V. M. Ostianu were devoted to various theoretical problems in the analysis and synthesis of relay-contact circuits.

*The Seminar activities until September 1959 have been reported in Avtomatika i Telemekhanika 18, No. 10 (1957); 20, No. 1 (1959); and 21, No. 1 (1960).

On October 9, 1959, I. L. Oifa read his report, "Topology of a neuron relay mockup." After considering various two-dimensional relay circuits, the author came to the conclusion that, from the point of view of efficiency, skeleton-symmetrical iterative circuits are the most satisfactory. By the term efficiency, it has been suggested to denote the optimum ratio of the circuit information capacity in bits to the number of elements in this circuit. The efficiency is the greater, the greater the number of closed loops that can be obtained with a given number of elements. The author found that a nine-element space-symmetrical circuit is the most efficient. Considering two types of inversions for this elementary space circuit, he further arrived at the conclusion that additional circuit improvements with the aim of realizing more complex logical functions, while maintaining the same efficiency, is possible only by means of a skeleton-symmetrical circuit which is isomorphous with an icosahedron.

The last part of the report was devoted to an attempt to construct a relay-contact neuron mockup on the basis of the above conclusions. As was shown in the discussion, such attempts are premature, since no sufficient data on neuron properties are yet available for an accurate statement of the problem.

In his report, "Certain problems in the matrix method for synthesizing relay circuits," which was read on October 16, 1959, A. D. Zakrevskii presented an original method for synthesizing functionally stable automatic devices. A. D. Zakrevskii considers as functionally stable those automatic devices whose functional properties cannot change if only one element of these devices breaks down in operation during any sufficient small time interval τ (the period of time during which the automatic device is checked and its structure restored). The high reliability (stability) of the automatic device is secured by the possibility of replacing elements or units as they break down. A. D. Zakrevskii's method for synthesizing functionally stable logical (n,m)-poles is similar to Hemming's method of noise-stable coding in communication systems, and represents a certain generalization of the latter.

In his report, "On a measure of the order in Boolean functions,"* which was presented on October 30, 1959, Yu. L. Sagalovich introduced as a measure of the order of a Boolean function the minimum number of sets of variable values for which the function is completely identified. It was shown how this number should be found for different ordered functions, for instance, for functions with an inertia group, functionally-divisible, nonrecurring II-class functions, particular functions, and others.

This report has been published in Izvest. Akad. Nauk SSSR, Tech. Sci. Div., Power Engineering and Automation No. 1 (1960).

A. D. Talantsev presented two closely related reports. In his report, "Logic algebra filtration operators in the small," which was read on March 18 and April 8, 1960, A. D. Talantsev presented a continuation of the work which he began with the introduction of logic algebra operators, formalizing changes in the logical variable values [see Avtomatika i Telemekhanika 20, No. 7 (1959)]. This paper is devoted to the logical investigation of the so-called "mixed" information processing systems, where information is assigned in discrete, digital, as well as in analog form. Such systems are asynchronous, and the necessity arises of distinguishing in such systems the characteristics of the input-signal behavior "in the small," i.e., in the neighborhood of an arbitrary instant of time. Such discrimination can be secured by electrical filters. Considerable space in the report was devoted to the determination of the "Z-type logical variable," which is a generalization of the potential, and the pulse logical variables. The following operators for the Z-type variable were then introduced: the state operator S(,), the discreteness operator i(,), the pulsed condition operator I(,), the potentiality operator p(,), the transition operator d(,), and the change operator D(,). The last two operators are identical to those introduced earlier (see the journal cited). All these operators, which are called "filtration operators in the small," can be simulated by various electrical filters. Thus, for instance, the p(,), operator can be simulated by means of a low-frequency filter; the i(,) operator by a high-frequency filter, the d(,) operator by a frequency band filter, etc.

It was shown in the report that the introduced system of operators is complete in the sense that any combination of the Z-type variable values in the recent past, present, and near future can be simulated by applying to Z any of these operators, or a certain number of them. A. D. Talantsev also indicated the possibility of constructing an axiomatic system which would reflect, to a certain degree, the logic of states of events.

*In the letters of invitation to the Seminar session, this report by Yu. L. Sagalovich was entitled "Entropy of Boolean functions as a measure of their order."

The other report by A. D. Talantsev, "An application of transition operators for the analysis and synthesis of final automatic devices," which was presented on January 15, 1960, was devoted to technical contributions concerning one of the logic algebra "filtration operators in the small" – the transition operator. The report was concerned with the so-called complex supply systems. A system from the field of electrical power engineering was used as an example to demonstrate how logical nets can be simplified by using the transition operator $\underline{d}$ in analyzing them. A. D. Talantsev explained, by means of an example, how the potential-pulse forms describing the circuits can be integrated.

On April 22, 1960, O. P. Kuznetsov presented his report, "On asynchronous logical nets." Such nets differ from the synchronous logical nets devised by Burkes and Wright by the fact that the lags in them are not equal, and that the action at the inputs of the elements and the supply of the output values are continuous. O. P. Kuznetsov expressed the functional relations between the inputs, states, and outputs of asynchronous logical nets (ALN), and he showed that the ALN class is wider than the class of final automatic devices in two respects: 1) self-contained ALN can produce nonperiodic-state sequences; 2) there exist ALN which represent irregular events.

On November 27, 1959, V. M. Ostianu presented her report, "On a class of scaling circuits," which was devoted to signal-corrector circuits. Three methods for correcting signal errors were presented: the Hemming method, the Gavrilov method, and the Varshamov method. The procedure to be used in designing corrector circuits was considered for each of these methods. Developing the material which has been published [see Bull. Math. de la Soc. Sci. Math. Phys. de la R.P.R. $\underline{2}$ (50). No. 3 (1958)], V. M. Ostianu extended her method of corrector-circuit design for the Gavrilov method to the case of different $C_1, C_2, \ldots, C_p$ functions, and she proved that a rectifier circuit constructed according to her method will not contain more than $2[2^p - (p + 1)]$ rectifiers.

On May 6, 1960, V. M. Ostianu presented her report, "Linear methods of coding for nonbinary error-correcting codes," which was concerned with the properties of linear nonbinary error-correcting codes, the method of their composition, and the determination of the number of signals in these codes. The reported results represent a development of the material in R. R. Varshamov's papers* for a code base $b > 2$.

The reports by A. M. Nechaev, A. S. Kotosonov, Daniel Muska, and A. D. Gorid'ko were devoted to the description of new circuits and machines for logical operations.

On December 11, 1959, A. M. Nechaev presented his report, "Ferrite-diode impedance circuits and their synthesis," which was devoted to a new universal element by means of which it is possible to simulate any logic-algebra function of arbitrary complexity. The possible technical uses of such elements were also described.

The report by A. S. Kotosonov, entitled "Logical nets based on cold-cathode thyratrons," which was presented on December 18, 1959, was devoted to new circuits for simulating logic-algebra functions.

Daniel Muska (Hungary) presented his report, "On the Szeged logical machine," on January 22, 1960. The first communication concerning this machine was presented by Professor L. Kalmar at the All-Union Conference on the Theory of Relay-Action Devices, which was held in 1957 in Moscow.**

On May 20, 1960, A. D. Gorid'ko reported on his circuit for a loss-proof game machine, and its algorithm.

On September 25, 1959, V. M. Ostianu presented the essence of G. K. Moisila's book Algebraic Theory of Automatic Devices, which was the first monograph on the theory of relay devices to be published in the Rumanian People's Republic. This book provides the results obtained in investigations performed by the author and his disciples. Not only the algebra of logic, but also multivalue logic and the theory of finite fields are used in the exposition. After discussing the contents of G. K. Moisila's book, the Seminar reached the conclusion that this book should be translated into Russian.

---

*Doklady Akad. Nauk SSSR $\underline{117}$, 5, 739 (1957); also Collection: Trudy Nauchno-Tekhnicheskogo Obshchestva Radiotekhniki i Elektrosvyazi im. A. S. Popova, No. 1 (1958).

**Avtomatika i Telemekhanika $\underline{19}$, No. 9 (1958) (Survey by G. K. Moskatov and V. M. Ostianu).